January 2010

Mechanisms of Copper-Dependent Notochord Formation in Zebrafish

John Gansner
Washington University in St. Louis

WASHINGTON UNIVERSITY

Division of Biology and Biomedical Sciences

Program in Molecular Cell Biology

Dissertation Examination Committee:
Jonathan D. Gitlin, Chair
Thomas J. Baranski
Stephen L. Johnson
Robert P. Mecham
Zsolt Urban
David B. Wilson

MECHANISMS OF COPPER-DEPENDENT NOTOCHORD FORMATION IN ZEBRAFISH

by

John Michael Gansner

A dissertation presented to the
Graduate School of Arts and Sciences
of Washington University in
partial fulfillment of the
requirements for the degree
of Doctor of Philosophy

May 2010

Saint Louis, Missouri

ABSTRACT OF THE DISSERTATION

Mechanisms of Copper-Dependent Notochord Formation in Zebrafish

by

John Michael Gansner

Doctor of Philosophy in Biology and Biomedical Sciences
(Molecular Cell Biology)

Washington University in St. Louis, 2010

Professor Jonathan D. Gitlin, Chair

The interplay of genes and nutrition during early development profoundly impacts fetal outcome. Copper is an essential nutrient required for the redox activity of many enzymes, and recent work in our laboratory has elucidated the phenotype of copper deficiency in zebrafish, which includes a strikingly distorted notochord. The studies described here establish the specific genetic etiology of this distortion and reveal a number of gene-gene and gene-nutrient interactions critical to notochord morphogenesis.

We first demonstrate that the notochord distortion observed in copper-deficient zebrafish results from lysyl oxidase cuproenzyme inhibition. Four lysyl oxidase family members are expressed throughout the developing zebrafish notochord, including *loxl1* and *loxl5b*. Morpholino antisense experiments reveal that knockdown of *loxl1* results in notochord distortion and also demonstrate overlapping roles for *loxl1* and *loxl5b* in notochord formation. Furthermore, partial knockdown of either *loxl1* or *loxl5b* sensitizes embryos to notochord distortion when combined with reduced copper availability, and

any of these treatments alone sensitizes embryos to notochord distortion after partial disruption of the gene encoding a lysyl oxidase substrate, *col2a1*.

To elucidate additional gene-nutrient interactions involved in notochord formation, we conducted a forward genetic screen for mutants that exhibit increased notochord distortion after partial lysyl oxidase inhibition. This screen was facilitated by the identification of a novel, highly potent lysyl oxidase inhibitor, 2-mercaptopyridine-*N*-oxide, and yielded a mutant with defects in notochord and vascular morphogenesis, *puff daddy*^{gw1}. Subsequent work demonstrated that the *puff daddy*^{gw1} phenotype results from loss of zebrafish fibrillin-2. Importantly, the notochords of *puff daddy*^{gw1} mutants are strikingly sensitized to distortion under conditions of suboptimal copper nutrition that do not affect wild-type embryos. This sensitization is also observed in a published notochord mutant, *gulliver*^{m208}, and we demonstrate that the *gulliver*^{m208} phenotype arises from a missense mutation in the alpha 1 chain of type VIII collagen.

Taken together, these studies demonstrate essential roles for copper and multiple extracellular matrix components in late notochord formation and suggest that nutritional status should be interpreted within the polymorphic genetic context of the developing embryo.

ACKNOWLEDGMENTS

I would like to thank Jonathan Gitlin for his time and commitment as a mentor. He has been a wonderful guide to the intellectual, ethical, and social aspects of both science and medicine. I have learned to pick important yet approachable problems, to ask key questions, and to observe closely for the answers. It has been a formative voyage, both professionally and personally.

I am grateful to members of the Gitlin laboratory for creating an exciting, earnest, and collegial laboratory environment in which to work. I am also grateful to my thesis committee for providing advice and helpful criticisms. Finally, I would like to acknowledge the MSTP program for its outstanding support.

This work is dedicated to my wife Rachel.

TABLE OF CONTENTS

LIST OF FIGURES

CHAPTER 1

CHAPTER 2

JOHN MICHAEL GANSNER

Date of Birth: October 1, 1980

Citizenship: Canadian

Permanent Address: 1650 Passageview Dr.
Campbell River, B.C. V9W 6L3 CANADA
Email: gansner@post.harvard.edu

Education:

2002 A.B. Biochemical Sciences, *magna cum laude*
Harvard College, Cambridge, Massachusetts

2010 M.D./Ph.D. Molecular Cell Biology (expected)
Washington University, Saint Louis, Missouri

Awards and Honors:

2002 Thomas Temple Hoopes Prize, Harvard College

2002 Phi Beta Kappa, Alpha Iota of Massachusetts

2005 Predoctoral Fellowship, American Heart Association

2009 Outstanding Scholar Award for the "most outstanding third year medical student," Saint Louis (John Cochran) VA

2009 American College of Physicians Clerkship Award (Missouri Chapter) for the "outstanding student in the internal medicine clerkship," Washington University School of Medicine

Research Experience:

2000-2002 Undergraduate thesis, Center for Blood Research,
Harvard Medical School, Boston, Massachusetts
Characterization of the Second DNase I Hypersensitivity Site in the Murine Interferon-Gamma (IFNγ) Gene
Advisor: Anjana Rao, Ph.D.

2005-Present Ph.D. candidate, Molecular Cell Biology,
Washington University, Saint Louis, Missouri
Mechanisms of Copper-Dependent Notochord Formation in Zebrafish
Advisor: Jonathan Gitlin, M.D.

Teaching Experience:

2004 Teaching Assistant, Molecular Foundations of Medicine
Washington University, Saint Louis, Missouri

2004-2007 Research mentor for several high school and college students pursuing independent laboratory projects
Washington University, Saint Louis, Missouri

Publications:

1. Anderson C, Bartlett SJ, **Gansner JM**, Wilson D, He L, Gitlin JD, Kelsh RN, and Dowden J. (2007). Chemical genetics suggests a critical role for lysyl oxidase in zebrafish notochord morphogenesis. *Mol Biosyst* 3, 51-59.
2. **Gansner JM**, Mendelsohn BA, Hultman KA, Johnson SL, and Gitlin JD. (2007). Essential role of lysyl oxidases in notochord development. *Dev Biol* 307, 202-213.
3. **Gansner JM**, Madsen EC, Mecham RP, and Gitlin JD. (2008). Essential role for fibrillin-2 in zebrafish notochord and vascular morphogenesis. *Dev Dyn* 237, 2844-2861.
4. **Gansner JM**, Gitlin JD. (2008). Essential role for the alpha 1 chain of type VIII collagen in zebrafish notochord formation. *Dev Dyn* 237, 3715-3726.

Abstracts:

1. **Gansner JM**, Mendelsohn BA, and Gitlin JD. Lysyl oxidases in notochord development and skeletal dysplasias. Poster, 7th International Conference on Zebrafish Development & Genetics, Madison, Wisconsin, June 14-18 2006.
2. **Gansner JM** and Gitlin JD. Lysyl oxidases in notochord development and skeletal dysplasias. Poster, 5th European Zebrafish Genetics and Development Meeting, Amsterdam, The Netherlands, July 12-15 2007.
3. **Gansner JM** and Gitlin JD. Lysyl oxidases in notochord development and skeletal dysplasias. Poster, Gordon Research Conference "Cell Biology of Metals," Newport, Rhode Island, July 29-August 3 2007.
4. **Gansner JM** and Cras JJ. Hypereosinophilia unmasked by discontinuation of long-term prednisone: a case of the hypereosinophilic syndrome. Poster, American College of Physicians, Missouri Chapter Meeting, Osage Beach, Missouri, September 25 2009.

CHAPTER 1

Introduction

Gene-nutrient interactions in early development

Adequate nutrition during embryogenesis is critical for preventing adverse developmental outcomes, and what is "adequate" is determined partly by genetic context. In the agouti mouse strain, dietary supplementation of female mice with vitamin B12 or other methyl-donors during pregnancy permanently alters gene expression and results in fewer offspring with obesity and an abnormal yellow coat color (1). Furthermore, different genetic breeds of ewes grazed on the same copper-deficient pasture give birth to offspring with strikingly dissimilar incidences of enzootic ataxia, a disease resulting from copper deficiency (2). In humans, a role for genetic susceptibility loci in the pathogenesis of fetal iodine deficiency disorder – the leading cause of preventable mental retardation in newborns – was likewise suggested by observations that not everyone born to an iodine-deficient mother is affected (3-5). A few of these genetic susceptibility loci have recently been identified (4, 6), and perinatal iodine supplementation should be particularly advantageous for mothers with these or other undiscovered genetic risk factors for iodine deficiency. Similarly, genetic susceptibility loci may determine the need for folate supplementation in the prevention of neural tube defects. Indeed, perinatal folate supplementation has been shown epidemiologically to reduce the risk of fetal neural tube defects by 50-70% and genetic risk factors have been described (7).

A great deal of evidence from animal models and epidemiologic studies supports the importance of diverse gene-nutrient interactions in determining developmental outcome (2, 8, 9). In essence, nutrient deprivation provides a stress that can result in the expression of congenital birth defects or other adverse fetal outcomes depending on

genetic background. The elucidation of gene-nutrient interactions during development is thus of particular relevance, since it can provide insight into the molecular pathways of organogenesis and may also allow for targeted therapeutic interventions designed to prevent disease.

Cuproenzymes in development

Copper is an essential nutrient required by many proteins as a cofactor for catalyzing electron transfer reactions (10). Cuproenzymes perform a number of functions critical to normal human development (Table 1), and these functions appear to be substantially conserved across species (10). Copper deficiency can result from insufficient dietary intake or from genetic factors (2). In humans, Menkes disease results from loss of function mutations in the intracellular copper transporter ATP7A, which delivers copper to the secretory pathway for incorporation into cuproenzymes or export from the cell (11). Children with Menkes disease appear normal at birth but soon exhibit many features attributable to loss of cuproenzyme activity, including skin hypopigmentation, kinky hair, cerebral and cerebellar degenerative symptoms such as hypotonia and seizures, lax skin, arterial tortuosity, emphysema, osteoporosis, and bladder diverticuli (11, 12). Subcutaneous copper injections fail to clinically reverse disease progression unless a small amount of residual ATP7A activity remains (12), as would be expected from a defect in copper delivery to the secretory pathway. Death generally occurs by three years of age, although survival is better in an allelic form of the disease known as Occipital Horn Syndrome where a greater degree of ATP7A activity is present (12, 13). In patients

with Occipital Horn Syndrome, scoliosis or kyphosis of the vertebral column are common and developmental delay is less profound (10).

Our laboratory has recently delineated the phenotype of copper deficiency in the zebrafish embryo, which can be induced either pharmacologically through incubation in copper chelators such as neocuproine or through genetic disruption of *atp7a*, as in the mutant *calamity* (14). Copper deficiency in zebrafish results in a pleiotropic phenotype including loss of melanin pigmentation, midbrain/hindbrain degeneration, and striking notochord distortion. The role for copper in notochord formation was previously unappreciated, and notochord distortion thus provides a new, highly visible phenotype that can be utilized for further study of copper homeostasis during embryonic development.

Enzyme	Function
Lysyl oxidase	Chemical crosslinking of collagens and elastin
Tyrosinase	Melanin pigment biogenesis
Ceruloplasmin	Ferroxidase
Peptidylglycine α-amidating monooxygenase	Peptide hormone activation
Cytochrome c oxidase	Electron transport and cellular respiration
Copper-zinc superoxide dismutase	Antioxidant defense
Sulfhydryl oxidase	Chemical cross-linking of keratin

Table 1. Select human cuproenzymes and functions.

Notochord formation

The notochord is a midline axial organ that specifies left-right asymmetry and provides structural support to the growing embryo. It also plays a critical role in patterning nearby ectodermal, mesodermal, and endodermal tissues including the neural tube, somites,

pancreas, heart, and dorsal aorta (15, 16). The notochord facilitates locomotion in lower chordates and is required for vertebral column formation. Indeed, defects in notochord formation have been linked to abnormalities in vertebral bone structure and other congenital birth defects in humans (15).

The notochord is specified early in embryogenesis and originates from the dorsal organizer. Notochord progenitors in this anatomic structure differentiate first into chordamesoderm and then into mature notochord. The transition from chordamesoderm to mature notochord involves the formation of an extracellular matrix sheath that constrains a single row of notochord vacuolar cells as their vacuoles inflate. This transition also correlates with the extinction of an embryonic gene program expressed by chordamesoderm (16). In zebrafish, a number of mutants with defects in different stages of notochord morphogenesis have been described (17-19). Of interest, defects in late notochord formation can arise from extracellular matrix abnormalities that impair the integrity of the notochord sheath (20).

Zebrafish as a model for studying gene-nutrient interactions in early development

Zebrafish provide a useful model for interrogating the relationship between genes and nutrition during early development. This vertebrate is genetically tractable and completes embryogenesis rapidly ex utero where organogenesis can be directly observed; furthermore, nutrient concentrations can be precisely controlled in the zebrafish embryonic milieu via pharmacologic manipulation.

Many phenotypes relevant to human development can be studied in zebrafish, and a number of zebrafish mutants identified in forward genetic screens have already

increased our understanding of the cell biologic mechanisms underlying human disease (21-23). Zebrafish are amenable to chemical mutagenesis, and phenotypic screening of mutant carriers can be conducted using haploid offspring, which complete the first few days of embryonic development relatively normally despite having half the normal complement of chromosomes (24). A major advantage of the haploid method is that F1 females (derived by fertilizing wild-type clutches with sperm from mutagenized males) can be utilized, eliminating the need to generate and maintain large families of F2 fish, which requires time and space (24). Once a mutant is identified, polymorphic strains of fish and large clutch sizes permit meiotic mapping of the lesion to a limited region of the genome for subsequent cloning of the affected gene (25, 26). Morpholino antisense oligonucleotides can be used to recapitulate the mutant phenotype in wild-type fish by altering splicing or inhibiting translation, resulting in transient knockdown of specific gene expression (27). Conversely, microinjection of wild-type mRNA into one-cell embryos will usually rescue the mutant phenotype. Importantly, forward genetic screens in zebrafish can be carried out in the presence of pharmacologic agents at doses just below what is required to elicit a phenotype in wild-type embryos. This permits the identification of hypomorphic alleles that might go undetected without pharmacologic stress, and focuses the screen on a biologic pathway of interest. When the pharmacologic agent alters nutrient metabolism, gene-nutrient interactions can be detected.

Summary

At present, zebrafish are the vertebrates most closely related to humans that are amenable to the application of powerful genetic techniques and also allow embryogenesis to be

observed in real-time. The studies in this thesis describe several gene-gene and gene-nutrient interactions critical to normal notochord morphogenesis. Chapter 2 demonstrates that the notochord distortion observed in copper-deficient zebrafish embryos results from inhibition of specific lysyl oxidase cuproenzymes. Chapter 3 describes the identification and characterization of 2-mercaptopyridine-*N*-oxide, a novel, highly potent lysyl oxidase inhibitor. Chapter 4 reports the use of this inhibitor in a forward genetic screen for mutants that exhibit increased notochord distortion after partial lysyl oxidase inhibition, and discusses the characterization of a mutant identified in the screen. Chapter 5 demonstrates that the phenotype of a published notochord mutant, *gulliver*, results from a missense mutation in the gene encoding the alpha 1 chain of type VIII collagen. Taken together, the data in this thesis contribute to an understanding of notochord formation and lysyl oxidase function, and elucidate some of the complex gene-nutrient interactions that shape development.

Developmental Biology
Vol. 307, Issue 2, pp. 202-213, 2007

CHAPTER 2

Essential role of lysyl oxidases in notochord development

John M. Gansner,[1] Bryce A. Mendelsohn,[1] Keith A. Hultman,[2]
Stephen L. Johnson,[2] and Jonathan D. Gitlin[1,2]

Departments of Pediatrics[1] and Genetics[2]
Washington University School of Medicine
St. Louis, Missouri 63110

Abstract

Recent studies reveal a critical role for copper in the development of the zebrafish notochord, suggesting that specific cuproenzymes are required for the structural integrity of the notochord sheath. We now demonstrate that β-aminopropionitrile, a known inhibitor of the copper-dependent lysyl oxidases, causes notochord distortion in the zebrafish embryo identical to that seen in copper deficiency. Characterization of the zebrafish lysyl oxidase genes reveals eight unique sequences, several of which are expressed in the developing notochord. Specific gene knockdown demonstrates that loss of *loxl1* results in notochord distortion, and that *loxl1* and *loxl5b* have overlapping roles in notochord formation. Interestingly, while notochord abnormalities are not observed following partial knockdown of *loxl1* or *loxl5b* alone, in each case this markedly sensitizes developing embryos to notochord distortion if copper availability is diminished. Likewise, partial knockdown of the lysyl oxidase substrate *col2a1* results in notochord distortion when combined with reduced copper availability or partial knockdown of *loxl1* or *loxl5b*. These data reveal a complex interplay of gene expression and nutrient availability critical to notochord development. They also provide insight into specific genetic and nutritional factors that may play a role in the pathogenesis of structural birth defects of the axial skeleton.

Introduction

Structural birth defects are a leading cause of morbidity and mortality in humans. Despite recent advances identifying the molecular genetic basis of several such disorders, the genetic and environmental determinants of most structural birth defects remain unknown (28). One of the most important environmental factors influencing the outcome of fetal development is nutrition, and epidemiologic data, twin studies, and phenotype-genotype correlations all suggest that specific nutritional influences in combination with genetic susceptibility at multiple loci have profound long-term effects on pregnancy outcome (29). While *in utero* development severely limits experimental elucidation of the mechanisms and timing of critical events affected by nutrition during early embryonic development, recent studies suggest that the zebrafish may be an informative, genetically tractable model organism for such analysis (14, 22, 30).

The notochord is a useful structure for examining the complex interplay of genes and nutrition in early vertebrate development. This organ is readily visible throughout early zebrafish development, is the first to fully differentiate during embryogenesis, and is essential for the patterning of surrounding ectodermal, mesodermal, and endodermal tissues (31). The notochord is also a critical midline structure required for locomotion in some chordates, and for axial skeletal formation in vertebrates (31). Furthermore, the cell biological mechanisms underlying notochord maturation, involving cell vacuolation, matrix biosynthesis, and sheath formation, have begun to be elucidated through a series of elegant genetic experiments (17-20). Given the critical role of the notochord in chondrogenesis and fate determination of surrounding tissues including neural tube,

heart, and skeleton (16), as well as the large number of human structural birth defects arising from these tissues, elucidation of the nutritional and genetic mechanisms of notochord formation may be of direct relevance to our understanding of the etiology of congenital malformations.

During studies examining the role of copper in embryonic development, we discovered a critical role for this nutrient in late notochord formation (14). These findings suggested that specific cuproenzymes may be required for the structural integrity of the zebrafish notochord sheath, a concept supported by recent studies in *Xenopus laevis* (32). In this current study we have determined a role for two specific lysyl oxidase genes in notochord formation, and defined a complex biological pathway modulated by copper nutrition that underlies this process. Our data suggest that copper status during embryonic development should be interpreted in the context of environmental and genetic modulators of cuproenzyme activity. Indeed, the results raise the intriguing possibility that suboptimal copper availability, due either to nutritional or genetic variation during embryonic development, contributes to human birth defects of the axial skeleton.

Materials and methods

Zebrafish strains and maintenance

Zebrafish were reared under standard conditions at 28.5°C (33) and staged as described (34). Synchronous, in vitro fertilized embryos were obtained from AB or AB/WIK stocks for all experiments.

Pharmacologic treatment

Pharmacologic compounds were purchased from Sigma (St. Louis, MO). β-aminopropionitrile (A3134) and neocuproine (N1501) were prepared as 100 mM stocks in egg water and dimethyl sulfoxide, respectively, and diluted in egg water. Embryos were incubated in compound starting at 3 hpf and examined with an Olympus SZX12 zoom stereomicroscope at 24, 30, 48, and 72 hpf. Images of representative fish mounted in 2% methylcellulose were acquired with an Olympus DP70 camera.

Identification and annotation of zebrafish lysyl oxidase genes

Exons encoding conserved regions of the lysyl oxidase catalytic domain (35) were detected by TBLASTN search of the Ensembl zebrafish genome (Zv5). A clone of *lox* was commercially available (Open Biosystems #6971279); full-length cDNA sequences of all other family members were obtained using 5' and 3' rapid amplification of cDNA ends (RACE) and RT-PCR based on sequence homology to human, mouse, and frog lysyl oxidase sequences. Primers were as follows: *loxl1* forward primer 5'-CGCCTTCTTTTATTAGTCTTCTGG-3' and reverse primer 5'-ACAGCGACGTCAGGAATTCC-3'; *loxl2a* – forward primer 5'-ATGGCGGTGTCTTCTGCATTGTGC-3' and reverse primer 5'-

CTATCTGAGGTGGTTCAGCTGGTTGC-3'; *loxl2b* – forward primer 5'-GCCATACAATCTGAGCCTCTGTC-3' and reverse primer 5'-CTTTACCTGTGGGTCACCTGG-3'; *loxl3a* – forward primer 5'-ATGGGACAGTTTGCTAACAGC-3' and reverse primer 5'-TTATGAGATCTTGTTGTTGAGCTGCC-3'; *loxl3b* – forward primer 5'-GTGTTTGTGTCCTTTGATGC-3' and reverse primer 5'-GCTGTACATGAAGAGTGATCT-3'; *loxl5a* – nested 5'RACE primers 5'-CACTCGAGCTGTACGCTGAACTGGAAAGGC-3' (first reaction) and 5'-GCACAGGGCTTGAACGCACCACATGCCC-3' (second reaction), and 3' PCR amplification with forward primer 5'-CATTAAGATGTGCCGCAGAGG-3'and reverse primer 5'-CTCACCCGGTGATCCTACAGTTG-3'; *loxl5b* – forward primer 5'-CCCACATCCAGAGGAGCGAA-3' and reverse primer 5'-TCCTCACCCAGTTATGATGCAG-3'. GenBank accession numbers are: *lox* – **EF030479**; *loxl1* – **EF030480**; *loxl2a* – **EF030481**; *loxl2b* – **EF030482**; *loxl3a* – **EF030483**; *loxl3b* – **EF030484**; *loxl5a* – **EF030485**; *loxl5b* – **EF030486**. An alignment of the C-terminal portion of zebrafish and human lysyl oxidases was created in ClustalW with human CD163 as outgroup (36, 37), and phylogenetic analysis carried out according to the parsimony method (38). Bootstrap values over 100 replicates are noted. Signal peptides and scavenger-receptor, cysteine rich domains were predicted using SignalP 3.0 and Motif scan (39, 40). Copper binding domains, Bone Morphogenetic Protein-1 (BMP-1) cleavage sites, and lysyl-tyrosyl quinone cofactor residues were identified based on homology to known lysyl oxidase sequences (41-43).

Whole mount in situ hybridization and frozen sections

Lysyl oxidase and *col2a1* (44) probe constructs were generated as partial clones by RT-PCR and ligated into pCRII (Invitrogen). DIG-labeled antisense RNA probes were synthesized from these constructs using a DIG-labeling kit (Roche), and whole mount in situ hybridization performed as previously described (14, 45). Embryos for frozen sections were subsequently embedded in PBS containing 1.5% agarose/5% sucrose. Blocks were equilibrated in 30% sucrose at 4°C, mounted with O.C.T. (Tissue-Tek), and cut on a Leica Cryostat after freezing with liquid nitrogen. 14 μM sections were collected on Superfrost slides (Fisher) and mounted in 50% glycerol-PBS for visualization on an Olympus BX60 microscope.

Morpholino and mRNA injections

Morpholino oligonucleotides (27) targeting splice sites of exons encoding the lysyl oxidase copper binding domain (43) were resuspended in Danieau buffer, diluted to include 0.05% phenol red, and injected into one- to four-cell embryos. Morpholinos targeting the start sites of *loxl1* and *loxl5b*, the 5' splice acceptor site of an exon corresponding to exon 48 of the human *col2a1* orthologue, and standard control morpholino (Gene Tools, LLC) were likewise prepared and injected. Morpholino sequences are as follows: *loxl1* (splice) – 5'- GTGTAGATGTGGACTCACTGATGGC-3'; *loxl1* (splice) – 5'- GTAATGCCTGATGGAGACAAGAGAC-3' (Fig. 7 and Fig. 8); *loxl1* (start) – 5'-AGTACATGCAGCATATTGAGAAGAC-3'; *loxl2b* – 5'-GATCTGGAGCAGCTAGAAAAAACAA-3'; *loxl3b* – 5'-CAGCTGCGGACATAAACAAACAAAT-3';

loxl5b (splice) – 5’-GCCTGTGGAATAAACACCAGCCTCA-3’; *loxl5b* (start) – 5’-TAAAGCTGTATGATTCGCTCCTCTG-3’; *col2a1* – 5’-CCTGAAGGTCCCTATTATAAATAAC-3’. Capped, polyadenylated mRNA for rescue experiments was generated from full-length clones of *loxl1*, *loxl5b*, and control transposase (46) using the mMESSAGE mMACHINE kit (Ambion), with 300 pg of mRNA injected per embryo. Rescue was calculated by taking the difference between the percentages of embryos with distorted notochords injected with lysyl oxidase and control mRNA, and then dividing this number by the percentage of embryos with distorted notochords injected with control mRNA. Statistical analysis was conducted using one-way ANOVA for independent samples based on the percentages of embryos with the distorted notochord phenotype from at least three separate experiments. In all cases, abnormal splicing was detected by RT-PCR of RNA from 15 embryos injected with control or lysyl oxidase morpholino using primers to exons flanking the putative splice site. Nucleotide sequencing of putative splice products identified on agarose or polyacrylamide gels confirmed the presence of a premature stop codon in the splice variants. The intensity of wild-type PCR products was quantified using non-saturated gel pictures and ImageJ 1.37v software (47), and the percentage of wild-type splice form remaining after morpholino knockdown calculated.

Transmission Electron Microscopy

Dechorionated embryos were fixed in 2.5% glutaraldehyde/0.1 M sodium cacodylate and sequentially stained with osmium tetroxide and uranyl acetate. They were then dehydrated, embedded in PolyBed 812, and thin sectioned on a Reichert-Jung Ultra-Cut.

Slices were post-stained in 4% uranyl acetate and lead citrate, and viewed on a Zeiss 902 electron microscope. Photographs were recorded with Kodak EM film.

Results

β-aminopropionitrile recapitulates the notochord phenotype of copper deficiency

Copper deficiency, induced by either chemical (neocuproine) or genetic (*calamity*^{vu69}) means, results in a pleiotropic phenotype that includes a distorted, wavy notochord (14). Lysyl oxidases are copper-dependent enzymes that stabilize extracellular matrix by crosslinking elastin and collagens (35, 43), a process thought to be important for maintaining notochord sheath integrity during notochord vacuolation. β-aminopropionitrile irreversibly inhibits lysyl oxidases by binding the active site of the catalytic domain (48, 49), and incubation of 3 hpf zebrafish embryos with β-aminopropionitrile resulted in striking notochord distortion and blunted somites, similar to what is observed with the copper chelator neocuproine (Fig. 1 and S. Fig. 1). Equivalent results were also obtained after incubation with semicarbazide, another known inhibitor of lysyl oxidases (data not shown), suggesting that these enzymes play a central role in notochord formation. β-aminopropionitrile treatment does not result in the pleiotropic phenotype of copper deficiency, including absence of melanin pigmentation, midbrain-hindbrain degeneration, and loss of red blood cells (Fig. 1B vs. 1C), reflecting the broader scope of cuproenzyme inhibition achieved with neocuproine. Furthermore, the effect of β-aminopropionitrile on notochord morphology was not due to copper chelation as this phenotype was not reversible with $CuCl_2$ (data not shown). Although the notochord distortion observed with β-aminopropionitrile in Figure 1 is less than that with neocuproine, the mechanisms resulting in this process are likely the same because ten-

fold higher doses of β-aminopropionitrile result in a degree of distortion identical to that seen with neocuproine (S. Fig. 1).

The zebrafish genome encodes eight lysyl oxidases

These data suggested a requirement for lysyl oxidase activity in zebrafish notochord development. The human genome encodes five lysyl oxidase family members characterized by the presence of a conserved copper binding domain and residues for a lysyl-tyrosyl quinone cofactor. Although experimental evidence suggests a role for two of these lysyl oxidases in elastin and collagen crosslinking (50-54), the precise role of each family member in extracellular matrix formation, cancer biology, and intracellular signaling remains undetermined. Using a bioinformatic approach, we identified and cloned eight unique zebrafish lysyl oxidase genes, revealing that each human lysyl oxidase has a zebrafish orthologue except LOXL4 (Fig. 2 and S. Fig. 2). While lysyl oxidase genes are well conserved between humans and zebrafish based on nucleotide sequence alignment, Loxl3a and Loxl3b lack a signal peptide and the full complement of scavenger receptor domains found in human LOXL3 (Fig. 2A and S. Fig. 2). Our analysis also revealed two novel zebrafish lysyl oxidases, Loxl5a and its paralogue Loxl5b, that are closely related to LOX and LOXL1 by phylogenetic analysis but have not been previously described in other species (Fig. 2B and S. Fig. 2A). The presence of paralogues for some zebrafish lysyl oxidases likely reflects a genome duplication event and subsequent partitioning of gene function (55, 56).

Four lysyl oxidases are expressed throughout the developing notochord

To elucidate the role of specific lysyl oxidases in notochord formation, we assessed lysyl oxidase mRNA expression in zebrafish embryos by whole-mount in situ hybridization. Four lysyl oxidase family members – *loxl1*, *loxl2b*, *loxl3b*, and *loxl5b* – were readily detected throughout the notochord during early zebrafish development (Fig. 3), and were specifically expressed within the vacuolar cells, as seen in frozen sections of 15 somite embryos (Fig. 4). Lysyl oxidase expression was observed as early as the 5 somite stage (Fig. 3A,M), well before notochord vacuolation begins, and was extinguished after vacuolation is complete, between 24 hpf and 48 hpf (data not shown). While *loxl1* and *loxl5b* were robustly expressed at the caudal tip (Fig. 3D,P, arrowheads), *loxl2b* and *loxl3b* were not (Fig. 3H,L), possibly reflecting a differential requirement for their activity during notochord elongation. Closer inspection revealed that *loxl5b* is expressed anterior to the notochord, in the prechordal plate region (Fig. 3O, asterix), and that *loxl1* is expressed in the hypochord (Fig. 4A, arrows), providing a new marker for this structure and suggesting a role for *loxl1* in crosslinking extracellular matrix near the developing aorta (57, 58). *lox*, *loxl3a*, and *loxl5a* were not expressed in or near the notochord between the 5 somite stage and 48 hpf, but could be detected by 5 dpf, while *loxl2a* was faintly and transiently expressed in a limited region of the anterior notochord before 24 hpf and was not studied further (data not shown).

Morpholino knockdown of* loxl1 *or* loxl1 *and* loxl5b *together results in a distorted notochord

To determine the precise developmental functions of individual lysyl oxidases expressed throughout the notochord, we conducted knockdown experiments using morpholino

antisense oligonucleotides (Fig. 5 and Table 1). Whereas control morpholino had no observable effect on developing zebrafish embryos (Fig. 5A and Table 1), a splice morpholino to *loxl1* recapitulated the notochord distortion and blunted somites observed with β-aminopropionitrile and neocuproine (Fig. 5B and Table 1), revealing that this family member is necessary for late notochord formation in zebrafish. Morpholino knockdown of *loxl2b*, *loxl3b*, and *loxl5b* induced minor changes to notochord architecture, including occasional notochord kinks (Fig. 5C-E and Table 1), and the *loxl5b* morpholino also caused caudal vein edema (Fig. 5E, arrows). In all cases, a specific effect of these splice morpholinos on lysyl oxidase gene transcription was confirmed by demonstrating abnormal splicing and generation of a premature stop codon (S. Fig. 3 and data not shown). Since very few embryos injected with morpholinos to *loxl2b*, *loxl3b*, and *loxl5b* alone developed the distorted notochord phenotype at high morpholino doses (Fig. 5C-E and Table 1), we tested all possible combinations of lysyl oxidase morpholinos. Morpholino doses of *loxl1* and *loxl5b* that did not result in notochord distortion when used alone, together recapitulated the notochord phenotype and blunted somites observed with β-aminopropionitrile and neocuproine (Fig. 5F and Table 1). This was the only morpholino combination resulting in a notochord phenotype (Table 1 and S. Table 1), and was similarly recapitulated with morpholinos targeting the start sites of *loxl1* and *loxl5b* (Table 1 and S. Fig. 1). Taken together, these observations indicate that these two lysyl oxidases have specific overlapping functions in notochord development. The notochord distortion elicited by combined knockdown of *loxl1* and *loxl5b* (Fig. 5F and Table 1) was specifically rescued with co-injection of either *loxl1* or

loxl5b mRNA (Fig. 5H,I and Table 2), but not control mRNA (Fig. 5G and Table 2). Importantly, each of the lysyl oxidase splice morpholinos also resulted in head necrosis (Fig. 5B-E) that was not rescued with specific mRNA injection (data not shown), suggesting that this phenotype results from a non-specific morpholino effect. Consistent with this concept, head necrosis is not observed following treatment with either β-aminopropionitrile or neocuproine (S. Fig. 1).

Nutrient, gene interactions in notochord distortion

Since the notochord phenotype observed with combined *loxl1* and *loxl5b* knockdown is identical to that seen with β-aminopropionitrile and neocuproine, we next examined the interaction of copper availability and lysyl oxidase gene expression in notochord formation (Fig. 6). For these experiments, doses of *loxl5b* morpholino and neocuproine were determined such that they did not cause notochord distortion when used alone (Fig. 6B,C and Table 3). In striking contrast, embryos subjected to combined treatment with these same doses of *loxl5b* morpholino and neocuproine developed distorted notochords (Fig. 6D and Table 3). Experiments using *loxl1* morpholino and neocuproine yielded similar results (Table 3), supporting the model that specific inhibition of two lysyl oxidases accounts for the notochord abnormalities observed with β-aminopropionitrile and neocuproine. Most significantly, these data also reveal that copper availability influences the phenotypic outcome of notochord development according to the genetic content of the embryo.

In this context, we also examined the role of collagen II, a structural component of the notochord sheath, in notochord formation. Collagen II is a lysyl oxidase substrate

whose spatio-temporal pattern of expression corresponds with that of the notochord-expressed lysyl oxidases during early zebrafish development (44). We determined the highest dose of *col2a1* morpholino that could be injected without phenotypic abnormalities (Fig. 6E), and incubated these injected embryos in a dose of neocuproine (2 μM) that was also without effect. This combined treatment resulted in notochord distortion (data not shown), revealing the importance of copper nutrition in the context of collagen II disruption and predicting a genetic interaction between collagen II and the notochord-expressed lysyl oxidases. Consistent with this prediction, about half of the embryos injected with *loxl5b* and *col2a1* morpholinos together revealed a conspicuously distorted notochord (Fig. 6F and Table 4), demonstrating that decreased expression of *loxl5b* sensitizes embryos to *col2a1* disruption. A comparable result was also obtained using the *loxl1* and *col2a1* morpholinos (Table 4). The specificity of this effect was confirmed by detection of a splicing defect resulting from the *col2a1* morpholino that causes a premature stop codon (S. Fig. 3 and data not shown). The observation that in each case only about 50% of the embryos displayed the abnormal notochord phenotype may be due either to additional lysyl oxidase substrates that play a role in notochord formation or to submaximal disruption of *col2a1* gene expression at this morpholino dose (S. Fig. 3). Taken together, these data illustrate the complex interplay of multigenic expression and nutrition required for notochord formation in developing zebrafish embryos.

col2a1 ***expression persists in notochord vacuolar cells after lysyl oxidase inhibition***

The foregoing experiments suggest that collagen II is a substrate for both Loxl1 and Loxl5b in zebrafish. As recently demonstrated (59), *col2a1* expression persists in the vacuolar cells of the notochord at 24 hpf when embryos are treated with a dose of neocuproine that causes notochord distortion (Fig. 7B). One possible explanation for this phenomenon is impairment of a feedback mechanism that normally downregulates production of *col2a1* upon collagen crosslinking in the notochord sheath. Consistent with this idea, embryos treated with β-aminopropionitrile (Fig. 7C) or injected with morpholinos to *loxl1* and *loxl5b* (Fig. 7D) continued to express *col2a1* in the vacuolar cells of the notochord at 24 hpf, whereas control embryos did not (Fig. 7A). The persistent expression of *col2a1* was not due to developmental delay, as embryos added somites at the same rate under all experimental conditions (data not shown).

We next considered whether the persistent *col2a1* expression was specific to a reduction in crosslinking or was a generalized response to mechanical distortion of the notochord. To explore this idea, we incubated embryos in a dose of neocuproine (2 μM) that did not cause notochord distortion but that partially disrupted crosslinking, as revealed by the combined neocuproine and *loxl5b* studies. Persistent *col2a1* expression was observed within the notochord vacuolar cells at 24 hpf under these conditions (S. Fig. 4), similar to what is observed in neocuproine-treated embryos incubated with anesthetic to prevent notochord distortion (59). These data are consistent with a feedback mechanism originating from the products of the crosslinking process.

The *col2a1* expression data suggest a model where lysyl oxidase inhibition affects the final stages of notochord development at a time when the extracellular matrix

components, including collagen II, are already in place in the notochord sheath. The notochord sheath in zebrafish is composed of three distinct layers: an internal basal lamina, a middle fibrillar layer, and an external granular layer (Fig. 8A) (16, 60). Inspection of the notochord sheath by electron microscopy revealed that inhibition of lysyl oxidase activity by neocuproine, β-aminopropionitrile, or combined *loxl1* and *loxl5b* knockdown was without effect on these layers (Fig. 8B-D). This observation is consistent with the idea that lysyl oxidase inhibition alters the final stages of notochord sheath formation.

Discussion

These studies reveal an essential role for two specific lysyl oxidase genes, *loxl1* and *loxl5b*, in notochord formation, and demonstrate a complex interplay of gene expression and nutrient availability that is relevant to the pathogenesis of human structural birth defects (Fig. 9A,B). A role for lysyl oxidases in notochord formation was hypothesized from previous work using small molecules (14, 32), and our current data establish a genetic basis for this pharmacologic notochord distortion. Various lysyl oxidases have been implicated in tumor metastasis, wound healing, cardiac fibrosis and elastin fiber homeostasis (50, 54, 61, 62). However, the precise function of individual lysyl oxidase family members in development has been difficult to discern given the lack of inhibitors unique to any given enzyme. This study is the first to demonstrate that genetic deficiency of specific lysyl oxidases results in notochord distortion, and elucidates a specific and novel interaction between gene function (lysyl oxidases) and nutrition (copper) during development. While it is logical that copper-dependent enzymes such as lysyl oxidases would be inactive in the complete absence of copper, it is more difficult to predict the effect of mild copper deficiency on enzyme activity, and more importantly, to determine what components of the developing notochord would become essential in the setting of impaired – but not absent – lysyl oxidase function. The specific role for *loxl1* and *loxl5b* in notochord formation is supported by sensitization experiments using neocuproine (Fig. 6 and Table 3), and these genes may be candidates for late notochord mutants identified in previous forward genetic screens (17, 18) or for human disorders of the axial skeleton. Though we cannot completely rule out the possibility that the low penetrance of a

distorted notochord phenotype using splice morpholinos to *loxl2b*, *loxl3b*, or *loxl5b* alone (Table 1) results from incomplete disruption of gene expression (S. Fig. 3), combinations involving these morpholinos did not convincingly demonstrate a role for *loxl2b* or *loxl3b* in notochord formation (Table 1 and S. Table 1).

Our data also demonstrate a genetic interaction between two lysyl oxidases (*loxl1* and *loxl5b*) and the collagen substrate *col2a1* (Fig. 6). This could reflect either direct crosslinking of this collagen substrate or crosslinking of additional extracellular matrix proteins that interact with collagen II for proper notochord formation. The latter possibility has been proposed in recent morphological studies on the notochord sheath of teleosts (63) and could account for observations in coatomer I protein complex mutants (19), where defects in the secretion of lysyl oxidases or additional such extracellular matrix components would give rise to the notochord sheath abnormalities. In all cases, reduced crosslinking of collagen fibrils from impaired lysyl oxidase activity would prevent the feedback inhibition of *col2a1* produced by notochord vacuolar cells, resulting in prolonged *col2a1* expression (Fig. 7). Alternatively, persistent *col2a1* expression could result indirectly from a general loss of notochord sheath integrity.

The observed lysyl oxidase expression patterns and phenotypes (Fig. 3, Fig. 4, Fig. 5 and data not shown) suggest that the zebrafish will be a useful model organism for elucidating the complex and specific roles of lysyl oxidases in development. In addition, the phylogenetic analysis (Fig. 2B) may prove helpful. The lack of a zebrafish orthologue to *LOXL4* is consistent with a BLAST search revealing such orthologues only in mammals (data not shown), and the markedly different expression patterns of this gene in

human and mouse (64-66) may indicate that it has divergent, specialized roles in these organisms. Moreover, it is now apparent that scavenger receptor, cysteine-rich domains are a more variable feature of lysyl oxidase structure than previously anticipated. LOXL2, LOXL3, and LOXL4 are considered related because they all possess four scavenger receptor, cysteine-rich domains, which are completely absent in LOX and LOXL1. However, zebrafish *loxl3a* and *loxl3b* encode only a single scavenger receptor, cysteine-rich domain that is truncated (Fig. 2A), as does a *Xenopus* clone of *loxl3* previously assumed to be partial (S. Fig. 2C) (32). While the function of these domains remains unknown, a splice variant of *LOXL3* that excludes some scavenger-receptor, cysteine-rich domains has recently been described, and appears to have altered substrate specificity (67).

Definitive demonstration of a role for specific lysyl oxidases in notochord formation is of direct relevance to embryonic environmental exposures to nitrile compounds in plasticizers and carbamates in pesticides. Recent toxicological studies demonstrate that such pesticides induce notochord distortion in developing zebrafish embryos (59, 68) as well as persistent expression of *col2a1* by vacuolar cells of the notochord (59). These findings are identical to our observations with *loxl1*, *loxl5b*, and *col2a1* morpholino knockdown combined with neocuproine treatment (Fig. 5B,F, Fig. 6 and Fig. 7), suggesting that the pesticides act through direct or indirect inhibition of these lysyl oxidase family members. Importantly, these data raise the distinct possibility that embryonic exposure to such toxins in specific genetic contexts may predispose to the later development of structural birth defects (Fig. 9B), where the inheritance of this

genetic variation would not be reflected in Mendelian ratios of the observable phenotypes.

The notochord is a critical structure required for vertebral column patterning in vertebrates (69) and its distortion in zebrafish phenotypically mimics a number of axial skeletal defects in humans including idiopathic scoliosis. Of note, while β-aminopropionitrile causes notochord distortion in zebrafish (Fig. 1B and S. Fig. 1), it is also well known to cause scoliosis in rats and other mammals (70). Interestingly, disruptions in extracellular matrix components involved in notochord formation have been identified in clinical syndromes that include scoliosis. Two different mutations in exon 48 of the *COL2A1* gene cause spondyloepiphyseal dysplasia with scoliosis in humans (71, 72). Furthermore, the kyphoscoliosis type of Ehler-Danlos syndrome (EDS VI) (73) results from loss of function mutations in the gene encoding lysyl hydroxylase type 1, which catalyzes the conversion of lysine to hydroxylysine in collagen prior to oxidization by lysyl oxidases. Taken together with the nutritional (copper) and toxicology findings noted above, these data raise the intriguing possibility that polymorphisms at multiple extracellular matrix component loci, including the lysyl oxidase genes identified here, may predispose to axial skeletal malformations in situations where nutrition or environment might otherwise be considered adequate (Fig. 9B). This concept is supported by our previous findings revealing a hierarchy of nutrient distribution to the developing embryo under limiting conditions (14) and as such is of broad relevance to our understanding of the pathogenesis of structural birth defects. The data reported here provide a testable model for these ideas with regards to common defects of the axial

skeleton and reveal that zebrafish permit unique insights into the complex interplay of genes, environment and nutrition in development and disease.

Acknowledgments

We thank Robert Mecham and Erik Madsen for critical review of the manuscript and Marilyn Levy for the electron microscopy. J.M.G and B.A.M. were supported by NIH Medical Scientist Training Program grant T32 GM07200. This work was supported by NIH grants GM56988 (S.L.J.), HD39952 (J.D.G.), DK61763 (J.D.G.), and DK44464 (J.D.G.).

Figure legends

Fig. 1. β-aminopropionitrile recapitulates the notochord phenotype of copper deficiency. Wild-type embryos were incubated in vehicle (A), 10 μM neocuproine (B), or 10 mM β-aminopropionitrile supplemented with 10 μM $CuCl_2$ (C). At 48 hpf, the notochord (arrowheads) is distorted in embryos treated with neocuproine (B) and β-aminopropionitrile (C); however, melanocytes (arrows) are present after β-aminopropionitrile (C) but not neocuproine treatment (B), demonstrating that β-aminopropionitrile does not act through copper chelation.

Fig. 2. Lysyl oxidase family members in zebrafish. (A) The zebrafish genome encodes eight distinct lysyl oxidases, all of which contain a conserved copper binding domain depicted in yellow. Scavenger receptor, cysteine-rich domains (SRCR) of unknown function are in blue and are truncated in Loxl3a and Loxl3b (SR with strikethrough). (B) Phylogenetic tree depicting the evolutionary relationship between human and zebrafish lysyl oxidases. HsCD163 is used as an outgroup, and bootstrap values over 100 replicates are noted. Loxl5a and Loxl5b (green) represent new additions to the lysyl oxidase family that closely resemble LOX and LOXL1 in structure. Zebrafish encode orthologues to all human lysyl oxidase genes except LOXL4.

Fig. 3. Four lysyl oxidases are expressed throughout the developing zebrafish notochord by in situ hybridization. (A-D) *loxl1*; (E-H) *loxl2b*; (I-L) *loxl3b*; and (M-P) *loxl5b*. Stages of development are 5 somites (A,E,I,M); 10 somites (B,F,J,N); 15 somites (C,G,K,O); and 20 somites (D,H,L,P). *loxl1* and *loxl5b* are robustly expressed at the

caudal notochord tip (arrowheads) while *loxl5b* is also expressed anterior to the notochord (asterix).

Fig. 4. Lysyl oxidases are expressed by notochord vacuolar cells. (A-D) Frozen cross-sections of 15 somite embryos were obtained after in situ hybridization with the following probes: (A) *loxl1*; (B) *loxl2b*; (C) *loxl3b*; and (D) *loxl5b*. The notochord is indicated (arrowheads). Hypochord staining of *loxl1* (arrows) suggests a role for this family member in extracellular matrix crosslinking near the developing aorta. (E) Cartoon demonstrating the location of the hypochord (h) and floorplate (f), which are closely apposed to the notochord (n). Lysyl oxidases are not expressed in the floorplate.

Fig. 5. Morpholino knockdown of *loxl1* or *loxl1* and *loxl5b* together results in notochord distortion. Wild-type embryos were injected with morpholinos (MO) to notochord-expressed lysyl oxidases and photographed at 24 hpf. (A) 12 ng standard control; (B) 6 ng *loxl1*; (C) 3.7 ng *loxl2b*; (D) 12 ng *loxl3b*; (E) 7.4 ng *loxl5b*; (F) 2.4 ng *loxl1* and 5 ng *loxl5b*. The notochord (arrowheads) is strikingly distorted after knockdown of *loxl1* (B), and caudal vein edema develops with the *loxl5b* morpholino (E, arrows). Combining doses of *loxl1* and *loxl5b* morpholino that do not cause notochord distortion alone also recapitulates the notochord phenotype seen with neocuproine and β-aminopropionitrile treatment (F). This distortion is specifically rescued by co-injection of mRNA encoding either *loxl1* (H) or *loxl5b* (I), but not control sequence (G).

Fig. 6. Partial knockdown of *loxl5b* sensitizes embryos to notochord distortion in the presence of suboptimal copper nutrition (A-D) or disruption of *col2a1* (E,F). Wild-type embryos were injected with 5 ng of control morpholino (A,C) or *loxl5b* morpholino

(B,D), and incubated with (C,D) or without (A,B) 2 μM neocuproine starting at 3 hpf. Embryos injected with *loxl5b* morpholino develop notochord distortion (arrowhead) in the context of diminished copper availability (D). Embryos injected with 7.4 ng of *col2a1* morpholino (E) are sensitized to develop notochord distortion (arrowhead) upon co-injection of 5 ng of *loxl5b* morpholino (F), demonstrating a genetic interaction between *col2a1* and *loxl5b*. Photographs were obtained at 30 hpf (A-D) and 24 hpf (E,F).

Fig. 7. Expression of *col2a1* mRNA by notochord vacuolar cells persists late following lysyl oxidase inhibition. Wild-type embryos were injected with 7.4 ng control morpholino (A), incubated in 10 μM neocuproine (B), incubated in 10 mM β-aminopropionitrile supplemented with 10 μM $CuCl_2$ (C), or injected with 3.7 ng each of *loxl1* and *loxl5b* morpholino (D). In situ hybridization was carried out at 24 hpf, and frozen sections confirmed persistent *col2a1* expression following lysyl oxidase inhibition (B-D, arrowhead), as well as floorplate and hypochord staining (A-D, arrows).

Fig. 8. Electron micrographs of the notochord sheath from cross-sections of 30 hpf embryos: (A) 7.4 ng control morpholino; (B) 10 μM neocuproine; (C) 10 mM β-aminopropionitrile; (D) 3.7 ng each of *loxl1* and *loxl5b* morpholino. Sheath components include a basal lamina (I), fibrillar layer (II), and granular layer (III). All three layers are preserved after lysyl oxidase inhibition.

Fig. 9. Model of pathways involved in notochord formation. (A) The cuproenzymes Loxl1 and Loxl5b crosslink collagen II in the notochord sheath, which suppresses vacuolar cell expression of *col2a1* as the notochord differentiates. (B) Polymorphisms at multiple genetic loci interact with environmental factors to cause disease. As a result,

what is normally considered adequate nutrition may in fact be suboptimal during a specific developmental window. The gene *atp7a* encodes a transporter required for copper uptake (14).

Table 1. *loxl1* is necessary for notochord formation in developing zebrafish embryos, and overlaps in function with *loxl5b*. Wild-type embryos were injected with morpholinos to notochord-expressed lysyl oxidases and examined at 24 hpf. The number and percentage of embryos with and without a distorted notochord phenotype is noted. Injection of 6 ng of *loxl1* splice morpholino causes notochord distortion in 88% of embryos, an effect not seen with morpholinos to *loxl2b*, *loxl3b*, or *loxl5b* alone. However, injection of 2.4 ng of *loxl1* morpholino and 5 ng of *loxl5b* morpholino together causes notochord distortion in 94% of embryos, demonstrating that *loxl1* and *loxl5b* have overlapping roles in notochord formation. This finding was recapitulated in separate experiments with start site (ATG) morpholinos to *loxl1* and *loxl5b*. The number of embryos examined includes dead embryos that could not be scored for notochord phenotype; the *loxl2b* morpholino causes significant embryo death at higher doses. Data shown are the pooled results of three independent experiments.

Table 2. The distorted notochord phenotype resulting from combined *loxl1* and *loxl5b* knockdown is specific and can be rescued by co-injection of mRNA encoding either *loxl1* or *loxl5b*. Wild-type embryos injected with control or *loxl1* and *loxl5b* morpholinos together were co-injected with control or lysyl oxidase mRNA, as indicated. The number and percentage of embryos with and without a distorted notochord phenotype at 24 hpf is noted, as well as the percentage rescue attributable to each mRNA.

Exogenously-supplied *loxl1* or *loxl5b* mRNA produces a marked improvement in notochord morphology, substantially decreasing the proportion of embryos with notochord distortion. Injection of lysyl oxidase mRNA alone did not result in any overexpression phenotype. The number of embryos examined includes dead embryos that could not be scored for notochord phenotype. Data shown are the pooled results of three independent experiments.

Table 3. Partial knockdown of *loxl1* or *loxl5b* sensitizes embryos to notochord distortion in the presence of suboptimal copper nutrition. Wild-type embryos were injected with control or lysyl oxidase-specific morpholino, as indicated, and incubated with or without neocuproine at doses that were determined not to cause notochord distortion alone. Embryos injected with lysyl oxidase-specific morpholino and incubated in 2 μM neocuproine were sensitized to develop notochord distortion. The number of embryos examined includes dead embryos that could not be scored for notochord phenotype. Each result is pooled from three independent experiments, which were scored at 24 hpf.

Table 4. Genetic interaction of *loxl1* and *loxl5b* with *col2a1*. Wild-type embryos were injected with the indicated morpholino combinations and scored for notochord distortion at 24 hpf. Partial knockdown of *loxl1* and *col2a1* together, but not alone, causes the distorted notochord phenotype. An identical result is obtained with morpholinos to *loxl5b* and *col2a1*, suggesting that diminished activity of these lysyl oxidases sensitizes embryos to notochord distortion in the presence of *col2a1* disruption. Importantly, collagen II is a lysyl oxidase substrate produced by the notochord vacuolar cells and present in the

notochord sheath. The number of embryos examined includes dead embryos that could not be scored for notochord phenotype. Each result is pooled from three independent experiments.

S. Fig. 1. Comparison of the notochord distortion obtained in zebrafish using three distinct methods of lysyl oxidase inhibition at 24 hpf. Wild-type embryos were incubated in 10 μM neocuproine (A), 10 mM β-aminopropionitrile supplemented with 10 μM $CuCl_2$ (B), 100 mM β-aminopropionitrile supplemented with 10 μM $CuCl_2$ (C), or injected with 6 ng each of *loxl1* and *loxl5b* start (ATG) morpholino (D). 10 μM neocuproine (A) causes greater notochord distortion than 10 mM β-aminopropionitrile (B), but an identical phenotype is obtained with 100 mM β-aminopropionitrile (A vs. C). Melanin pigmentation has not yet developed in the embryos pictured, but is not affected by β-aminopropionitrile treatment or by the morpholino injection.

S. Fig. 2. Protein sequence alignment of zebrafish lysyl oxidase family members with human orthologues. (A) *lox*, *loxl1*, *loxl5a*, and *loxl5b*; (B) *loxl2*a and *loxl2b*; (C) *loxl3*a and *loxl3b* with *Xenopus laevis* clone XL051k10 included for comparison. A number of conserved elements are indicated including predicted signal peptides (bold, underlined), BMP-1 cleavage sequences (bold, italicized), scavenger receptor cysteine-rich domains (gray, underlined), copper binding domains (gray), and lysyl-tyrosyl quinone cofactor residues (bold).

S. Fig. 3. Lysyl oxidase and collagen II splice morpholinos decrease the abundance of wild-type splice forms and cause specific changes in splice site usage. (A) *loxl1* (B) *loxl2b* (C) *loxl3b* (D) *loxl5b* and (E) *col2a1*. Wild-type embryos injected with the

indicated doses of morpholino were harvested at 20 hpf and cDNA prepared from equal amounts of RNA. The intensity of the wild-type (WT) product obtained by PCR was quantified and the percentage of wild-type splice form remaining after morpholino knockdown determined, as noted. This measure is independent of processes that may depress levels of the mutant (Mut) splice products, including degradation through nonsense-mediated decay. The primer set used to amplify *loxl1* does not amplify the mutant band.

S. Fig. 4. Persistent expression of *col2a1* by notochord vacuolar cells after lysyl oxidase inhibition is not due to mechanical distortion of the notochord. Wild-type embryos incubated with (B) or without (A) 2 μM neocuproine were probed for *col2a1* expression at 24 hpf. *col2a1* expression persists in the notochord vacuolar cells after treatment with 2 μM neocuproine, which affects crosslinking but does not cause mechanical distortion. This suggests that the signal to downregulate *col2a1* expression in the vacuolar cells of the notochord originates from the products of the crosslinking reaction.

S. Table 1. Morpholinos to combinations of lysyl oxidase family members other than *loxl1* and *loxl5b* do not result in notochord distortion. Wild-type embryos were injected with the indicated morpholino doses and examined at 24 hpf for notochord distortion. The number of embryos examined includes dead embryos that could not be scored for notochord phenotype. Each result is pooled from three independent experiments.

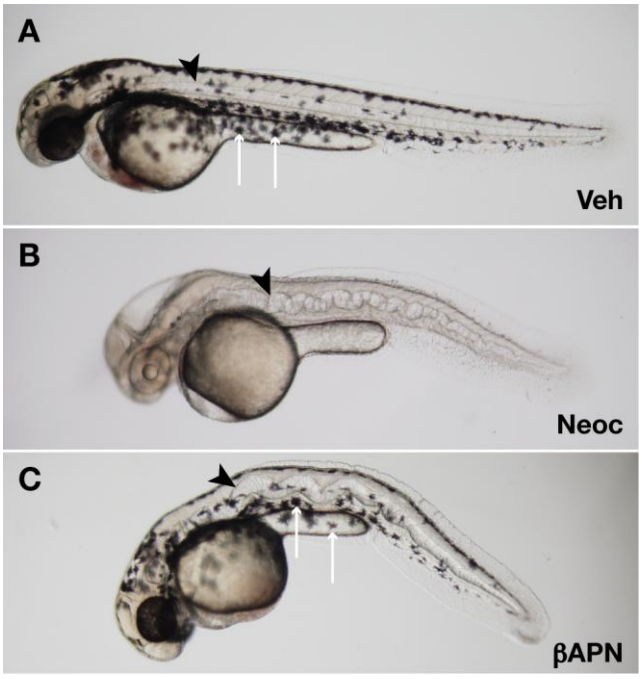

Figure 1

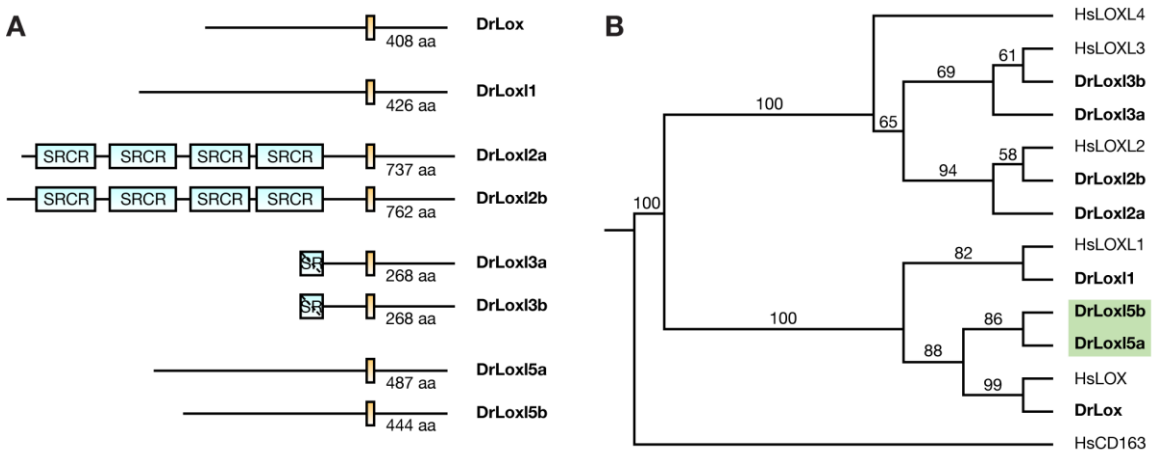
A
DrLox
408 aa
DrLoxl1
426 aa
SRCR
SRCR
SRCR
SRCR
DrLoxl2a
737 aa
DrLoxl2b
762 aa
DrLoxl3a
268 aa
DrLoxl3b
268 aa
DrLoxl5a
487 aa
DrLoxl5b
444 aa
B
HsLOXL4
HsLOXL3
DrLoxl3b
DrLoxl3a
HsLOXL2
DrLoxl2b
DrLoxl2a
HsLOXL1
DrLoxl1
DrLoxl5b
DrLoxl5a
HsLOX
DrLox
HsCD163
100
61
69
65
100
58
94
100
82
86
100
88
99

Figure 2

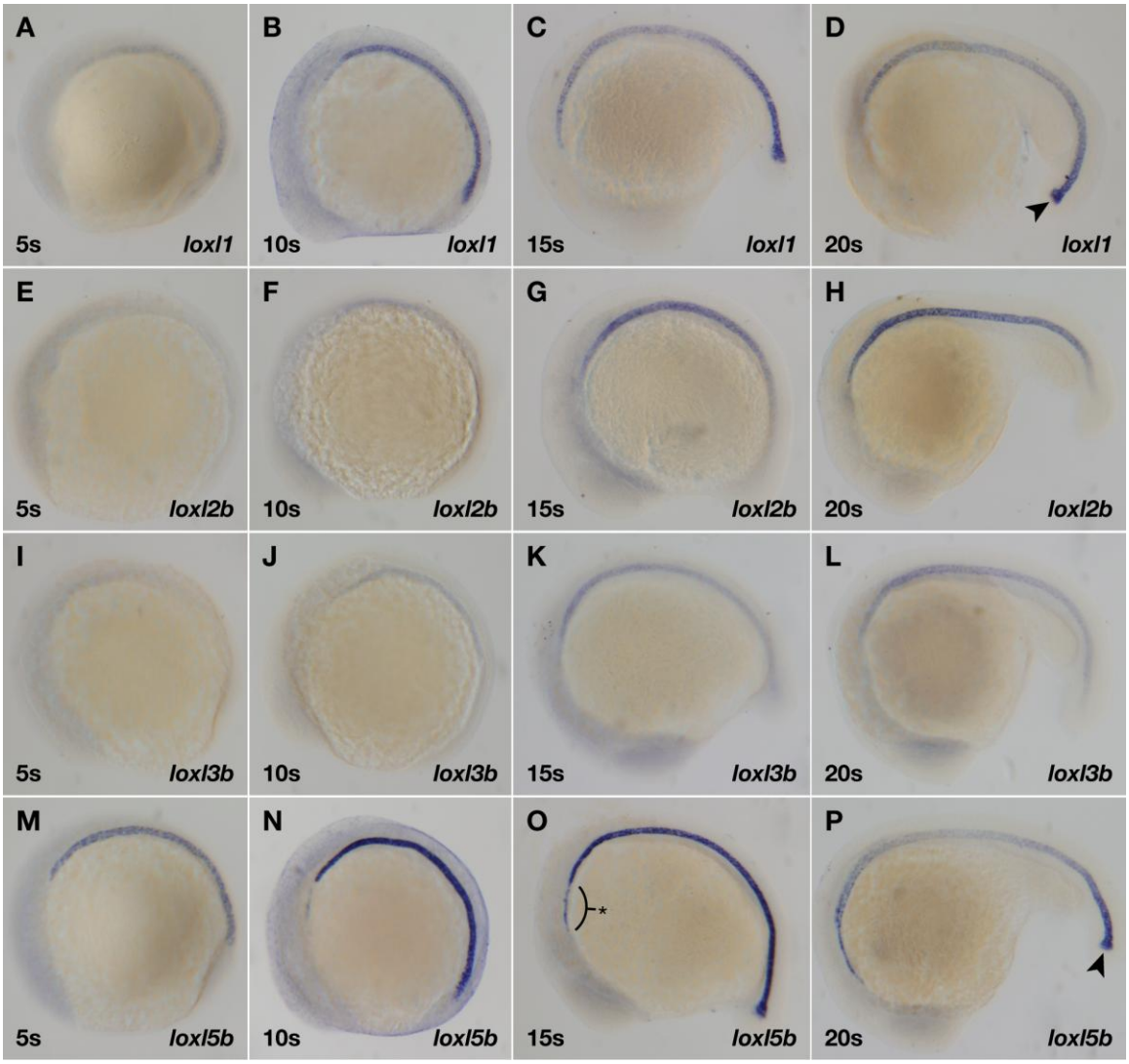
A
5s
loxl1
B
10s
loxl1
C
15s
loxl1
D
20s
loxl1
E
5s
loxl2b
F
10s
loxl2b
G
15s
loxl2b
H
20s
loxl2b
I
5s
loxl3b
J
10s
loxl3b
K
15s
loxl3b
L
20s
loxl3b
M
5s
loxl5b
N
10s
loxl5b
O
15s
loxl5b
P
20s
loxl5b

Figure 3

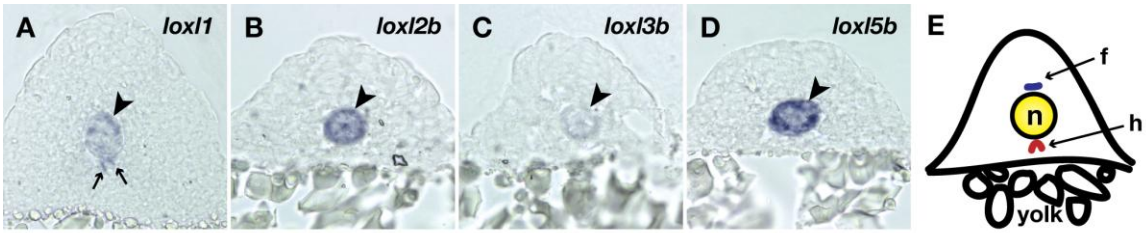

Figure 4

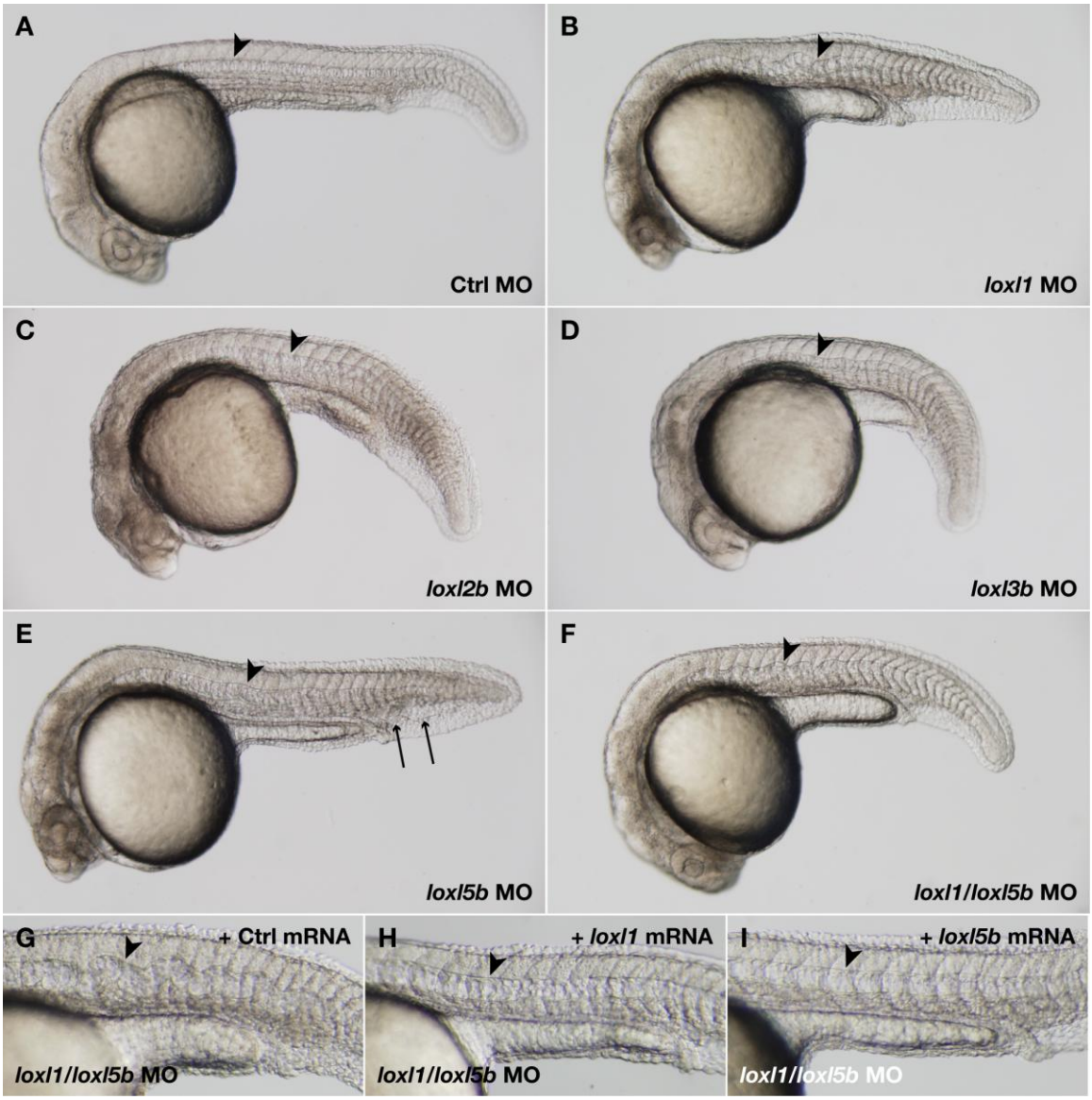
A
Ctrl MO
B
loxl1 MO
C
loxl2b MO
D
loxl3b MO
E
loxl5b MO
F
loxl1/loxl5b MO
G
+ Ctrl mRNA
loxl1/loxl5b MO
H
+ loxl1 mRNA
loxl1/loxl5b MO
I
+ loxl5b mRNA
loxl1/loxl5b MO

Figure 5

Specific Morpholino	Dose of morpholino (ng)	# of embryos examined	Phenotype of notochord distortion -	+
Ctrl	12	302	278 (**100%**)	0 (**0%**)
loxl1	6	271	30 (**12%**)	217 (**88%***)
loxl2b	2.4	212	122 (**98%**)	3 (**2%**)
loxl3b	12	190	128 (**96%**)	6 (**4%**)
loxl5b	5	263	237 (**98%**)	6 (**2%**)
loxl1	2.4	297	272 (**99%**)	2 (**1%**)
loxl1/loxl5b	2.4/5	292	17 (**6%**)	254 (**94%***)
Ctrl	12	173	138 (**100%**)	0 (**0%**)
***loxl1* ATG**	12	158	145 (**100%**)	0 (**0%**)
***loxl5b* ATG**	12	159	140 (**92%**)	12 (**8%**)
***loxl1* ATG/*loxl5b* ATG**	6/6	188	33 (**19%**)	145 (**81%***)

*$p < 0.01$ versus controls by ANOVA

Table 1

Specific Morpholino	**Dose of morpholino (ng)**	**Specific mRNA**	**# of embryos examined**	**Phenotype of notochord distortion**		**Rescue of notochord phenotype**
				-	**+**	
Ctrl	7.4	Ctrl	240	226 (**100%**)	0 (**0%**)	**NA**
loxl1/loxl5b	2.4/5	Ctrl	223	8 (**4%**)	195 (**96%**)	**NA**
loxl1/loxl5b	2.4/5	*loxl1*	238	137 (**63%**)	80 (**37%***)	**62%**
loxl1/loxl5b	2.4/5	*loxl5b*	251	197 (**86%**)	33 (**14%***)	**85%**

*$p < 0.01$ versus *loxl1*/*loxl5b* MO with Ctrl mRNA by ANOVA

Table 2

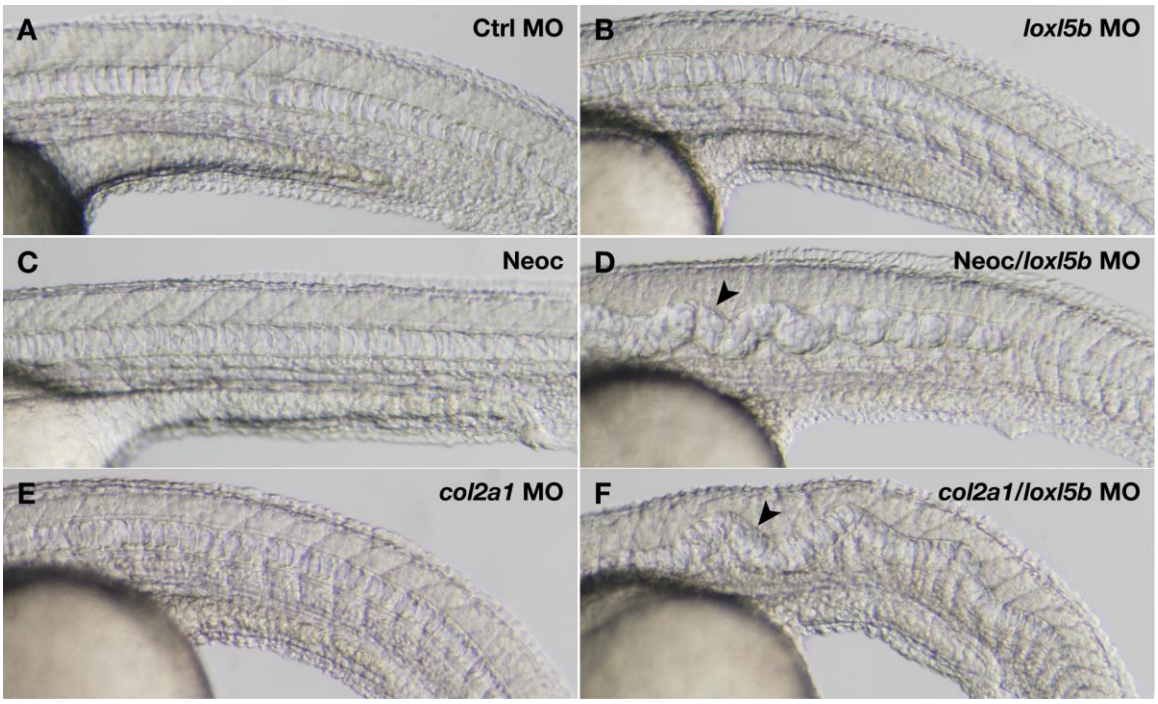
A
Ctrl MO
B
loxl5b MO
C
Neoc
D
Neoc/loxl5b MO
E
col2a1 MO
F
col2a1/loxl5b MO

Figure 6

Specific Morpholino	**Dose of morpholino (ng)**	**Pharmacologic treatment**	**# of embryos examined**	**Phenotype of notochord distortion**	
				-	**+**
Ctrl	2.4	None	104	104 (**100%**)	0 (**0%**)
Ctrl	2.4	2 μM neocuproine	113	111 (**98%**)	2 (**2%**)
loxl1	2.4	None	143	127 (**100%**)	0 (**0%**)
loxl1	2.4	2 μM neocuproine	132	49 (**39%**)	77 (**61%***)
Ctrl	5	None	139	136 (**100%**)	0 (**0%**)
Ctrl	5	2 μM neocuproine	138	132 (**99%**)	2 (**1%**)
loxl5b	5	None	147	126 (**95%**)	7 (**5%**)
loxl5b	5	2 μM neocuproine	147	1 (**1%**)	140 (**99%***)

*$p < 0.01$ versus controls by ANOVA

Table 3

Specific Morpholino	**Dose of morpholino (ng)**	**# of embryos examined**	**Phenotype of notochord distortion**	
			-	**+**
***loxl1*/ctrl**	2.4 /7.4	202	146 (**99%**)	1 (**1%**)
***col2a1*/ctrl**	7.4 /2.4	206	161 (**98%**)	4 (**2%**)
col2a1*/*loxl1	7.4/2.4	258	118 (**58%**)	84 (**42%***)
***loxl5b*/ctrl**	5/7.4	151	137 (**93%**)	10 (**7%**)
***col2a1*/ctrl**	7.4/5	122	116 (**99%**)	1 (**1%**)
col2a1*/*loxl5b	7.4/5	217	111 (**54%**)	96 (**46%***)

*$p < 0.01$ versus controls by ANOVA

Table 4

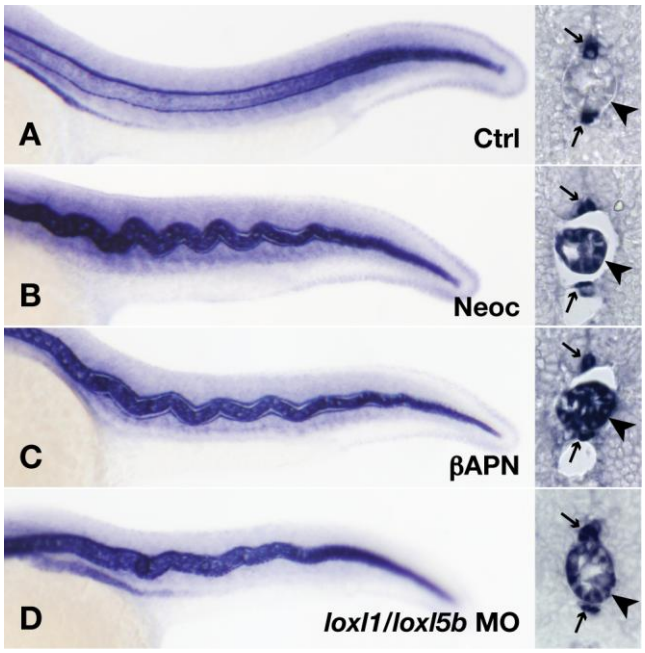

Figure 7

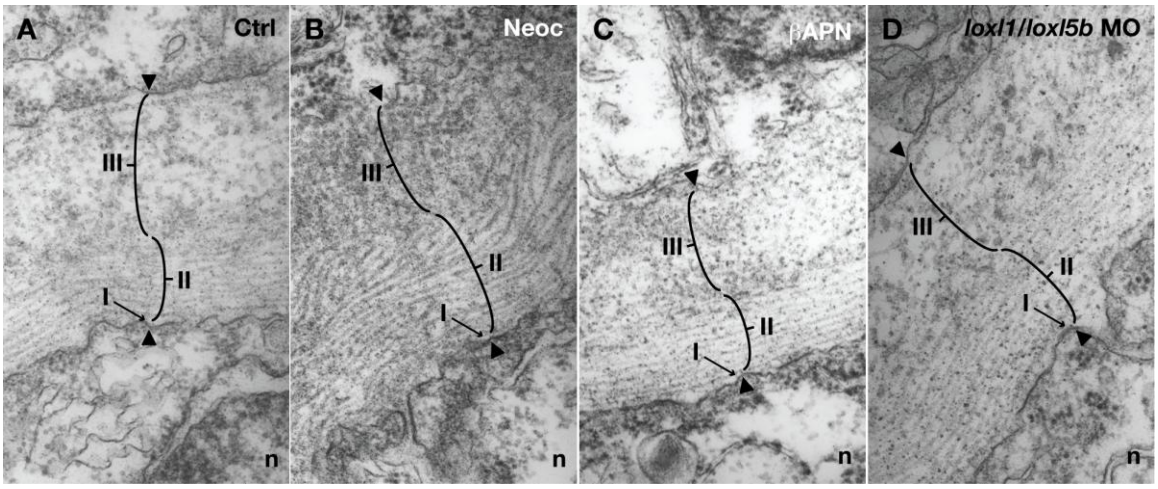

Figure 8

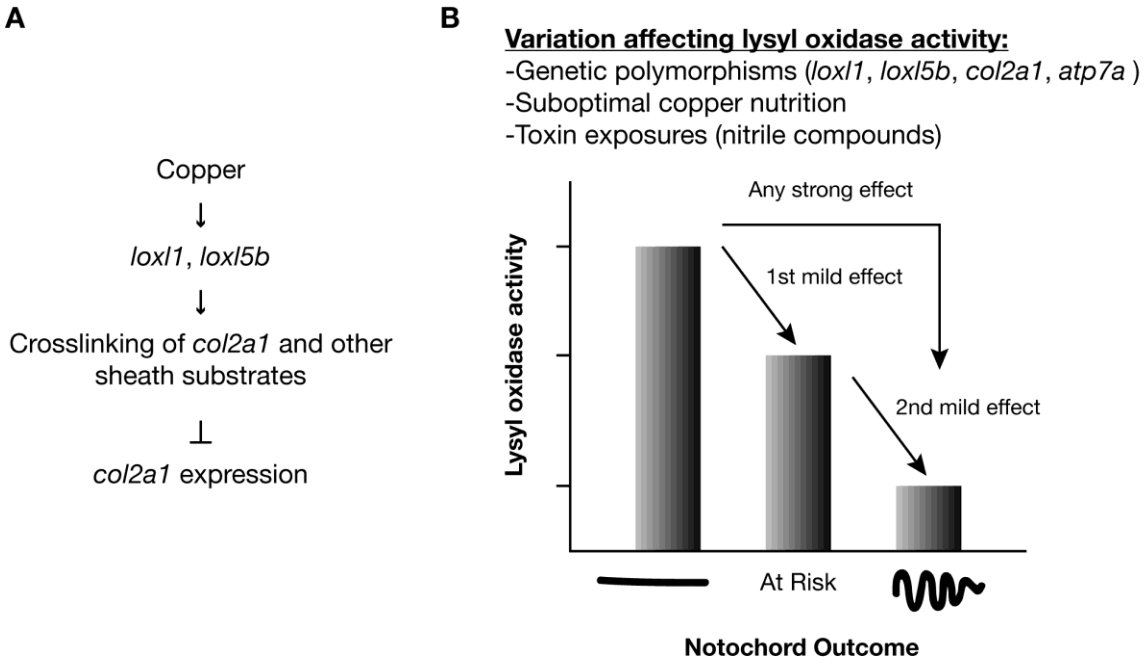
A
Copper
↓
loxl1, loxl5b
↓
Crosslinking of col2a1 and other sheath substrates
⊥
col2a1 expression
B
Variation affecting lysyl oxidase activity:
-Genetic polymorphisms (loxl1, loxl5b, col2a1, atp7a)
-Suboptimal copper nutrition
-Toxin exposures (nitrile compounds)
Any strong effect
1st mild effect
2nd mild effect
Lysyl oxidase activity
At Risk
Notochord Outcome

Figure 9

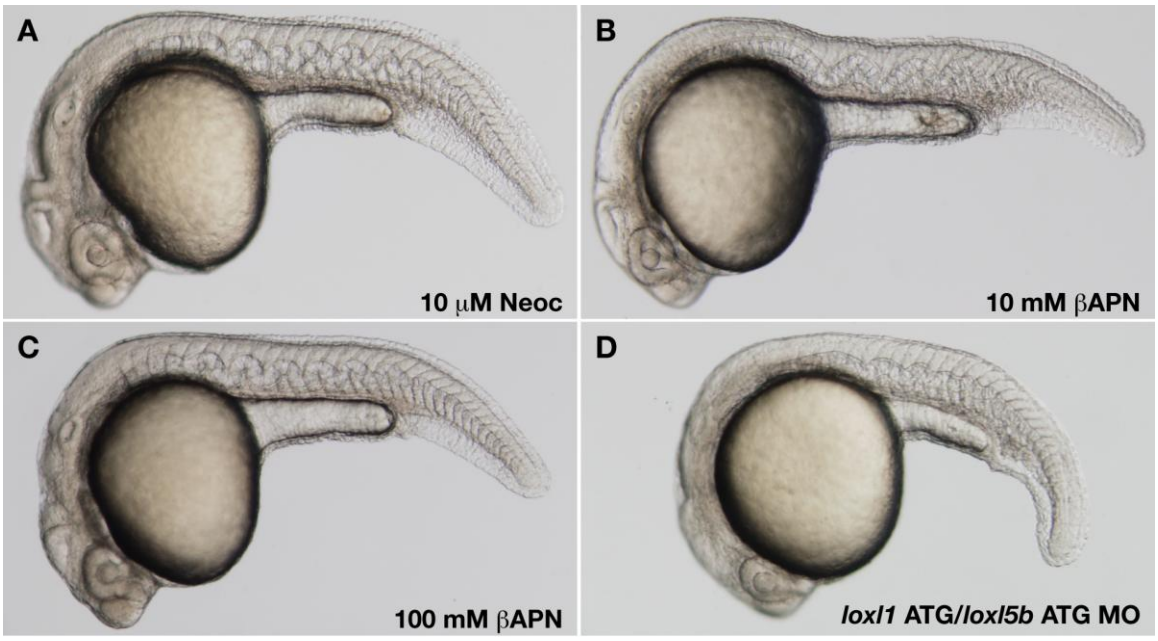

Supplementary Figure 1

A

```
HsLOX          MRFAWTVLLLGPLQLCALVHCAPPAAGQQQPPREPPAAPGAWRQQIQWENNGQVFSLLSL 60
DrLox          MSMSLIDTFIYAFAHVCLLSCIAQTG---QTQRQGNTGAAALRQTIQWQHNGKLFSILSQ 57
HsLOXL1        MALARGSRQLGALVWGACLCVLVHGQ---QAQPGQGSDPARWRQLIQWENNGQVYSLLNS 57
DrLoxl1        --------MLHVLLMSLWVLGSVTGQ---SQS--QPDDTNPWRQMIQWENNGRVYSLLNS 47
DrLoxl5a       --MTKYSFIFCLSIHLCVLVFLNTAQ-----------NHGAWQHKVKWETNGQVYSLLSA 47
DrLoxl5b       MFFTISNFIFFLYL-LQGLNNLTSAQ-----------SSAQWRNRVRWVNNGQVFSLMST 48
                         :       :                    :: ::*  **:::*::.

HsLOX          GSQYQPQ--RRRDP----------GAAVPGAANASAQQPRTPILLIRDNRTA------AA 102
DrLox          GSEYQPP--LKRD-----------GNKEQAQARPVAIVRNDDAATRTDSSAP------SR 98
HsLOXL1        GSEYVPAGPQRSES----------SSRVLLAGAPQAQQRRSHGSPRRRQAPSLPLPGRVG 107
DrLoxl1        GAEYVPARNQERDR----------NHRVLLADAP---NRRSQGGNVRRQAPS-----RGS 89
DrLoxl5a       SSQYHAPASGKQHARFLLRRQIIPSFTGRIFMGQFAKTRMHTAGHVVRSSPVPGHIGLNA 107
DrLoxl5b       GSEFHAPVPSRRQSRVYQ------SSRTDAVPGRSMQIRLEAMDRPANSAPDSALLGPDR 102
               .::: .    . .          .                       . .

HsLOX          RTRTAGSSGVTAGR-PRPTARHWFQAGYSTSRARERGASRAENQTAPGEVPALSNLRPPS 161
DrLox          ASQSRGSVRVPSGTGARGGASRWLSG----DGARTRGVHGRRNHTDP-LRSINGTDRPAG 153
HsLOXL1        SDTVRGQARHPFGFGQVPDNWREVAVGDSTGMARARTSVSQQRHGG--SASSVSASAFAS 165
DrLoxl1        SETVRGQARHPFGFGQVPENWRQQQG----AVGRSETSRFQSQTGSRYRPSSGASSSASS 145
DrLoxl5a       KHMISGHIRNNNQLPLHAKKVAFSSD----ETLRTQTWPYRTSPTGTTTHGPVKNSEISR 163
DrLoxl5b       AQYIMANSRAPGARQMQVMQRHRAPP----ASRNNSTVPSEYSGGGGRTG------ENTR 152
                    .                          .                      .

HsLOX          RV-------------------------------------------DGMVG--------- 168
DrLox          DD-------------------------------------------EVMVG--------- 160
HsLOXL1        TYRQQPSYPQQFPYPQAPFVSQYENYDPASRTYDQGFV---YYRPAGGGVGAGAAAVASA 222
DrLoxl1        SYPQYP-IPQ-----QPPFGAPYDQVS--DRSYEPPFLGTGYSAGTGGGFGGGSYGGYST 197
DrLoxl5a       APKQHK-------------------------------------ITSQPVAKQPSPATGK 185
DrLoxl5b       R------------------------------------------GQAVAN-------- 159
                                                          ..

HsLOX          ------------------------------------------------DDPYNPYKYSD- 179
DrLox          ------------------------------------------------DDPYNPYKSTDP 172
HsLOXL1        GVIYPYQPRARYEEYGGGEELPEYPPQGFYPAPERPYVPPPPPPPDGLDRRYSHSLYSEG 282
DrLoxl1        GSFGGGNP-ANDDRYR------FYPPFG-QQYQAVPAQPAQPPFSDGLDHRYTHSLFNED 249
DrLoxl5a       PPTPEEKQHAKPQPIS-----------NATNKSKLSPSLDAPSASGNVRNVRNPLVQVEA 234
DrLoxl5b       -----FQQIAAPTDNS-----------NTVN-------------SDNENEARTPNVPAEQ 190
                                                          .     :

HsLOX          --------------------DNPYYNYYDTYERPRP------------------------ 195
DrLox          --------------------DNPYYNYYDTYERPRP------------------------ 188
HsLOXL1        TPGFEQAYPDPGPEAAQAHGGDPRLGWYPPYANPPPEAYGPPRALEPPYLPVRSSDTPPP 342
DrLoxl1        NPAVPNGASSNTGSSFQPAVQSPQYEQFPPYGRPQP---------QPPFLQPAPRNPLVS 300
DrLoxl5a       RG-GESMIDDEPTN--HQANRNSFYNLLPYGNTNRS------------------------ 267
DrLoxl5b       GATSETMPGDDPRN--RNT---VFYNIYPPGGRTII------------------------ 221


HsLOX          ------GGRYRPGYGTGYFQYG----LPDLVADPYYIQASTYVQKMSMYNLRCAAEENCL 245
DrLox          ------AQ--RPGYGTGYFQNG----LPDLVGDPYYIQASTYVQRVPMYNLRCAAEENCL 236
HsLOXL1        GGERNGAQQGRLSVGSVYRPNQNGRGLPDLVPDPNYVQASTYVQRAHLYSLRCAAEEKCL 402
DrLoxl1        ----NTAENPNINVGSVYRPQQ--RGLPDLVPDPNYVQASTYVQRAHMYSLRCAAEEKCL 354
DrLoxl5a       ----PQRE---TGHGTRYFLNG----LPDLIPDPYYIQAASYIQRVQMYTLRCAAEENCL 316
DrLoxl5b       ----PRRPPPGTGYGTRFFQNG----LPDLVPDPYSIQAGSYIQRVQMYALRCAAEENCL 273
                         . *: :        ****: **  :**.:*:*:  :* *******:**

HsLOX          ASTAYRADVRDYDHRVLLRFPQRVKNQGTSDFLPSRPRYSWEWHSCHQHYHSMDEFSHYD 305
DrLox          ASSAYRSSVRDYDMRMLLRFPQRVKNQGTSDFLPSRPRYTWEWHSCHQHYHSMDEFSHYD 296
HsLOXL1        ASTAYAPEATDYDVRVLLRFPQRVKNQGTADFLPNRPRHTWEWHSCHQHYHSMDEFSHYD 462
DrLoxl1        ASSAYNAETTDYSVRVLLRFPQRVKNQGTADFMPNRPRHTWEWHSCHQHYHSMDEFSHYD 414
DrLoxl5a       SSSAYSSSVRDLDYRVLLRFPQRVKNQGTADFLPVKPHYDWEWHSCHQHYHSMDAFSNYD 376
DrLoxl5b       ARTAYRPTVRDLDYRVLLRFPQKVRNMGTADFLPVKPRHQWEWHSCHQHYHSMDAFSHYD 333
               : :** . . * . *:******:*:* **:**:* :*:: ************** **:**
```

```
HsLOX          LLDANTQRRVAEGHKASFCLEDTSCDYGYHRRFACTAHTQGLSPGCYDTYGADIDCQWID 365
DrLox          LLDATTHRRVAEGHKASFCLEDTSCDYGYYRRYACTSHTQGLSPGCYDTYNADIDCQWID 356
HsLOXL1        LLDAATGKKVAEGHKASFCLEDSTCDFGNLKRYACTSHTQGLSPGCYDTYNADIDCQWID 522
DrLoxl1        LLEVSSGRKVAEGHKASFCLEDTTCDFGHLKRYACTAHTQGLSPGCFDTYNADIDCQWID 474
DrLoxl5a       LLDAATGRKVAEGHKASFCLEDTSCDPGVRRRYACTAHTQGLGPGCYDTYHANIDCQWID 436
DrLoxl5b       LLDISTGRKVAEGHKASFCLEDTGCDPGFHRRYACTAHTQGLSPGCHDTYAANIDCQWID 393
               **:  : ::************: ** *  :*:***:*****.***.*** *:*******

HsLOX          ITDVKPGNYILKVSVNPSYLVPESDYTNNVVRCDIRYTGHHAYASGCTISPY 417
DrLox          ITDVKPGNYILKVSVNPSYQVPESDYSNNVVRCDVRYTGNYAYVSGCHISQY 408
HsLOXL1        ITDVQPGNYILKVHVNPKYIVLESDFTNNVVRCNIHYTGRYVSATNCKIVQS 574
DrLoxl1        ITDVQPGNYILKLQVNPKYLVLESDFTNNIVRCNIHYTGRYAKTTNCKISQS 526
DrLoxl5a       ITDVSPGDYILKVTVNPGFQVQGSDFSNNIVRCDIRYTGLYVQTNNCRITG- 487
DrLoxl5b       ITDVPPGNYILKVTVNPDFLVAESDFSNNVVRCEVIYTGIYIQTRNCIITG- 444
               **** **:****: *** : *  **::**:***:: *** :  . .* *
```

B

```
HsLOXL2        MERPLCSHLCSCLAMLALLSPLSLAQYDSWPHYPEYFQQPAPEYHQPQAPANVAKIQLRL 60
DrLoxl2a       ------MAVSSA----LCVFGL-------LVLVQAQSELQQ------------PKIELRL 31
DrLoxl2b       -----MLALWSISFVLLCSWRLSYAQYEHLGFAIAYQEPEQDLYTPPELPADTPRIQLRL 55
                     : *          *              :              .:*:***

HsLOXL2        AGQKRKHSEGRVEVYYDGQWGTVCDDDFSIHAAHVVCRELGYVEAKSWTASSSYGKGEGP 120
DrLoxl2a       AGDKRKHYEGRLEVFYNNEWGTVCDDDFSIEAAHVACRQLGFLGAVAWSPSAKFGQGEGR 91
DrLoxl2b       AGEKRKHNEGRVEVFYEGEWGTVCDDDFTIHAAQVICRELGYFEAISWSPSSKYGKGEGR 115
               **:**** ***:**:*:.:*********:*.**:* **:**:. * :*:.*:.:*:***

HsLOXL2        IWLDNLHCTGNEATLAACTSNGWGVTDCKHTEDVGVVCSDKRIPGFKFDNSLINQIENLN 180
DrLoxl2a       IWLDNVHCTGRENSLAACPSNGFGVSDCRHSEDVGVICNQKRIPGHRFINIMNNNIETLE 151
DrLoxl2b       IWFDNVHCKGKEKSLAQCESNGIGVSDCKHSEDVGVVCSDKRIPGFKFVNTLTNNINSLN 175
               **:**:**.*.* :** * *** **:**:*:*****:*.:*****.:* * : *:*:.*:

HsLOXL2        IQVEDIRIRAILSTYRKRTPVMEGYVEVKEGKTWKQICDKHWTAKNSRVVCGMFGFPGER 240
DrLoxl2a       ERVEEIRIRPISS-HLKRIPITEGYVEVKEWGKWRQICDEEWTPLNSRVVCGMYGFPGEK 210
DrLoxl2b       IQVEDVRIRPILASYRKRIPVTEGYVEVKDGGKWKQICDDEWTQMNSRVICGMFSFPGQK 235
                :**::***.* : : ** *: *******:  .*:****..**  ****:***:.***::

HsLOXL2        TYNTKVYKMFASRRKQRYWPFSMDCTGTEAHISSCKLGPQVSLDPMKNVTCENGLPAVVS 300
DrLoxl2a       NYNNKVYRSLSMRKKKNYWGFLVNCTGNEAHMSSCRLG--KALEPKRNGTCGRGLPVVVS 268
DrLoxl2b       RYNTRVYKMFARRRKPSYWDYTINCTGKEAHLSSCTLG--HTLS---NSTCEEGTPVVVS 290
                **.:**: :: *:*  ** : ::***.***:*** **   :*.   * ** .* *.***

HsLOXL2        CVPGQVFSPDGPSRFRKAYKPEQPLVRLRGGAYIGEGRVEVLKNGEWGTVCDDKWDLVSA 360
DrLoxl2a       CVPGRAFAPSSSIGFRKAYRPEQPLVRLRGGANVGEGRVEVLKNGVWGTVCDDNWNLKAA 328
DrLoxl2b       CIPGRAFAPTPMTGYKKAFRQEQPLVRLRGGAVVGEGRVEVLKNGEWGTICDDNWNLLAA 350
               *:**:.*:*     ::**:: *********** :*********** ***:***:*:* :*

HsLOXL2        SVVCRELGFGSAKEAVTGSRLGQGIGPIHLNEIQCTGNEKSIIDCKFNA--ESQGCNHEE 418
DrLoxl2a       TVVCRELGFGSAKEALTGAKLGQGMGPVHMNEVECSGFEKSLTDCYFNN--DALGCSHEE 386
DrLoxl2b       TVVCRELGFGSAKEALSGGQLGQGMGPVHMNEVQCSGFEKSVTECSFNMEKDSEGCSHEE 410
               :***************::*.:****:**:*:**::*:* ***: :* **   :: **.***

HsLOXL2        DAGVRCNTPAMGLQKKLRLNGGRNPYEGRVEVLVERNGSLVWGMVCGQNWGIVEAMVVCR 478
DrLoxl2a       DAAVRCNVPAMGFQKRIRLSGGRNPFEGRVEVLAEKNGSLVWGTVCSENWGIIEAMVVCR 446
DrLoxl2b       DAGVKCNVPAMGFQQRLRLSGGRNPFEGRVEVLVERNGSLVWGTVCGEGWTTMEAMVVCR 470
               **.*:**.****:*:::**.*****:*******.*:******* **.:.*  :*******

HsLOXL2        QLGLGFASNAFQETWYWHGDVNSNKVVMSGVKCSGTELSLAHCRHDGEDVACPQGGVQYG 538
DrLoxl2a       QLGLGFASHAFQETWYWAGDANADNVVMSGVRCSGTEMSLPQCLHHGKHINCPKGGGRFA 506
DrLoxl2b       QLGLGFASNAFQETWYWPGAVNADAVVMSGVRCAGTEMSLSHCLHHGEYLSCPKGGGRFA 530
               ********:******** * .*:: ******:*:***:**.:* *.*: : **:** ::.

HsLOXL2        AGVACSETAPDLVLNAEMVQQTTYLEDRPMFMLQCAMEENCLSASAAQTDPTTGYRRLLR 598
DrLoxl2a       AGVSCSDTAPDLVLNAQLVEQTTYLEDRPMYALQCALEENCLSSTARKNDHSS-YRRLLR 565
DrLoxl2b       AGVSCSETAPDLVLNPQVVEQTTYLEDRPMFMLQCAYEENCLASTSSATPANS-PRRLLR 589
               ***:**:********.::*:**********: **** *****::::  .  .:  *****
```

```
HsLOXL2         FSSQIHNNGQSDFRPKNGRHAWIWHDCHRHYHSMEVFTHYDLLNLNGTKVAEGHKASFCL 658
DrLoxl2a        FSSQIHNVGQSDFRPKLGYHAWTWHECHRHYHSMEVFTHYDLLSLNGTKVAEGHKASFCL 625
DrLoxl2b        FSSQIHNNGQSDFRPKISRENWVWHDCHRHYHSMEVFTHYDLLSTNGTKVAEGHKASFCL 649
                ******* ******** . . * **:*****************. ***************

HsLOXL2         EDTECEGDIQKNYECANFGDQGITMGCWDMYRHDIDCQWVDITDVPPGDYLFQVVINPNF 718
DrLoxl2a        EDTHCDEGISKRYHCANFGEQGITVGCWDTYRHDIDCQWIDVTDVKPGDYIFQVVINPNY 685
DrLoxl2b        EDSECDEGIEKRYECANFGEQGITVGCWDTYRHDIDCQWVDITDVKPGDYIFQIVINPNY 709
                **:.*: .*.*.*.*****:****:**** *********:*:*** ****:**:*****:

HsLOXL2         EVAESDYSNNIMKCRSRYDGHRIWMYNCHIGGSFSEETEKKFEHFSGLLNNQLSPQ 774
DrLoxl2a        DVAESDYTNNVMKCKCRYDGYRIWTYSCHIGGSRSSD-MDEYS---GMSNQLNHLR 737
DrLoxl2b        EVAESDYTNNIVKCRCRYDGHRIWMYNCHIGGSFSAETEDTFP---GLINNQVTHR 762
                :******:**::**:.****:*** *.****** * :  . :    *: *:    :
```

C

```
HsLOXL3         MRPVSVWQWSPWGLLLCLLCSSCLGSPSPSTGPEKKAGSQGLRFRLAGFPRKPYEGRVEI 60
DrLoxl3a        ------------------------------------------------------------
DrLoxl3b        ------------------------------------------------------------
XlLoxl3         ------------------------------------------------------------

HsLOXL3         QRAGEWGTICDDDFTLQAAHILCRELGFTEATGWTHSAKYGPGTGRIWLDNLSCSGTEQS 120
DrLoxl3a        ------------------------------------------------------------
DrLoxl3b        ------------------------------------------------------------
XlLoxl3         ------------------------------------------------------------

HsLOXL3         VTECASRGWGNSDCTHDEDAGVICKDQRLPGFSDSNVIEVEHHLQVEEVRIRPAVGWGRR 180
DrLoxl3a        ------------------------------------------------------------
DrLoxl3b        ------------------------------------------------------------
XlLoxl3         ------------------------------------------------------------

HsLOXL3         PLPVTEGLVEVRLPDGWSQVCDKGWSAHNSHVVCGMLGFPSEKRVNAAFYRLLAQRQQHS 240
DrLoxl3a        ------------------------------------------------------------
DrLoxl3b        ------------------------------------------------------------
XlLoxl3         ------------------------------------------------------------

HsLOXL3         FGLHGVACVGTEAHLSLCSLEFYRANDTARCPGGGPAVVSCVPGPVYAASSGQKKQQQSK 300
DrLoxl3a        ------------------------------------------------------------
DrLoxl3b        ------------------------------------------------------------
XlLoxl3         ------------------------------------------------------------

HsLOXL3         PQGEARVRLKGGAHPGEGRVEVLKASTWGTVCDRKWDLHAASVVCRELGFGSAREALSGA 360
DrLoxl3a        ------------------------------------------------------------
DrLoxl3b        ------------------------------------------------------------
XlLoxl3         ------------------------------------------------------------

HsLOXL3         RMGQGMGAIHLSEVRCSGQELSLWKCPHKNITAEDCSHSQDAGVRCNLPYTGAETRIRLS 420
DrLoxl3a        ------------------------------------------------------------
DrLoxl3b        ------------------------------------------------------------
XlLoxl3         ------------------------------------------------------------

HsLOXL3         GGRSQHEGRVEVQIGGPGPLRWGLICGDDWGTLEAMVACRQLGLGYANHGLQETWYWDSG 480
DrLoxl3a        ------------------------------------------------------------
DrLoxl3b        ------------------------------------------------------------
XlLoxl3         ------------------------------------------------------------
```

Supplementary Figure 2

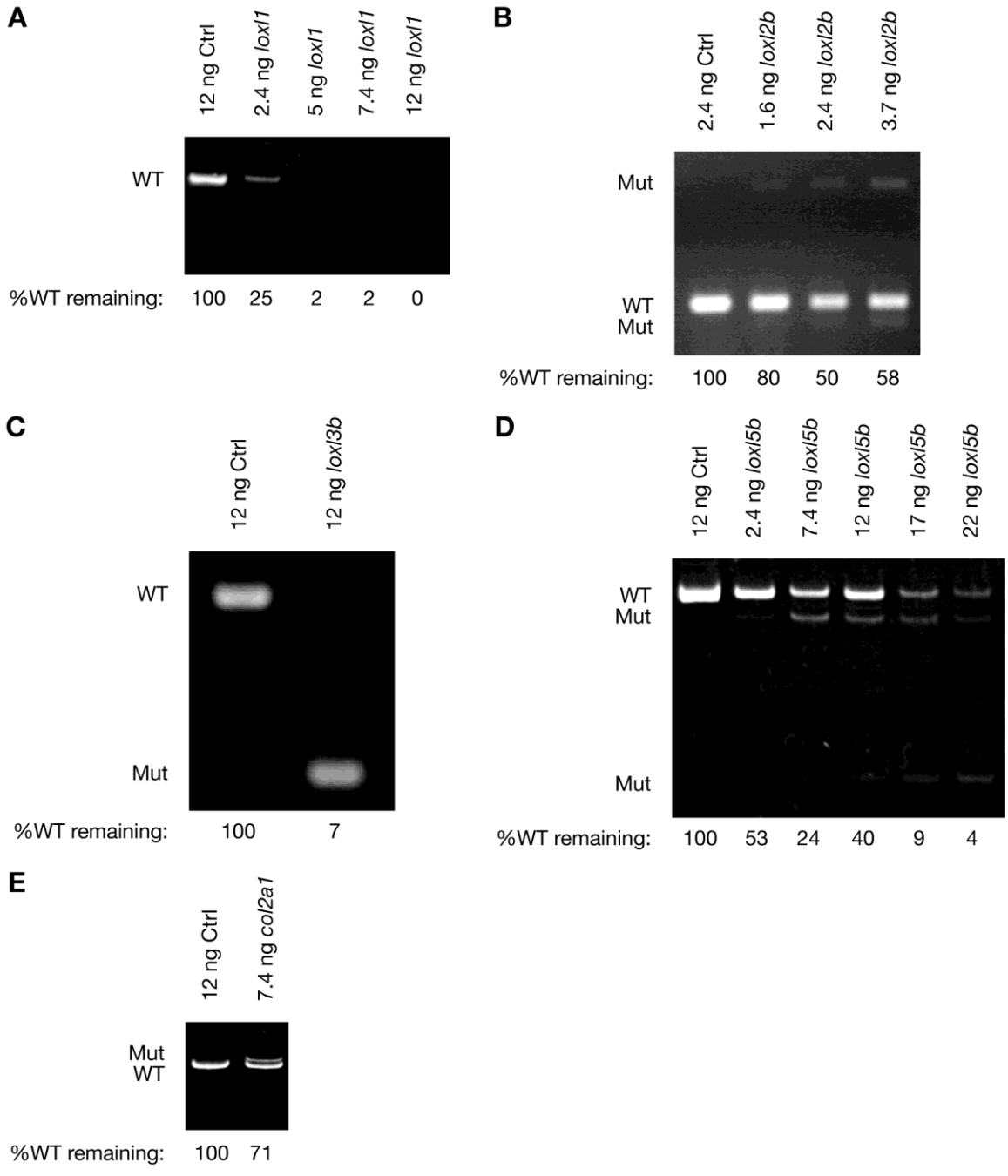

Supplementary Figure 3

Specific Morpholino	Dose of morpholino (ng)	# of embryos examined	Phenotype of notochord distortion	
			-	+
loxl1*/*loxl2b	2.4/1.6	53	49 (**100%**)	0 (**0%**)
loxl1*/*loxl3b	2.4/5	49	32 (**78%**)	9 (**22%**)
loxl2b*/*loxl3b	1.6/5	44	18 (**100%**)	0 (**0%**)
loxl2b*/*loxl5b	1.6/5	45	26 (**90%**)	3 (**10%**)
loxl3b*/*loxl5b	5/5	42	32 (**86%**)	5 (**14%**)

Supplementary Table 1

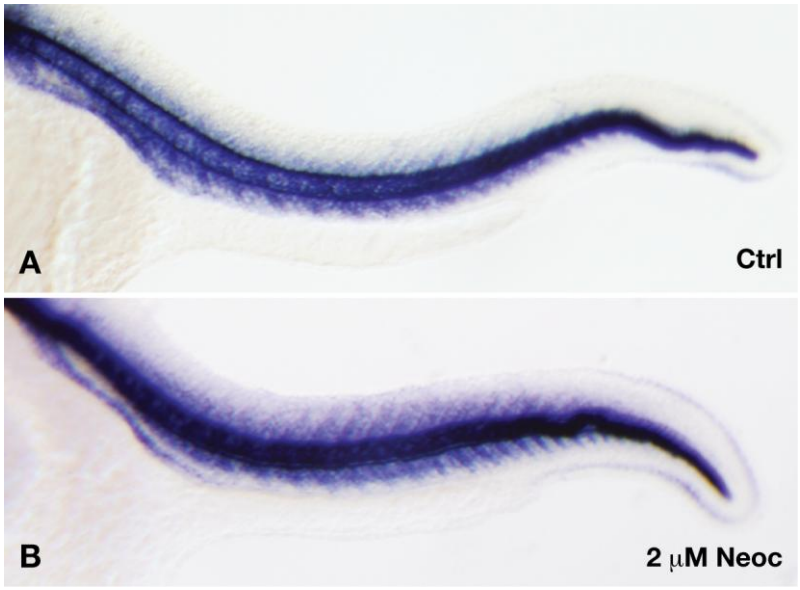

Supplementary Figure 4

Molecular BioSystems
Vol. 3, Issue 1, pp. 51-59, 2007

CHAPTER 3

2-Mercaptopyridine-*N*-oxide is a novel, potent lysyl oxidase inhibitor

Unpublished material and material excerpted from:
Chemical genetics suggests a critical role for lysyl oxidase in zebrafish notochord morphogenesis

Carrie Anderson,[‡a] Stephen J. Bartlett,[‡b] John M. Gansner,[c] Duncan Wilson,[a] Ling He,[a] Jonathan D. Gitlin,[c] Robert N. Kelsh,[a] and James Dowden[bd]

[a]Centre for Regenerative Medicine, Department of Biology & Biochemistry, University of Bath, Bath, UK BA2 7AY
[b]Wolfson Laboratory of Medicinal Chemistry, Department of Pharmacy and Pharmacology, University of Bath, Bath, UK BA2 7AY
[c]Edward Mallinckrodt Department of Pediatrics, Washington University School of Medicine, 660 South Euclid Ave, St. Louis, Missouri, 63110, USA
[d]School of Chemistry, University of Nottingham, University Park, Nottingham, UK NG7 2RD

‡These authors have contributed equally and are to be considered joint first authors

Abstract

2-Mercaptopyridine-*N*-oxide causes notochord distortion in zebrafish embryos similar to what is observed after lysyl oxidase cuproenzyme inhibition with β-aminopropionitrile. We demonstrate in vitro that 2-mercaptopyridine-*N*-oxide potently inhibits amine oxidase activity in adult zebrafish extracts. We also demonstrate that 2-mercaptopyridine-*N*-oxide causes notochord distortion in haploid embryos at nanomolar concentrations, making it practical to conduct forward genetic sensitivity screens using a sub-threshold dose of this compound.

Introduction

The notochord is one of the most conspicuous organs visible during zebrafish embryogenesis, allowing pharmacologic compounds that affect notochord formation to be easily identified. 2-Mercaptopyridine-*N*-oxide was noted to recapitulate the notochord distortion observed in copper-deficient zebrafish embryos without diminishing melanin pigmentation except at very high concentrations (74). Based on the known hierarchy of copper metabolism (14), this suggested that copper chelation is not the principal mode of action of 2-mercaptopyridine-*N*-oxide and that this compound directly inhibits the lysyl oxidases required for notochord formation. We demonstrate by biochemical assay that 2-mercaptopyridine-*N*-oxide potently diminishes amine oxidase activity in adult zebrafish extracts and that it causes notochord distortion in gynogenetic haploid embryos.

Materials and methods

Zebrafish maintenance

Zebrafish were reared under standard conditions at 28.5°C (33) and staged as described (34). All experiments were carried out in accordance with Washington University's Division of Comparative Medicine guidelines.

Pharmacologic treatment

Pharmacologic compounds were purchased from Sigma-Aldrich (St. Louis, MO). β-Aminopropionitrile (A3134) and 2-mercaptopyridine-*N*-oxide (188549) were prepared as 100 mM stocks in water and dimethyl sulfoxide, respectively, and diluted in water. For experiments with haploid embryos, egg water (33) was used instead of water and embryos were placed in compound between 3 and 6 hpf.

Lysyl oxidase assay (75)

Fish were euthanized and pulverized in liquid nitrogen with a mortar and pestle. The powder was collected in PBS and rocked for 1 h at 4 °C before centrifuging at 10 000 g for 30 min to obtain an insoluble fraction, which was mechanically homogenized and extracted overnight in 6 M urea–50 mM sodium borate pH 8.2 with agitation at 4 °C. The supernatant was isolated after a second centrifugation at 30 000 g for 30 min and diluted to 1.2 M urea with 50 mM sodium borate, pH 8.2. Lysates were then concentrated using Amicon YM-10 columns and the flow-through saved.

Assays were carried out in triplicate at 37 °C using 150 µL of lysate or flow-through and 50 µL of a 4x reaction buffer containing 4 U mL^{-1} type II horseradish peroxidase, 40 mM cadaverine, and 40 µM Amplex UltraRed in 1.2 M urea–50 mM

sodium borate, pH 8.2. Amplex UltraRed fluorescence was measured at defined intervals using an excitation of 560 nm and an emission of 590 nm. For each sample, the background fluorescence of the corresponding flow-through with or without drug was subtracted to generate a corrected fluorescence, reported in relative fluorescent units (RFU).

Haploid embryo generation

Gynogenetic haploid embryos were generated as described (33). Briefly, sperm from multiple adult male fish was pooled in 300 μL of Hank's buffer ("Final"), deposited on a chilled watch glass, and subjected to UV irradiation for 7 seconds at maximum power in a UV Stratalinker 1800 (Stratagene). It was then collected with a new tip and stored on ice. 10 μL aliquots were used to fertilize individual clutches from female fish.

Results

2-Mercaptopyridine-N-*oxide inhibits zebrafish amine oxidase activity in vitro*

Work performed by our collaborators demonstrated that wild-type diploid embryos exposed to nanomolar concentrations of 2-mercaptopyridine-*N*-oxide develop a phenotype of notochord distortion similar to the one obtained with lysyl oxidase inhibition. To determine whether 2-mercaptopyridine-*N*-oxide inhibits zebrafish amine oxidase activity in vitro, we performed a biochemical assay (75) using extracts from adult fish. In this assay, addition of 500 μM β-aminopropionitrile inhibited amine oxidase activity almost 80%, while addition of 5 μM 2-mercaptopyridine-*N*-oxide reduced activity by almost 30% (Fig. 1). Interestingly, addition of both compounds resulted in an additive effect, suggesting that the mechanisms of action of β-aminopropionitrile and 2-mercaptopyridine-*N*-oxide are different. Approximately the same amount of inhibition is obtained with 100 μM β-aminopropionitrile as with 5 μM 2-mercaptopyridine-*N*-oxide (data not shown), reflecting the greater potency of β-aminopropionitrile as a lysyl oxidase inhibitor in vitro. Importantly, β-aminopropionitrile causes notochord distortion in wild-type zebrafish embryos at millimolar concentrations (see Chapter 2), confirming that 2-mercaptopyridine-*N*-oxide also has superior potency in vivo. Concentrations of 2-mercaptopyridine-*N*-oxide higher than 5 μM could not be used in the assay because they diminished fluorescence non-specifically.

2-mercaptopyridine-N-*oxide causes notochord distortion in haploid embryos*

We next tested the effect of 2-mercaptopyridine-*N*-oxide on wild-type gynogenetic haploid embryos to determine if this compound would be useful in a forward genetic

sensitivity screen. Titration experiments revealed consistent notochord distortion at concentrations of 200 nM and no distortion at 50 nM (Table 1). This was of particular interest because β-aminopropionitrile lacks the potency to induce notochord distortion in gynogenetic haploid embryos at concentrations as high as 1 mM (Table 2).

Discussion

Taken together with detailed studies conducted by our collaborators, the phenotypic and biochemical data presented here demonstrate that lysyl oxidases are direct targets of 2-mercaptopyridine-*N*-oxide. In addition, the titration experiments (Table 1) reveal that this compound induces notochord distortion in gynogenetic haploid embryos, a finding that now permits forward genetic sensitivity screens where notochord formation is examined in the context of impaired lysyl oxidase function.

The in vitro inhibition of amine oxidase activity observed with β-aminopropionitrile provides biochemical evidence for the evolutionary conservation of lysyl oxidase enzymatic activity between zebrafish and mammals. While 1 mM β-aminopropionitrile does not cause notochord distortion in gynogenetic haploids, higher concentrations of this inhibitor may result in the anticipated phenotype.

These studies suggest that high-throughput screening of pharmacologic compounds could be used to identify additional lysyl oxidase inhibitors by examining embryos for the phenotype of notochord distortion in the context of normal melanin pigmentation. Inhibitors of specific lysyl oxidase family members would help elucidate the individual roles of these proteins in development and could be useful in preventing hypoxia-induced cancer metastasis (54).

Figure legends

Fig. 1. 2-Mercaptopyridine-*N*-oxide inhibits lysyl oxidase activity. Lysyl oxidase activity in crude fish extracts was measured in the absence and presence of a known lysyl oxidase inhibitor β-aminopropionitrile (βAPN) or 2-mercaptopyridine-*N*-oxide (MCP) or both combined. Data shown is representative of three separate experiments and activity is presented in relative fluorescent units with each data point as the mean of three triplicate measurements, error bars indicate standard deviation.

Table 1. 2-Mercaptopyridine-*N*-oxide causes notochord distortion in haploid embryos. Gynogenetic haploid embryos were incubated in increasing concentrations of 2-mercaptopyridine-*N*-oxide and examined for notochord distortion at 24 hpf. Some but not all embryos in 75 nM 2-mercaptopyridine-*N*-oxide exhibited notochord distortion. All embryos in 200 nM 2-mercaptopyridine-*N*-oxide exhibited notochord distortion.

Table 2. Effect of β-aminopropionitrile on notochord formation in haploid embryos. Gynogenetic haploid embryos were incubated in increasing concentrations of β-aminopropionitrile and examined for notochord distortion at 24 hpf. Notochord distortion was not observed at concentrations of β-aminopropionitrile ranging from 50 μM to 1 mM.

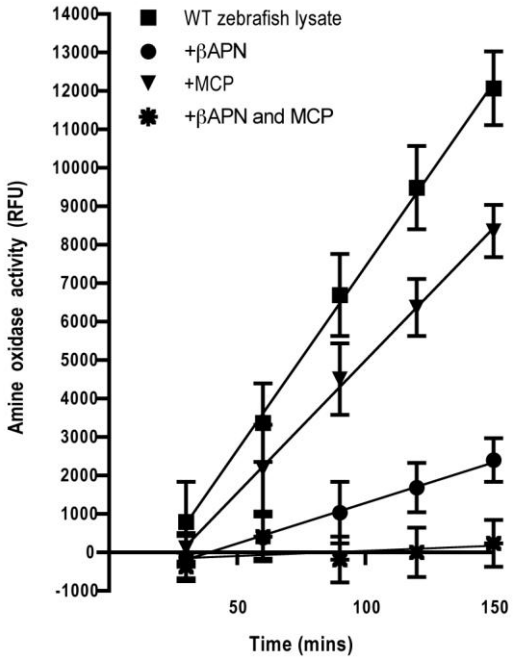
WT zebrafish lysate
+βAPN
+MCP
+βAPN and MCP
Amine oxidase activity (RFU)
14000
13000
12000
11000
10000
9000
8000
7000
6000
5000
4000
3000
2000
1000
0
-1000
50
100
150
Time (mins)

Figure 1

2-Mercaptopyridine-*N*-oxide concentration (nM):	**0**	**12.5**	**25**	**50**	**75**	**100**	**200**	**250**
Notochord distortion?	No	No	No	No	Some	Some	All	All

Table 1

β-aminopropionitrile concentration (μM):	**0**	**50**	**100**	**200**	**400**	**600**	**800**	**1 000**
Notochord distortion?	No	No	No	No	No	No	No	No

Table 2

Developmental Dynamics
Vol. 237, Issue 10, pp. 2844-2861, 2008

CHAPTER 4

Essential role for fibrillin-2 in zebrafish notochord and vascular morphogenesis

John M. Gansner,[1] Erik C. Madsen,[1] Robert P. Mecham,[2] and Jonathan D. Gitlin[1]

Departments of Pediatrics[1] and Cell Biology and Physiology[2]
Washington University School of Medicine
St. Louis, Missouri 63110

Abstract

Recent studies demonstrate that lysyl oxidase cuproenzymes are critical for zebrafish notochord formation, but the molecular mechanisms of copper-dependent notochord morphogenesis are incompletely understood. We therefore conducted a forward genetic screen for zebrafish mutants that exhibit notochord sensitivity to lysyl oxidase inhibition, yielding a mutant with defects in notochord and vascular morphogenesis, *puff daddy*^{gw1} (*pfd*^{gw1}). Meiotic mapping and cloning reveal that the *pfd*^{gw1} phenotype results from disruption of the gene encoding the extracellular matrix protein fibrillin-2, and the spatio-temporal expression of fibrillin-2 is consistent with the *pfd*^{gw1} phenotype. Furthermore, each aspect of the *pfd*^{gw1} phenotype is recapitulated by morpholino knockdown of fibrillin-2. Taken together, the data reveal a genetic interaction between fibrillin-2 and the lysyl oxidases in notochord formation and demonstrate the importance of fibrillin-2 in specific early developmental processes in zebrafish.

Introduction

Structural birth defects are a significant cause of morbidity and mortality in humans and result from both genetic and environmental factors (76-78). Nutrition is a critical environmental factor affecting early development (29), and deficiencies in several nutrients during pregnancy are known to cause structural birth defects (77, 79). As nutritional status can now be increasingly interpreted within a specific genetic context, identification of alleles that confer susceptibility to nutritional or metabolic abnormalities may allow for therapeutic intervention or prevention of birth defects. Zebrafish provide a genetically tractable model to examine gene-nutrient interactions during early vertebrate development as early morphogenesis can be directly observed and levels of specific nutrients precisely controlled in the embryonic milieu via pharmacologic manipulation (14, 30, 80).

The zebrafish notochord is well suited to the study of gene-nutrient interactions during development. This prominent organ is easily visualized, consisting of a series of notochord vacuolar cells that exert turgor pressure on an extracellular matrix sheath (31). The notochord provides axial support to the growing embryo, is essential for subsequent vertebral column formation, and secretes signaling molecules required for neural patterning, muscle differentiation, and cardiac formation (16). Furthermore, defects in extracellular matrix formation lead to compromised notochord sheath function and notochord abnormalities and therefore can be readily detected. Indeed, large forward genetic screens (17, 18) have established the importance of laminins and coatomer proteins in notochord differentiation and sheath formation (19, 20).

The fibrillins are a family of extracellular matrix proteins that form 10 nm-diameter microfibrils around the notochord and in other tissues during development (81-84). The human genome encodes three fibrillins which are numbered sequentially, have a highly modular and conserved domain organization, and exhibit about 68% amino acid identity with each other (85). Because of this similarity, fibrillin family members have historically been distinguished by a few salient features, including a single internal unique region which is proline-rich in fibrillin-1, glycine-rich in fibrillin-2, and proline/glycine-rich in fibrillin-3 (84). The composition of this domain, which may act as a hinge region (86), is thought to contribute to functional differences between individual family members (84). In addition, the number and location of integrin-binding RGD-motifs and *N*-glycosylation sites differ between family members (84). While little is known about fibrillin-3, the other fibrillins have a long history and were first studied in avian development using monoclonal antibodies to fibrillin-1 (clone 201) (87) and fibrillin-2 (the JB3 antibody) (82). In particular, the role of fibrillin-2 in embryo patterning and axis formation has been extensively studied in avians (88-90).

Our laboratory has recently delineated the phenotype of copper deficiency in a zebrafish model of Menkes disease, which includes a strikingly distorted notochord (14). This notochord distortion is due to the inhibition of two specific copper-dependent lysyl oxidases that normally crosslink collagens and other extracellular matrix proteins in the notochord sheath (80). Partial disruption of collagen II, a lysyl oxidase substrate and notochord sheath protein, sensitizes embryos to notochord distortion after suboptimal copper nutrition or partial lysyl oxidase inhibition, demonstrating a complex interplay of

gene dosage and nutrient availability critical to notochord formation (80). To understand the molecular mechanisms of notochord formation in relation to copper nutrition, we conducted a forward genetic screen for mutants exhibiting notochord sensitivity to lysyl oxidase inhibition. In this current study, we report the identification and characterization of one such mutant with defects in notochord and vascular morphogenesis, *puff daddy* (*pfd*^{gw1}).

Materials and methods

Zebrafish maintenance

Zebrafish were reared under standard conditions at 28.5°C (33) and staged as described (34). Synchronous, *in vitro* fertilized embryos were obtained for all experiments, which were carried out in accordance with Washington University's Division of Comparative Medicine guidelines. AB stocks were used except when *pfd*^{gw1} was crossed to WIK for mapping and to *Tg(fli1a:EGFP)*^{y1} (91) for visualization of vascular defects. In Figs. 1, 2, 3A-D, 4, 5, 7A-J, and 8, "wild-type" refers to either +/+ or +/- embryos, which could not be phenotypically distinguished.

Chemical mutagenesis and forward genetic screening

Mutagenesis was carried out with *N*-ethyl-*N*-nitrosourea according to standard methods (92). Briefly, male zebrafish were incubated for 1 hour in 3 mM *N*-ethyl-*N*-nitrosourea at weekly intervals for five consecutive weeks and outcrossed to generate F1 carriers (AB*/AB) after a rest period. Gynogenetic haploid offspring from F1 females were screened using a dose (50 nM) of the lysyl oxidase inhibitor 2-mercaptopyridine-*N*-oxide (74) that is slightly lower than the dose required to cause notochord distortion in haploids. In addition, frank notochord mutants detected in concurrent screens were also interrogated for notochord sensitivity to partial lysyl oxidase inhibition by this method. Random intercrosses of F2 progeny confirmed transmission of the mutation.

Microscopy

Live embryos were anesthetized in tricaine, mounted in 2% methylcellulose, and imaged using either Olympus SZX12 (bright-field) or Olympus MVX10 (fluorescent)

microscopes fitted with Olympus DP70 cameras. Frozen sections mounted on slides were imaged using an Olympus BX60 microscope fitted with a Zeiss AxioCam. Electron microscopy was carried out as previously described (80).

Pharmacologic treatment

All pharmacologic compounds were purchased from Sigma-Aldrich (St. Louis, MO) except losartan, which was purchased from AK Scientific, Inc. (Mountain View, CA). β-Aminopropionitrile (A3134) was prepared as a 100 mM stock in egg water (33) and diluted in egg water; neocuproine (N1501) and 2-mercaptopyridine-*N*-oxide (188549) were prepared as 100 mM stocks in dimethyl sulfoxide and diluted in egg water. Losartan (I497) was prepared as a 50 mM stock in dimethyl sulfoxide, diluted in water, and used at final concentrations of 5 and 50 μM. Embryos were incubated in each compound starting at 3-6 hpf. Statistical analysis was performed as previously described (80).

Meiotic mapping

F2 carriers were mapcrossed to the polymorphic WIK strain and the progeny (AB*/WIK) raised to adulthood. The *pfd*^{gw1} mutation was assigned to chromosome 22 by centromeric linkage analysis (26, 93) using simple sequence length polymorphism (SSLP) markers (94) and DNA from early pressure gynogenetic diploids. For fine mapping, 597 mutant embryos from AB*/WIK females crossed to AB*/AB males were collected and assessed for recombination along chromosome 22 by SSLP analysis. Embryos were incubated in 2 μM neocuproine to accentuate the mutant phenotype and facilitate rapid mutant identification. When necessary, candidate marker primer pairs for BAC sequences were generated using the Zebrafish SSR search website of the Massachusetts General Hospital

(http://danio.mgh.harvard.edu/markers/ssr.html). Primers for the BAC markers used in Fig. 6A are: zC124A3 – forward 5'-GAGTGTTGCAAGTGTAACTTGCCC-3' and reverse 5'-ATGGGAAACTAGTTATTTGGCACAG-3'; zC239M17 – forward 5'-GAGTCTAATCAGTGGAGACTTGG-3' and reverse 5'-CGTACAGATGCTGATCTGGG-3'; zK49M19 – forward 5'-GCATCGTTGCAACTTGCTT-3' and reverse 5'-TGATGGCAGAATAGTTTCACACA-3'; bZ36A1 – forward 5'-GGCAATAGATTTCAAAGGTGTTTT-3' and reverse 5'-AATCCAAGGCAATGCAGAAA-3'. DNA from wild-type and heterozygote embryos as well as WIK and AB grandparents was used to ensure polymorphism between AB and WIK. Based on available genetic maps of the zebrafish genome (94, 95), the *pfd*^{gw1} mutation was localized to a telomeric region of chromosome 22.

Cloning and protein annotation

Zebrafish fibrillin-2 was cloned first in pieces and then in its entirety using Superscript III reverse transcriptase (Invitrogen) and Phusion DNA polymerase with high-fidelity buffer (Finnzymes). The *pfd*^{gw1} mutation was initially detected by cloning the 5' end of fibrillin-2 from mutant embryo and wild-type adult fin cDNA into pCRII (Invitrogen) using forward primer 5'-AGGGTGAGGCACATTTACCG-3' and reverse primer 5'-GTGTCTTCACACTCGTCGATG-3'. Full-length wild-type fibrillin-2 was subsequently cloned into pCR-XL-TOPO (Invitrogen) after amplification from 52 hpf embryo cDNA using forward primer 5'-AGGGTGAGGCACATTTACCG-3' and reverse primer 5'-CTGCAGTGAAGGGCATAGGG-3'. Full-length clones from 3 separate PCR reactions

were sequenced and compared, allowing mutations introduced during PCR to be identified. No alternative splice forms were detected. The start site of fibrillin-2 was confirmed by 5' rapid amplification of cDNA ends (RACE) using wild-type RACE-ready cDNA from 15-somite embryos and the primer 5'-GACCCTCTGCTGCACCTCCCCCTCAG-3'. The full-length zebrafish *fbn2* sequence is available at Genbank (accession number **EU449516**). The 5' portion of zebrafish fibrillin-4 (accession number **EU854565**) was cloned in two overlapping pieces using the following primer sets: A) forward primer 5'-GCAGTCCTTCTGTTGTCCAGG-3' and reverse primer 5'-CAGACAGATGATGACCAGGCGG-3' and B) forward primer 5'-CCTTTCACTGTGCAATGGAGGC-3' and reverse primer 5'-CCACATTATTGACACACCGACC-3'. The start site was inferred from an EST (**EE319589**). The 3' portion of zebrafish fibrillin-4 (accession number **EU854566**) was cloned in multiple overlapping pieces using the following primer sets: A) forward primer 5'-CGAATGTGGTCAGAATCCTC-3' and reverse primer 5'-CCCATGACCTCCATTACAGC-3' B) forward primer 5'-GTGAATGTGGTGTTGGGTTC-3' and reverse primer 5'-GGTGTTGTGTGTAACCCTGTGG-3' C) forward primer 5'-CCTGGGATATGTGCTCCTGG-3' and reverse primer 5'-CCCATGACCTCCATTACAGC-3' D) forward primer 5'-CGTTTAACACCACCAAAGCC-3' and reverse primer 5'-GCAGTGGCATCTGTAAGAGC-3'. An 86 bp sequence connecting the 5' and 3' portions was inferred from Zv7_Scaffold988 based on the modular nature of fibrillins. A

253 bp extension to the 3' end was also inferred in this manner. The far 3' end and stop codon could not be determined. For both fibrillins, conserved protein domains were identified using Motif Scan (40) and by comparison with annotated orthologues (84). The NetNGlyc 1.0 Server (http://www.cbs.dtu.dk/services/NetNGlyc/) was used to predict *N*-glycosylation sites with a potential greater than 0.32.

Phylogenetic analysis

DNA coding sequences were aligned using ClustalW2 (96) and a phylogenetic tree was constructed in TOPALi v2.5 by the maximum likelihood method (PhyML) using HKY substitution and gamma rate models (97-99). 100 bootstrap runs were performed. Similar trees were obtained with MEGA4.0 using maximum parsimony or minimum evolution methods (100), except that pDr*fbn4* diverged before all other fibrillins to form its own one-member group. Accession numbers for the non-zebrafish sequences used were: Hs*FBN1* – **NM_000138**; Hs*FBN2* – **NM_001999**; Hs*FBN3* – **NM_032447**; Mm*Fbn1* – **NM_007993**; Mm*Fbn2* – **NM_010181**; Rn*Fbn1* – **NM_031825**; Rn*Fbn2* – **NM_031826**; Bt*Fbn1* – **NM_174053**; pXl*fbn* – **DQ310728**; and Hs*LTBP1* – **NM_000627**.

Whole-mount in situ hybridization and frozen sections

Embryos from pfd^{gw1}/+ intercrosses were manually dechorionated at the indicated developmental stages, fixed in 4% paraformaldehyde-PBS, and dehydrated by methanol series. Three fibrillin-2 probe constructs were generated by cloning nonoverlapping fragments of the cDNA into pCRII (Invitrogen). DIG-labeled antisense RNA probes were synthesized from these constructs using a DIG-labeling kit (Roche), and whole-mount in situ hybridization performed as previously described (14, 45). All embryos of the same

developmental stage were processed in a single well to ensure identical reaction conditions. Frozen sections were prepared as described (80).

Genotyping

DNA was extracted from embryos or caudal fin tissue and PCR amplified using primers flanking the mutation: forward primer 5'-GCGGTGTGCGAGAGCGGATG-3' and reverse primer 5'-GCATTCTTGAAGGAGCCCCG-3'. The resulting product was then digested with the restriction enzyme AvaII (New England Biolabs) for 5 hrs at 37°C and a small aliquot run on a 10% TBE polyacrylamide gel for visualization. PCR product derived from the mutant allele is not cut by AvaII. For genotyping after whole-mount in situ hybridization, embryos were first rehydrated to PBS and incubated in 300 mM NaCl for 4 hours at 65°C to reverse crosslinking. They were then placed in DNA extraction buffer (80 mM KCl, 10 mM Tris pH 8, 1 mM EDTA, 0.3% Tween 20, 0.3% Igepal), boiled 10 minutes, and the DNA phenol-chloroform extracted. Genotyping was performed by restriction digest, as described above.

Reverse transcriptase-polymerase chain reaction (RT-PCR)

RNA was obtained from pooled wild-type embryos or unfertilized eggs using Trizol reagent (Invitrogen) and RT-PCR performed with the SuperScript III One-Step RT-PCR Platinum *Taq* HiFi kit (Invitrogen). Half a microgram of total RNA was used per 25 μL reaction. The primer annealing temperature was 57°C and 30 cycles of PCR were performed. Fibrillin-2 primers were: forward primer 5'-CACCTGTAAATGCCCCTCGG-3' and reverse primer 5'-GAAGCCCACCCCATTGATGC-3'. Spadetail primers were: forward primer 5'-

GAAGATGTTTACTGACCACTCAG-3' and reverse primer 5'-GCCTGTTTGTTTAAGACATT-3'.

Morpholino and mRNA injections

Morpholino oligonucleotides (27) targeting start and splice sites in fibrillin-2 were resuspended in Danieau buffer (start MO) or water (splice MO), diluted to include 0.05% phenol red, and injected into 1-cell embryos. Standard control morpholino (Gene Tools, LLC) was resuspended in Danieau buffer and likewise injected. Morpholino sequences were: 5'-GCGACTCCTGAAGCGCCGGTAAATG-3' (start MO) and 5'-GGGATACTTACGAACTATACACTGG-3' (splice MO). The splice MO was used at a dose of 1.7 ng. The *loxl5b* splice morpholino (5'-GCCTGTGGAATAAACACCAGCCTCA-3') was prepared as previously described (80) and was used at a dose of 5 ng. Capped, polyadenylated mRNA for rescue experiments was generated from a full-length clone of zebrafish fibrillin-2 using the mMESSAGE mMACHINE kit (Ambion). Individual embryos from *pfd*^{gw1}/+ intercrosses were injected with between 100 and 1000 pg of mRNA in multiple separate experiments. Statistical analysis was performed as previously described (80).

Results

The pfd^{gw1} *mutation disrupts notochord and vascular development*

To elucidate the role of copper homeostasis in development, we performed a screen that couples *N*-ethyl-*N*-nitrosourea mutagenesis to pharmacologic sensitization using a sub-threshold dose of the lysyl oxidase inhibitor 2-mercaptopyridine-*N*-oxide (74). A mutant, *puff daddy* (*pfd*^{gw1}), was identified with notochord abnormalities (Fig. 1B, black arrow) and normal melanin pigmentation (Fig. 1B, white arrowhead) characteristic of the previously identified phenotype of impaired lysyl oxidase function. *pfd*^{gw1} mutants also display a cavernous caudal vein (Figs. 1B, D, white arrows) and fin fold attenuation (Figs. 1B, D, black arrowheads) not present in wild-type (+/+ and +/-) embryos at 30 hpf (Figs. 1A, C). Skin distention secondary to edema occurs in the lateral truncal region near the yolk-sac extension of *pfd*^{gw1} mutants by 30 hpf (Fig. 1F vs. Fig. 1E, arrowheads), and blood cell extravasation is visible in this space (Fig. 1F, arrow).

The pfd^{gw1} *mutation disrupts venous plexus and axial vessel formation*

To examine vascular development in *pfd*^{gw1} fish, *pfd*^{gw1} was crossed to a transgenic line that expresses enhanced green fluorescent protein in vascular endothelial cells (91). In wild-type embryos, the caudal vein forms a venous plexus with a characteristic reticular pattern (Fig. 2A, arrowheads), and the dorsal aorta and cardinal vein are appropriately lumenized (Fig. 2C, circles). In *pfd*^{gw1} mutants, endothelial cells are disorganized around a cavernous caudal vein (Fig. 2B, arrowheads), and the diameters of the large axial vessels are reduced to a variable degree (Fig. 2D, circles). Blood cells do not circulate in mutants with particularly small-diameter axial vessels despite a pumping heart (data not

shown), and increased vascular resistance due to reduced vessel diameter may contribute to the observed impaired heart contractility in *pfd*^{gw1} mutants (data not shown). The distended area in the lateral truncal region of *pfd*^{gw1} mutants (Fig. 1F, arrowheads) is not lined by *fli1*-expressing cells (data not shown), a finding consistent with edema. While the notochord, fin fold, and vascular abnormalities are consistently penetrant in clutches from *pfd*^{gw1} fish, by 3 dpf, the truncal edema resolves and blood flow occurs through the caudal vein in most *pfd*^{gw1} mutants. However, the swim bladder does not inflate, resulting in embryonic lethality (data not shown).

The outer layer of the notochord sheath is disrupted in* pfd^{gw1} *mutants

The phenotype of *pfd*^{gw1} mutants suggested a defect in notochord sheath formation, and we therefore imaged this organ in *pfd*^{gw1} mutants and wild-type embryos by transmission electron microscopy (Figs. 3A-D). Ultrastructurally, the notochord sheath consists of inner, medial, and outer layers, all of which are clearly visible in a cross-section from a wild-type embryo at 30 hpf (Figs. 3A, C). While the inner and medial sheath layers are present in *pfd*^{gw1} mutants, the outer layer is strikingly diminished in size at the region of notochord folding (Figs. 3B, D).

pfd^{gw1} ***mutants are sensitized to lysyl oxidase inhibition***

Interestingly, lysyl oxidase inhibition results in impaired notochord formation without an effect on the outer sheath layer (Figs. 3E, F and Gansner et al., 2007), suggesting that the product of the *pfd*^{gw1} locus has roles in addition to those related to lysyl oxidase crosslinking. To examine this, we first incubated clutches from *pfd*^{gw1}/+ intercrosses in vehicle (Figs. 4A, B and Table 1) or a dose of the copper chelator neocuproine that does

not cause notochord distortion in wild-type embryos (Fig. 4C, Table 1, and Gansner et al., 2007). Consistent with the results of our original screen, *pfd*^{gw1} mutants were sensitized to increased notochord distortion under copper-limiting conditions (Fig. 4D vs. Fig. 4B and Table 1), presumably due to partial inhibition of lysyl oxidase activity (80). To confirm this finding, we incubated clutches from *pfd*^{gw1}/+ intercrosses in a dose of the irreversible lysyl oxidase inhibitor β-aminopropionitrile that causes very mild notochord herniation in wild-type embryos (Fig. 4E, white arrowhead). Under these conditions, notochord sensitization in *pfd*^{gw1} mutants was again observed (Fig. 4F vs. Fig. 4B and Table 1). Importantly, *pfd*^{gw1} mutants could be distinguished from heterozygote and wild-type siblings in these experiments by the cavernous caudal vein and truncal edema present in the mutants. These additional phenotypes are never observed after lysyl oxidase inhibition with neocuproine or β-aminopropionitrile, even when higher doses of these compounds are used (80).

We next tested for a genetic interaction between the lysyl oxidases involved in late notochord formation (80) and the *pfd*^{gw1} product by injecting clutches from *pfd*^{gw1}/+ intercrosses with control morpholino (Figs. 5A, B and Table 2) or morpholino targeting *loxl5b* (Figs. 5C, D and Table 2). The specificity of this lysyl oxidase morpholino has been demonstrated previously (80), and partial morpholino knockdown of *loxl5b* that does not cause notochord distortion in wild-type embryos (Fig. 5C and Gansner et al., 2007) exacerbates the notochord phenotype of *pfd*^{gw1} mutants compared to control morpholino (Fig. 5D vs. Fig. 5B and Table 2). Once the *pfd*^{gw1} lesion was identified (see below), we genotyped a subset of 32 embryos from these experiments to confirm the

genotype assignments in Table 2. Each directly-determined genotype matched the one assigned in Table 2 (data not shown), and testing of 17 phenotypically wild-type embryos that appeared worse after *loxl5b* morpholino injection (Table 2) revealed that 15 were heterozygous for the *pfd*^{gw1} lesion (data not shown), possibly due to a slight increase in the sensitivity of heterozygote embryos to lysyl oxidase inhibition.

The consistent worsening of the notochord phenotype in *pfd*^{gw1} mutants after partial lysyl oxidase inhibition demonstrates an interaction between the *pfd*^{gw1} product and the lysyl oxidases. However, the notochord distortion observed in *pfd*^{gw1} mutants in these sensitization experiments does not adopt the characteristic sine-wave pattern seen in wild-type embryos treated with high-dose neocuproine (Fig. 5E), and at this dose of neocuproine, the notochords of *pfd*^{gw1} mutants never develop this classic shape (Fig. 5F vs. Fig. 5E). These observations, taken together with the electron microscopy studies (Fig. 3), suggest that the *pfd*^{gw1} product and the lysyl oxidases have overlapping but also distinct roles in late notochord formation.

The pfd^{gw1} *mutation disrupts the zebrafish* fibrillin-2 *gene*

To determine the molecular basis for the notochord sensitivity to lysyl oxidase inhibition and other phenotypes observed in *pfd*^{gw1} mutants, we identified the locus mutated in *pfd*^{gw1} fish (Fig. 6). Meiotic mapping localized the *pfd*^{gw1} lesion to a telomeric region of chromosome 22, and inspection of the physical genome assembly (Zv6) for candidate genes in this region revealed sequence coding for an extracellular matrix protein of the fibrillin family (Fig. 6A). A fragment of this gene is annotated as fibrillin-3 in the current zebrafish genome assembly (Zv7), and human orthologues to the flanking genes

timm44 and *trh1* (Fig. 6A) flank human fibrillin-3. However, BLAST searches using the translated fibrillin EST sequences (Fig. 6A) demonstrated better hits in both cases with human fibrillin-1 and fibrillin-2 than with fibrillin-3 (data not shown), suggesting that the zebrafish gene might exhibit greater amino acid identity to a fibrillin besides fibrillin-3.

Sequencing of a 5' segment of the zebrafish fibrillin on chromosome 22 revealed a nonsense mutation in *pfd*^{gw1} mutant embryos that was absent in adult, wild-type fish (Fig. 6B). This mutation abrogates an AvaII restriction enzyme site, allowing wild-type and heterozygote embryos to be distinguished (Fig. 6C) and permitting genotyping of fish stocks. Genotyping of stored DNA samples confirmed that the original *pfd*^{gw1} mutant identified in our screen was heterozygous for the nonsense mutation indicated in Fig. 6B, and that this mutation was absent in both the WIK grandparent used for the mapcross (see Experimental Procedures) and the AB fish used for the outcross (data not shown). Since all 7 recombinants at the flanking markers shown in Fig. 6A were homozygous for the mutation (data not shown), the recombination rate at this location is 0% (0 out of 597 meiotic events), consistent with the hypothesis that the nonsense mutation causes the *pfd*^{gw1} phenotype.

Cloning of the full-length zebrafish fibrillin on chromosome 22 revealed that it encodes a 2868 amino acid protein highly similar to human, mouse, and rat fibrillin-2 (Figs. 6D, E and S. Fig. 1). In particular, the glycine-rich domain and location of the RGD motifs are characteristic of fibrillin-2 but not fibrillin-1 or fibrillin-3 (Figs. 6D, E and S. Fig. 1) (84, 85). In addition, 11 of 12 potential *N*-glycosylation site are conserved (S. Fig. 1) and two calcium-binding EGF-like domains are encoded before the first TGF-

β binding (TB) domain (Fig. 6D and S. Fig. 1), a sequence arrangement that is observed in human fibrillin-2 but not in human fibrillin-3 (Fig. 6E) (85). Overall, the zebrafish fibrillin on chromosome 22 exhibits 75% amino acid identity with human fibrillin-2 but only 67% and 68% identity with human fibrillin-1 and fibrillin-3, respectively (Fig. 6E). In view of the high amino acid sequence identity with human fibrillin-2 and the presence of functional domains that have historically been used to distinguish fibrillin-2 from other fibrillins (the glycine-rich domain, RGD motifs, and *N*-glycosylation sites), we name this gene fibrillin-2 (*fbn2*). The premature stop codon identified in pfd^{gw1} mutants is predicted to result in a severely truncated protein product of only 161 amino acids (Fig. 6D).

Since the current zebrafish genome assembly (Zv7) contains a gene fragment annotated as fibrillin-2 on chromosome 10 (data not shown), we cloned the majority of this gene to determine whether it is a paralogue of zebrafish *fbn2* (S. Fig. 2). Surprisingly, the fibrillin gene on chromosome 10 encodes a protein without RGD motifs and with a novel proline/glutamine-rich domain not found in any fibrillin reported to date (Fig. 6E and S. Fig. 3). Consistent with previous nomenclature that differentiates fibrillins based on these attributes (84), we name this gene fibrillin-4 (*fbn4*) (Fig. 6E). Compared to the three human fibrillins, zebrafish fibrillin-4 exhibits highest amino acid identity with human fibrillin-2 (Fig. 6E). However, this identity (68%) is relatively low, since it is comparable to the identity between individual human fibrillin family members (85). Importantly, zebrafish fibrillin-2 exhibits greater amino acid identity with human fibrillin-2 than does zebrafish fibrillin-4 (Fig. 6E). In addition, zebrafish fibrillin-2 and

fibrillin-4 are only 66% identical, suggesting that these zebrafish fibrillins are not paralogues created by a genome duplication event in teleosts (55).

In order to determine the evolutionary relationship of zebrafish fibrillin-2 and fibrillin-4 to fibrillins in other species, we performed a phylogenetic analysis based on nucleotide coding sequences (Fig. 6F). This revealed that zebrafish fibrillin-2 is evolutionarily related to human fibrillin-3, and that zebrafish fibrillin-4 is distantly related to human fibrillin-2 (Fig. 6F). These findings were corroborated by examining the exon structure of the zebrafish fibrillins. In zebrafish *fbn2*, a single exon encodes both the sixth calcium-binding EGF-like motif and the first half of the second TB domain (data not shown), analogous to what is observed in human fibrillin-3 but not in other human fibrillins (85). By contrast, the exon structure of zebrafish *fbn4* at this location is identical to that of human fibrillin-2 (data not shown). Importantly, a putative orthologue of fibrillin-2 in *Xenopus laevis* (101, 102) clusters with zebrafish *fbn2* and human *FBN3* in the phylogenetic tree (Fig. 6F, arrow). This suggests that in fish and amphibians, a fibrillin with highest amino acid identity to human fibrillin-2 has evolved at the fibrillin-3 locus.

fbn2 ***expression is consistent with the*** **pfd**^{gw1} ***phenotype and dramatically reduced in*** **pfd**^{gw1} ***mutants***

To determine the developmental expression of zebrafish *fbn2*, whole-mount in situ hybridization was performed on embryos from *pfd*^{gw1}/+ intercrosses (Fig. 7). *fbn2* expression is first visible during gastrulation in the hypoblast (mesendoderm) of embryos at 9 hpf (Fig. 7A). In 3-somite embryos, *fbn2* expression occurs in the paraxial mesoderm

(Fig. 7B, arrowheads) and notochord (Fig. 7B, arrow), consistent with a role for zebrafish fibrillin-2 in notochord morphogenesis. In 7-somite embryos, *fbn2* is expressed in the somites and notochord (Fig. 7C, arrow), with foci of increased staining present near notochord-somite boundaries (Fig. 7C, arrowheads). By the 20-somite stage, *fbn2* is also expressed in the developing venous plexus (Fig. 7D, arrowhead), which forms abnormally in *pfd*^{gw1} mutants, and in the eye (Fig. 7D, arrow). Frozen sections of 20-somite embryos revealed that this eye expression is restricted to the lens placode (Fig. 8A, arrowheads) and demonstrated *fbn2* expression in the notochord, hypochord, floorplate, and paraxial mesoderm (Fig. 8B). At 24 hpf, *fbn2* is expressed in the hypochord (Fig. 7E and Fig. 8C, arrows), which plays a critical role in axial vascular development (57, 58), and in the fin fold epidermis (Fig. 7E and Fig. 8C, arrowheads), where *fbn2*-expressing cells form two parallel lines on either side of the midline (Figs. 8C, D, arrowheads). Despite expression of *fbn2* in the lens placode (Fig. 8A), no differences in lens morphology were observed by electron microscopy between *pfd*^{gw1} mutants and wild-type embryos at 30 hpf (data not shown).

Expression of *fbn2* was almost completely absent in a quarter of embryos from *pfd*^{gw1}/+ intercrosses at each developmental stage (Figs. 7F-J and data not shown). At 24 hpf, the mutant phenotype correlated with loss of *fbn2* expression, and genotyping of embryos after in situ hybridization demonstrated an exact concordance between the homozygous mutant genotype and abrogation of *fbn2* expression at three different stages of development examined (data not shown). Furthermore, heterozygote embryos exhibited an intermediate level of *fbn2* expression (Fig. 9), revealing that compensatory

up-regulation of the wild-type allele does not occur in heterozygous mutant embryos. The reduced amount of staining in heterozygous and homozygous mutant embryos supports the specificity of the in situ hybridization reactions. Given the distribution of the in situ probes across the entire length of the zebrafish cDNA (see Experimental Procedures), these findings mitigate against the presence of alternative splice products and suggest nonsense-mediated decay of the *fbn2* transcript (103).

We also examined the developmental onset of *fbn2* expression by reverse transcriptase-polymerase chain reaction (RT-PCR), which is more sensitive than in situ hybridization (Fig. 7K). This revealed that fibrillin-2 mRNA is expressed at very low levels in wild-type embryos maternally and until 6-7 hpf, when it is upregulated but is not yet detectable by in situ hybridization (Fig. 7K and data not shown). At 9 hpf and the 3-somite stage, more robust *fbn2* expression is apparent (Fig. 7K), and this correlates with the detection of *fbn2* by in situ hybridization (Figs. 7A, B). As a control, RT-PCR was performed in parallel with primers to the gene *spadetail* (*spt*) (Fig. 7K). *spt* expression is relatively constant over the time period examined except that it is not present maternally (Fig. 7K) (104). Importantly, an RT-PCR product was not obtained if the reactions were performed in the absence of RNA (Fig. 7K).

fbn2 *knockdown recapitulates the* pfd^{gw1} *phenotype*

To confirm that the *pfd*^{gw1} phenotype directly results from loss of fibrillin-2, we designed morpholinos to abrogate zebrafish *fbn2* expression (Fig. 10). Whereas wild-type embryos injected with control morpholino demonstrated normal formation of the notochord, caudal vein, and fin folds (Figs. 10A, C), embryos injected with a *fbn2* start morpholino

exhibited notochord kinks (Fig. 10B, black arrows), a cavernous caudal vein without venous plexus formation (Figs. 10B, D, white arrows), and fin fold attenuation (Figs. 10B, D, arrowheads). The *fbn2* start morpholino also caused truncal skin distention characteristic of *pfd*^{gw1} mutants (Fig. 10F, arrowheads) that was not observed with control morpholino (Fig. 10E, arrowheads). These findings were consistent and were dose dependent (Table 3). The *fbn2* start morpholino had no visible effect on embryos at a dose of 0.12 ng (Table 3), and at an intermediate dose of 0.48 ng, only a cavernous caudal vein with truncal edema was observed (data not shown), possibly reflecting differences in transcript abundance between notochord and caudal vein. At a dose of 7.2 ng, embryos developed non-specific findings suggestive of morpholino toxicity, such as reduced melanin pigmentation and mild necrosis (data not shown). Injection of *fbn2* start morpholino into *pfd*^{gw1} mutant embryos did not alter their phenotype (Fig. 10H vs. Fig. 10G), indicating that the *pfd*^{gw1} mutation results in a null phenotype, consistent with the early location of the premature stop codon and the in situ hybridization findings (Fig. 6D and Figs. 7F-J). Importantly, it also did not result in the reduced melanin pigmentation or necrosis observed with high dose (7.2 ng) *fbn2* start morpholino, providing evidence that these phenotypes are non-specific. Injection of a morpholino targeting a splice site in *fbn2* also recapitulated the *pfd*^{gw1} phenotype (data not shown), further confirming the specificity of the *fbn2* knockdown.

Injection of mRNA encoding full-length (9 kb) *fbn2* into clutches from *pfd*^{gw1}/+ intercrosses did not rescue the *pfd*^{gw1} phenotype, but expression of zebrafish fibrillin-2 in

mutant embryos could not be confirmed by western immunoblotting since none of the available antibodies cross-reacted with zebrafish fibrillin-2 (data not shown).

Discussion

These data reveal a previously unappreciated role for fibrillin-2 in zebrafish notochord and vascular morphogenesis. Fibrillins are large glycoproteins that polymerize to form microfibrils in a wide variety of elastic and non-elastic connective tissues (84). Microfibrils associate with many different extracellular matrix proteins, bind cell-surface integrins, and have recently been shown to modulate the activity of soluble signaling factors (105). The demonstration in this current work that the notochords of *pfd*^{gw1} mutants are sensitized to lysyl oxidase inhibition (Fig. 4 and Fig. 5) is consistent with the recent realization that microfibril structural elements are part of larger, more complex networks associated with impaired morphogenesis (106). Indeed, our data reveal gene-gene and gene-nutrient interactions between fibrillin-2 and the copper-dependent lysyl oxidases in notochord formation that were not previously apparent. Interestingly, our findings are consistent with the recent discovery in yeast that whereas only ~20% of gene deletions have an obvious phenotypic consequence, 97% exhibit a measurable growth phenotype under situations of specific chemical or environmental stress (107). In addition, the findings add to previous elegant genetic studies that elucidated novel molecular pathways required for notochord sheath formation in zebrafish (16, 19, 20).

Fibrillin gene nomenclature in zebrafish

The zebrafish genome appears to encode three fibrillins, similar to what is observed in human and other vertebrate genomes (data not shown). In the current work, we present sequences for two of these fibrillins, which we name fibrillin-2 (*fbn2*) and fibrillin-4 (*fbn4*) (Figs. 6D, E). The third fibrillin, a putative orthologue of fibrillin-1 (*fbn1*), has not

been cloned but has been targeted using morpholinos (108), and we have independently confirmed its embryonic expression (data not shown).

The two cloned zebrafish fibrillins are named based on amino acid identity to human fibrillins and on the presence of unique domains that are thought to modulate fibrillin function. Zebrafish fibrillin-2 exhibits the highest amino acid identity with human fibrillin-2 (Fig. 6E) and encodes a glycine-rich internal unique region characteristic of fibrillin-2 in other species (S. Fig. 1). It also possesses two RGD motifs located in the same relative positions as human fibrillin-2 (Figs. 6D, E, and S. Fig. 1). Fibrillin RGD motifs mediate interactions with specific cell-surface integrins, and increasing data suggest that these interactions are determined in part by the surrounding amino acid sequence (109-112). It is therefore not surprising that the two RGD motifs in fibrillin-2 have different receptor specificities (111), and the spacing of the RGD motifs, which differs between human fibrillin-2 and fibrillin-3, may thus affect integrin binding and protein function.

In contrast to zebrafish fibrillin-2, zebrafish fibrillin-4 exhibits relatively low amino acid identity to human fibrillins, with only 68% identity to human fibrillin-2 (Fig. 6E). Furthermore, zebrafish fibrillin-4 contains a novel proline/glutamine-rich internal unique region not found in other fibrillins and also completely lacks RGD motifs. Zebrafish *fbn4* is thus unlikely to function as a fibrillin-2 orthologue, although it appears to be a distant evolutionary relative of human fibrillin-2 by phylogenetic analysis (Fig. 6F) and is flanked by the zebrafish orthologue of *SLC27A6* that flanks human fibrillin-2 (data not shown).

The zebrafish fibrillin nomenclature presented here has been informed by studies in amphibians (101, 102). *Xenopus laevis* fibrillin contains an antigenic determinant recognized by the JB3 antibody to fibrillin-2, and the cloned 3' fragment of this fibrillin exhibits 77% amino acid identity with human fibrillin-2 but only 68% and 71% identity with fibrillin-1 and fibrillin-3, respectively (101). Although the 5' sequence of *Xenopus* fibrillin is unknown, it seems likely based on the published expression and functional data that this fibrillin is an orthologue of human fibrillin-2 (101, 102). Importantly, the amino acid sequences of *Xenopus* fibrillin and zebrafish *fbn2* are 75% identical over the region cloned, and their expression patterns are similar (see below). Since both genes cluster phylogenetically with human fibrillin-3 (Fig. 6F), the data suggest that *Xenopus* fibrillin and zebrafish *fbn2* are functional orthologues of fibrillin-2 that have evolved at the human fibrillin-3 locus. The fact that fibrillin family members are already fairly similar (~68% amino acid identity in humans), may help to explain how this could have occurred.

Conservation of fibrillin-2 gene expression

The spatiotemporal expression of zebrafish *fbn2* is similar to that of fibrillin-2 in other vertebrates. In chick and quail, fibrillin-2 protein localization has been directly and extensively studied using the JB3 monoclonal antibody (82, 90, 113, 114). In chick, the earliest fibrillin-2 immunostaining is detected in the primitive streak, which gives rise to notochord and mesodermal structures that exhibit persistent fibrillin-2 staining throughout development (82, 114). In particular, fibrillin-2 containing microfibrils are detected extracellularly around the notochord and somites (compare Figs. 7B, C), and

also in splanchnic mesoderm and segmental plate mesoderm, which is equivalent to paraxial mesoderm in zebrafish (Fig. 7B) (82, 114). In quail, immunostaining using the JB3 antibody revealed prominent fibrillin-2 deposition around the notochord and somites, as well as fibrillin-2 immunoreactivity in the primitive mesocardium and segmental plate mesoderm (90). Of note, fibrillin-2 appeared to physically integrate somites and notochord (90), which may explain the increased *fbn2* expression at notochord-somite boundaries observed in zebrafish (Fig. 7C, arrowheads). Overall, the findings in avian species using the JB3 antibody are consistent with the zebrafish RT-PCR and in situ hybridization results reported above (Fig. 7 and Fig. 8), both in terms of time of onset (pre-gastrulation) and tissue distribution (compare Fig. 7B with Fig. 3 of Rongish et al., 1998).

Zebrafish *fbn2* expression is also similar to that of *Xenopus* fibrillin, a putative orthologue of fibrillin-2 (101, 102). RNase protection assays demonstrate that *Xenopus* fibrillin is markedly upregulated in mid-gastrula embryos (101), which correlates well with the initial increase in zebrafish *fbn2* transcript at 6-7 hpf observed by RT-PCR (Fig. 7K). In addition, fibrillin-2 expression is first detectable by in situ hybridization during gastrulation in both organisms (Fig. 7A) (101). Exact comparison of fibrillin-2 expression between *Xenopus* and zebrafish at post-gastrula stages is difficult because *Xenopus* has a distinct neurulation period before segmentation whereas these stages overlap in zebrafish and a distinct neurulation period is absent (34). Nevertheless, *Xenopus* fibrillin is expressed in the notochord, somites, floorplate, hypochord, and eye by in situ hybridization (101), analogous to what is observed in zebrafish (Figs. 7B-D and Figs. 8A,

B). At later stages, *Xenopus* fibrillin is also expressed in tail fins (101), mimicking zebrafish fin fold expression (Fig. 7E and Figs. 8C, D). Interestingly, while notochord staining is stronger than somite staining in *Xenopus* (101), the opposite is true in zebrafish (Figs. 7B, C and Fig. 8B), possibly due to a differential requirement for fibrillin-2 in axial extension. Future studies using antibodies to zebrafish fibrillin-2 will be required to determine the exact timing of zebrafish fibrillin-2 protein deposition in the notochord-somite boundary during gastrulation, but this may occur later in zebrafish than in *Xenopus*, as is the case in chick (101).

Fibrillin-2 expression has also been studied during human and mouse embryonic development. In humans, immunostaining demonstrates that fibrillin-2 has a wide tissue distribution and is present in fetal eye as well as in the notochordal sheath and perinotochordal mesenchyme (83, 115). In mouse, a wide tissue distribution with prominent mesenchyme staining has been noted (116). The overall conserved expression pattern of fibrillin-2 argues for conservation of function among these different species.

Functions of microfibrils

The functions of specific microfibrillar proteins in various tissues during development are incompletely characterized (105). Fibrillin-2 binds multiple other microfibrillar proteins *in vitro*, including microfibril-associated glycoprotein-1 and fibrillin-1 (117-119), and morpholino knockdown of zebrafish microfibril-associated glycoprotein-1 or the predicted zebrafish fibrillin-1 results in caudal vein dilation and altered plexus formation (108) similar to what is observed in *pfd*^{gw1} mutants (Fig. 2B). A specialized type of heterofibril composed of fibrillin-1, fibrillin-2, and microfibril-associated glycoprotein-1

may thus be required for venous plexus formation in zebrafish. By contrast, tissue-specific roles unique to fibrillin-2 are indicated by the notochord kinks, reduced axial vessel diameters, fin fold attenuation, and truncal edema observed in *pfd*^{gw1} mutants but not fibrillin-1 or microfibril-associated glycoprotein-1 morphants (Fig. 1 and Fig. 2 vs. Chen et al., 2006).

The precise role of microfibrils in notochord formation is unclear, but our results suggest that microfibrils contribute to the strength of the sheath that envelops the notochord, at least in zebrafish. The sensitivity of the notochord phenotype in *pfd*^{gw1} mutants to lysyl oxidase inhibition (Fig. 4 and Fig. 5) may result in part from an impaired ability to recruit or correctly position lysyl oxidases at their site of action in the notochord sheath, a hypothesis supported by studies demonstrating a role for microfibril-associated proteins in this process (50, 120). This model is also consistent with the observation that the heterozygote *pfd*^{gw1} mutants are largely unaffected by lysyl oxidase inhibition (Fig. 4 and Fig. 5), provided that enough fibrillin-2 is present in these fish to allow for proper targeting of lysyl oxidase.

Our data from mutant and morphant zebrafish demonstrate that loss of fibrillin-2 causes early embryonic phenotypes in zebrafish (Fig. 1B, Figs. 2B, D, and Fig. 10B). Interestingly, morpholino knockdown of *Xenopus* fibrillin-2 results in gastrulation arrest (102), a finding that likely reflects differences in the mechanisms of axial extension employed by *Xenopus* and zebrafish embryos. Alternatively, an additional fibrillin family member may compensate for the loss of fibrillin-2 in zebrafish but not in *Xenopus* during gastrulation. In this regard, mice homozygous for a null allele of fibrillin-2 are viable but

die *in utero* when crossed into a fibrillin-1 deficient background, suggesting partial functional redundancy between fibrillin-1 and fibrillin-2 (121-123). Fibrillin-2 knockout mice exhibit syndactyly and congenital contractures of the forelimbs (122) but not notochord or vascular abnormalities, possibly due to evolutionary differences between mice and zebrafish.

Microfibril signaling

Microfibrils have recently been demonstrated to modulate critical morphogenetic signaling events (122, 124-127), and the phenotypes observed in *pfd*^{gw1} mutants may therefore result in part from altered signaling. While the notochord distortion observed in *pfd*^{gw1} mutants (Fig. 1B) likely results from weakness of the notochord sheath due to disruption of the outer sheath layer (Figs. 3B, D), the etiology of the endothelial cell disorganization and altered caudal vein formation in *pfd*^{gw1} mutants (Fig. 2B) is less certain. The mechanisms of venous plexus formation may be similar to those involved in epithelial branching morphogenesis, where signaling by bone morphogenetic protein-7 plays a prominent role (128, 129). A genetic interaction between fibrillin-2 and bone morphogenetic protein-7 has been demonstrated in fibrillin-2 knockout mice (122), and epithelial branching morphogenesis is inhibited in embryonic lung cultures after fibrillin-2 knockdown (130). Signaling by bone morphogenetic protein-7 or other morphogens may therefore be required for endothelial cell branching and venous plexus morphogenesis in *pfd*^{gw1} mutants. Since heterofibrils of fibrillin-2 and fibrillin-1 may be required for caudal vein formation, and mutations in fibrillin-1 lead to excessive transforming growth factor-β activity (124-127), we considered whether increased

transforming growth factor-β signaling could explain the caudal vein abnormalities in *pfd*^{gw1} mutants. However losartan, an inhibitor of transforming growth factor-β signaling (126) does not rescue the vascular phenotype of *pfd*^{gw1} mutants (data not shown).

Microfibrils in human disease

Mutations in human fibrillin-2 cause congenital contractural arachnodactyly, a rare disease with autosomal dominant inheritance that is characterized by congenital joint contractures, arachnodactyly, kyphoscoliosis, malformed ear helices, and vascular abnormalities (131). The pathogenesis of congenital contractural arachnodactyly is uncertain and could result from haploinsufficiency or a gain of function mutation (antimorphic and/or neomorphic) in fibrillin-2. Our results demonstrate that *heterozygosity* for a null allele at the *fbn2* locus in zebrafish does not cause any overt phenotype (Figs. 1A, C, E and data not shown) even in mature fish (data not shown), a finding corroborated by mice heterozygous for a null allele of fibrillin-2 (121-123). Furthermore, the mutations that are known to cause congenital contractural arachnodactyly all cluster within a well-defined region near the middle of human fibrillin-2, a finding that is statistically unexpected and suggests a role for this region in mediating interactions with other proteins (131-133). These data suggest that a gain of function mutation (antimorphic and/or neomorphic) in human fibrillin-2 is required to cause congenital contractural arachnodactyly, a hypothesis now testable through transgenic expression experiments in the *pfd*^{gw1} mutant. Taken together, the data reveal a genetic interaction between fibrillin-2 and the lysyl oxidases in late notochord formation, demonstrate the importance of fibrillin-2 in specific early developmental processes in

zebrafish, and provide insight into the pathogenesis of congenital contractural arachnodactyly. Furthermore, the *pfd*^{gw1} mutant described here should now permit studies to elucidate the cell biological mechanisms of fibrillin-2 in early development.

Acknowledgments

We thank Stephen Johnson for help with meiotic mapping, Marilyn Levy for the electron microscopy, Bryce Mendelsohn for helpful suggestions, and Stephen Johnson and David Wilson for careful review of the manuscript. This work was supported by NIH Medical Scientist Training Program grant T32 GM07200 (J.M.G. and E.C.M.) and by NIH grant DK44464 (J.D.G.).

Figure legends

Fig. 1. The *pfd*^{gw1} mutation disrupts notochord and vascular development. (A) The notochord (black arrow), caudal vein (white arrow), and fin fold (black arrowheads) form normally in wild-type embryos, and melanin pigmentation is present (white arrowhead). (B) *pfd*^{gw1} mutants exhibit notochord kinking (black arrow), a cavernous caudal vein with loss of the usual reticular venous plexus (white arrow), and fin fold attenuation (black arrowheads). Melanin pigmentation is present (white arrowhead). (C) Fin fold (arrowheads) and caudal vein (arrow) in a wild-type embryo. (D) Attenuated fin fold (arrowheads) and cavernous caudal vein (arrow) typical of *pfd*^{gw1} mutants. (E, F) Ventral views of a wild-type embryo (E) and a *pfd*^{gw1} mutant (F) demonstrating skin distention secondary to edema in the mutant (F, arrowheads). Red blood cells have extravasated into the edematous area (F, arrow). All embryos were photographed at 30 hpf.

Fig. 2. The *pfd*^{gw1} mutation disrupts venous plexus and axial vessel formation. (A-D) *pfd*^{gw1} was crossed into a *fli1*:EGFP transgenic line to allow visualization of endothelial cells. (A) The caudal vein of wild-type embryos has a well-formed venous plexus (arrowheads). (B) The caudal vein of *pfd*^{gw1} mutants has lost its characteristic reticular pattern, and endothelial cells are disorganized (arrowheads). (C, D) Dorsal aorta (upper circle) and cardinal vein (lower circle) in a wild-type embryo (C) and a *pfd*^{gw1} mutant (D), demonstrating reduced axial vessel diameters in the mutant (D, circles). Embryos were photographed at 30 hpf (C, D) and 35 hpf (A, B).

Fig. 3. The outer layer of the notochord sheath is disrupted in *pfd*^{gw1} mutants. (A-F) Transmission electron micrographs of truncal cross-sections from embryos at 30 hpf. (A)

Notochord sheath of a wild-type embryo (between arrows). The area in the white square is shown at higher magnification in panel C. (B) Notochord sheath of a *pfd*^{gw1} mutant (between arrows). The area in the white square is shown at higher magnification in panel D. (C) Notochord sheath of a wild-type embryo with inner (i), medial (m), and outer (o) layers. (D) Notochord sheath of a *pfd*^{gw1} mutant where inner (i) and medial (m) layers are normal, but the outer (o) layer is reduced in size. (E, F) Notochord sheaths of wild-type embryos treated with 10 μM neocuproine (E) or 10 mM β-aminopropionitrile (F). Not = notochord.

Fig. 4. *pfd*^{gw1} mutants are sensitized to inhibition of lysyl oxidase. Clutches from *pfd*^{gw1}/+ intercrosses were incubated in vehicle (A, B), the copper chelator neocuproine (2 μM) (C, D), or the lysyl oxidase inhibitor β-aminopropionitrile (1 mM) (E, F). Notochord is normal in wild-type embryos treated with vehicle or neocuproine (A, C) and shows a very mild herniation event in β-aminopropionitrile (E, arrowhead). Notochords of *pfd*^{gw1} mutants in neocuproine and β-aminopropionitrile (D, F, arrowheads) are substantially more distorted than mutants incubated in vehicle (B, arrowhead). Embryos were incubated in PTU to inhibit melanin pigmentation and photographed at 30 hpf.

Fig. 5. *pfd*^{gw1} mutants are sensitized to notochord distortion after partial knockdown of *loxl5b*. Embryos from *pfd*^{gw1}/+ intercrosses were injected with 5 ng control MO (A, B) or 5 ng *loxl5b* MO (C, D) and examined at 30 hpf. Neither morpholino induced notochord distortion in wild-type embryos (A, C). However, *pfd*^{gw1} mutants injected with lysyl oxidase morpholino developed striking notochord distortion (D, arrowheads) compared to mutants injected with control morpholino (B, arrowheads). (E) Wild-type

embryo incubated in high-dose (6 μM) neocuproine, demonstrating classic sine-wave appearance of lysyl oxidase inhibition at 30 hpf. (F) *pfd*^{gw1} mutant at 30 hpf with irregular notochord distortion after incubation in 6 μM neocuproine. Embryos were treated with PTU to inhibit melanin pigmentation.

Fig. 6. The *pfd*^{gw1} mutation disrupts the zebrafish *fbn2* gene. (A) The *pfd*^{gw1} lesion was meiotically mapped to a telomeric region bounded by markers zC124A3 and z33723 on chromosome 22. The number of recombinants is noted for each marker; a single recombinant was identified at z33723. Marker, gene, and fibrillin EST locations relative to BACs and scaffolds (scfld) are illustrated on the physical map, which is based on Zv6. (B) Sequencing traces from the fibrillin on chromosome 22 revealed a nonsense mutation (arrow) in *pfd*^{gw1} mutants that abrogates an AvaII restriction enzyme site. (C) Genotyping of *pfd*^{gw1} fish by restriction digest of a PCR product encompassing the mutated sequence. PCR product from the wild-type allele (+) is cleaved to generate fragments of 143 bp and 43 bp; product from the mutant allele (-) is not cleaved. (D) Structure of zebrafish fibrillin-2 illustrating the conserved modular domains of this 2868 amino acid protein. The glycine-rich domain and location of the RGD motifs (asterisks) are characteristic of fibrillin-2 but not fibrillin-1 or fibrillin-3 orthologues. The *pfd*^{gw1} mutation is predicted to result in a truncated protein product (arrow). (E) Structure of the three human fibrillins and zebrafish fibrillin-4. The percent amino acid identity with zebrafish fibrillin-2 and fibrillin-4 is indicated. The dashed line indicates sequence that is presumed to exist but has not been determined. (F) Phylogenetic tree of fibrillin DNA coding sequences from various vertebrate species. Latent transforming growth factor-beta binding protein 1

(LTBP1) is used as the outgroup. Species are identified using standard two-letter abbreviations with zebrafish genes in bold. The arrow indicates *Xenopus laevis* fibrillin, a predicted fibrillin-2 orthologue. The scale bar reflects expected substitutions per site, and partial sequences begin with "p".

Fig. 7. *fbn2* expression is consistent with the *pfd*^{gw1} phenotype and dramatically reduced in *pfd*^{gw1} mutants. (A-J) Clutches from *pfd*^{gw1}/+ intercrosses were subjected to whole-mount in situ hybridization at the indicated developmental stages using probes to *fbn2*. (A) Lateral view of a wild-type embryo at 9 hpf. (B) Dorsal view of a wild-type embryo at the 3-somite stage demonstrating *fbn2* expression in the notochord (arrow) and paraxial mesoderm (arrowheads). (C) Dorsal view of a wild-type embryo at the 7-somite stage demonstrating *fbn2* expression in the notochord (arrow) and somites, with foci of increased staining near notochord-somite boundaries (arrowheads). (D) Lateral view of a wild-type embryo at the 20-somite stage with *fbn2* expression in the region of the developing caudal vein (arrowhead) and eye (arrow). (E) Lateral view of a wild-type embryo at 24 hpf with hypochord (arrow) and prominent fin fold expression (arrowheads). (F-J) *fbn2* expression is dramatically reduced in *pfd*^{gw1} mutants at all stages analyzed. (K) RT-PTCR for fibrillin-2 (*fbn2*) or spadetail (*spt*) using RNA from embryos at the indicated developmental stages. Unfert. = unfertilized.

Fig. 8. *fbn2* expression in frozen sections (A-C), and at high-power magnification in a whole-mount specimen (D). (A) Cross-section through the head of a wild-type embryo at the 20-somite stage demonstrating *fbn2* expression in the lens placodes (arrowheads). (B) Cross-section through the trunk of a wild-type embryo at the 20-somite stage

demonstrating *fbn2* expression in the notochord (n), floorplate (arrow), hypochord (arrowhead), and paraxial mesoderm (p). (C) Cross-section through the trunk of a wild-type embryo at 24 hpf demonstrating *fbn2* expression in the hypochord (arrow) and fin fold (arrowheads). The plane of section is schematized for A-C. (D) Dorsal view of a wild-type embryo at 24 hpf demonstrating *fbn2* expression in two parallel lines of fin fold cells.

Fig. 9. *pfd*^{gw1} heterozygote embryos exhibit an intermediate level of *fbn2* expression. (A-C) Clutches from *pfd*^{gw1}/+ intercrosses were subjected to whole-mount in situ hybridization at the 20-somite stage using probes to *fbn2*, photographed, and then genotyped. *fbn2* expression is robust in wild-type embryos (A), dramatically reduced in mutant embryos (C), and intermediate in heterozygote embryos (B).

Fig. 10. Morpholino knockdown of *fbn2* recapitulates the *pfd*^{gw1} phenotype. (A) Wild-type embryos injected with 2.4 ng of control morpholino exhibit normal notochord (black arrow), caudal vein (white arrow), and fin fold formation (arrowheads). (B) Embryos injected with 2.4 ng of a start morpholino targeting *fbn2* develop notochord kinks (black arrows), a cavernous caudal vein with loss of the usual reticular venous plexus (white arrow), and fin fold attenuation (arrowheads). The caudal vein and fin fold abnormalities in *fbn2* morphants are better appreciated at higher magnification (D vs. C). (E, F) Ventral views demonstrating truncal edema with skin distention in wild-type fish injected with *fbn2* morpholino (F, arrowheads) but not control morpholino (E, arrowheads). (G, H) *pfd*^{gw1} mutants injected with control morpholino (G) or *fbn2* morpholino (H) are indistinguishable. All embryos were treated with PTU to inhibit

melanin pigmentation and photographed at 30 hpf. Embryos in G and H were photographed and then genotyped.

Table 1. *pfd*^{gw1} mutants are sensitized to pharmacologic inhibition of lysyl oxidase. Embryos were treated as indicated and scored for notochord phenotype at 30 hpf. Embryos with mild notochord herniation events in β-aminopropionitrile were scored as normal (if wild-type) or mild (if *pfd*). Data shown are the pooled results of four independent experiments.

Table 2. Genetic interaction between *loxl5b* and the *pfd*^{gw1} locus. Embryos were injected with morpholino as indicated and the number of live embryos sorted to new dishes at 10 hpf noted; these embryos were scored for notochord phenotype at 30 hpf. The number of sorted embryos that were either dead or dysmorphic at 30 hpf is also noted. Data shown are the pooled results of three independent experiments.

Table 3. Morpholino knockdown of *fbn2* consistently recapitulates the *pfd*^{gw1} mutant phenotype. Wild-type embryos were injected with morpholino as indicated and the number of live embryos sorted to new dishes at 10 hpf noted; these embryos were scored for the *pfd*^{gw1} mutant phenotype at 30 hpf. The number of sorted embryos that were either dead or dysmorphic at 30 hpf is also noted. Data shown are the pooled results of three or more independent experiments.

S. Fig. 1. Protein sequence alignment of zebrafish fibrillin-2 with human, mouse, and rat orthologues. Conserved elements are highlighted using colors as follows: predicted furin cleavage sites, purple (2); EGF-like domains (3), light gray; hybrid motifs (2), red; TB domains (7), blue; calcium-binding EGF-like domains (43), dark gray;

glycine-rich domain (1), gold; potential *N*-glycosylation sites (12-13), green; RGD motifs (2), yellow. The number of times each element is observed is in parentheses.

S. Fig. 2. Partial sequence of zebrafish fibrillin-4. (A) Nucleotide sequence with the predicted translation start site highlighted in red. EST sequence from EE319589 is in small caps and is supported by BAC CT027715. Sequence in pink is inferred from Zv7_scaffold988. All other sequence was cloned, suggesting that CT027715 should be joined to Zv7_scaffold988 in the physical genome assembly. (B) Protein sequence derived from translation of the nucleotide sequence in A.

S. Fig. 3. Protein sequence alignment of zebrafish, *Xenopus laevis*, and human fibrillins. Conserved elements are highlighted using colors as follows: predicted furin cleavage sites, purple; EGF-like domains, light gray; hybrid motifs, red; TB domains, blue; calcium-binding EGF-like domains, dark gray; internal unique domains (glycine-rich, proline-rich, proline/glycine-rich or proline/glutamine-rich), gold; RGD motifs, yellow.

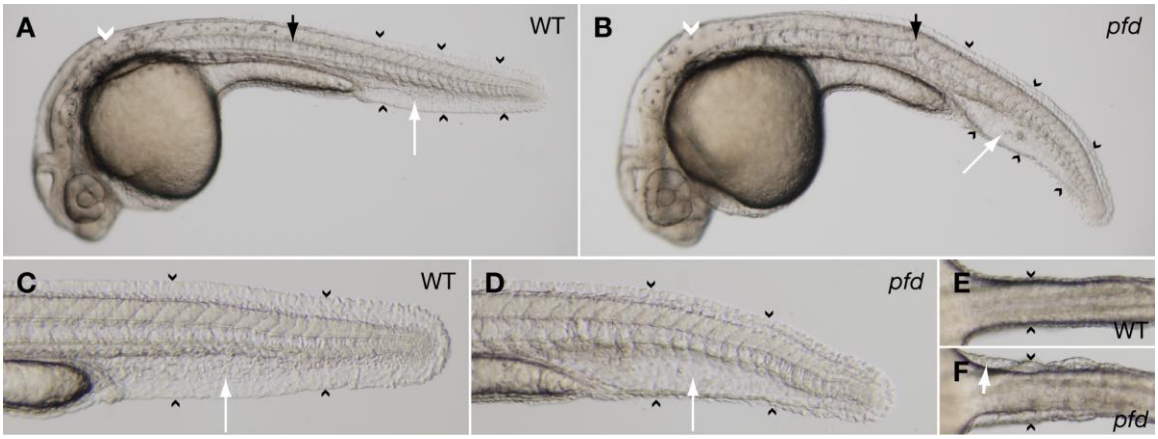

Figure 1

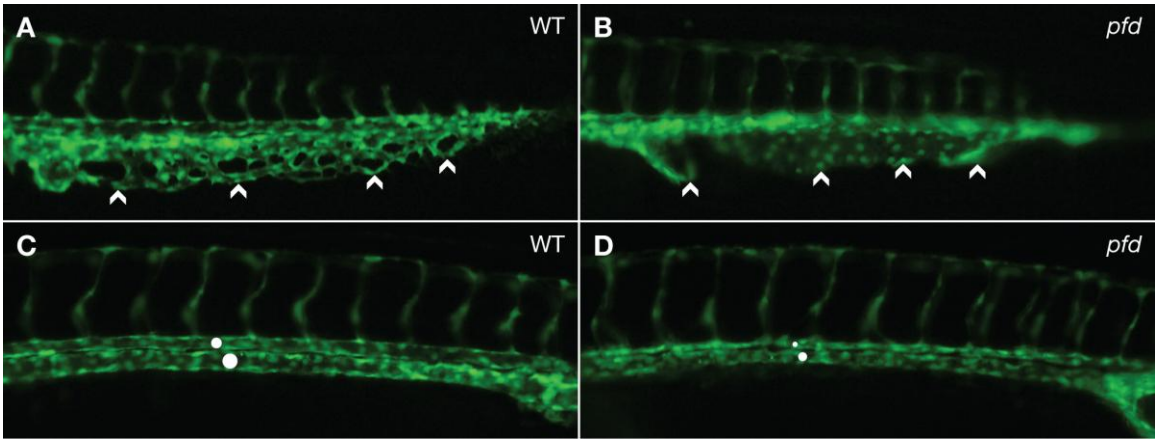

Figure 2

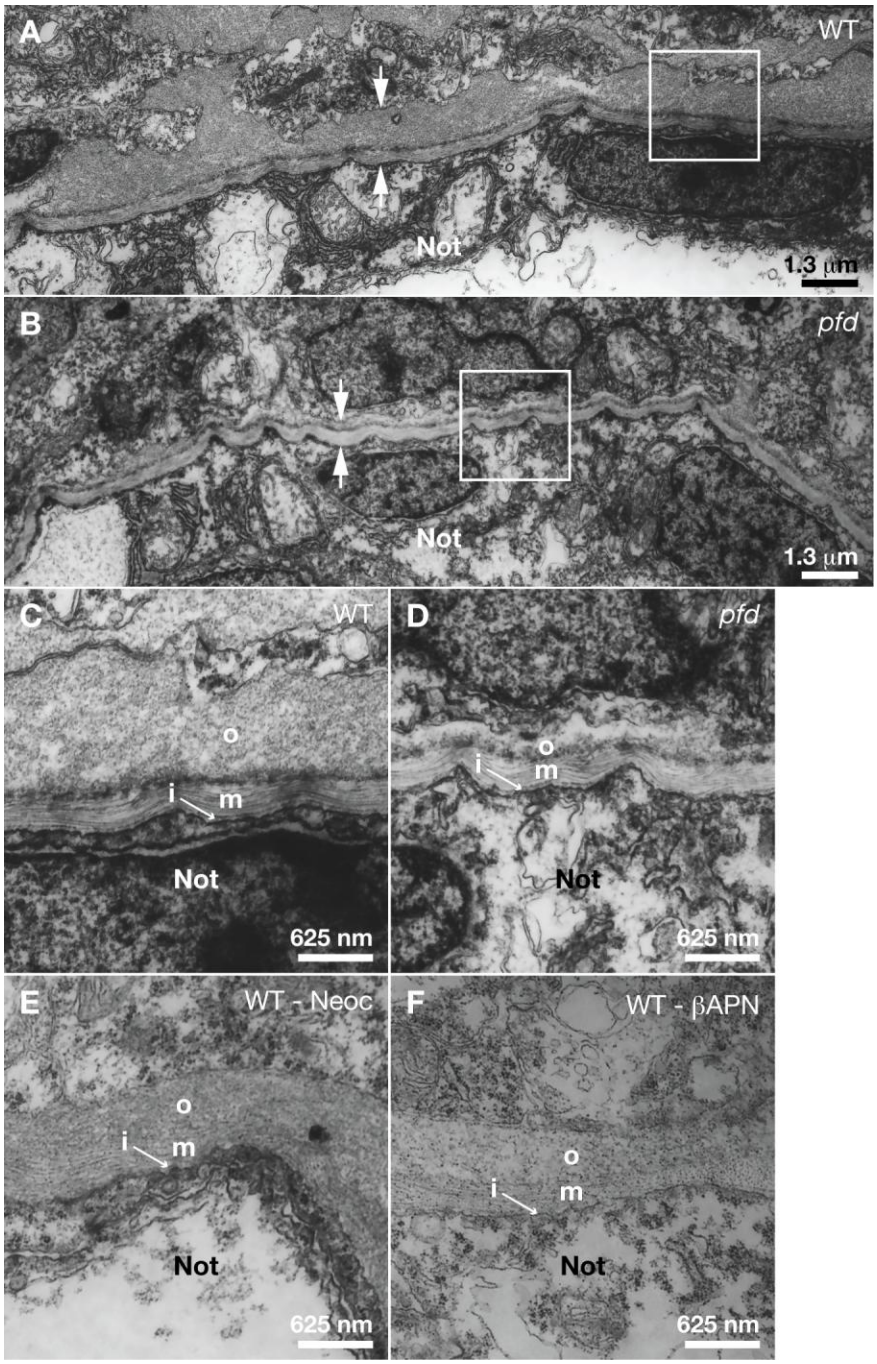
A
WT
Not
1.3 μm
B
pfd
Not
1.3 μm
C
WT
o
i
m
Not
625 nm
D
pfd
o
i
m
Not
625 nm
E
WT - Neoc
o
i
m
Not
625 nm
F
WT - βAPN
o
m
i
Not
625 nm

Figure 3

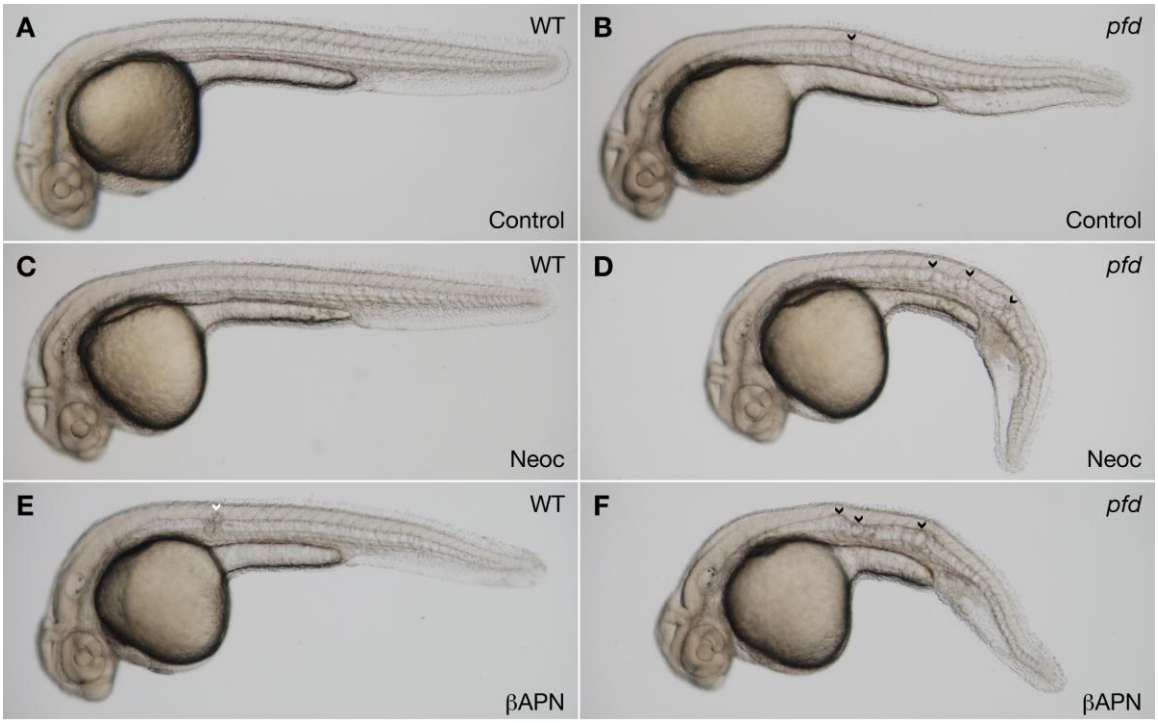
A
WT
Control
B
pfd
Control
C
WT
Neoc
D
pfd
Neoc
E
WT
βAPN
F
pfd
βAPN

Figure 4

Pharmacologic treatment	**Observed Phenotype**			
	Wild-type		***pfd* mutant**	
	Normal	**Worse**	**Mild**	**Severe**
None	110 (**100%**)	0 (**0%**)	33 (**97%**)	1 (**3%**)
Neocuproine (2 μM)	114 (**99%**)	1 (**1%****)	0 (**0%**)	35 (**100%***)
β-aminopropionitrile (1 mM)	114 (**96%**)	5 (**4%****)	1 (**3%**)	31 (**97%***)

*p < 0.01 vs. no treatment by 1-way ANOVA

**p not significant vs. no treatment by 1-way ANOVA

Table 1

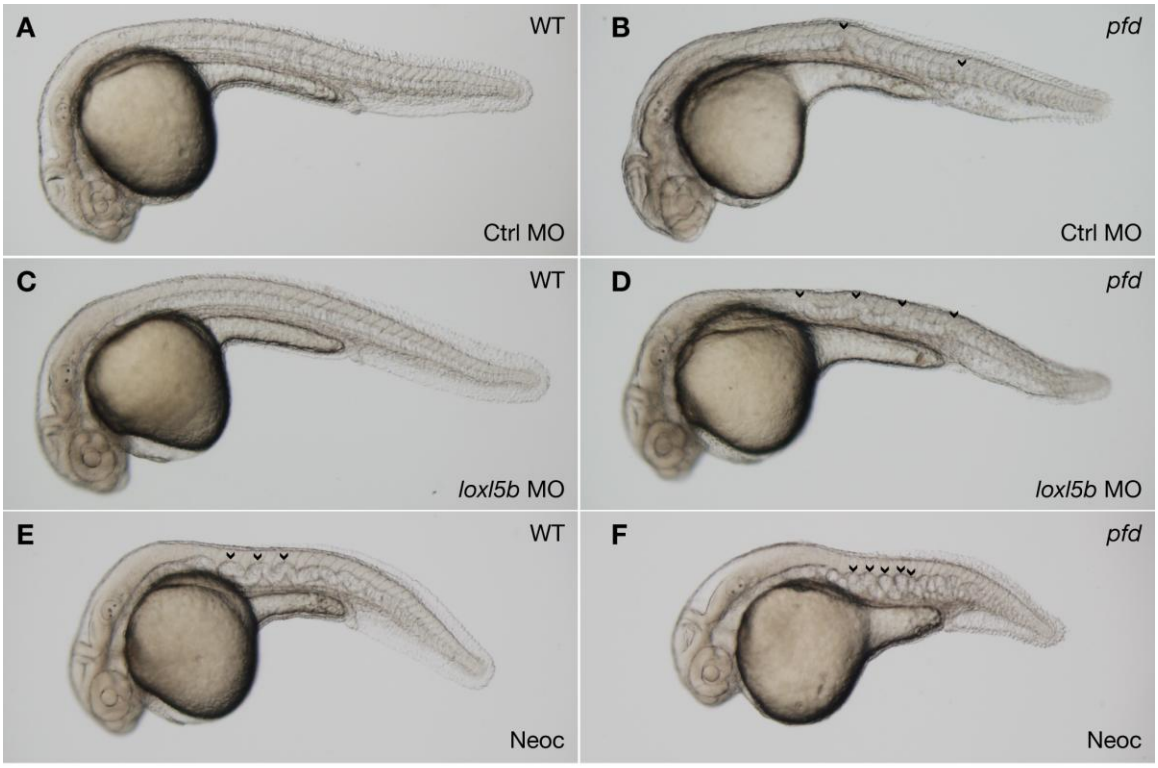
A
WT
Ctrl MO
B
pfd
Ctrl MO
C
WT
loxl5b MO
D
pfd
loxl5b MO
E
WT
Neoc
F
pfd
Neoc

Figure 5

Specific Morphol-ino	Dose of Morphol-ino (ng)	Embryos injected (#)	Embryos sorted/ scored (#)	Dead or dysmorphic embryos (#)	Observed Phenotype			
					Wild-type		*pfd*	
					Normal	Worse	Mild	Severe
Control	5	280	191	13	135 (**100%**)	0 (**0%**)	41 (**95%**)	2 (**5%**)
loxl5b	5	300	222	13	143 (**88%**)	19 (**12%***)	3 (**6%**)	44 (**94%*†**)

*p < 0.01 vs. no treatment by 1-way ANOVA
†p < 0.05 vs. wild-type by 1-way ANOVA

Table 2

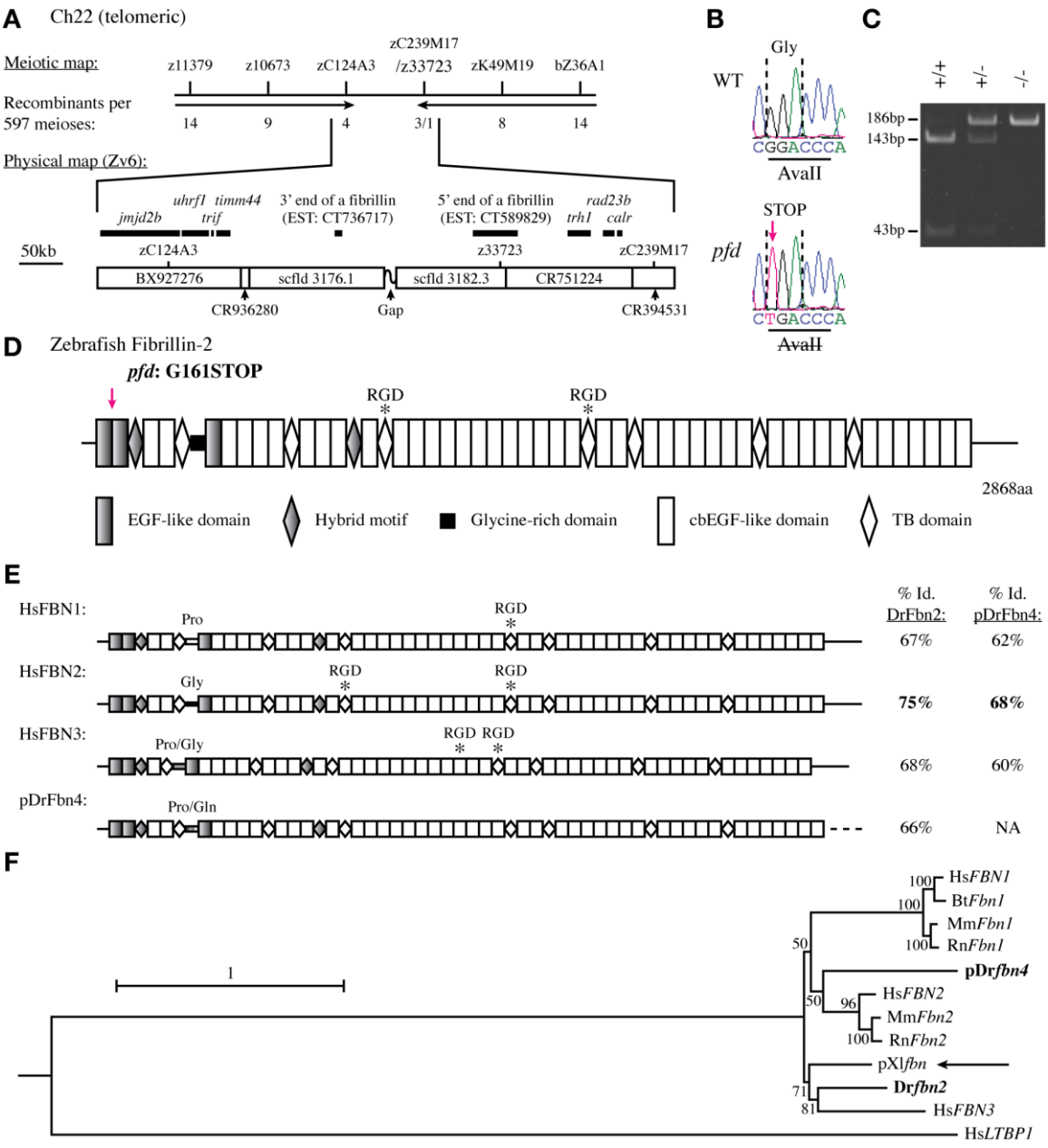
A
Ch22 (telomeric)
Meiotic map:
z11379
z10673
zC124A3
zC239M17
/z33723
zK49M19
bZ36A1
Recombinants per
597 meioses:
14
9
4
3/1
8
14
Physical map (Zv6):
jmjd2b
uhrf1
timm44
trif
3' end of a fibrillin
(EST: CT736717)
5' end of a fibrillin
(EST: CT589829)
trh1
rad23b
calr
50kb
zC124A3
z33723
zC239M17
BX927276
scfld 3176.1
scfld 3182.3
CR751224
CR936280
Gap
CR394531
B
WT
Gly
CGGACCCA
AvaII
pfd
STOP
CTGACCCA
AvaII
C
+/+
+/-
-/-
186bp
143bp
43bp
D
Zebrafish Fibrillin-2
pfd: G161STOP
RGD
RGD
2868aa
EGF-like domain
Hybrid motif
Glycine-rich domain
cbEGF-like domain
TB domain
E
% Id.
DrFbn2:
% Id.
pDrFbn4:
HsFBN1:
Pro
RGD
67%
62%
HsFBN2:
Gly
RGD
RGD
75%
68%
HsFBN3:
Pro/Gly
RGD RGD
68%
60%
pDrFbn4:
Pro/Gln
66%
NA
F
1
100
HsFBN1
100
BtFbn1
MmFbn1
50
100
RnFbn1
pDrfbn4
50
96
HsFBN2
MmFbn2
100
RnFbn2
pXlfbn
71
Drfbn2
81
HsFBN3
HsLTBP1

Figure 6

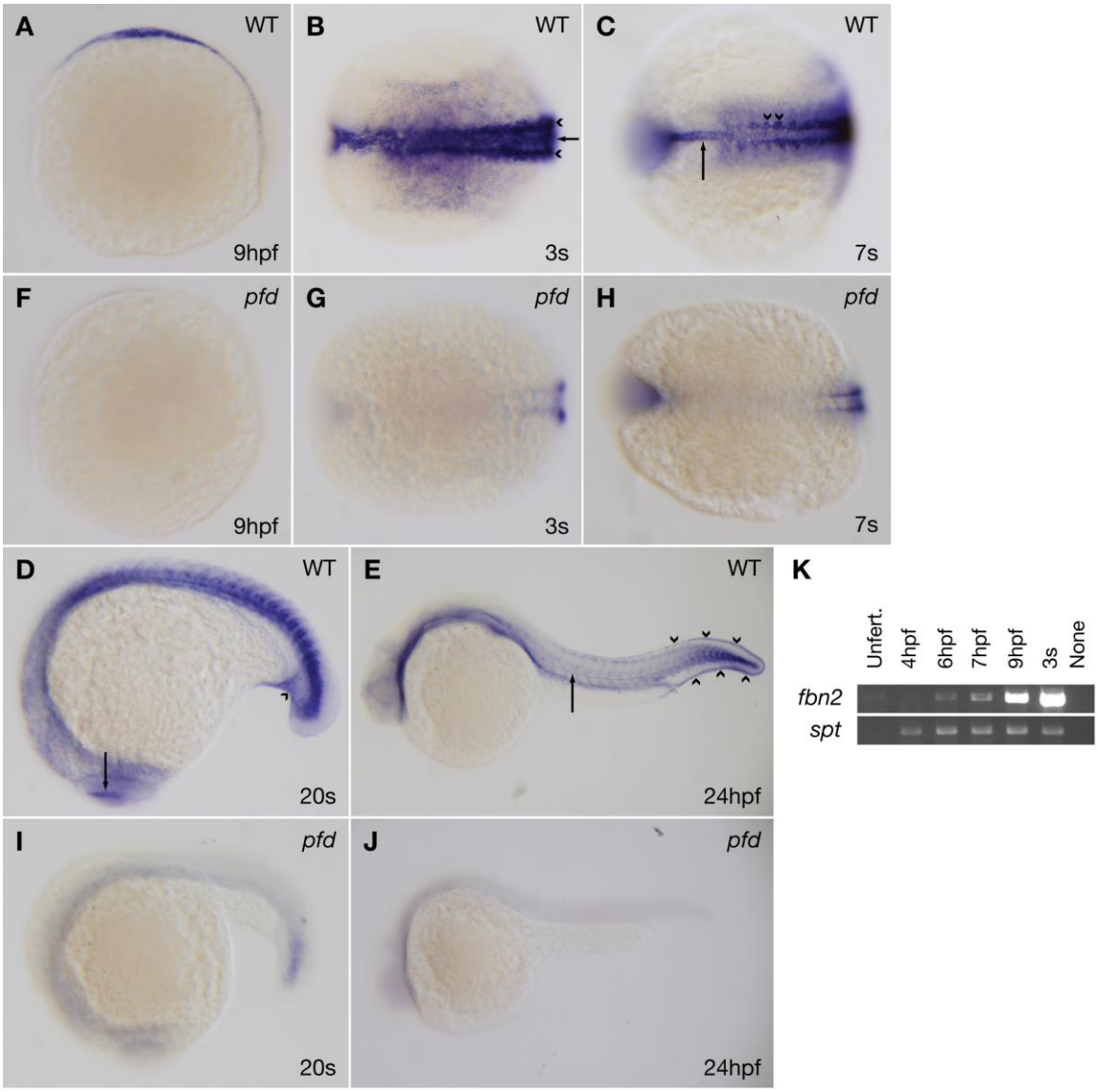
A
WT
9hpf
B
WT
3s
C
WT
7s
F
pfd
9hpf
G
pfd
3s
H
pfd
7s
D
WT
20s
E
WT
24hpf
K
Unfert.
4hpf
6hpf
7hpf
9hpf
3s
None
fbn2
spt
I
pfd
20s
J
pfd
24hpf

Figure 7

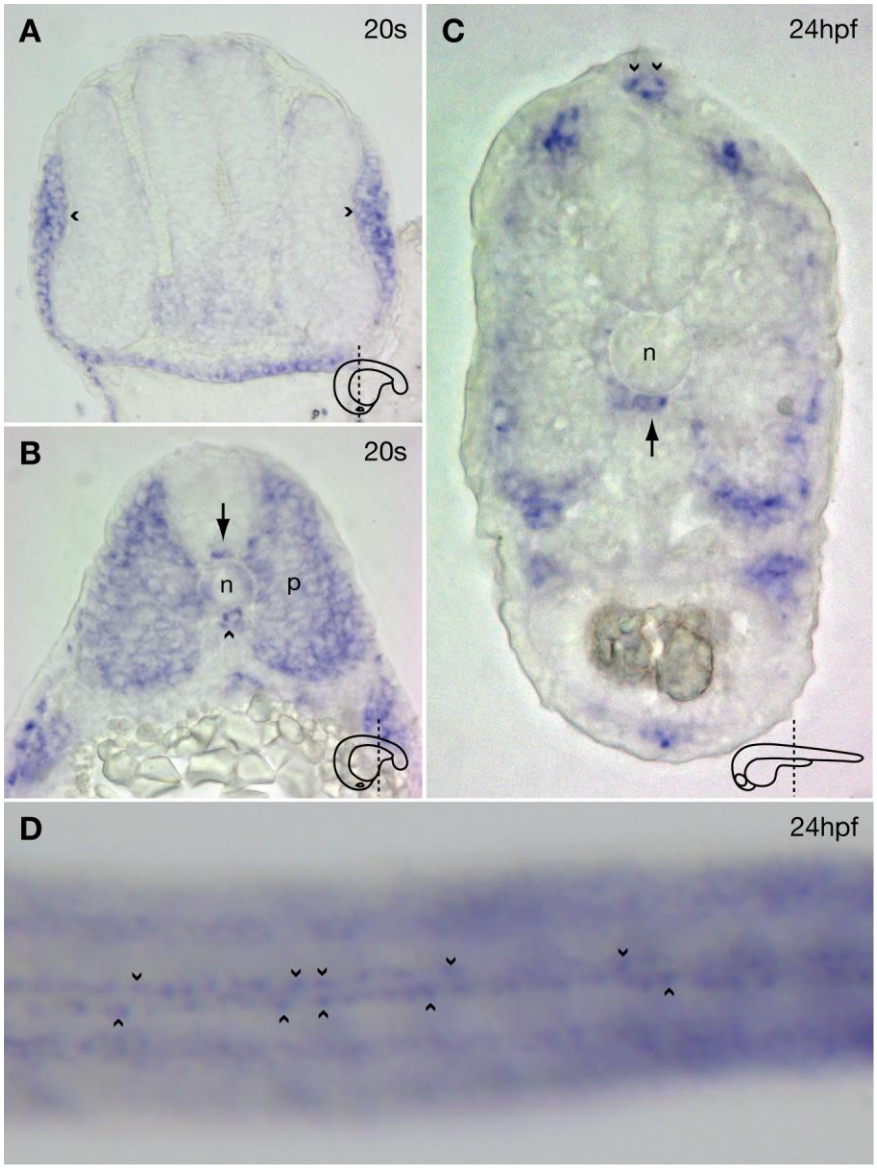

Figure 8

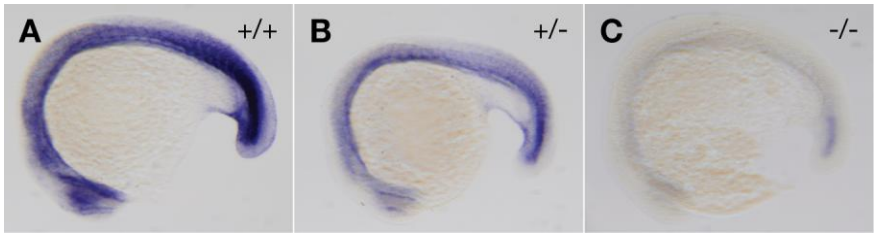

Figure 9

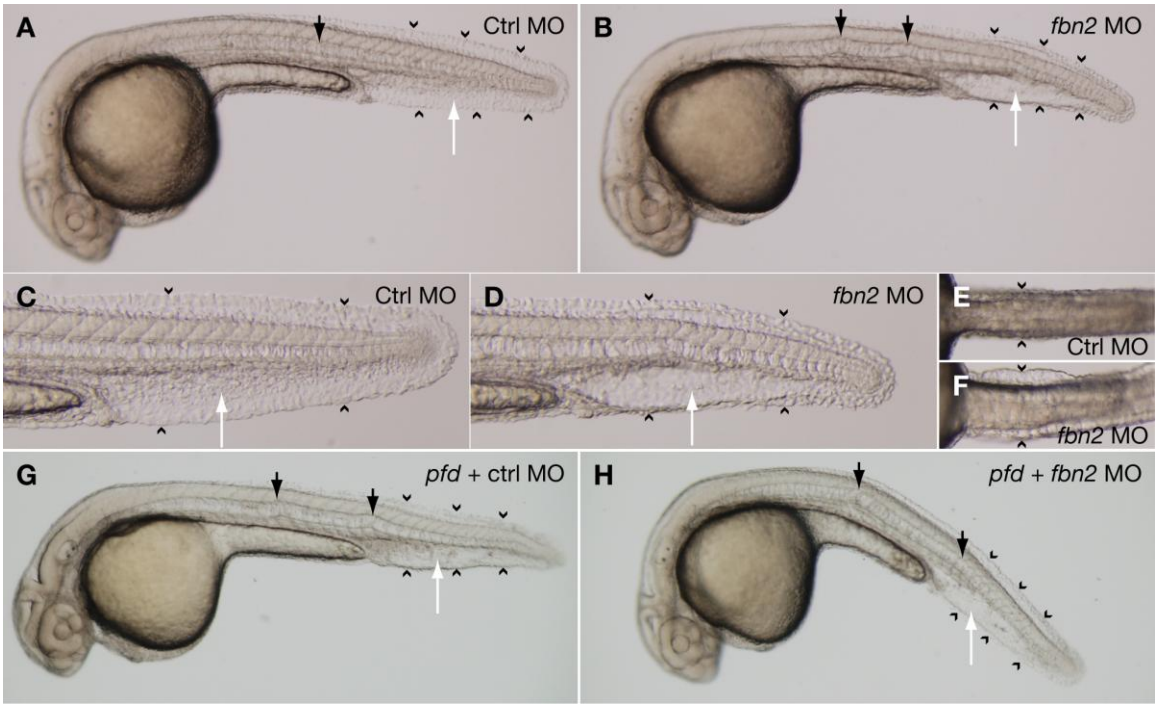
A
Ctrl MO
B
fbn2 MO
C
Ctrl MO
D
fbn2 MO
E
Ctrl MO
F
fbn2 MO
G
pfd + ctrl MO
H
pfd + fbn2 MO

Figure 10

Specific Morpholino	Dose of morpholino (ng)	Embryos injected (#)	Embryos sorted/ scored (#)	Dead or dysmorphic embryos (#)	Observed Phenotype	
					Wild-type	Mutant
Control	7.2	533	377	39	338 (**100%**)	0 (**0%**)
***fbn2* (start)**	2.4	545	406	33	8 (**2%**)	365 (**98%***)
***fbn2* (start)**	0.12	320	212	37	175 (**100%**)	0 (**0%****)

*p < 0.01 vs. control by 1-way ANOVA

**p not significant vs. control by 1-way ANOVA

Table 3

```
DrFbn2          MGVWK----------LANVVLWWA---------------------AVHSVQGQGDGDIQA 29
HsFBN2          MGRRRRLCLQLYFLWLGCVVLWAQGTAGQPQPPPPKPPRPQPPPQQVRSATAGSEGGFLA 60
MmFBN2          MGRRRRLCLQPYFVWLGCVALWAQGTDGQPQPPPPKTLRPQPPPQQVRPAVAGSEGGFMG 60
RnFBN2          MGRRRRLCLRPYFVWLGCVALWAQGTDGQPQPPPPKTLRPQPPPQQVRPAGAS-EGGFAG 59
                **  :          *. *.**                        *:.. .  :*.: .

DrFbn2          SRFTGKPEGEVQQRVRRRGQ-ESLRGPNVCGSRFHSYCCPGWKTLPGGNQCIVPICRNSC 88
HsFBN2          PEYREE-GAAVASRVRRRGQQDVLRGPNVCGSRFHSYCCPGWKTLPGGNQCIVPICRNSC 119
MmFBN2          PEYRDE-GAVAASRVRRRGQQEILRGPNVCGSRFHSYCCPGWKTLPGGNQCIVPICRNSC 119
RnFBN2          PEYRDE-GALAASRVRRRGQQEILRGPNVCGSRFHSYCCPGWKTLPGGNQCIVPICRNSC 118
                ..:  :  . . .******* : ************************************

DrFbn2          GDGFCSRPNMCTCSSGHLAPSCGAAAVQSCSVRCMNGGMCNEDACSCQKGYTGTHCGQPV 148
HsFBN2          GDGFCSRPNMCTCSSGQISSTCGSKSIQQCSVRCMNGGTCADDHCQCQKGYIGTYCGQPV 179
MmFBN2          GDGFCSRPNMCTCSSGQISPTCGAKSIQQCSVRCMNGGTCADDHCQCQKGYIGTYCGQPV 179
RnFBN2          GDGFCSRPNMCTCSSGQISPTCGGKSIQQCSVRCMNGGTCADDHCQCQKGYIGTYCGQPV 178
                ****************:::.:**. ::*.********* * :* *.***** **:*****

DrFbn2          CESGCQNGGRCIGPNRCACVYGFTGPQCERDYRTGPCFTQVNNQMCQGQLSGIVCTKTLC 208
HsFBN2          CENGCQNGGRCIGPNRCACVYGFTGPQCERDYRTGPCFTQVNNQMCQGQLTGIVCTKTLC 239
MmFBN2          CENGCQNGGRCIGPNRCACVYGFTGPQCERDYRTGPCFTQVNNQMCQGQLTGIVCTKTLC 239
RnFBN2          CETGCQNGGRCIGPNRCACVYGFTGPQCERDYRTGPCFTQVNNQMCQGQLTGIVCTKTLC 238
                **.*************************************************:*********

DrFbn2          CATIGRAWGHPCEMCPAQPHPCRRGFIPNIRTGACQDVDECQAVPGLCAGGNCINTVGSY 268
HsFBN2          CATIGRAWGHPCEMCPAQPQPCRRGFIPNIRTGACQDVDECQAIPGICQGGNCINTVGSF 299
MmFBN2          CATIGRAWGHPCEMCPAQPQPCRRGFIPNIRTGACQDVDECQAIPGLCQGGNCINTVGSF 299
RnFBN2          CATIGRAWGHPCEMCPAQPQPCRRGFIPNIRTGACQDVDECQAIPGLCQGGNCINTVGSF 298
                ******************:**********************:**:* **********:

DrFbn2          ECKCPAGHRQSETNQKCEDIDECATISGVCDGGECTNTAGSYVCTCPRGYITSTDGSRCV 328
HsFBN2          ECRCPAGHKQSETTQKCEDIDECSIIPGICETGECSNTVGSYFCVCPRGYVTSTDGSRCI 359
MmFBN2          ECRCPAGHKQSETTQKCEDIDECSVIPGVCETGDCSNTVGSYFCLCPRGFVTSTDGSRCI 359
RnFBN2          ECRCPAGHKQSETTQKCEDIDECSVVPGICETGDCSNTVGSYFCLCPRGFVTSTDGSRCI 358
                **:*****:****.*********: :.*:*: *:*:**.***.* ****::********:

DrFbn2          DHRIGTCFSSLANGRCASELSGQYTKMQCCCDTGRCWALGHIPEMCPVRGSDEYRRLCIQ 388
HsFBN2          DQRTGMCFSGLVNGRCAQELPGRMTKMQCCCEPGRCWGIGTIPEACPVRGSEEYRRLCMD 419
MmFBN2          DQRAGTCFSGLVNGRCAQELPGRMAKAQCCCEPGRCWSIGTIPEACPVRGSEEYRRLCLD 419
RnFBN2          DQRTGTCFSGLVNGRCAQELPGRMAKAQCCCEPGRCWGIGTIPEACPVRGSEEYRRLCLD 418
                *:* * ***.*.*****.**.*: :* ****:.****.:* *** ******:******::

DrFbn2          RLPFG--TGNGGIIHDGNGGLN------IGGYGKGPS--QNGNGGGGYIYGSEHTFTNGN 438
HsFBN2          GLPMGGIPGSAGSRPGGTGGNGFAPSGNGNGYGPGGTGFIPIPGGNGFSPGVGGAGVGAG 479
MmFBN2          GLPMGGIPGSSVSRPGGTGST-------GNGYGPGGTGFLPIPGDNGFSPGVGGAGVGAG 472
RnFBN2          GLPMGGIPGSSVSRPGGSGSN-------SNGYGPGGTGFLPIPGGNGFSPGVGGAGVGAG 471
                 **:*  .*..    .*.*.         .*** * :      *..*:  *   : ....

DrFbn2          GNGGQKIQISQLNETTIDVCKHFTNLCLNGRCIPTPTSYRCECNMGYRQDVRGECIDVDE 498
HsFBN2          GQGPIITGLTILNQT-IDICKHHANLCLNGRCIPTVSSYRCECNMGYKQDANGDCIDVDE 538
MmFBN2          GQGPIITGLTILNQT-IDICKHHANLCLNGRCIPTVSSYRCECNMGYKQDANGDCIDVDE 531
RnFBN2          GQGPIITGLTILNQT-IDICKHHANLCLNGRCIPTVSSYRCECNMGYKQDANGDCIDVDE 530
                *:*     :: **:* **:***.:*********** :**********:**..*:******

DrFbn2          CVSNPCVNGDCVNTQGSYHCKCHEGYQGTPTKQACIDIDECIVNGVMCRNGRCVNTDGSF 558
HsFBN2          CTSNPCTNGDCVNTPGSYYCKCHAGFQRTPTKQACIDIDECIQNGVLCKNGRCVNTDGSF 598
MmFBN2          CTSNPCSNGDCVNTPGSYYCKCHAGFQRTPTKQACIDIDECIQNGVLCKNGRCVNTDGSF 591
RnFBN2          CTSNPCSHGDCVNTPGSYYCKCHAGFQRTPTKQACIDIDECIQNGVLCKNGRCVNTDGSF 590
                *.**** :****** ***:**** *:* ************** ***:*:***********

DrFbn2          QCICNAGFEISPDGKNCIDHDECATTNMCLNGMCINEDGSFKCICKPGFALAPNGRYCTD 618
HsFBN2          QCICNAGFELTTDGKNCVDHDECTTTNMCLNGMCINEDGSFKCICKPGFVLAPNGRYCTD 658
MmFBN2          QCICNAGFELTTDGKNCVDHDECTTTNMCLNGMCINEDGSFKCVCKPGFILAPNGRYCTD 651
RnFBN2          QCICNAGFELTTDGENCVGHDECTTTNMCLNGMCINEDGSFKCVCKPGFVLAPNGRCCTD 650
                *********::.**:**:.****:******************:***** ****** ***
```

```
DrFbn2          IDECHTSGICMNGRCVNTEGSFRCECPPGLAIDVDGRVCVDTHMRTTCYGAIKMGVCSRP 678
HsFBN2          VDECQTPGICMNGHCINSEGSFRCDCPPGLAVGMDGRVCVDTHMRSTCYGGIKKGVCVRP 718
MmFBN2          VDECQTPGICMNGHCINNEGSFRCDCPPGLAVGVDGRVCVDTHMRSTCYGEIKKGVCVRP 711
RnFBN2          VDECQTPGICMNGHCINNEGSFRCDCPPGLAVGVDGRVCVDTHMRSTCYGEIKKGVCVRP 710
                :***:*.******:*:*.******:******:.:***********:**** ** *** **

DrFbn2          FPGAVTKSECCCANPEHGFGEPCQPCPAFNSAEFQAVCSSGPGITTDGRDINECALDPDI 738
HsFBN2          FPGAVTKSECCCANPDYGFGEPCQPCPAKNSAEFHGLCSSGVGITVDGRDINECALDPDI 778
MmFBN2          FPGAVTKSECCCANPDYGFGEPCQPCPAKNSAEFHGLCSSGIGITVDGRDINECALDPDI 771
RnFBN2          FPGAVTKYECCCANPDYGFGEPCQPCPAKNSAEFHGLCSGGVGITVDGRDINECALDPDI 770
                ******* *******::*********** *****:.:**.* ***.**************

DrFbn2          CQNGICENLRGSYRCICNIGYESDASGKNCVDINECLVNRLLCDNGMCRNTPGSYTCSCP 798
HsFBN2          CANGICENLRGSYRCNCNSGYEPDASGRNCIDIDECLVNRLLCDNGLCRNTPGSYSCTCP 838
MmFBN2          CANGICENLRGSYRCNCNSGYEPDASGRNCIDIDECLVNRLLCDNGLCRNTPGSYSCTCP 831
RnFBN2          CANGICENLRGSYRCNCNSGYEPDASGRNCIDIDECLVNRLLCDNGLCRNTPGSYSCTCP 830
                * ************* ** ***.****:**:**:************:********:*:**

DrFbn2          KGFSFKADSETCEDINECDSNPCINGICRNIAGSFNCECSHGSKLDSTNTVCVDSMKGTC 858
HsFBN2          PGYVFRTETETCEDINECESNPCVNGACRNNLGSFNCECSPGSKLSSTGLICIDSLKGTC 898
MmFBN2          PGYVFRTETETCEDVNECESNPCVNGACRNNLGSFHCECSPGSKLSSTGLICIDSLKGTC 891
RnFBN2          PGYVFRTETETCEDVNECESNPCVNGACRNNLGSFHCECSPGSKLSSTGLICIGSLKGTC 890
                 *: *::::*****:***:****:** ***  ***:**** ****.**. :*:.*:****

DrFbn2          WLNIQDGRCEVNINGATLKSECCSTLGAAWGSPCERCEIDPACSKGFGRMKGLVCEDINE 918
HsFBN2          WLNIQDSRCEVNINGATLKSECCATLGAAWGSPCERCELDTACPRGLARIKGVTCEDVNE 958
MmFBN2          WLNIQDNRCEVNINGATLKSECCATLGAAWGSPCERCELDAACPRGFARIKGVTCEDVNE 951
RnFBN2          WLNIQDNRCEVNINGATLKSECCATLGTAWGSPCERCELDAACPRGFARIKGVTCEDVNE 950
                ******.****************:***:**********:*.**.:*:.*:**:.***:**

DrFbn2          CEVFPGVCTNGRCVNTQGSFRCECPEGLTLDGAGRTCVDVRSEQCYMKWDEDECVEPLPG 978
HsFBN2          CEVFPGVCPNGRCVNSKGSFHCECPEGLTLDGTGRVCLDIRMEQCYLKWDEDECIHPVPG 1018
MmFBN2          CEVFPGVCPNGRCVNSKGSFHCECPEGLTLDGTGRVCLDIRMEHCFLKWDEDECIHPVPG 1011
RnFBN2          CEVFPGVCPNGRCVNNKGSFHCECPEGLTLDGTGRVCLDVRMEHCFLKWDEDECVHPVPG 1010
                ********.******.:***:**********:**.*:*:* *:*::*******:.*:**

DrFbn2          RYRVDMCCCTVGAAWGVDCEACPKPNTNEFKTICPRGPGIANRGDILTGRPFYKDVNECK 1038
HsFBN2          KFRMDACCCAVGAAWGTECEECPKPGTKEYETLCPRGAGFANRGDVLTGRPFYKDINECK 1078
MmFBN2          KFRMDACCCAVGAAWGTECEECPKPGTKEYETLCPRGPGFANRGDILTGRPFYKDINECK 1071
RnFBN2          KFRMDACCCAVGAAWGTECEECPKPGTKEYETLCPRGPGFANRGDILTGRPFYKDINECK 1070
                ::*:* ***:******.:** ****.*:*::*:****.*:*****:*********:****

DrFbn2          VFRGLCTHGTCRNTIGSFKCRCDSGFALTMEERNCTDIDECTISPDLCGHGVCVNTPGSF 1098
HsFBN2          AFPGMCTYGKCRNTIGSFKCRCNSGFALDMEERNCTDIDECRISPDLCGSGICVNTPGSF 1138
MmFBN2          AFPGMCTYGKCRNTIGSFKCRCNNGFALDMEERNCTDIDECRISPDLCGSGICVNTPGSF 1131
RnFBN2          ALPGMCTYGKCRNTIGSFKCRCNSGFALDMEERNCTDIDECRISPDLCGNGICVNTPGSF 1130
                .: *:**:*.************:.**** ************ ******* *:********

DrFbn2          ECECFDGYESGFMMMKNCMDIDECERDPLLCRGGTCLNTEGSYECDCPPGHQLSTEASAC 1158
HsFBN2          ECECFEGYESGFMMMKNCMDIDECERNPLLCRGGTCVNTEGSFQCDCPLGHELSPSREDC 1198
MmFBN2          ECECFEGYESGFMMMKNCMDIDECERNPLLCRGGTCVNTEGSFQCDCPLGHELSPSREDC 1191
RnFBN2          ECECFEGYESGFMMMKNCMDIDECERNPLLCRGGTCVNTEGSFQCDCPLGHELSPSREDC 1190
                *****:********************:*********:*****::**** **:**.. . *

DrFbn2          EDVNECQLSDNLCKHGQCVNMVGTYQCSCETGYQVTPDRQGCVDIDECTIMNGGCDTHCT 1218
HsFBN2          VDINECSLSDNLCRNGKCVNMIGTYQCSCNPGYQATPDRQGCTDIDECMIMNGGCDTQCT 1258
MmFBN2          VDINECSLSDNLCRNGKCVNMIGTYQCSCNPGYQATPDRQGCTDIDECMIMNGGCDTQCT 1251
RnFBN2          IDINECSLSDNLCRNGKCVNMIGTYQCSCNPGYQATPDRQGCSDIDECMIMNGGCDTQCT 1250
                 *:***.******::*:****:*******:.***.******* ***** ********:**

DrFbn2          NSEGSYECSCSEGYALMPDLRTCADIDECEDTPDICDGGQCTNIPGEYRCLCYDGFMASM 1278
HsFBN2          NSEGSYECSCSEGYALMPDGRSCADIDECENNPDICDGGQCTNIPGEYRCLCYDGFMASM 1318
MmFBN2          NSEGSYECSCSEGYALMPDGRSCADIDECENNPDICDGGQCTNIPGEYRCLCYDGFMASM 1311
RnFBN2          NSEGSYECSCSEGYALMPDGRSCADIDECENNPDICDGGQCTNIPGEYRCLCYDGFMASM 1310
                ****************** *:********:.**************************
```

```
DrFbn2          DMRTCIDVNECDLNPNICLHGDCENTKGSFICHCQLGYFVKKGSTGCTDVDECEIGAHNC 1338
HsFBN2          DMKTCIDVNECDLNSNICMFGECENTKGSFICHCQLGYSVKKGTTGCTDVDECEIGAHNC 1378
MmFBN2          DMKTCIDVNECDLNPNICMFGECENTKGSFICHCQLGYSVKKGTTGCTDVDECEIGAHNC 1371
RnFBN2          DMKTCIDVNECDLNPNICMFGECENTKGSFICHCQLGYSVKKGATGCTDVDECEIGAHNC 1370
                **:***********.***:.*:**************** ****:****************

DrFbn2          DLHAACVNAPGSFKCRCRDGWEGDGIKCIDVDECVTEEHNCNPNAECLNTPGSYRCSCKE 1398
HsFBN2          DMHASCLNIPGSFKCSCREGWIGNGIKCIDLDECSNGTHQCSINAQCVNTPGSYRCACSE 1438
MmFBN2          DMHASCLNVPGSFKCSCREGWVGNGIKCIDLDECANGTHQCSINAQCVNTPGSYRCACSE 1431
RnFBN2          DMHASCLNVPGSFKCSCREGWVGNGIKCIDLDECANGTHQCSINAQCVNTPGSYRCACSE 1430
                *:**:*:* ****** **:** *:******:*** .  *:*. **:*:********:*.*

DrFbn2          GFNGDGFSCSDMDECADNVNLCENGQCLNAPGGYRCECEMGFTPTEDSKACQDIDECNFQ 1458
HsFBN2          GFTGDGFTCSDVDECAENINLCENGQCLNVPGAYRCECEMGFTPASDSRSCQDIDECSFQ 1498
MmFBN2          GFTGDGFTCSDVDECAENTNLCENGQCLNVPGAYRCECEMGFTPASDSRSCQDIDECSFQ 1491
RnFBN2          GFTGDGFTCSDVDECAENINLCENGQCLNVPGAYRCECEMGFTPASDSRSCQDIDECSFQ 1490
                **.****:***:****:* **********.**.***********:.**::*******.**

DrFbn2          NICVFGSCQNLPGMFRCVCDYGYELDRSGGNCTDINECFDPVNCINGVCVNLPGSYLCNC 1518
HsFBN2          NICVFGTCNNLPGMFHCICDDGYELDRTGGNCTDIDECADPINCVNGLCVNTPGRYECNC 1558
MmFBN2          NICVFGTCNNLPGMFHCICDDGYELDRTGGNCTDIDECADPINCVNGLCVNTPGRYECNC 1551
RnFBN2          NICVFGTCNNLPGMFHCICDDGYGLDRTGGHCTDIDECADPINCVNGLCVNTPGRYECNC 1550
                ******:*:******:*:** ** ***:**:****:** **:**:**:*** ** * ***

DrFbn2          PPDFELNPSGVGCVDTRVGNCFLDTLDRGDGGISCSAEIGVGVTRASCCCSLGGAWGNPC 1578
HsFBN2          PPDFQLNPTGVGCVDNRVGNCYLKFGPRGDGSLSCNTEIGVGVSRSSCCCSLGKAWGNPC 1618
MmFBN2          PPDFQLNPTGVGCVDNRVGNCYLKFGPRGDGSLSCNTEVGVGVSRSSCCCSLGKAWGNPC 1611
RnFBN2          PPDFQLNATGVGCVDNRVGNCYLKFGPRGDGSLSCKTEVGVGVSCSSCCCSLGKAWGNPC 1610
                ****:**.:******.*****:*.   ****.:**.:*:****: :******* ******

DrFbn2          ELCPFVNSTEYKTLCPGGEGFRPNPITVILEDIDECQELPGLCQGGNCVNTFGSFQCECP 1638
HsFBN2          ETCPPVNSTEYYTLCPGGEGFRPNPITIILEDIDECQELPGLCQGGNCINTFGSFQCECP 1678
MmFBN2          ETCPPVNSTEYYTLCPGGEGFRPNPITIILEDIDECQELPGLCQGGNCINTFGSFQCECP 1671
RnFBN2          ETCPPVNSTEYYSLCPGGEGFRPNQITIILEDIDECQELPGLCQGGNCINTFGSFQCECP 1670
                * ** ****** :*********** **:*********************:***********

DrFbn2          AGYYLNEETRICEDIDECTAHIGICGPGTCYNTLGNYTCVCPPEYMQVNGGNNCMDMRKS 1698
HsFBN2          QGYYLSEDTRICEDIDECFAHPGVCGPGTCYNTLGNYTCICPPEYMQVNGGHNCMDMRKS 1738
MmFBN2          QGYYLSEETRICEDIDECFAHPGVCGPGTCYNTLGNYTCICPPEYMQVNGGHNCMDMRKS 1731
RnFBN2          QGYYLSEETRICEDIDECFAHPGVCGPGTCYNTLGNYTCICPPEYMQVNGGHNCMDMRKS 1730
                 ****.*:********** ** *:***************:***********:********

DrFbn2          VCYRNFN-DTCENELSFNMTKKMCCCAYNVGKAWNRPCEACPTPATSEYQLLCGNQAPGF 1757
HsFBN2          FCYRSYNGTTCENELPFNVTKRMCCCTYNVGKAWNKPCEPCPTPGTADFKTICGN-IPGF 1797
MmFBN2          FCYRSYNGTTCENELPFNVTKRMCCCTYNVGKAWNKPCEPCPTPGTADFKTICGN-IPGF 1790
RnFBN2          FCYRSYNGTTCENELPFNVTKRMCCCTYNVGKAWNKPCEPCPTPGTADFKTICGN-IPGF 1789
                .***.:*  ******.**:**:****:********:***.****.*:::: :***  ***

DrFbn2          IIDIHTGKPIDIDECREIPGICANGVCINQIGSFRCECPMGFSYNNILLICEDIDECNSG 1817
HsFBN2          TFDIHTGKAVDIDECKEIPGICANGVCINQIGSFRCECPTGFSYNDLLLVCEDIDECSNG 1857
MmFBN2          TFDIHTGKAVDIDECKEIPGICANGVCINQIGSFRCECPTGFSYNDLLLVCEDIDECSNG 1850
RnFBN2          TFDIHTGKAVDIDECKEIPGICANGVCINQIGSFRCECPTGFSYNDLLLVCEDIDECSNG 1849
                 :******.:******:********************** *****::**:*******..*

DrFbn2          DNLCQRNANCINIPGSYRCECSAGFKLSPSGACIDRNECQEIPNVCSHGECIDTQGSFRC 1877
HsFBN2          DNLCQRNADCINSPGSYRCECAAGFKLSPNGACVDRNECLEIPNVCSHGLCVDLQGSYQC 1917
MmFBN2          DNLCQRNADCINSPGSYRCECAAGFKLSPNGACVDRNECLEIPNVCSHGLCVDLQGSYQC 1910
RnFBN2          DNLCQRNADCINSPGSYRCECAAGFKLSPNGACVDRNECLEIPNVCSHGLCVDLQGSYQC 1909
                ********:*** ********:*******.***:***** ********* *:* ***::*

DrFbn2          LCHNGFKTTPDQTMCMDIDECDRQPCGNGTCKNTVGSYNCLCFPGFELTHNNDCMDIDEC 1937
HsFBN2          ICHNGFKASQDQTMCMDVDECERHPCGNGTCKNTVGSYNCLCYPGFELTHNNDCLDIDEC 1977
MmFBN2          ICNNGFKASQDQTMCMDVDECERHPCGNGTCKNTVGSYNCLCYPGFELTHNNDCLDIDEC 1970
RnFBN2          ICNNGFKASQDQTMCMDVDECERHPCGNGTCKNTVGSYNCLCYPGFELTHNNDCLDIDEC 1969
                :*:****:: *******:***:*:******************:***********:*****
```

```
DrFbn2          SVHASQVCRNGQCINNMGSFKCLCLDGYNLTPDGKNCVDINECVTLPGACQPGTCQNLDG 1997
HsFBN2          SSFFGQVCRNGRCFNEIGSFKCLCNEGYELTPDGKNCIDTNECVALPGSCSPGTCQNLEG 2037
MmFBN2          SSFFGQVCRNGRCFNEIGSFKCLCNEGYELTPDGKNCIDTNECVALPGSCSPGTCQNLEG 2030
RnFBN2          SSFFGQVCRNGRCFNEIGSFKCLCNEGYELTPDGKNCIDTNECVALPGSCSPGTCQNLEG 2029
                * . .******:*:*::******* :**:********:* ****:***:*.*******:*

DrFbn2          SFRCICPPGYEVQNDKCVDINECNVEPNICQFGTCKNTPGSFQCICQPGFVLSDNGRRCF 2057
HsFBN2          SFRCICPPGYEVKSENCIDINECDEDPNICLFGSCTNTPGGFQCLCPPGFVLSDNGRRCF 2097
MmFBN2          SFRCICPPGYEVRSENCIDINECDEDPNICLFGSCTNTPGGFQCICPPGFVLSDNGRRCF 2090
RnFBN2          SFRCICPPGYEVKSENCIDINECDEDPNICLFSSCTNTPGGFQCICPPGFVLSDNGRRCF 2089
                ************:.::*:*****: :**** *.:*.****.***:* *************

DrFbn2          DTRESFCFTRFEAGKCSVPKPRNTTKAKCCCSLLPGEGWGDPCELCPRDTEEAAFHTLCP 2117
HsFBN2          DTRQSFCFTNFENGKCSVPKAFNTTKAKCCCSKMPGEGWGDPCELCPKD-DEVAFQDLCP 2156
MmFBN2          DTRQSFCFTNFENGKCSVPKAFNTTKAKCCCSKMPGEGWGDPCELCPKD-DEVAFQDLCP 2149
RnFBN2          DTRQSFCFTNFENGKCSVPKAFNTTKAKCCCSKMPGEGWGDPCELCPKD-DEVAFQDLCP 2148
                ***:*****.** *******. ********** :**************:* :*.**: ***

DrFbn2          YGHEAVP-KPEGREDMNECVENPEICGNGLCINTDGSFRCECPFGYNLDYTGVNCVDTDE 2176
HsFBN2          YGHGTVPSLHDTREDVNECLESPGICSNGQCINTDGSFRCECPMGYNLDYTGVRCVDTDE 2216
MmFBN2          YGHGTVPSLHDTREDVNECLESPGICSNGQCINTDGSFRCECPMGYNLDYTGVRCVDTDE 2209
RnFBN2          YGHGTVPSLHDTREDVNECLESPGICSNGQCINTDGSFRCECPMGYNLDYSGVRCVDTDE 2208
                *** :**   : ***:***:*.* **.** *************:******:**.******

DrFbn2          CSIGNPCGNGTCSNVPGGFECSCQEGFEPGPMMTCEDINECAVNPLLCAFRCVNTFGSYE 2236
HsFBN2          CSIGNPCGNGTCTNVIGSFECNCNEGFEPGPMMNCEDINECAQNPLLCAFRCMNTFGSYE 2276
MmFBN2          CSIGNPCGNGTCTNVIGSFECTCNEGFEPGPMMNCEDINECAQNPLLCAFRCMNTFGSYE 2269
RnFBN2          CSIGNPCGNGTCANVIGSFECNCNEGFEPGPMMNCEDINECAQNPLFCAFRCMNTFGSYE 2268
                ************:** *.***.*:**********.******** ***:*****:*******

DrFbn2          CMCPTGYVLRDDNRMCRDQDECAEGLDDCASRGMACKNQIGTFMCICPPGMTRRPDGEGC 2296
HsFBN2          CTCPIGYALREDQKMCKDLDECAEGLHDCESRGMMCKNLIGTFMCICPPGMARRPDGEGC 2336
MmFBN2          CTCPVGYALREDQKMCKDLDECAEGLHDCESRGMMCKNLIGTFMCICPPGMARRPDGEGC 2329
RnFBN2          CTCPVGYALREDQKMCKDLDECAEGLHDCESRGMMCKNLIGTFMCICPPGMARRPDGEGC 2328
                * ** **.**:*::**:* *******.** **** *** ************:********

DrFbn2          MDLNECRSKPGICKNGRCVNTVGSYRCECNEGFEASATGTECIDNRKGFCFTEVLQTMCQ 2356
HsFBN2          VDENECRTKPGICENGRCVNIIGSYRCECNEGFQSSSSGTECLDNRQGLCFAEVLQTICQ 2396
MmFBN2          VDENECRTKPGICENGRCVNIIGSYRCECNEGFQSSSSGTECLDNRQGLCFAEVLQTMCQ 2389
RnFBN2          VDENECRTKPGICENGRCVNIIGSYRCECNEGFQSSSSGTECLDNRQGLCFAEVLQTMCQ 2388
                :* ****:*****:****** :***********::*::****:***:*:**:*****:**

DrFbn2          QSSTNRNTVTKSECCCNGGRGWGSLCELCPLPGTIQYKKMCPLGPGYTTDGRDINECEVM 2416
HsFBN2          MASSSRNLVTKSECCCDGGRGWGHQCELCPLPGTAQYKKICPHGPGYTTDGRDIDECKVM 2456
MmFBN2          MASSSRNLVTKSECCCDGGRGWGHQCELCPLPGTAQYKKICPHGPGYATDGRDIDECKVM 2449
RnFBN2          MASSSRNLVTKSECCCDGGRGWGHQCELCPLPGTAQYKKICPHGPGYATDGRDIDECKVM 2448
                 :*:.** ********:******  ********* ****:** ****:******:**:**

DrFbn2          PNLCKNGQCINSVGSFRCHCNVGYTNDFTGTSCIDMDECSQSPKPCNFLCKNTEGSYLCS 2476
HsFBN2          PNLCTNGQCINTMGSFRCFCKVGYTTDISGTSCIDLDECSQSPKPCNYICKNTEGSYQCS 2516
MmFBN2          PSLCTNGQCVNTMGSFRCFCKVGYTTDISGTACVDLDECSQSPKPCNFICKNTKGSYQCS 2509
RnFBN2          PSLCTNGLCVNTMGSFRCFCKVGYTTDISGTACVDLDECSQSPKPCNFICKNTEGSYQCS 2508
                *.**.** *:*::*****.*:****.*::**:*:*:***********::****:*** **

DrFbn2          CPRGYILQPDGKTCKDLDECSTKQHNCQFLCVNTIGGFTCKCPSGFTQHQTACIDNNECS 2536
HsFBN2          CPRGYVLQEDGKTCKDLDECQTKQHNCQFLCVNTLGGFTCKCPPGFTQHHTACIDNNECG 2576
MmFBN2          CPRGYVLQEDGKTCKDLDECQTKQHNCQFLCVNTLGGFTCKCPPGFTQHHTACIDNNECG 2569
RnFBN2          CPRGYVLQEDGKTCKDLDECQTKQHNCQFLCVNTLGGFTCKCPPGFTQHHTACIDNNECG 2568
                *****:** ***********.*************:********.*****:*********.

DrFbn2          NQPNICGSRASCLNSPGSFNCECQKGFSLDATGLNCDDVDECGGNHRCQHGCQNMMGGYR 2596
HsFBN2          SQPSLCGAKGICQNTPGSFSCECQRGFSLDATGLNCEDVDECDGNHRCQHGCQNILGGYR 2636
MmFBN2          SQPSLCGAKGICQNTPGSFSCECQRGFSLDASGLNCEDVDECDGNHRCQHGCQNILGGYR 2629
RnFBN2          SQPSLCGAKGICQNTPGSFSCECQRGFSLDASGLNCEDVDECDGNHRCQHGCQNILGGYR 2628
                .**.:**::. * *:****.****:******:****:*****.***********::****
```

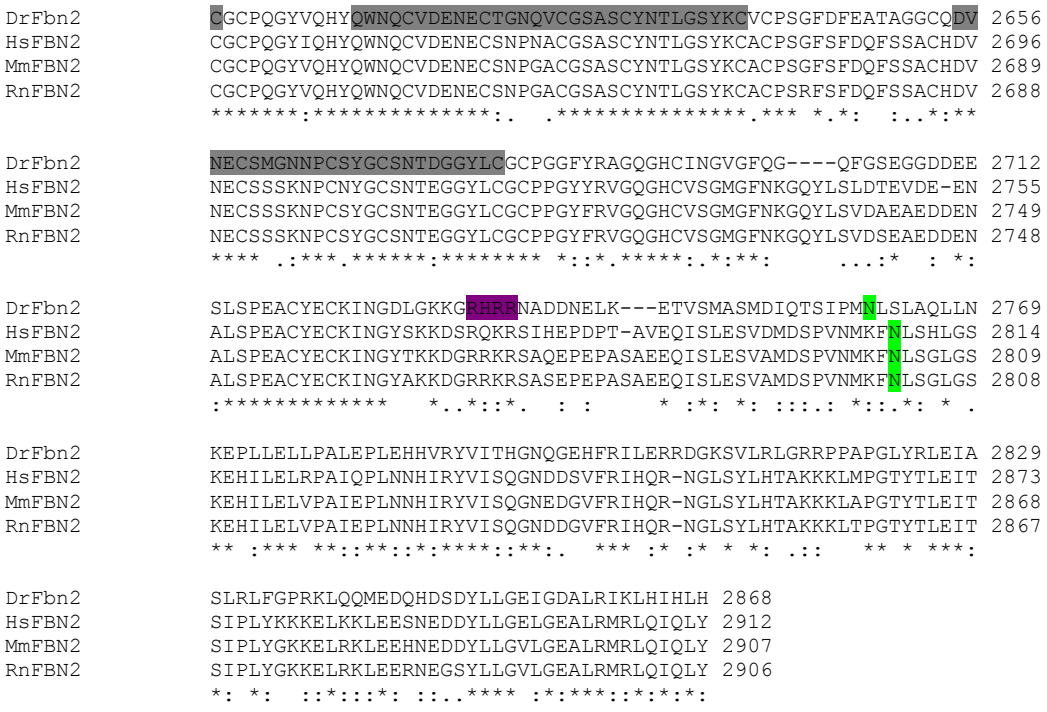

Supplementary Figure 1

A)

gaggatttaggagggaattgggaatatgacagtttcggtccggggttcccgggatctttaaaacaacgtagccaatcagctaatgtaataattaaccccttttat
taattgaatattttattgcgtttacgtttcatcagtcagtcgaacaaatatgcgctattcatattattattattatctggttaaattaaagaacgatttgctatagcaatac
ccattcactcaagagtgcagagagttttgtcgcgtccagctgctagtgggtaacgttaggatagattggtgctggctggcgtcatgattttatatcgttcagtca
aacgtttaggatcctccttcattctcttcactaagtgcgctcctcctgtacttcaattcttattcttgtagctttacttttctggtcaaaaaccggatatgttatgatttcc
ctttcatctcatggactaacagactgtaaaggtacactgggttaaattgcactaggatatatcatgtcatctcaggggggacctcaggtgtttatttggatttgttgct
ctgttgggaattttaacggggaaaatctctggaattcatggaaaagcaactgttcatattgatggatcacagagacgccaaaaacaagagtccctgagaggc
cctaatgtgtgtggatctcgtctGCAGTCCTTCTGTTGTCCAGGCTGGAAGACTCTGCCTGGGGGCAACCAGT
GTGTTGTGCCTATTTGCCGGAGTGACTGTGGGGATGGTTTCTGCTCCAGACCTAACATGTGCA
CATGTCCTGGTGGACAAACAGCTACAACCTGTTTTACTAAATCATCCAAACAATGCAAAATAA
GGTGTATGAATGGAGGAGTGTGTGAAGATGACTATTGTCAGTGTCCAAAGGGATATACAGGA
AGCTTTTGTGGACAACCTGTCTGTGAAAAAAACTGTCAGAATGGTGGACACTGCATTGGACCG
AACAGATGCGCGTGTGGATACGGCTTCACTGGACCACAGTGTGAGAGAGACTACCGGACAGG
CCCATGCTTCATCCAAGTGCACAGCAGGAAGTGTGCAGGTCAGAGCAGTGAATTTGTTTGCAG
TAAGGCCTTGTGCTGTGCCACAGTGGGTCAAGCGTGGGGTCACTCGTGCGAGCAGTGCCCACC
TATCAGCTCGCCCTGCACCAGAGGGTTCATCCCAAACACCCGCACAGGAGCCTGCCAAGATGT
TGATGAATGCAAGGTTGTCCCCGATCTGTGTAAAGGAGGAAGATGCATCAACACATTGGGTTC
ATATCAGTGCACGTGTCCTGTCGGTTACCAACAGCATGTGAGCATTTTGAAGTGCGAGGATGT
GGATGAATGCTCCACCATTGAACGTGCGTGTGAAGCGGGACACTGCATTAATTCGGCGGGCA
GTTTCTCCTGTGTGTGTCCTTCTGGATATGTGCTGTCTGCAGACCGGACTCGCTGTCTTGACCA
GCACACAGGGATCTGCTTTGCGTCAGTTGTGAATGGACGCTGTGCTCATGAAATCAGCGGACG
TTTCAATAAAATCCAGTGCTGCTGTGATCGTGGCCGGTGCTGGAGTCAAAGAACAACTCATGA
AATGTGTCCTGTACCAGGATCAGATGAATACTTGAGGATTTGTCTGGTAGGCTCTGCTCTGAG
TGGCTACAATGAGGAGGATCCTGAAATGAGCCCTCACCACCACAGCAGCTTCAGTGTTTCCCC
TAATGACCAGATACTTCACCCACATAATGGCAATGGACAAATAAAACCCCAGATTCGCCAAA
CACCTCAAATTCTGCAGTTTCCACAGATTCCACAGATCCCAAGGCATGACAATGGATTTAAAC
CACAACGACCTGTTGTTAGTGTGAATGAGACTGTGAACAGGTGCCGTTTGCTTCCTAATTTGT
GTCTGAATGGACGCTGTATTCCCATGGAGTCTGACTACCGATGTGACTGTAACACCGGATTCA
AAGAAGACAACAGAGGAGAGTGCTCAGATGTAGATGAGTGTGAGTTTGACCCCTGTGCTAAT
GGAAACTGCATCAACACTCCTGGTTCCTACTACTGCAGATGCCACACAGGCTTTCTTAGGGTT
ACAGGCAAACAAACCTGCATAGATATTGATGAATGTCTTCAGAATGGAGTGCTCTGTAAGAA
CGGCCGCTGTCTGAACACTGAGGGAAGCTTTCAGTGCATCTGCAACTCTGGATTTAAGCTTTC
ACCTGATGGGAGAAACTGTGTAGATCATGATGAATGTGCCGCCACAAACATGTGTCTTAACGG
CATGTGTATTAACGAAGACGGCAGCTTTAAATGTGTGTGTAAACCTGGATTCACCCTCAACTC
TAGTGGACGATACTGTACAGAAATCGATGAGTGCCGGACTCCAGGTGTGTGCATGAATGGAC
GATGTGTAAACACACAGGGCTCTTTCAGGTGTGAGTGTTTTGCAGGTCTTACTGTTGGAATAG
ACGGCCGAACATGTGTAGACACACACATGCGTAGCACCTGTTATGGGGCTGTAAAAAGAGGT
TTGTGTTTACGACCCTTCCAGCGTGCTGTCACCAAGTCACAGTGCTGCTGTGCCAACCCTGACT
ATGCCTTCGGTGAACCCTGCCATCCCTGCCCTGCCAAACACTCAGCTGAGTTTCAGGTCTTGTG
TGCGAGCGGTGTTGGATTTTCTGCTGATGGCAAAGACATTAATGAGTGCGCTCTGGATCCGGA
TATCTGCTCAAATGGAGTGTGTGAGAATCTCCGAGGAAATTTCCGCTGCATCTGTAACATTGG
CTATGAAAGTGACCAGAGCGGCAGAAACTGTTTAGATATTGATGAATGTGTGGTGAACAGTCT
CCTCTGTGATAATGGCCTGTGCCGGAATGTTCCAGGAAGCTACAGTTGCACCTGCCCGGCGGG
GTTCATCTTCAGACATGACACAGAGACATGTGAGGATGTGAATGAGTGTGTGAGCAGCCCAT
GCGTCAATGGAGTGTGTAAAAACAGTGCAGGCTCTTTCTACTGTGAATGTTCACAAGGAAGTA
AACTGGACAGCACTGGACTTTTATGTGTTGACAGTGTGAAGGGTTCATGCTGGTTAACTCTTC
AGGATGGTCGTTGTGAAGTTAACATCAACGGAGCTACACTGAGATCACAGTGCTGTGCCACAC
TAGGATTGGCGTGGGGCAGCCCATGTGAACCATGTCAAACTGATCTAGTGTGCGAACGAGGA
TTTGCTCGGTCAAGAGGGGCTTCATGTGAAGATGTGAATGAATGTGAGGTGTTTCCTGGTGTG
TGTCACAATGGACACTGTGTGAACACTAGAGGCTCATTTAAATGTCAGTGCCCAGAAAGCCTC
ACACTGGATGTCACTGGACGCCTCTGTGTTGATGTTCGTTCAGAGCCGTGCTTTCTTACTTACG
AAGAAGATGTGTGTACACAGCCGGTACCAGGACGCTTCCGCATGGACATGTGTTGCTGTACGG
TGGGTTTGGCTTGGGGCAAAGATTGTGACTTATGTCCTGAGCCTGGTACTCGGCAGTTTGACA

CCCTGTGCCCAAGAGGACCAGGCTTCGCCAACAAAGGAGACGTGCTCACTGGCAGAGCTGTC
TATAAAGATATTAATGAGTGCAAAGTTTTCCAAAGCATTTGTGTCCATGGGAAATGTCGGAAC
ACCATTGGGAGCTTCAGATGTCGCTGTGATAGTGGATTTGCACTGGATACCAATGAGAAAAAC
TGCACAGATATTGACGAGTGCATGATCTCTCCTGATGTCTGTGGTCATGGCACATGTGTGAAC
ACTTTGGGCAGTTTCCAATGTGACTGTTTTCCTGGCTACGAAAGTGGAATCATGATGATGAAG
AACTGCATGGATATTGATGAATGTGAGCGTAACCTTTCACTGTGCAATGGAGGCACCTGTGAA
AACACTGACGGCAGCTACAAGTGTGTGTGTCCGCCTGGTCATCATCTGTCTGTGGATGGCAGT
GCCTGTGAAGACGTGAACGAGTGTGATCTGAGTAGCACACTTTGTCCTAATGGCTGGTGTGTG
AATTTGGTGGGAACCTACCAGTGCTCATGTAACTCTGGCTACCAGACGGCACCTGATTGGAAG
GGTTGCACAGATATAGATGAGTGCACAATAGAGAACGGAGGATGTGAGCTGTACTGTAGTAA
CTCAGAGGGCAGTTACTCCTGCAGCTGTGGTCAGGGTTACAGTCTCACGCCGGACCAGCGGAC
ATGTTCAGATGTGAATGAATGTGAAGAGGTTTTAGACATCTGTGAAGGTGGTCAGTGCACTAA
CGTTCCTGGAGCATATCATTGTTTGTGTTACGAAGGATTTATGGCTTCCGTGGACATGAAGAC
ATGTATTGATGTGAATGAGTGTGAACTGAACGACAACATCTGTGCATTTGGGGAGTGTGAGAA
CACCAAGGGTTCTTTCATCTGTCATTGTGACATAGGTTACGCCGTAAAAAAAGGAACCTCTGG
CTGCACTGATGTTAATGAGTGTGAGATTAACAGTCATAACTGTGACACACATGCCACCTGTGT
CAACACACCAGGACATTACCACTGCTCCTGCGGGGACGGATGGTTTGGAGATGGAGTCAAAT
GTGCTGATGTGGATGAGTGTGCTAACAGGACTAGCGTCTGCAGCGCTGATGCCGAGTGTGTGA
ACACAGCTGGCTCATACCACTGTGAATGTTCAGACGGGTTTATTGGAGACGGGGTTATCTGCT
CAGATTTGGATGAATGCGCTGAAGATGTGGATCTGTGTGAAAATGGCCAGTGTCTAAATGTTC
CTGGCAGCTATCGCTGTGAATGTGAGATGGGCTTCACACACACTTCAAACAGAAAAACCTGTC
GAGATATAGACGAGTGCTCCTTCCAGAACATCTGTGTGTTTGGCACATGTCAGAATATTCCAG
GAATGTTTCGCTGTATTTGTGATGAGGGGTATGAGCTGGACAGGACAGGTGGAAATTGCACA
GATGTGGACGAGTGTCTCGATTCCTTAAACTGTGTTAATGGTCACTGTGAGAACACAGCCGGC
TCGTACCAGTGTAACTGTCCTATTGACTTCGAGCTCAATCCTACTGGAATTGGATGCGTTGACA
CCCGGGTTGGAAACTGTTTTCTGGAGGTGGCGTACCATAGTAAGCTGGCATGTAGTGCTGAAA
TTGGATTTGGAGTCAGTCGTTCCTCATGTTGCTGTTCTCTGGGACGGGTGTGGGGTTACCCATG
TGACCACTGCCCTACACTCAACACCTCGGAATATAACACACTCTGTCCTGGAGGAGAGGGGTT
CAAACCCAACCCTGTCACCATCATCTTGGAAGATATCGATGAGTGTCAGGAGCTGCCCGGCCT
CTGTCAGGGTGGAAACTGTGTTAACACATTCGGAAGTTTCCAGTGTGAATGTCCAGCCGGATT
CTACCTTAACACACAGAGCCGCATCTGTGAAGATATCGATGAGTGTGTGCTCAGTTTGGGGGT
TTGTGGTCCAGGCACCTGCTACAACACACTGGGAAACTACACTTGTGTCTGTCCACAGGAATA
CATTCAGGTGAATGGAGGACACAGATGCATGGATATGAGGAAAAGTTTGTGCTATCGCAGCT
ACAATGGCAGTGCCTGTGAACATCAGCTCAACTTTAACATCACACACCGATTGTGTTGCTGTT
CCTACAATGTGGGAAAAGCCTGGAACAAGCCATGCCATGCCTGCCCGATACCTGGAACTGAT
GACTACAGCAGTCTTTGTGGCAGTGTGACTGGATTCTGGATCAACATTGCAACTGGAAAGCCA
AAAGATATTGACGAATGTCATGAAATCCCGGGAGTTTGTGCTCATGGTGTGTGTATAAACCAC
ATGGGCAGTTTCCACTGCGAGTGTCCCACTGGCTTCCTTTATAATGACCTGCTGCTCATCTGTG
AAGACATTGATGAATGCAGCAGCAGAGAGCCTGTGTGTCAGAGAAATGCAGACTGCATCAAC
CGTCCAGGCGGTTATCAGTGTGAATGTTCTGATGGGTATATACTCACACCTAATGGAGACTGT
AATGATCGTAATGAGTGCTTGGAGACACCCAGTGTGTGTCGTCATGGTGACTGTGTGGATATT
CCAGGAGGGTATGAGTGCATGTGCCACACCGGATTTACAGTAACACCAAACCGCAGGATGTG
TGTAGATGTCAATGAATGTTCACCTCAGCCGTGTGGGAATGGCACATGTAAAAACTCTGTTGG
ATCATTTAACTGTATCTGCCATCACGGATTTGAGCTCGCCACTAATAACTACTGTACAGATATC
GATGAGTGTGCAGTTTTTCACTCTCAGCTCTGCAGGAATGGTCGGTGTGTCAATAATGTGGGC
TCCTTCCAGTGTCTCTGTAGAGAAGGTTATGAACTCACTTTTGATGGCAAGACTTGTATGGATG
TTAATGAGTGTACAATCATTCCTGGGATATGTGCTCCTGGAACTTGTCTGAATCTGGATGGTTC
TTTCAGATGTGTCTGTCCTGATGGGTACATTGTCCAGAGTGATCACTGCGTAGATGTAAACGA
GTGTTCGGAGGAGCCTGGGATCTGCACATATGGGACCTGCTTCAACAGTCTGGGCAGCTTTGA
GTGTGTGTGTAAACCAGGATTTGTGCTGTCAGAAGATAAGCGCAGATGTTATGACACCAGAG
AGAGCTTCTGTTTCACACGCTTTGAGAACAGCAAGTGCTCTGTCCCGCAGGCGTTTAACACCA
CCAAAGCCAAGTGCTGCTGTAGTATCATGGCCAAGGAGGGCTGGGGCGACCCGTGTGAGCTG
TGCCCTAAAGAACATGATGCATTTCAGGATCTGTGCCCGTTTGGTCATGGGATCATTCCTGGT

GTTGGGGACACACGTGTAGATTTAAACGAGTGTGTGGAGAATCCAGAGATCTGTGTAAACGG
ACGCTGCATCAACATGGATGGTTCCTTTCGCTGTGAGTGTCCAGCAGGGTACACTCTTGACTA
CACAGGAACACATTGTGATGATATCGATGAATGTTCAGTGAGAAACCCATGTGGAAACGGCA
CGTGCTCCAATGTAATCGGGGCATTTGAGTGTTTGTGTGAAGAAGGATTTGAGCCTGGACCGA
TGATGAGCTGTGAAGATGTGAACGAATGTGGTCAGAATCCTCTGCTCTGTGCATTTCGCTGCA
TCAACACTTTCGGGAGTTATGAATGCAGCTGTCCATCTGGTTACACACTGAGAGAGGATGGAC
GCATGTGTCAAGATGTAGACGAGTGTGCAGAAGATCTTCATAACTGTGACTCCAGAGGAATG
GAATGTAGCAACCTAATTGGCACATTTATGTGTGTTTGTCCGGCCGGTATGATCCGCAGGATG
AGTGATGAGGCCTGTCAAGATGAAAATGAATGCTTGACTCAGCCTGGTGTTTGTGAAAATGGC
CGTTGTGTGAACACTGTTGGCAGCTACACTTGTGAATGTGGTGTTGGGTTCAAAACGGACTCA
TCAGCCACACAATGTCTTGATTACAGGAAAGGCTTCTGTTTCACTGAAGTTCTGCACACCATG
TGTCAGATGTCGTCCAGCAGTCGTGTTCCTGTCAGCAGGTCTCAGTGCTGCTGTAATGGAGGT
CATGGGTGGGGGGATCAGTGTGAGCTCTGCCCTCTGCCTGCCACTGCCAACTACAAAAAACTC
TGTCCATATGGTCATGGATACGCCATAGACGGAACAGATATAGATGAGTGTAAACTAATTCCA
GATGTCTGTGCCAATGGCGCTTGTATCAACATGATGGGCTCTTACAGATGCCACTGCAAACCA
GGATACATAGCATCTACTGCAGGAACCGCATGTGTTGATGTCGATGAATGTGGTATGTCTCCA
AAACCCTGTAACTTCATATGTAAGAACACCGAGGGCAGCTATGCATGTTCCTGTCCCCGTGGT
TACACTCTGCAGAATGACAACAGGTCATGCAAAGATGTGGATGAATGTCAGAGCAGACGACA
CAACTGCCAGTTCTCGTGCATGAACACCATCGGTGGATTCACATGCAAGTGTCCAGCAGGTTT
CAGCCAGCATCACAGAGCTTGCAGAGATATTGATGAATGTTTGTCAGACCTAACACCGTGTGG
CCTGCAAGGAGCATGTCAGAATTCAGTGGGAAGCTTCAGCTGTGAGTGTCCCCAGGGCTTCAG
TCTGGACTCTCTCGGCCACAACTGTGATGATGTAGATGAGTGTGCACGGGATCACAGGTGTCA
GTTCGGTTGTCAGAATGTTGCTGGAGGTTTTCGCTGCAGCTGTCCACAGGGTTACACACAACA
CCAGCAGTGGAACCAGTGTGTGGATGACAATGAGTGCTTGAACGCAGACAACTGTGGTTCAG
CTTCCTGTTTCAACACTTTGGGCAGTTTCAAGTGTGGCTGCCCATCTGGCTTCACCTTTGATCC
TGCATCTACTAGCTGTGAGGATGTAGACGAGTGCGGGTCCTTCATGAACCCCTGCAGATACGG
CTGCTCTAACACACAGGGTGGATTTGCGTGCGGGTGCCCAGCTGGTTATTACAGAGCAGGACA
GGG

B)

MSSQGDLRCLFGFVALLGILTGKISGIHGKATVHIDGSQRRQKQESLRGPNVCGSRLQSFCCPGWK
TLPGGNQCVVPICRSDCGDGFCSRPNMCTCPGGQTATTCFTKSSKQCKIRCMNGGVCEDDYCQCP
KGYTGSFCGQPVCEKNCQNGGHCIGPNRCACGYGFTGPQCERDYRTGPCFIQVHSRKCAGQSSEF
VCSKALCCATVGQAWGHSCEQCPPISSPCTRGFIPNTRTGACQDVDECKVVPDLCKGGRCINTLGS
YQCTCPVGYQQHVSILKCEDVDECSTIERACEAGHCINSAGSFSCVCPSGYVLSADRTRCLDQHTG
ICFASVVNGRCAHEISGRFNKIQCCCDRGRCWSQRTTHEMCPVPGSDEYLRICLVGSALSGYNEED
PEMSPHHHSSFSVSPNDQILHPHNGNGQIKPQIRQTPQILQFPQIPQIPRHDNGFKPQRPVVSVNETV
NRCRLLPNLCLNGRCIPMESDYRCDCNTGFKEDNRGECSDVDECEFDPCANGNCINTPGSYYCRC
HTGFLRVTGKQTCIDIDECLQNGVLCKNGRCLNTEGSFQCICNSGFKLSPDGRNCVDHDECAATN
MCLNGMCINEDGSFKCVCKPGFTLNSSGRYCTEIDECRTPGVCMNGRCVNTQGSFRCECFAGLTV
GIDGRTCVDTHMRSTCYGAVKRGLCLRPFQRAVTKSQCCCANPDYAFGEPCHPCPAKHSAEFQVL
CASGVGFSADGKDINECALDPDICSNGVCENLRGNFRCICNIGYESDQSGRNCLDIDECVVNSLLC
DNGLCRNVPGSYSCTCPAGFIFRHDTETCEDVNECVSSPCVNGVCKNSAGSFYCECSQGSKLDSTG
LLCVDSVKGSCWLTLQDGRCEVNINGATLRSQCCATLGLAWGSPCEPCQTDLVCERGFARSRGAS
CEDVNECEVFPGVCHNGHCVNTRGSFKCQCPESLTLDVTGRLCVDVRSEPCFLTYEEDVCTQPVP
GRFRMDMCCCTVGLAWGKDCDLCPEPGTRQFDTLCPRGPGFANKGDVLTGRAVYKDINECKVF
QSICVHGKCRNTIGSFRCRCDSGFALDTNEKNCTDIDECMISPDVCGHGTCVNTLGSFQCDCFPGY
ESGIMMMKNCMDIDECERNLSLCNGGTCENTDGSYKCVCPPGHHLSVDGSACEDVNECDLSSTL
CPNGWCVNLVGTYQCSCNSGYQTAPDWKGCTDIDECTIENGGCELYCSNSEGSYSCSCGQGYSLT
PDQRTCSDVNECEEVLDICEGGQCTNVPGAYHCLCYEGFMASVDMKTCIDVNECELNDNICAFGE
CENTKGSFICHCDIGYAVKKGTSGCTDVNECEINSHNCDTHATCVNTPGHYHCSCGDGWFGDGV
KCADVDECANRTSVCSADAECVNTAGSYHCECSDGFIGDGVICSDLDECAEDVDLCENGQCLNVP
GSYRCECEMGFTHTSNRKTCRDIDECSFQNICVFGTCQNIPGMFRCICDEGYELDRTGGNCTDVDE

CLDSLNCVNGHCENTAGSYQCNCPIDFELNPTGIGCVDTRVGNCFLEVAYHSKLACSAEIGFGVSR
SSCCCSLGRVWGYPCDHCPTLNTSEYNTLCPGGEGFKPNPVTIILEDIDECQELPGLCQGGNCVNTF
GSFQCECPAGFYLNTQSRICEDIDECVLSLGVCGPGTCYNTLGNYTCVCPQEYIQVNGGHRCMDM
RKSLCYRSYNGSACEHQLNFNITHRLCCCSYNVGKAWNKPCHACPIPGTDDYSSLCGSVTGFWINI
ATGKPKDIDECHEIPGVCAHGVCINHMGSFHCECPTGFLYNDLLLICEDIDECSSREPVCQRNADCI
NRPGGYQCECSDGYILTPNGDCNDRNECLETPSVCRHGDCVDIPGGYECMCHTGFTVTPNRRMCV
DVNECSPQPCGNGTCKNSVGSFNCICHHGFELATNNYCTDIDECAVFHSQLCRNGRCVNNVGSFQ
CLCREGYELTFDGKTCMDVNECTIIPGICAPGTCLNLDGSFRCVCPDGYIVQSDHCVDVNECSEEP
GICTYGTCFNSLGSFECVCKPGFVLSEDKRRCYDTRESFCFTRFENSKCSVPQAFNTTKAKCCCSIM
AKEGWGDPCELCPKEHDAFQDLCPFGHGIIPGVGDTRVDLNECVENPEICVNGRCINMDGSFRCEC
PAGYTLDYTGTHCDDIDECSVRNPCGNGTCSNVIGAFECLCEEGFEPGPMMSCEDVNECGQNPLL
CAFRCINTFGSYECSCPSGYTLREDGRMCQDVDECAEDLHNCDSRGMECSNLIGTFMCVCPAGMI
RRMSDEACQDENECLTQPGVCENGRCVNTVGSYTCECGVGFKTDSSATQCLDYRKGFCFTEVLH
TMCQMSSSSRVPVSRSQCCCNGGHGWGDQCELCPLPATANYKKLCPYGHGYAIDGTDIDECKLIP
DVCANGACINMMGSYRCHCKPGYIASTAGTACVDVDECGMSPKPCNFICKNTEGSYACSCPRGY
TLQNDNRSCKDVDECQSRRHNCQFSCMNTIGGFTCKCPAGFSQHHRACRDIDECLSDLTPCGLQG
ACQNSVGSFSCECPQGFSLDSLGHNCDDVDECARDHRCQFGCQNVAGGFRCSCPQGYTQHQQW
NQCVDDNECLNADNCGSASCFNTLGSFKCGCPSGFTFDPASTSCEDVDECGSFMNPCRYGCSNTQ
GGFACGCPAGYYRAGQG

Supplementary Figure 2

```
HsFBN1          ----------MRRGRLLEIALGFT----------------------VLLASYTSHGADAN 28
HsFBN2          MGRRRRLCLQLYFLWLGCVVLWAQGTAGQPQPPPPKPPRPQPPPQQVRSATAGSEGGFLA 60
DrFbn2          ----------MGVWKLANVVLWWA----------------------AVHSVQGQGDGDIQA 29
pXlFbn          ------------------------------------------------------------
pDrFbn4         ---------MSSQGDLRCLFG-------------------------FVALLGILTGKISG 26
HsFBN3          ---MTLEGLYLARGPLARLLLAWS----------------------ALLCMAGGQGRWDG 35

HsFBN1          LEAGNVKETRASRAKRRGGGGHDALKGPNVCGSRYNAYCCPGWKTLPGGNQCIVPICRHS 88
HsFBN2          PEYREEGAAVASRVRRRGQ--QDVLRGPNVCGSRFHSYCCPGWKTLPGGNQCIVPICRNS 118
DrFbn2          SRFTGKPEGEVQQRVRRRG--QESLRGPNVCGSRFHSYCCPGWKTLPGGNQCIVPICRNS 87
pXlFbn          ------------------------------------------------------------
pDrFbn4         IHGKATVHIDGSQRRQKQE----SLRGPNVCGSRLQSFCCPGWKTLPGGNQCVVPICRSD 82
HsFBN3          ----ALEAAGPGRVRRRGS--PGILQGPNVCGSRFHAYCCPGWRTFPGRSQCVVPICRRA 89

HsFBN1          CGDGFCSRPNMCTCPSGQIAPSCGSRSIQHCNIRCMNGGSCSDDHCLCQKGYIGTHCGQP 148
HsFBN2          CGDGFCSRPNMCTCSSGQISSTCGSKSIQQCSVRCMNGGTCADDHCQCQKGYIGTYCGQP 178
DrFbn2          CGDGFCSRPNMCTCSSGHLAPSCGAAAVQSCSVRCMNGGMCNEDACSCQKGYTGTHCGQP 147
pXlFbn          ------------------------------------------------------------
pDrFbn4         CGDGFCSRPNMCTCPGGQTATTCFTKSSKQCKIRCMNGGVCEDDYCQCPKGYTGSFCGQP 142
HsFBN3          CGEGFCSQPNLCTCADGTLAPSCGVSRGSGCSVSCMNGGTCRGASCLCQKGYTGTVCGQP 149

HsFBN1          VCESGCLNGGRCVAPNRCACTYGFTGPQCERDYRTGPCFTVISNQMCQGQLSGIVCTKTL 208
HsFBN2          VCENGCQNGGRCIGPNRCACVYGFTGPQCERDYRTGPCFTQVNNQMCQGQLTGIVCTKTL 238
DrFbn2          VCESGCQNGGRCIGPNRCACVYGFTGPQCERDYRTGPCFTQVNNQMCQGQLSGIVCTKTL 207
pXlFbn          ------------------------------------------------------------
pDrFbn4         VCEKNCQNGGHCIGPNRCACGYGFTGPQCERDYRTGPCFIQVHSRKCAGQSSEFVCSKAL 202
HsFBN3          ICDRGCHNGGRCIGPNRCACVYGFMGPQCERDYRTGPCFGQVGPEGCQHQLTGLVCTKAL 209

HsFBN1          CCATVGRAWGHPCEMCPAQPHPCRRGFIPNIRTGACQDVDECQAIPGLCQGGNCINTVGS 268
HsFBN2          CCATIGRAWGHPCEMCPAQPQPCRRGFIPNIRTGACQDVDECQAIPGICQGGNCINTVGS 298
DrFbn2          CCATIGRAWGHPCEMCPAQPHPCRRGFIPNIRTGACQDVDECQAVPGLCAGGNCINTVGS 267
pXlFbn          ------------------------------------------------------------
pDrFbn4         CCATVGQAWGHSCEQCPPISSPCTRGFIPNTRTGACQDVDECKVVPDLCKGGRCINTLGS 262
HsFBN3          CCATVGRAWGLPCELCPAQPHPCRRGFIPNIHTGACQDVDECQAVPGLCQGGSCVNMVGS 269

HsFBN1          FECKCPAGHKLNEVSQKCEDIDECSTIPGICEGGECTNTVSSYFCKCPPGFYTSPDGTRC 328
HsFBN2          FECRCPAGHKQSETTQKCEDIDECSIIPGICETGECSNTVGSYFCVCPRGYVTSTDGSRC 358
DrFbn2          YECKCPAGHRQSETNQKCEDIDECATISGVCDGGECTNTAGSYVCTCPRGYITSTDGSRC 327
pXlFbn          ------------------------------------------------------------
pDrFbn4         YQCTCPVGYQQHVSILKCEDVDECSTIERACEAGHCINSAGSFSCVCPSGYVLSADRTRC 322
HsFBN3          FHCRCPVGHRLSDS-------------------------------------------SAAC 287

HsFBN1          IDVRPGYCYTALTNGRCSNQLPQSITKMQCCCDAGRCWSPGVTVAPEMCPIRATEDFNKL 388
HsFBN2          IDQRTGMCFSGLVNGRCAQELPGRMTKMQCCCEPGRCWGIGT--IPEACPVRGSEEYRRL 416
DrFbn2          VDHRIGTCFSSLANGRCASELSGQYTKMQCCCDTGRCWALGH--IPEMCPVRGSDEYRRL 385
pXlFbn          ------------------------------------------------------------
pDrFbn4         LDQHTGICFASVVNGRCAHEISGRFNKIQCCCDRGRCWSQRT--THEMCPVPGSDEYLRI 380
HsFBN3          EDYRAGACFSVLFGGRCAGDLAGHYTRRQCCCDRGRCWAAGP--VPELCPPRGSNEFQQL 345

HsFBN1          CSVPMVIPGRPEYPPPPLGPIPPVLPVPPGFPPGPQIPVPRPP----------------- 431
HsFBN2          CMDGLPMGGIPGSAGSRPGGTGGNGFAPSGNGNGYGPGGTGFIPIPGGNGFSPGVGGAGV 476
DrFbn2          CIQRLPFG--TGNGGIIHDGNGGLNIGGYGKGPSQNGNGGGGYIYGSEHTFTN------- 436
pXlFbn          ------------------------------------------------------------
pDrFbn4         CLVGSALSGYNEEDPEMSPHHHSSFSVSPNDQILHPHNGNGQIKPQIRQTPQILQFPQIP 440
HsFBN3          CAQRLPLLPGHPGLFPGLLGFGSNGMGPPLGPARLNPHGSDARGIPS------------- 392
```

```
HsFBN1          VEYLYPS---REPPRVLPVNVTDYCQLVRYLCQNGRCIPTPGSCRCECNKGFQLDLRGEC 488
HsFBN2          GAGGQGP---IITGLTILNQTIDICKHHANLCLNGRCIPTVSSYRCECNMGYKQDANGDC 533
DrFbn2          GNGNGGQ---KIQISQLNETTIDVCKHFTNLCLNGRCIPTPTSYRCECNMGYRQDVRGEC 493
pXlFbn          ------------------------------------------------------------
pDrFbn4         QIPRHDNGFKPQRPVVSVNETVNRCRLLPNLCLNGRCIPMESDYRCDCNTGFKEDNRGEC 500
HsFBN3          --LGPGN---SNIGTATLNQTIDICRHFTNLCLNGRCLPTPSSYRCECNVGYTQDVRGEC 447

HsFBN1          IDVDECEKNPCAGGECINNQGSYTCQCRAGYQSTLTRTECRDIDECLQNGRICNNGRCIN 548
HsFBN2          IDVDECTSNPCTNGDCVNTPGSYYCKCHAGFQRTPTKQACIDIDECIQNGVLCKNGRCVN 593
DrFbn2          IDVDECVSNPCVNGDCVNTQGSYHCKCHEGYQGTPTKQACIDIDECIVNGVMCRNGRCVN 553
pXlFbn          ------------------------------------------------------------
pDrFbn4         SDVDECEFDPCANGNCINTPGSYYCRCHTGFLRVTGKQTCIDIDECLQNGVLCKNGRCLN 560
HsFBN3          IDVDECTSSPCHHGDCVNIPGTYHCRCYPGFQATPTRQACVDVDECIVSGGLCHLGRCVN 507

HsFBN1          TDGSFHCVCNAGFHVTRDGKNCEDMDECSIRNMCLNGMCINEDGSFKCICKPGFQLASDG 608
HsFBN2          TDGSFQCICNAGFELTTDGKNCVDHDECTTTNMCLNGMCINEDGSFKCICKPGFVLAPNG 653
DrFbn2          TDGSFQCICNAGFEISPDGKNCIDHDECATTNMCLNGMCINEDGSFKCICKPGFALAPNG 613
pXlFbn          ------------------------------------------------------------
pDrFbn4         TEGSFQCICNSGFKLSPDGRNCVDHDECAATNMCLNGMCINEDGSFKCVCKPGFTLNSSG 620
HsFBN3          TEGSFQCVCNAGFELSPDGKNCVDHNECATSTMCVNGVCLNEDGSFSCLCKPGFLLAPGG 567

HsFBN1          RYCKDINECETPGICMNGRCVNTDGSYRCECFPGLAVGLDGRVCVDTHMRSTCYGGYKRG 668
HsFBN2          RYCTDVDECQTPGICMNGHCINSEGSFRCDCPPGLAVGMDGRVCVDTHMRSTCYGGIKKG 713
DrFbn2          RYCTDIDECHTSGICMNGRCVNTEGSFRCECPPGLAIDVDGRVCVDTHMRTTCYGAIKMG 673
pXlFbn          ------------------------------------------------------------
pDrFbn4         RYCTEIDECRTPGVCMNGRCVNTQGSFRCECFAGLTVGIDGRTCVDTHMRSTCYGAVKRG 680
HsFBN3          HYCMDIDECQTPGICVNGHCTNTEGSFRCQCLGGLAVGTDGRVCVDTHVRSTCYGAIEKG 627

HsFBN1          QCIKPLFGAVTKSECCCASTEYAFGEPCQPCPAQNSAEYQALCSSGPGMTSAGSDINECA 728
HsFBN2          VCVRPFPGAVTKSECCCANPDYGFGEPCQPCPAKNSAEFHGLCSSGVGITVDGRDINECA 773
DrFbn2          VCSRPFPGAVTKSECCCANPEHGFGEPCQPCPAFNSAEFQAVCSSGPGITTDGRDINECA 733
pXlFbn          ------------------------------------------------------------
pDrFbn4         LCLRPFQRAVTKSQCCCANPDYAFGEPCHPCPAKHSAEFQVLCASGVGFSADGKDINECA 740
HsFBN3          SCARPFPGTVTKSECCCANPDHGFGEPCQLCPAKDSAEFQALCSSGLGITTDGRDINECA 687

HsFBN1          LDPDICPNGICENLRGTYKCICNSGYEVDSTGKNCVDINECVLNSLLCDNGQCRNTPGSF 788
HsFBN2          LDPDICANGICENLRGSYRCNCNSGYEPDASGRNCIDIDECLVNRLLCDNGLCRNTPGSY 833
DrFbn2          LDPDICQNGICENLRGSYRCICNIGYESDASGKNCVDINECLVNRLLCDNGMCRNTPGSY 793
pXlFbn          ------------------------------------------------------------
pDrFbn4         LDPDICSNGVCENLRGNFRCICNIGYESDQSGRNCLDIDECVVNSLLCDNGLCRNVPGSY 800
HsFBN3          LDPEVCANGVCENLRGSYRCVCNLGYEAGASGKDCTDVDECALNSLLCDNGWCQNSPGSY 747

HsFBN1          VCTCPKGFIYKPDLKTCEDIDECESSPCINGVCKNSPGSFICECSSESTLDPTKTICIET 848
HsFBN2          SCTCPPGYVFRTETETCEDINECESNPCVNGACRNNLGSFNCECSPGSKLSSTGLICIDS 893
DrFbn2          TCSCPKGFSFKADSETCEDINECDSNPCINGICRNIAGSFNCECSHGSKLDSTNTVCVDS 853
pXlFbn          ------------------------------------------------------------
pDrFbn4         SCTCPAGFIFRHDTETCEDVNECVSSPCVNGVCKNSAGSFYCECSQGSKLDSTGLLCVDS 860
HsFBN3          SCSCPPGFHFWQDTEICKDVDECLSSPCVSGVCRNLAGSYTCKCGPGSRLDPSGTFCLDS 807

HsFBN1          IKGTCWQTVIDGRCEININGATLKSQCCSSLGAAWGSPCTLCQVDPICGKGYSRIKGTQC 908
HsFBN2          LKGTCWLNIQDSRCEVNINGATLKSECCATLGAAWGSPCERCELDTACPRGLARIKGVTC 953
DrFbn2          MKGTCWLNIQDGRCEVNINGATLKSECCSTLGAAWGSPCERCEIDPACSKGFGRMKGLVC 913
pXlFbn          ------------------------------------------------------------
pDrFbn4         VKGSCWLTLQDGRCEVNINGATLRSQCCATLGLAWGSPCEPCQTDLVCERGFARSRGASC 920
HsFBN3          TKGTCWLKIQESRCEVNLQGASLRSECCATLGAAWGSPCERCEIDPACARGFARMTGVTC 867
```

```
HsFBN1          EDIDECEVFPGVCKNGLCVNTRGSFKCQCPSGMTLDATGRICLDIRLETCFLRYEDEECT 968
HsFBN2          EDVNECEVFPGVCPNGRCVNSKGSFHCECPEGLTLDGTGRVCLDIRMEQCYLKWDEDECI 1013
DrFbn2          EDINECEVFPGVCTNGRCVNTQGSFRCECPEGLTLDGAGRTCVDVRSEQCYMKWDEDECV 973
pXlFbn          ------------------------------------------------------------
pDrFbn4         EDVNECEVFPGVCHNGHCVNTRGSFKCQCPESLTLDVTGRLCVDVRSEPCFLTYEEDVCT 980
HsFBN3          DDVNECESFPGVCPNGRCVNTAGSFRCECPEGLMLDASGRLCVDVRLEPCFLRWDEDECG 927

HsFBN1          LPIAGRHRMDACCCSVGAAWGTEECEECPMRNTPEYEELCPRGPGFATK-EITNGKPFFK 1027
HsFBN2          HPVPGKFRMDACCCAVGAAWG-TECEECPKPGTKEYETLCPRGAGFANRGDVLTGRPFYK 1072
DrFbn2          EPLPGRYRVDMCCCTVGAAWG-VDCEACPKPNTNEFKTICPRGPGIANRGDILTGRPFYK 1032
pXlFbn          ------------------------------------------------------------
pDrFbn4         QPVPGRFRMDMCCCTVGLAWG-KDCDLCPEPGTRQFDTLCPRGPGFANKGDVLTGRAVYK 1039
HsFBN3          VTLPGKYRMDVCCCSIGAVWG-VECEACPDPESLEFASLCPRGLGFASR-DFLSGRPFYK 985

HsFBN1          DINECKMIPSLCTHGKCRNTIGSFKCRCDSGFALDSEERNCTDIDECRISPDLCGRGQCV 1087
HsFBN2          DINECKAFPGMCTYGKCRNTIGSFKCRCNSGFALDMEERNCTDIDECRISPDLCGSGICV 1132
DrFbn2          DVNECKVFRGLCTHGTCRNTIGSFKCRCDSGFALTMEERNCTDIDECTISPDLCGHGVCV 1092
pXlFbn          ------------------------------------------------------------
pDrFbn4         DINECKVFQSICVHGKCRNTIGSFRCRCDSGFALDTNEKNCTDIDECMISPDVCGHGTCV 1099
HsFBN3          DVNECKVFPGLCTHGTCRNTVGSFHCACAGGFALDAQERNCTDIDECRISPDLCGQGTCV 1045

HsFBN1          NTPGDFECKCDEGYESGFMMMKNCMDIDECQRDPLLCRGGVCHNTEGSYRCECPPGHQLS 1147
HsFBN2          NTPGSFECECFEGYESGFMMMKNCMDIDECERNPLLCRGGTCVNTEGSFQCDCPLGHELS 1192
DrFbn2          NTPGSFECECFDGYESGFMMMKNCMDIDECERDPLLCRGGTCLNTEGSYECDCPPGHQLS 1152
pXlFbn          ------------------------------------------------------------
pDrFbn4         NTLGSFQCDCFPGYESGIMMMKNCMDIDECERNLSLCNGGTCENTDGSYKCVCPPGHHLS 1159
HsFBN3          NTPGSFECECFPGYESGFMLMKNCMDVDECARDPLLCRGGTCTNTDGSYKCQCPPGHELT 1105

HsFBN1          PNISACIDINECELSAHLCPNGRCVNLIGKYQCACNPGYHSTPDRLFCVDIDECSIMNGG 1207
HsFBN2          PSREDCVDINECSLSDNLCRNGKCVNMIGTYQCSCNPGYQATPDRQGCTDIDECMIMNGG 1252
DrFbn2          TEASACEDVNECQLSDNLCKHGQCVNMVGTYQCSCETGYQVTPDRQGCVDIDECTIMNGG 1212
pXlFbn          ------------------------------------------------------------
pDrFbn4         VDGSACEDVNECDLSSTLCPNGWCVNLVGTYQCSCNSGYQTAPDWKGCTDIDECTIENGG 1219
HsFBN3          AKGTACEDIDECSLSDGLCPHGQCVNVIGAFQCSCHAGFQSTPDRQGCVDINECRVQNGG 1165

HsFBN1          CETFCTNSEGSYECSCQPGFALMPDQRSCTDIDECEDNPNICDGGQCTNIPGEYRCLCYD 1267
HsFBN2          CDTQCTNSEGSYECSCSEGYALMPDGRSCADIDECENNPDICDGGQCTNIPGEYRCLCYD 1312
DrFbn2          CDTHCTNSEGSYECSCSEGYALMPDLRTCADIDECEDTPDICDGGQCTNIPGEYRCLCYD 1272
pXlFbn          ------------------------------------------------------------
pDrFbn4         CELYCSNSEGSYSCSCGQGYSLTPDQRTCSDVNECEEVLDICEGGQCTNVPGAYHCLCYE 1279
HsFBN3          CDVHCINTEGSYRCSCGQGYSLMPDGRACADVDECEENPRVCDQGHCTNMPGGHRCLCYD 1225

HsFBN1          GFMASEDMKTCVDVNECDLNPNICLSGTCENTKGSFICHCDMGYSGKKGKTGCTDINECE 1327
HsFBN2          GFMASMDMKTCIDVNECDLNSNICMFGECENTKGSFICHCQLGYSVKKGTTGCTDVDECE 1372
DrFbn2          GFMASMDMRTCIDVNECDLNPNICLHGDCENTKGSFICHCQLGYFVKKGSTGCTDVDECE 1332
pXlFbn          ------------------------------------------------------------
pDrFbn4         GFMASVDMKTCIDVNECELNDNICAFGECENTKGSFICHCDIGYAVKKGTSGCTDVNECE 1339
HsFBN3          GFMATPDMRTCVDVDECDLNPHICLHGDCENTKGSFVCHCQLGYMVRKGATGCSDVDECE 1285

HsFBN1          IGAHNCGKHAVCTNTAGSFKCSCSPGWIGDGIKCTDLDECSNGTHMCSQHADCKNTMGSY 1387
HsFBN2          IGAHNCDMHASCLNIPGSFKCSCREGWIGNGIKCIDLDECSNGTHQCSINAQCVNTPGSY 1432
DrFbn2          IGAHNCDLHAACVNAPGSFKCRCRDGWEGDGIKCIDVDECVTEEHNCNPNAECLNTPGSY 1392
pXlFbn          ------------------------------------------------------------
pDrFbn4         INSHNCDTHATCVNTPGHYHCSCGDGWFGDGVKCADVDECANRTSVCSADAECVNTAGSY 1399
HsFBN3          VGGHNCDSHASCLNIPGSFSCRCLPGWVGDGFECHDLDECVSQEHRCSPRGDCLNVPGSY 1345
```

```
HsFBN1          RCLCKEGYTGDGFTCTDLDECSENLNLCGNGQCLNAPGGYRCECDMGFVPSADGKACEDI 1447
HsFBN2          RCACSEGFTGDGFTCSDVDECAENINLCENGQCLNVPGAYRCECEMGFTPASDSRSCQDI 1492
DrFbn2          RCSCKEGFNGDGFSCSDMDECADNVNLCENGQCLNAPGGYRCECEMGFTPTEDSKACQDI 1452
pXlFbn          ------------------------------------------------------------
pDrFbn4         HCECSDGFIGDGVICSDLDECAEDVDLCENGQCLNVPGSYRCECEMGFTHTSNRKTCRDI 1459
HsFBN3          RCTCRQGFAGDGFFCEDRDECAENVDLCDNGQCLNAPGGYRCECEMGFDPTEDHRACQDV 1405

HsFBN1          DECSLPNICVFGTCHNLPGLFRCECEIGYELDRSGGNCTDVNECLDPTTCISGNCVNTPG 1507
HsFBN2          DECSFQNICVFGTCNNLPGMFHCICDDGYELDRTGGNCTDIDECADPINCVNGLCVNTPG 1552
DrFbn2          DECNFQNICVFGSCQNLPGMFRCVCDYGYELDRSGGNCTDINECFDPVNCINGVCVNLPG 1512
pXlFbn          ------------------------------------------------------------
pDrFbn4         DECSFQNICVFGTCQNIPGMFRCICDEGYELDRTGGNCTDVDECLDSLNCVNGHCENTAG 1519
HsFBN3          DECAQGNLCAFGSCENLPGMFRCICNGGYELDRGGGNCTDINECADPVNCINGVCINTPG 1465

HsFBN1          SYICDCPPDFELNPTRVGCVDTRSGNCYLDIRPRGDNGDTACSNEIGVGVSKASCCCSLG 1567
HsFBN2          RYECNCPPDFQLNPTGVGCVDNRVGNCYLKFGPRGDGS-LSCNTEIGVGVSRSSCCCSLG 1611
DrFbn2          SYLCNCPPDFELNPSGVGCVDTRVGNCFLDTLDRGDGG-ISCSAEIGVGVTRASCCCSLG 1571
pXlFbn          ------------------------------------------------------------
pDrFbn4         SYQCNCPIDFELNPTGIGCVDTRVGNCFLEVAYH---SKLACSAEIGFGVSRSSCCCSLG 1576
HsFBN3          SYLCSCPQDFELNPSGVGCVDTRAGNCFLETHDRGDSG-ISCSAEIGVGVTRASCCCSLG 1524

HsFBN1          KAWGTPCEMCPAVNTSEYKILCPGGEGFRPNPITVILEDIDECQELPGLCQGGKCINTFG 1627
HsFBN2          KAWGNPCETCPPVNSTEYYTLCPGGEGFRPNPITIILEDIDECQELPGLCQGGNCINTFG 1671
DrFbn2          GAWGNPCELCPFVNSTEYKTLCPGGEGFRPNPITVILEDIDECQELPGLCQGGNCVNTFG 1631
pXlFbn          ------------------------------------------------------------
pDrFbn4         RVWGYPCDHCPTLNTSEYNTLCPGGEGFKPNPVTIILEDIDECQELPGLCQGGNCVNTFG 1636
HsFBN3          RAWGNPCELCPMANTTEYRTLCPGGEGFQPNRITVILEDIDECQELPGLCQGGDCVNTFG 1584

HsFBN1          SFQCRCPTGYYLNEDTRVCDDVNECETP-GICGPGTCYNTVGNYTCICPPDYMQVNGGNN 1686
HsFBN2          SFQCECPQGYYLSEDTRICEDIDECFAHPGVCGPGTCYNTLGNYTCICPPEYMQVNGGHN 1731
DrFbn2          SFQCECPAGYYLNEETRICEDIDECTAHIGICGPGTCYNTLGNYTCVCPPEYMQVNGGNN 1691
pXlFbn          ------------------------------------------------------------
pDrFbn4         SFQCECPAGFYLNTQSRICEDIDECVLSLGVCGPGTCYNTLGNYTCVCPQEYIQVNGGHR 1696
HsFBN3          SFQCECPPGYHLSEHTRICEDIDECSTHSGICGPGTCYNTLGNYTCVCPAEYLQVNGGNN 1644

HsFBN1          CMDMRRSLCYRNYYADNQTCDGELLFNMTKKMCCCSYNIGRAWNKPCEQCPIPSTDEFAT 1746
HsFBN2          CMDMRKSFCYRSYNG--TTCENELPFNVTKRMCCCTYNVGKAWNKPCEPCPTPGTADFKT 1789
DrFbn2          CMDMRKSVCYRNFN---DTCENELSFNMTKKMCCCAYNVGKAWNRPCEACPTPATSEYQL 1748
pXlFbn          ---------RRNYN---DTCENELSSNMTKKMCCCSYNIGKAWNKPCEPCPSPATPEYIF 48
pDrFbn4         CMDMRKSLCYRSYNG--SACEHQLNFNITHRLCCCSYNVGKAWNKPCHACPIPGTDDYSS 1754
HsFBN3          CMDMRKSVCFRHYN---GTCQNELAFNVTRKMCCCSYNIGQAWNRPCEACPTPISPDYQI 1701
                          * :     :*: :*  *:*:::***:**:*:***:**. ** * : ::

HsFBN1          LCGSQRPGFVIDIYTGLPVDIDECREIPGVCENGVCINMVGSFRCECPVGFFYNDKLLVC 1806
HsFBN2          ICGN-IPGFTFDIHTGKAVDIDECKEIPGICANGVCINQIGSFRCECPTGFSYNDLLLVC 1848
DrFbn2          LCGNQAPGFIIDIHTGKPIDIDECREIPGICANGVCINQIGSFRCECPMGFSYNNILLIC 1808
pXlFbn          LCGNQAPGFIIDIRTGKPMDIDECSEIPAICSNGVCINQIGTFRCECPMGFSYNNILLIC 108
pDrFbn4         LCGS-VTGFWINIATGKPKDIDECHEIPGVCAHGVCINHMGSFHCECPTGFLYNDLLLIC 1813
HsFBN3          LCGNQAPGFLTDIHTGKPLDIDECGEIPAICANGICINQIGSFRCECPAGFNYNSILLAC 1761
                :**.  .**  :* ** . ***** ***.:* :*:*** :*:*:**** ** **. ** *

HsFBN1          EDIDECQNG-PVCQRNAECINTAGSYRCDCKPGYRFTSTGQCNDRNECQEIPNICSHGQC 1865
HsFBN2          EDIDECSNGDNLCQRNADCINSPGSYRCECAAGFKLSPNGACVDRNECLEIPNVCSHGLC 1908
DrFbn2          EDIDECNSGDNLCQRNANCINIPGSYRCECSAGFKLSPSGACIDRNECQEIPNVCSHGEC 1868
pXlFbn          EDIDECSSGENLCQRNADCINIPGSYRCECSSGYKLSPSGACVGRNECQEIPNVCSHGTC 168
pDrFbn4         EDIDECSSREPVCQRNADCINRPGGYQCECSDGYILTPNGDCNDRNECLETPSVCRHGDC 1873
HsFBN3          EDVDECGSRESPCQQNADCINIPGSYRCKCTRGYKLSPGGACVGRNECREIPNVCSHGDC 1821
                **:*** .    **:**:*** .*.*:*.*  *: ::. * * .**** * *.:* **
```

```
HsFBN1          IDTVGSFYCLCHTGFKTNDDQTMCLDINECERDACGNGTCRNTIGSFNCRCNHGFILSHN 1925
HsFBN2          VDLQGSYQCICHNGFKASQDQTMCMDVDECERHPCGNGTCKNTVGSYNCLCYPGFELTHN 1968
DrFbn2          IDTQGSFRCLCHNGFKTTPDQTMCMDIDECDRQPCGNGTCKNTVGSYNCLCFPGFELTHN 1928
pXlFbn          MDTEGSYICVCHNGFKASGDQTMCMDIDECDRQPCGNGTCKNTVGSYNCLCFPGFELTHN 228
pDrFbn4         VDIPGGYECMCHTGFTVTPNRRMCVDVNECSPQPCGNGTCKNSVGSFNCICHHGFELATN 1933
HsFBN3          MDTEGSYMCLCHRGFQASADQTLCMDIDECDRQPCGNGTCKNIIGSYNCLCFPGFVVTHN 1881
                :*  *.: *:** ** .. :: :*:*::**. ..******:* :**:** *  ** :: *

HsFBN1          NDCIDVDECASGNGNLCRNGQCINTVGSFQCQCNEGYEVAPDGRTCVDINECLLEPRKCA 1985
HsFBN2          NDCLDIDECSSFFGQVCRNGRCFNEIGSFKCLCNEGYELTPDGKNCIDTNECVALPGSCS 2028
DrFbn2          NDCMDIDECSVHASQVCRNGQCINNMGSFKCLCLDGYNLTPDGKNCVDINECVTLPGACQ 1988
pXlFbn          NDCMDIDECSSLVGQVCRNGQCINNVGSFQCLCQEGYEITPDGKNCMDINECTSLPATCS 288
pDrFbn4         NYCTDIDECAVFHSQLCRNGRCVNNVGSFQCLCREGYELTFDGKTCMDVNECTIIPGICA 1993
HsFBN3          GDCVDFDECTTLVGQVCRFGHCLNTAGSFHCLCQDGFELTADGKNCVDTNECLSLAGTCL 1941
                . * *.***:   .::** *:*.*  ***:* * :*:::: **:.*:* ***   .  *

HsFBN1          PGTCQNLDGSYRCICPPGYSLQNEKCEDIDECVEEPEICALGTCSNTEGSFKCLCPEGFS 2045
HsFBN2          PGTCQNLEGSFRCICPPGYEVKSENCIDINECDEDPNICLFGSCTNTPGGFQCLCPPGFV 2088
DrFbn2          PGTCQNLDGSFRCICPPGYEVQNDKCVDINECNVEPNICQFGTCKNTPGSFQCICQPGFV 2048
pXlFbn          PGTCQNLEGSFRCICPPGFEVQNDNCIDINECDEEPNICLFGTCTNTPGSFQCVCPPGFV 348
pDrFbn4         PGTCLNLDGSFRCVCPDGYIVQSDHCVDVNECSEEPGICTYGTCFNSLGSFECVCKPGFV 2053
HsFBN3          PGTCQNLEGSFRCICPPGFQVQSDHCIDIDECSEEPNLCLFGTCTNSPGSFQCLCPPGFV 2001
                **** **:**:**:** *: ::.::* *::**  :* :*  *:* *: *.*:*:*  **

HsFBN1          LSSSGRRCQDLRMSYCYAKFEGGKCSSPKSRNHSKQECCCALK-GEGWGDPCELCPTE-P 2103
HsFBN2          LSDNGRRCFDTRQSFCFTNFENGKCSVPKAFNTTKAKCCCSKMPGEGWGDPCELCPKD-D 2147
DrFbn2          LSDNGRRCFDTRESFCFTRFEAGKCSVPKPRNTTKAKCCCSLLPGEGWGDPCELCPRDTE 2108
pXlFbn          LSDNGRRCFDTRQSFCFTRFDNGKCSVPKAFNTTKARCCCSKMPGEGWGDPCELCPQE-G 407
pDrFbn4         LSEDKRRCYDTRESFCFTRFENSKCSVPQAFNTTKAKCCCSIMAKEGWGDPCELCPKE-- 2111
HsFBN3          LSDNGHRCFDTRQSFCFTRFEAGKCSVPKAFNTTKTRCCCSKRPGEGWGDPCELCPQE-G 2060
                **.. :** * * *:*::.*: .*** *:. * :* .***:    ********** :

HsFBN1          DEAFRQICPYGSGIIVGPDDSAVDMDECKE-PDVCKHGQCINTDGSYRCECPFGYILAGN 2162
HsFBN2          EVAFQDLCPYGHGTVPSLHDTREDVNECLESPGICSNGQCINTDGSFRCECPMGYNLDYT 2207
DrFbn2          EAAFHTLCPYGHEAVP-KPEGREDMNECVENPEICGNGLCINTDGSFRCECPFGYNLDYT 2167
pXlFbn          SVAFQELCPYGHGSIPGMGDTREDVNECSESPGICVNGVCINTDGSFRCECPFGYNLDYT 467
pDrFbn4         HDAFQDLCPFGHGIIPGVGDTRVDLNECVENPEICVNGRCINMDGSFRCECPAGYTLDYT 2171
HsFBN3          SAAFQELCPFGHGAVPGPDDSREDVNECAENPGVCTNGVCVNTDGSFRCECPFGYSLDFT 2120
                  **: :**:*   :    :   *::** * * :* :* *:* ***:***** ** *  .

HsFBN1          --ECVDTDECSVGNPCGNGTCKNVIGGFECTCEEGFEPGPMMTCEDINECAQNPLLCAFR 2220
HsFBN2          GVRCVDTDECSIGNPCGNGTCTNVIGSFECNCNEGFEPGPMMNCEDINECAQNPLLCAFR 2267
DrFbn2          GVNCVDTDECSIGNPCGNGTCSNVPGGFECSCQEGFEPGPMMTCEDINECAVNPLLCAFR 2227
pXlFbn          GVNCVDTDECSIGNPCGNGTCSNVVGGFECACDEGFEPGPMMTCEDINECTN-PLLCAFR 526
pDrFbn4         GTHCDDIDECSVRNPCGNGTCSNVIGAFECLCEEGFEPGPMMSCEDVNECGQNPLLCAFR 2231
HsFBN3          GINCVDTDECSVGHPCGQGTCTNVIGGFECACADGFEPGLMMTCEDIDECSLNPLLCAFR 2180
                  .* * ****: :***:***.** *.*** * :***** **.***::**   *******

HsFBN1          CVNTYGSYECKCPVGYVLREDRRMCKDEDECEEGKHDCTEKQMECKNLIGTYMCICGPGY 2280
HsFBN2          CMNTFGSYECTCPIGYALREDQKMCKDLDECAEGLHDCESRGMMCKNLIGTFMCICPPGM 2327
DrFbn2          CVNTFGSYECMCPTGYVLRDDNRMCRDQDECAEGLDDCASRGMACKNQIGTFMCICPPGM 2287
pXlFbn          CINTYGSYECTCPSGYTLREDQRMCKDLDECAEGLHDCESRGMMCKNLIGTFMCICPPGL 586
pDrFbn4         CINTFGSYECSCPSGYTLREDGRMCQDVDECAEDLHNCDSRGMECSNLIGTFMCVCPAGM 2291
HsFBN3          CHNTEGSYLCTCPAGYTLREDGAMCRDVDECADGQQDCHARGMECKNLIGTFACVCPPGM 2240
                * ** *** * ** **.**:*  **:* *** :. .:*  : * *.* ***: *:* .*

HsFBN1          QRRP-DGEGCVDENECQTKPGICENGRCLNTRGSYTCECNDGFTASPNQDECLDNREGYC 2339
HsFBN2          ARRP-DGEGCVDENECRTKPGICENGRCVNIIGSYRCECNEGFQSSSSGTECLDNRQGLC 2386
DrFbn2          TRRP-DGEGCMDLNECRSKPGICKNGRCVNTVGSYRCECNEGFEASATGTECIDNRKGFC 2346
pXlFbn          QRRP-DGEGCMDENECRTKPGICANGRCVNTIGSYKCDCNEGFQVSSSGTECVDTRQGFC 645
pDrFbn4         IRRM-SDEACQDENECLTQPGVCENGRCVNTVGSYTCECGVGFKTDSSATQCLDYRKGFC 2350
HsFBN3          RPLPGSGEGCTDDNECHAQPDLCVNGRCVNTAGSFRCDCDEGFQPSPTLTECHDIRQGPC 2300
                     ..*.* * *** ::*.:* ****:*  **: *:*. **  ...  :* * *:* *
```

```
HsFBN1          FTEVLQNMCQIGSSNRNPVTKSECCCDGGRGWGPHCEICPFQGTVAFKKLCPHGRGFMTN 2399
HsFBN2          FAEVLQTICQMASSSRNLVTKSECCCDGGRGWGHQCELCPLPGTAQYKKICPHGPGYTTD 2446
DrFbn2          FTEVLQTMCQQSSTNRNTVTKSECCCNGGRGWGSLCELCPLPGTIQYKKMCPLGPGYTTD 2406
pXlFbn          FTEVLQTMCQLSSTNRNMVTKSECCCNSGRGWGNQCEICPLPGTGAFKKMCPHGAGFSTD 705
pDrFbn4         FTEVLHTMCQMSSSSRVPVSRSQCCCNGGHGWGDQCELCPLPATANYKKLCPYGHGYAID 2410
HsFBN3          FAEVLQTMCRSLSSSSEAVTRAECCCGGGRGWGPRCELCPLPGTSAYRKLCPHGSGYTAE 2360
                *:***:.:*:  *:.   *::::***..*:***  **:**: .*  ::*:** * *:  :

HsFBN1          GADIDECKVIHDVCRNGECVNDRGSYHCICKTGYTPDITGTSCVDLNECNQAPKPCNFIC 2459
HsFBN2          GRDIDECKVMPNLCTNGQCINTMGSFRCFCKVGYTTDISGTSCIDLDECSQSPKPCNYIC 2506
DrFbn2          GRDINECEVMPNLCKNGQCINSVGSFRCHCNVGYTNDFTGTSCIDMDECSQSPKPCNFLC 2466
pXlFbn          GRDIDECKVLPNLCKNGQCINTIGSFRCHCKLGYTTDITGTTCVDLDECAQSPKPCNFIC 765
pDrFbn4         GTDIDECKLIPDVCANGACINMMGSYRCHCKPGYIASTAGTACVDVDECGMSPKPCNFIC 2470
HsFBN3          GRDVDECRMLAHLCAHGECINSLGSFRCHCQAGYTPDATATTCLDMDECSQVPKPCTFLC 2420
                * *::**.:: .:* :* *:*  **::* *: **  . :.*:*:*::**   ****.::*

HsFBN1          KNTEG-SYQCSCPKGYILQEDGRSCKDLDECATKQHNCQFLCVNTIGGFTCKCPPGFTQH 2518
HsFBN2          KNTEG-SYQCSCPRGYVLQEDGKTCKDLDECQTKQHNCQFLCVNTLGGFTCKCPPGFTQH 2565
DrFbn2          KNTEG-SYLCSCPRGYILQPDGKTCKDLDECSTKQHNCQFLCVNTIGGFTCKCPSGFTQH 2525
pXlFbn          KNTEGKSITCSCPTAYILQEDGKRCKDLDECSTKQHNCQFLCVNTIGSFTCKCPPGFTQH 825
pDrFbn4         KNTEG-SYACSCPRGYTLQNDNRSCKDVDECQSRRHNCQFSCMNTIGGFTCKCPAGFSQH 2529
HsFBN3          KNTKG-SFLCSCPRGYLLEEDGRTCKDLDECTSRQHNCQFLCVNTVGAFTCRCPPGFTQH 2479
                ***:* *  **** .* *: *.: ***:*** :::***** *:**:*.***:**.**:**

HsFBN1          HTSCIDNNECTSDINLCGSKGICQNTPGSFTCECQRGFSLDQTGSSCEDVDECEGNHRCQ 2578
HsFBN2          HTACIDNNECGSQPSLCGAKGICQNTPGSFSCECQRGFSLDATGLNCEDVDECDGNHRCQ 2625
DrFbn2          QTACIDNNECSNQPNICGSRASCLNSPGSFNCECQKGFSLDATGLNCDDVDECGGNHRCQ 2585
pXlFbn          QSSCIDNNECNAQPNLCGSRGTCQNNPGSFTCECQKGFSLDNSGSNCEDVDECDGNHRCQ 885
pDrFbn4         HRACRDIDECLSDLTPCGLQGACQNSVGSFSCECPQGFSLDSLGHNCDDVDECARDHRCQ 2589
HsFBN3          HQACFDNDECSAQPGPCGAHGHCHNTPGSFRCECHQGFTLVSSGHGCEDVNECDGPHRCQ 2539
                : :* * :**  :   ** :. * *. *** *** :**:*   * .*:**:**   ****

HsFBN1          HGCQNIIGGYRCSCPQGYLQHYQWNQCVDENECL-SAHICGGASCHNTLGSYKCMCPAGF 2637
HsFBN2          HGCQNILGGYRCGCPQGYIQHYQWNQCVDENECS-NPNACGSASCYNTLGSYKCACPSGF 2684
DrFbn2          HGCQNMMGGYRCGCPQGYVQHYQWNQCVDENECT-GNQVCGSASCYNTLGSYKCVCPSGF 2644
pXlFbn          HGCQNVLGGFRCGCPQRYVQHYQWNQCVDENECA-SQSACGSASCYNTLGSFKCVCPSGF 944
pDrFbn4         FGCQNVAGGFRCSCPQGYTQHQQWNQCVDDNECL-NADNCGSASCFNTLGSFKCGCPSGF 2648
HsFBN3          HGCQNQLGGYRCSCPQGFTQHSQWAQCVDENECALSPPTCGSASCRNTLGGFRCVCPSGF 2599
                .****  **:**.*** : ** ** ****:***  .   **.*** ****.::* **:**

HsFBN1          QYEQFSGGCQDINECGSAQ-APCSYGCSNTEGGYLCGCPPGYFRIGQGHCVSGMGMGRGN 2696
HsFBN2          SFDQFSSACHDVNECSSSK-NPCNYGCSNTEGGYLCGCPPGYYRVGQGHCVSGMGFNKGQ 2743
DrFbn2          DFEATAGGCQDVNECSMGN-NPCSYGCSNTDGGYLCGCPGGFYRAGQGHCINGVGF-QGQ 2702
pXlFbn          DFDQSFGGCQDVDECSSGGGNPCSYGCSNTDGGYLCGCPGGYFRAGQGHCVSGMGFGKGS 1004
pDrFbn4         TFDPASTSCEDVDECGSFM-NPCRYGCSNTQGGFACGCPAGYYRAGQG------------ 2695
HsFBN3          DFDQALGGCQEVDECAGRR-GPCSYSCANTPGGFLCGCPQGYFRAGQGHCVSGLGFSPGP 2658
                 ::    .*.:::**.     ** *.*:** **: **** *::* ***

HsFBN1          PEPPVSGEMDDNSLSPEACYECKINGYPKR-GRKRRSTNETDASNIEDQSETEANVSLAS 2755
HsFBN2          YLSLDTEVDEENALSPEACYECKINGYSKKDSRQKRSIHEPDPT-------AVEQISLES 2796
DrFbn2          FGSEGG--DDEESLSPEACYECKINGDLGKKGRHRRNADDNE---------LKETVSMAS 2751
pXlFbn          YLQAPVEEDEENVLSPESCYECKINGYPKR-GRQRRNADDINGN-------EIQNVSLAS 1056
pDrFbn4         ------------------------------------------------------------
HsFBN3          Q----DTPDKEELLSSEACYECKINGLSPR-DRPRRSAHRDH------------QVNLAT 2701


HsFBN1          WDVEKTAIFAFNISHVSNKVRILELLPALTTLTNHNRYLIESGNEDGFFKINQK-EGISY 2814
HsFBN2          VDMDSPVNMKFNLSHLGSKEHILELRPAIQPLNNHIRYVISQGNDDSVFRIHQR-NGLSY 2855
DrFbn2          MDIQTSIPMNLSLAQLLNKEPLLELLPALEPLEHHVRYVITHGNQGEHFRILERRDGKSV 2811
pXlFbn          VDIDAPLNMTLNISDLANKQHIFEFIPALESLENRVRYIISHGNEGGIFHIHQR-DGISY 1115
pDrFbn4         ------------------------------------------------------------
HsFBN3          LDSEALLTLGLNLSHLGRAERILELRPALEGLEGRIRYVIVRGNEQGFFRMHHL-RGVSS 2760
```

```
HsFBN1          LHFTKKKPVAGTYSLQISSTPLYKKKELNQLEDKYDKDYLSGELGDNLKMKIQVLLH 2871
HsFBN2          LHTAKKKLMPGTYTLEITSIPLYKKKELKKLEESNEDDYLLGELGEALRMRLQIQLY 2912
DrFbn2          LRLGRRPPAPGLYRLEIASLRLFGPRKLQQMEDQHDSDYLLGEIGDALRIKLHIHLH 2868
pXlFbn          LHLGHKKVATGIYNLEIASVSLYRKKELQKLEDEKDHNYLSGEVGQTLKMKLHIHLY 1172
pDrFbn4         ------------------------------------------------------------
HsFBN3          LQLGRRRPGPGTYRLEVVSH-MAGPWGVQPEGQP-------GPWGQALRLKVQLQLL 2809
```

Supplementary Figure 3

Developmental Dynamics
Vol. 237, Issue 12, pp. 3715-3726, 2008

CHAPTER 5

Essential role for the alpha 1 chain of type VIII collagen in zebrafish notochord formation

John M. Gansner and Jonathan D. Gitlin

Edward Mallinckrodt Department of Pediatrics
Washington University School of Medicine
St. Louis, Missouri 63110

Abstract

A number of zebrafish mutants identified in large-scale forward genetic screens exhibit notochord distortion. We now report the cloning and further characterization of one such mutant, *gulliver*^{m208} (*gul*^{m208}). The notochord defect in *gul*^{m208} mutants is exacerbated under conditions of copper depletion or lysyl oxidase cuproenzyme inhibition that are without a notochord effect on wild-type embryos. The *gul*^{m208} phenotype results from a missense mutation in the gene encoding Col8a1, a lysyl oxidase substrate, and morpholino knockdown of *col8a1* recapitulates the notochord distortion observed in *gul*^{m208} mutants. Interestingly, the amino acid mutated in *gul*^{m208} Col8a1 is highly conserved, and the equivalent substitution in a closely related human protein, COL10A1, causes Schmid metaphyseal chondrodysplasia. Taken together, the data identify a new protein essential for notochord morphogenesis, extend our understanding of gene-nutrient interactions in early development, and suggest that human mutations in *COL8A1* may cause structural birth defects.

Introduction

The notochord is a midline structure that functions both as an axial skeleton and as an important signaling center to other tissues during embryogenesis (31). It is one of the defining structures of the chordate phylum, and is the first organ to fully differentiate in vertebrates (31). The notochord arises from the dorsal organiser and likely represents a primitive form of cartilage, as indicated by its expression of type II collagen, type IX collagen, sox9, aggrecan, and chondromodulin (16). In higher chordates, the notochord plays a critical role in vertebral column formation and persists post-embryonically as the nucleus pulposus of intervertebral discs (16).

In zebrafish, studies of notochord morphogenesis are facilitated by the genetic tractability of this model organism and by the ease with which its notochord is visualized throughout early development (16, 19, 20). During late notochord morphogenesis, chordamesoderm differentiates into mature notochord, a transition that involves the downregulation of specific marker genes and the inflation of notochord cell vacuoles which exert turgor pressure on an extracellular matrix sheath (31). If sheath formation is impaired, this turgor pressure results in notochord abnormalities that are readily observed, permitting insight into the mechanisms of both notochord morphogenesis and extracellular matrix formation. Indeed, a number of zebrafish notochord mutants have already been identified during large-scale forward genetic screens (17, 18), and early studies of these mutants established the importance of laminins and coatomer proteins in notochord differentiation and sheath formation (19, 20). Since notochord abnormalities and extracellular matrix defects have both been implicated in the development of

structural birth defects (11, 15, 134), elucidating the mechanisms of notochord formation will not only permit a greater understanding of the biology of this important organ, but may also allow for the therapeutic intervention or prevention of structural birth defects, which are a major cause of morbidity and mortality in children (135).

Previous work in our laboratory has demonstrated that copper deficiency causes notochord distortion in zebrafish embryos and that this distortion results from the inhibition of specific lysyl oxidase cuproenzymes, which crosslink collagens in the notochord sheath (14, 80). In addition, we have recently conducted a forward genetic screen for zebrafish mutants that exhibit increased notochord distortion after partial lysyl oxidase inhibition, identifying one such mutant (136). These studies raised the intriguing possibility that notochord mutants previously identified in large-scale forward genetic screens (17, 18) could provide insight into the molecular mechanisms of copper-dependent notochord formation. We now report the mapping and further characterization of one such recessive lethal mutant, *gulliver*^{m208} (17). The analysis presented here demonstrates a role for the alpha 1 chain of type VIII collagen in zebrafish notochord formation and an interaction with lysyl oxidase cuproenzymes.

Materials and methods

Zebrafish maintenance

Gulliver^{m208} was obtained from the Zebrafish International Resource Center (Eugene, OR). Zebrafish were reared under standard conditions at 28.5°C (33) and staged as described (34). Synchronous, in vitro fertilized embryos were obtained for all experiments, which were carried out in accordance with Washington University's Division of Comparative Medicine guidelines. In Figs. 1, 2, and the first two lanes of 5B, "wild-type" refers to either +/+ or +/- embryos.

Microscopy

Live embryos were anesthetized in tricaine, mounted in 2% methylcellulose, and imaged using an Olympus SZX12 zoom stereomicroscope fitted with an Olympus DP70 camera. Electron microscopy was carried out as previously described (80) except that negatives were directly scanned using a Canon Canoscan 8400F. For the electron microscopy, sections from two wild-type and two mutant embryos were examined.

Pharmacologic treatment and yolk sac extension measurements

Pharmacologic compounds were purchased from Sigma (St. Louis, MO). β-aminopropionitrile (A3134) and neocuproine (N1501) were prepared as 100 mM stocks in egg water (33) and dimethyl sulfoxide, respectively, and diluted in egg water. Tunicamycin (T7765) was prepared as a 1 mg/mL stock in DMSO and used at a concentration of 2 μg/mL. 4-Phenylbutyric acid (P21005) was prepared as a 2 M stock in DMSO and used at a concentration of 5 mM in buffered egg water adjusted to a pH of 6.9 (137). In all cases, embryos were placed in compound between 6 and 10 hpf. Lengths of

individual yolk sac extensions were measured from photographs of 10 mutant and 10 wild-type embryos per pharmacologic treatment using ImageJ software (47). Values are reported in arbitrary units, with standard deviations noted.

Meiotic mapping

Gulliver^{m208} was mapcrossed to the polymorphic WIK strain and the progeny (AB*/WIK) raised to adulthood. The *gul*^{m208} mutation was assigned to chromosome 9 by centromeric linkage analysis (26, 93) using simple sequence length polymorphism (SSLP) markers (94) and DNA from early pressure gynogenetic diploids. For fine mapping, 1295 mutant embryos from AB*/WIK females crossed to AB*/AB males were collected and assessed for recombination along chromosome 9 by SSLP analysis. Embryos were incubated in 2 μM neocuproine to accentuate the mutant phenotype and facilitate rapid mutant identification. When necessary, candidate marker primer pairs for BAC sequences were generated using the Zebrafish SSR search website of the Massachusetts General Hospital (http://danio.mgh.harvard.edu/markers/ssr.html). Primers for the BAC markers used in Fig. 3 are: zC81J7 – forward 5'-TTGTTCTGCAAATTTTGTTGG-3' and reverse 5'-GGGGCAACCCCTCTAAAGT-3'; zK46K9 – forward 5'-AACACAAGCTGGGACTGGAC-3' and reverse 5'-GATGTCTAACACAAACACATTGG-3'; zC206L17 – forward 5'-GAGTATCACCTCTGACAGATGGG-3' and reverse 5'-GCAGCATTGACGGTGAAGGTCAC-3'; zK229B18 – forward 5'-TGATTAATACAACATGGGCA-3' and reverse 5'-CGCACTGTGAAATAACATGA-3'; zC184M13 – forward 5'-GGAAGTGTGTGTGTGCGTTT-3' and reverse 5'-

GGCCACAAGAACCATGACA-3' (descendents of one WIK grandparent) and also forward 5'-TGGTGTAGGGGGCTAACAAG-3' and reverse 5'-TGAACTGAACTGGCATGAACA-3' (descendents of the other WIK grandparent). DNA from wild-type and heterozygote embryos as well as WIK and AB grandparents was used to ensure polymorphism between AB and WIK.

Cloning and annotation

Full-length *col8a1* was amplified from wild-type and mutant cDNA and cloned into pCR-XL-TOPO (Invitrogen). cDNA for these reactions was generated with Superscript III reverse transcriptase (Invitrogen) and PCR carried out using Phusion DNA polymerase and high-fidelity buffer (Finnzymes). The primers used for PCR were: forward primer 5'-GAGTGAGCCCACCAATCCTTG-3' and reverse primer 5'-CCTTCAAATTCTTACTTATTCTTGC-3'. The full-length zebrafish *col8a1* coding sequence is available at Genbank (accession number **EU781032**). The protein sequence alignment of zebrafish Col8a1 with orthologues from other species was created using ClustalW2 (96). Signal peptides were predicted using SignalP 3.0 (39).

Trimerization assay

Wild-type and mutant *col8a1* sequences were subcloned into pCS2+ and in vitro transcribed and translated in the presence of TRAN35S-LABEL (MP Biomedicals) using the SP6 TNT Coupled Reticulocyte Lysate System (Promega) essentially as described (138, 139). 5 µl of each 25 µl reaction was mixed with an equal volume of 2X sample buffer containing 250 mM Tris pH 6.8, 4 M urea, 4% sodium dodecyl sulfate (SDS), 24 mM dithiothreitol, and a small amount of bromophenol blue. Samples were heated at

50°C for 5 minutes and subjected to SDS-PAGE on a 1 mm gel with 3.5% stacking and 7.5% resolving layers. The gel was fixed for 30 minutes in a mixture of 20% methanol and 10% glacial acetic acid, washed in water for 5 minutes, and vacuum dried at 80° C for 2 hours before exposure of a low-energy phosphor screen (Amersham) and image acquisition using a Storm imaging system (Amersham).

Whole-mount in situ hybridization and frozen sections

Embryos were manually dechorionated at the indicated developmental stages, fixed in 4% paraformaldehyde-PBS overnight at 4°C, and dehydrated by methanol series. The probe construct was generated by cloning the 5' end of zebrafish *col8a1* into pCRII (Invitrogen). The primers used for the PCR amplification reaction were: forward primer 5'-GAGTGAGCCCACCAATCCTTG-3' and reverse primer 5'-CTCCTGGACTTCCAATACCC-3'. DIG-labeled antisense RNA probes were synthesized using a DIG-labeling kit (Roche), and whole-mount in situ hybridization was performed as previously described (14, 45).

Reverse transcriptase-polymerase chain reaction (RT-PCR)

RNA was obtained from pooled embryos or unfertilized eggs using Trizol reagent (Invitrogen). For Figs. 4J and 5B, cDNA was prepared from 500 ng of RNA using an oligo dT primer and Superscript III reverse transcriptase (Invitrogen). PCR amplification over 35 cycles was subsequently performed using 1 μL of cDNA and GoTaq polymerase (Promega) in a final volume 25 μL. The annealing temperature was 57°C and the extension time 1 minute. Primers to *col8a1* were: forward primer 5'-GAGTGAGCCCACCAATCCTTG-3' and reverse primer 5'-

CCTCTGGGAATGGTCTCACC-3'. Primers to *xbp1* were: forward primer 5'-GTTCAGGTACTGGAGTCCGC-'3 (140) and reverse primer 5'-GGATGTCCAGAATACCAAGCAGG-3'. Primers to *ampka1* and *spt* (also known as *tbx16*) have been reported previously (141). For Fig. 6C, cDNA was prepared from 1 μg of RNA and the annealing temperature was 55°C. The forward primer to *col8a1* was as noted above, but the reverse primer was 5'- GACATTCCTGGCTTACCAATTCC-3'. Band quantitation was performed using ImageJ software (47). For Fig. 4J, band quantitation of *col8a1* was calculated using a different exposure of the same gel where the bands were not saturated.

Morpholino and mRNA injections

Morpholino oligonucleotides (27) targeting start and splice sites in *col8a1* were resuspended in Danieau buffer (start MO) or water (splice MO), diluted to include 0.05% phenol red, and injected into 1-cell embryos. Standard control morpholino (Gene Tools, LLC) was resuspended in Danieau buffer and likewise injected. Morpholino sequences were: 5'-CCGTAGGAGAAGATAATCTCAAGGA-3' (start MO) and 5'-TAAAGTGTATCTCCTTACCTTTCCT-3' (splice MO). The start MO was used at doses of 2.4 ng and 7.2 ng. Capped, polyadenylated mRNA for rescue experiments was generated from wild-type or mutant full-length clones of zebrafish *col8a1* using the mMESSAGE mMACHINE kit (Ambion). Individual embryos from *gul*^{m208}/+ intercrosses were injected with either 200 or 800 pg of mRNA.

Results

gul^{m208} *mutants are sensitized to lysyl oxidase inhibition*

Gulliver^{m208} (*gul*^{m208}) mutants exhibit notochord distortion similar to what is obtained under conditions of copper deficiency or direct pharmacologic lysyl oxidase cuproenzyme inhibition (14, 17, 74, 80). However, the distortion observed in *gul*^{m208} mutants is less robust, and we therefore tested these mutants for sensitivity to lysyl oxidase inhibition (Fig. 1). Clutches from *gul*^{m208}/+ intercrosses were incubated in vehicle (Fig. 1A, B) or in a dose of the copper chelator neocuproine (Fig. 1C, D) that does not cause notochord distortion in wild-type embryos (Fig. 1C and Gansner et. al, 2007). Under such copper-limiting conditions, *gul*^{m208} mutants exhibited increased notochord distortion (Fig. 1D vs. Fig. 1B, arrowheads), presumably due to the partial inhibition of lysyl oxidase activity (80). This hypothesis was confirmed by incubating clutches from *gul*^{m208}/+ intercrosses in a dose of the irreversible lysyl oxidase inhibitor β-aminopropionitrile that does not cause notochord distortion in wild-type embryos (Fig. 1E). Under these conditions, increased notochord distortion in *gul*^{m208} mutants was again observed (Fig. 1F vs. Fig. 1B, arrowheads).

Interestingly, the notochord distortion observed in *gul*^{m208} mutants is accompanied by a decrease in the length of the yolk sac extension (wild-type length = 3.23 ±0.09 vs. mutant length = 2.64 ±0.18 in vehicle), and the increased notochord distortion observed after neocuproine or β-aminopropionitrile treatment is associated with a further shortening of this structure in mutant but not wild-type embryos (wild-type length = 3.33 ±0.15 vs. mutant length = 2.31 ±0.09 in neocuproine; wild-type length = 3.22 ± 0.12 vs.

mutant length = 2.13 ± 0.16 in β-aminopropionitrile) (Fig. 1). These data suggest that force generation in the notochord is impaired in *gul*^{m208} mutants and confirms a synergy between the *gul*^{m208} locus and both copper chelation and lysyl oxidase inhibition.

Electron microscopy reveals notochord abnormalities in* gul^{m208} *mutants

To determine if a defect in notochord sheath formation could explain the notochord phenotype of *gul*^{m208} mutants, we imaged truncal cross-sections from *gul*^{m208} mutant and wild-type embryos by transmission electron microscopy. This revealed abnormalities in both the vacuolated notochord cells and notochord sheath of *gul*^{m208} mutants at 24 hpf (Fig. 2). In the vacuolated notochord cells of *gul*^{m208} mutants, the rough endoplasmic reticulum exhibits striking areas of engorgement compared to wild-type embryos, presumably due to retention of protein that fails to be secreted and instead forms large circular aggregates (Fig. 2B vs. Fig. 2A, arrows). These aggregates are also observed in the hypochord, which is closely apposed to the ventral aspect of the notochord (Fig. 2C, red arrows) and plays a critical role in the formation of the dorsal aorta (57, 58). While the inner (i), medial (m), and outer (o) layers of the notochord sheath are present in both wild-type embryos and *gul*^{m208} mutants, the fibrillar medial layer appears disordered in *gul*^{m208} mutants (Fig. 2E vs. Fig. 2D).

The* gul^{m208} *mutation disrupts the zebrafish* col8a1 *gene

To determine the molecular basis of the *gul*^{m208} phenotype, we meiotically mapped the *gul*^{m208} locus to a centromeric region of chromosome 9 (Fig. 3A). This region contains twenty-six genes (S. Fig. 1) one of which encodes the alpha 1 chain of type VIII collagen (Col8a1), a known lysyl oxidase substrate (67). Cloning and sequencing of zebrafish

col8a1 revealed a missense mutation in *gul*^{m208} mutants that is absent in wild-type embryos (Fig. 3B). This mutation results in the substitution of histidine for tyrosine in the C1q-like domain of Col8a1 (Y628H) (Fig. 3C). Protein sequence alignment demonstrates that the tyrosine mutated in *gul*^{m208} fish is highly conserved (Fig. 3D; see also the Discussion), and that zebrafish Col8a1 is similar to homologues in other species (S. Fig. 2). Sequencing of other genes located in the region between our flanking markers did not identify any additional mutations capable of causing the *gul*^{m208} phenotype (S. Fig. 1).

The expression of* col8a1 *is consistent with the* gul^{m208} *phenotype

To determine the spatio-temporal expression of zebrafish *col8a1*, we performed whole-mount in situ hybridization on wild-type embryos at various stages of development (Fig. 4). Consistent with the hypothesis that the Y628H substitution disrupts notochord morphogenesis, *col8a1* is robustly expressed in the notochord at the 5-, 10-, 15-, and 20-somite stages (Fig. 4A-D, arrows). Starting at the 10-somite stage and continuing through 24-30 hpf, expression is also observed in the prechordal plate region (Fig. 4B-E, asterix), floorplate (Fig. 4B-E, G, black arrowhead), and hypochord (Fig. 4B-E, G, white arrowhead). At 24 hpf, notochord staining is diminished (Fig. 4E) and *col8a1* is expressed in the caudal somites (Fig. 4F, arrowheads). By 48 hpf, *col8a1* expression is restricted to the forming jaw cartilages (Fig. 4H, I, arrows). A difference in staining intensity was not detected between *gul*^{m208} mutant and wild-type embryos processed in the same basket (data not shown), suggesting that mutant *col8a1* transcripts are not degraded or overexpressed.

To precisely map the onset of *col8a1* expression, we employed a more sensitive method for transcript detection, reverse transcriptase-polymerase chain reaction (RT-PCR). This revealed that *col8a1* is expressed at very low levels maternally and is upregulated between 9 hpf and the 3-somite stage (Fig. 4J). Importantly, a PCR product was not obtained if the reactions were performed in the absence of cDNA (Fig. 4J).

The Y628H substitution prevents Col8a1 trimerization but does not activate the unfolded protein response

Since C1q-like domains are important for oligomerization (142), we tested whether the Y628H substitution impairs zebrafish Col8a1 trimer formation using an in vitro assay previously validated in studies of a closely-related collagen, collagen X (138, 139, 143). While transcription and translation from either wild-type or mutant plasmid contructs results in the production of Col8a1 monomers (Fig. 5A, lanes 1 and 2), only wild-type zebrafish Col8a1 is able to trimerize (Fig. 5A, lane 1). Co-transcription and translation of half the amounts of wild-type and mutant Col8a1 together did not prevent trimerization (Fig. 5A, lane 3), consistent with loss of function of mutant Col8a1. Bands migrating faster than monomer may represent late initiation products, as they were not present in a negative control lane and were not cleaved in reactions supplemented with canine pancreatic microsomes, which facilitate proteolytic processing of the Col8a1 signal peptide (data not shown).

We also considered whether the *gul*^{m208} phenotype could result from a toxic effect of mutant Col8a1 aggregates, which are observed in the endoplasmic reticulum of *gul*^{m208} mutants at 24 hpf (Fig. 2B, E). These aggregates could lead to endoplasmic reticulum

stress, which results in the processing of x-box binding protein-1 (*xbp1*) mRNA to a splice form encoding an activator of the unfolded protein response (144). However, *xbp1* splicing is not observed in wild-type embryos or *gul*^{m208} mutants at 24 hpf (Fig. 5B). Furthermore, incubation of wild-type embryos in tunicamycin, an inhibitor of *N*-glycosylation that causes endoplasmic reticulum stress, results in *xbp1* splicing (Fig. 5B) but does not cause the *gul*^{m208} phenotype (data not shown). Finally, 4-phenylbutyric acid, a chemical chaperone that reduces endoplasmic reticulum stress (145, 146), does not rescue the *gul*^{m208} phenotype (data not shown). These data suggest that the Y628H substitution causes notochord distortion through insufficient Col8a1 deposition in the notochord sheath rather than through activation of the unfolded protein response.

Morpholino knockdown of* col8a1 *recapitulates the* gul^{m208} *phenotype

To determine if loss of *col8a1* recapitulates the notochord phenotype observed in *gul*^{m208} mutants, we designed morpholinos to knock down *col8a1* in zebrafish. While injection of standard control morpholino into wild-type embryos did not result in any visible phenotypic effect (Fig. 6A and Table 1), injection of a splice morpholino targeting *col8a1* caused notochord distortion indistinguishable from what is observed in *gul*^{m208} mutants (Fig. 6B and Table 1). Importantly, this splice morpholino also caused a dose-dependent reduction in *col8a1* transcript, as detected by RT-PCR (Fig. 6C). Injection of a second, distinct morpholino targeting the start site of *col8a1* gave identical phenotypic results when used at a dose of 2.4 ng (data not shown), confirming that the *gul*^{m208} phenotype results from loss of Col8a1. Interestingly, injection of either the start or splice morpholinos at higher doses resulted in more robust notochord distortion (Fig. 6D and

data not shown). Neither morpholino altered melanin pigment formation (data not shown).

Injection of 200 pg of mRNA encoding full-length *col8a1* into clutches from *gul*^{m208}/+ intercrosses did not rescue the *gul*^{m208} phenotype (data not shown), whereas injection of 800 pg of mRNA caused dysmorphism during epiboly and at 26 hpf (data not shown). This suggests that *col8a1* expression must be restricted to specific cell types during early development in order for rescue to be successful.

Discussion

These data reveal a previously unappreciated role for the alpha 1 chain of type VIII collagen (Col8a1) in zebrafish notochord formation. Type VIII collagen is formed through homopolymerization of either alpha 1 or alpha 2 polypeptide chains (147) and is a member of the short-chain collagen family that includes type X collagen. The experiments with neocuproine (Fig. 1C, D) reveal a gene-nutrient interaction between copper and *col8a1* that significantly alters notochord morphogenesis. The notochord sensitivity of *gul*^{m208} mutants to lysyl oxidase inhibition (Fig. 1D, F) suggests that some mutant Col8a1 may be able to fold in vivo, and residual Col8a1 function could explain the enhanced notochord distortion observed with higher doses of *col8a1* morpholino (Fig. 6D). Importantly, the mechanism by which morpholinos decrease specific gene transcription precludes the accumulation of protein aggregates in the rough endoplasmic reticulum, arguing that mutant Col8a1 aggregates do not cause the *gul*^{m208} phenotype. In addition, no mutant Col8a1 is present in the morpholino-injected wild-type embryos, and thus mutant protein cannot be interfering with normal collagen assembly in the extracellular space. Taken together, the data presented here strongly suggest that the Y628H substitution causes notochord distortion through insufficient Col8a1 deposition in the notochord sheath.

Implications for other notochord mutants

Our results advance the possibility that published late notochord mutants such as *crash test dummy*, *zickzack*, *wavy tail*, *quasimodo*, and *kinks* (17, 18) may encode mutations in lysyl oxidases, proteins required for lysyl oxidase activity, or lysyl oxidase substrates. In

some cases, additional phenotypes may help to identify the mutant gene. For instance, *quasimodo* exhibits defects in both notochord and melanin pigment formation (18), suggesting a mutation in a protein required for global copper homeostasis. The lesion in *quasimodo* has been mapped to a region near the *atp7a* locus (148), and may thus be allelic to *calamity* (14).

Our data also suggest that force generation in the notochord can be indirectly measured by quantitating the length of the yolk sac extension, which is simple to do and could prove useful in studies of other notochord mutants. Since *col8a1* is not expressed in the yolk sac extension (Fig. 4), the reduction in the length of this structure in *gul*^{m208} mutants, both before and after pharmacologic treatment (Fig. 1), provides evidence for impaired force generation in the notochord, and implicates Col8a1, copper, and lysyl oxidases in this force generation process.

Conservation of amino acid Y628

The Y628H substitution identified in *gul*^{m208} mutants is located within the C1q-like domain of Col8a1 (Fig. 3C). This domain is present in a number of other proteins, including the structurally similar collagen paralogues COL8A2 and COL10A1 (Fig. 3D) (143, 149, 150). Alignment of all 31 human C1q-like domain-containing proteins reveals only eight invariant residues, including the tyrosine corresponding to Y628 in zebrafish Col8a1 (151). Furthermore, this tyrosine is conserved in all predicted 52 zebrafish C1q-like domain-containing proteins (152). In view of such notable evolutionary conservation, it is not surprising that the Y628H substitution present in *gul*^{m208} mutants could be deleterious. Indeed, an identical substitution at the equivalent position in human

COL10A1 (Y597H) causes Schmid metaphyseal chondrodysplasia, an autosomal dominant skeletal disorder (153). The Y597H mutation is predicted to prevent proper folding of the COL10A1 C-terminal noncollagenous domain (NC1) in the endoplasmic reticulum and to cause disease by haploinsufficiency (149). This mechanism may also account for the *gul*^{m208} phenotype since the crystal structures of the COL10A1 and COL8A1 NC1 domains are very similar and in each case the histidine would destabilise the hydrophobic core of the protein (149, 150).

Our data support the hypothesis that the Y628H substitution inhibits proper folding of individual Col8a1 chains. First, the large circular aggregates visualized by electron microscopy are consistent with unfolded Col8a1 monomer that is retained in the rough endoplasmic reticulum (Fig. 2B, E, arrows). Similar aggregates resulting from protein retention in the endoplasmic reticulum are observed in three zebrafish coatomer mutants, although the cause of retention is different in these mutants and leads to a more severe phenotype (19). Second, the in vitro trimerization assay directly demonstrates a defect in mutant Col8a1 trimerization (Fig. 5A, lane 2 vs. lane 1). This presumably results from a primary defect in NC1 domain folding rather than a defect in inter-chain assembly because the mutated tyrosine is buried in the NC1 domain (150). We propose that the Y628H substitution in Col8a1 inhibits monomer folding in *gul*^{m208} mutants. Since the NC1 domain nucleates trimer formation (154-156), this unfolded Col8a1 monomer would subsequently fail to trimerize and form higher-order assemblies (Fig. 7).

Comparative expression of type VIII collagen

Zebrafish *col8a1* expression is restricted to a few tissues during early development (Fig. 4), and the absence of *col8a1* expression in zebrafish eye was initially puzzling because Type VIII collagen is a major component of Descemet's membrane in other vertebrates (157-160). However, zebrafish encode a paralogue of *col8a1* located on chromosome 22 (BAC CR956626), and an EST encoding part of this paralogue (DN898414) has been isolated from zebrafish eye, specifically from the anterior segment where Descemet's membrane is located. Thus, it appears that partitioning of tissue-specific patterns of expression has occurred (56), and type VIII collagen distribution in zebrafish is expected to be broader than what is predicted from the expression data presented here (Fig.4).

Previous work demonstrates that type VIII collagen is distributed in the cartilage matrix and perichondrium of fetal calf tissues (161). The zebrafish notochord is most closely related to cartilage as a tissue (16), and expression of *col8a1* in notochord and jaw cartilages (Fig. 4A-D, H, I) suggests an association between cartilage and type VIII collagen deposition that is evolutionarily conserved during early development. This association is supported by the similar spatio-temporal expression profiles of *col8a1* and cartilage-expressed *col2a1* in zebrafish embryos (compare Fig. 4 with Fig. 3 of Yan et al., 1995) (44). Importantly, loss of wild-type *col8a1* expression in jaw cartilages likely causes the severe head malformation noted in gul^{m208} mutants by 72 hpf (17) and thus the two principal phenotypes of gul^{m208} mutants (notochord distortion and head malformation) involve the major cartilage and cartilage-related tissues of zebrafish during early embryogenesis. Mice lacking both alpha 1 and alpha 2 chains of type VIII collagen exhibit anterior segment abnormalities in the eye but are not noted to have notochord or

jaw malformations (162). The reasons for these differences are presently unknown, though *Col8a1* is expressed in at least some cartilages of newborn mice (163).

Short-chain collagens in human disease

Col8a1 belongs to a small group of highly-related short-chain collagens, and the *gul*^{m208} mutant zebrafish may provide insight into the mechanism by which specific types of point mutations in these collagens cause disease. Indeed, our findings may be relevant to the molecular pathogenesis of Schmid metaphyseal chondrodysplasia, which is currently debated. Schmid metaphyseal chondrodysplasia results from mutations at multiple sites in *COL10A1*, and functional haploinsufficiency due to nonsense-mediated decay of mutant message appears to cause this disorder (164, 165). However, an effect of misfolded protein on chondrocyte differentiation secondary to activation of the unfolded protein response has also been invoked (166, 167). The determination of whether a missense mutation causes disease through loss of function or endoplasmic reticulum stress is potentially critical because treatment options may differ. 4-Phenylbutyric acid has been shown to reduce endoplasmic reticulum stress and restore glucose homeostasis in a mouse model of type 2 diabetes (145) and is already approved by the U.S. Food and Drug Administration for the chronic management of certain urea-cycle disorders (168). Thus, a disease caused by endoplasmic reticulum stress may be amenable to treatment with this chemical chaperone. Our data suggest that mutations affecting monomer folding (Fig. 7) cannot be rescued by 4-phenylbutyric acid (Fig. 5B and data not shown).

To date, no human disease has been shown to result from mutations in *COL8A1*. While *COL8A1* has been evaluated as a candidate gene for certain eye disorders due to

the presence of type VIII collagen in Descemet's membrane and to the fact that mutations in *COL8A2* cause corneal dystrophies (169-171), the data presented here suggest that a role for *COL8A1* in cartilage development should now be considered. Indeed, the expression pattern of *col8a1* in zebrafish (Fig. 4) and the notochord and head phenotypes of gul^{m208} mutants (17) suggest that mutations in *COL8A1* could result in chondrodysplasias. A number of different mutations in *COL10A1* cause Schmid metaphyseal chondrodysplasia (172), but not all patients with this disease have an identifiable mutation in *COL10A1* and additional unknown loci are implicated in its pathogenesis (153, 173-175). *COL8A1* may thus be a candidate gene for Schmid metaphyseal chondrodysplasia or another chondrodysplasia.

Acknowledgments

We thank Marilyn Levy for the electron microscopy and Stephen Johnson for help with meiotic mapping. We also thank Stephen Johnson, Erik Madsen, and Robert Mecham for careful review of the manuscript. This work was supported by NIH Medical Scientist Training Program grant T32 GM07200 (J.M.G.) and by NIH grant DK44464 (J.D.G.).

Figure legends

Fig. 1. *gul*^{m208} mutants are sensitized to lysyl oxidase inhibition. Clutches from *gul*^{m208}/+ intercrosses were incubated in vehicle (A, B), the copper chelator neocuproine (2 μM) (C, D), or the lysyl oxidase inhibitor β-aminopropionitrile (1 mM) (E, F). The notochord is normal in wild-type embryos treated with vehicle, neocuproine, or β-aminopropionitrile (A, C, E). Notochords of *gul*^{m208} mutants incubated in neocuproine and β-aminopropionitrile (D, F, arrowheads) are substantially more distorted than mutants incubated in vehicle (B, arrowheads). Insets show notochord at higher magnification. Embryos were treated with PTU to inhibit melanin pigmentation and photographed at 30 hpf.

Fig. 2. Electron microscopy reveals notochord abnormalities in *gul*^{m208} mutants. (A-E) Transmission electron micrographs of truncal cross-sections from embryos at 24 hpf. (A) Notochord sheath and vacuolated notochord cell of a wild-type embryo, with small areas of protein accumulation visible in the rough endoplasmic reticulum (arrow). (B) Notochord sheath and vacuolated notochord cell of a *gul*^{m208} mutant with large circular aggregates of protein in the rough endoplasmic reticulum (arrow). (C) Notochord and hypochord of a *gul*^{m208} mutant with large circular aggregrates of protein in the hypochord (red arrows) and notochord (yellow arrow). (D) Notochord sheath of a wild-type embryo with inner (i), medial (m), and outer (o) layers indicated. Small areas of protein accumulation are visible in the rough endoplasmic reticulum (red arrow). (E) Notochord sheath of a *gul*^{m208} mutant where the collagen fibrils in the medial (m) layer appear

disorganized. A large circular aggregate of protein is visible in the rough endoplasmic reticulum (red arrow). Not = vacuolated notochord cell; Hyp = hypochord.

Fig. 3. The *gul*^{m208} mutation disrupts the *col8a1* gene. (A) The *gul*^{m208} lesion was meiotically mapped to a centromeric region of chromosome 9 bounded by markers zK46K9 and zK229B18. The number of recombinants at each marker is noted. According to the physical genome assembly (Zv7), 26 genes are located within the critical region, including the alpha 1 chain of type VIII collagen (*col8a1*). (B) Sequencing of wild-type and *gul*^{m208} mutant cDNAs revealed a missense mutation in *gul*^{m208} mutant *col8a1* that changes a tyrosine to a histidine. (C) Structure of the predicted 711-amino acid zebrafish Col8a1 protein. NC1 and NC2 are two non-collagenous domains. The Y628H substitution present in *gul*^{m208} mutants (arrow) is located within the C1q-like domain (grey) of NC1. (D) Protein sequence alignment of N-terminal portions of select C1q-like domains. Conserved residues, including Y628 (arrow), are shaded yellow. Sequence numbering refers to the zebrafish Col8a1 sequence (DrCol8a1).

Fig. 4. *col8a1* expression is consistent with the *gul*^{m208} phenotype.

(A-I) Whole-mount in situ hybridization for *col8a1* was performed on wild-type embryos at various developmental stages. (A) Lateral view of a 5-somite embryo with *col8a1* expression in the vacuolated notochord cells (arrow). (B-D) Lateral views of 10- (B), 15- (C), or 20- (D) somite embryos with *col8a1* expression in the notochord (arrow), floorplate (black arrowhead), hypochord (white arrowhead), and prechordal plate region (asterix). (E) Lateral view of an embryo at 24 hpf with *col8a1* expression in the floorplate (black arrowhead), hypochord (white arrowhead), and prechordal plate region (asterix).

(F) Dorsal view of an embryo at 24 hpf with *col8a1* expression in the caudal somites (arrowheads). (G) Lateral view of an embryo at 30 hpf with *col8a1* expression in the floorplate (black arrowhead) and hypochord (white arrowhead). (H) Dorsal view of an embryo at 48 hpf with *col8a1* expression in jaw cartilages (arrows). (I) Lateral view of an embryo at 48 hpf with *col8a1* expression in jaw cartilages (arrows). (J) RT-PCR for *col8a1* at the indicated developmental stages. As controls, maternally-expressed 5'-AMP-activated protein kinase catalytic subunit alpha-1 (*ampka1*) and zygotically-expressed spadetail (*spt*) were amplified in parallel (104, 176). The fold induction of *col8a1* relative to *ampka1* is noted. Unfert. = unfertilized; NA = not applicable.

Fig. 5. The Y628H substitution prevents Col8a1 trimerization. (A) Constructs encoding wild-type (lane 1) or *gul*^{m208} mutant (lane 2) Col8a1 were transcribed and translated in the presence of radiolabelled methionine, and the products analyzed as described under Experimental Procedures. Col8a1 monomers and trimers are indicated. Co-transcription and translation of half the amounts of wild-type and mutant construct together does not prevent trimerization (lane 3). The approximate location of molecular weight markers (kDa) is noted. (B) RT-PCR to assess the splice status of *xbp1* in wild-type embryos and *gul*^{m208} mutants at 24 hpf. Splicing of *xbp1* is not observed in *gul*^{m208} mutants but occurs after incubation of wild-type embryos in tunicamycin. U = unspliced; S = spliced. Amplification of the gene *spt* was performed in parallel to confirm that equal amounts of cDNA were used for each condition.

Fig. 6. Morpholino knockdown of *col8a1* recapitulates the *gul*^{m208} phenotype.

(A) Wild-type embryos injected with 12 ng of control morpholino exhibit normal morphology. (B) Embryos injected with 2.4 ng of a splice morpholino targeting *col8a1* develop notochord distortion (arrowheads) characteristic of *gul*^{m208} mutants. (C) RT-PCR at 24 hpf demonstrating a dose-dependent reduction in *col8a1* transcript after morpholino injection. (D) Embryos injected with 12 ng of a splice morpholino targeting *col8a1* develop notochord distortion (arrowheads) that is worse than in *gul*^{m208} mutants. Insets show notochord at higher magnification. All embryos were treated with PTU to inhibit melanin pigmentation and photographed at 30 hpf.

Fig. 7. Model of Col8a1 assembly in wild-type and *gul*^{m208} mutant embryos. Col8a1 monomer containing the Y628H mutation is unable to fold, preventing trimer formation and higher-order assembly that occurs in the absence of the mutation. The Y628H mutation is located within the NC1 domain of Col8a1 (asterisk).

Table 1. Morpholino knockdown of *col8a1* recapitulates the notochord distortion observed in *gul*^{m208} mutants. Wild-type embryos were injected with morpholino and live embryos sorted to new dishes at 10 hpf; these embryos were scored for notochord distortion at 30 hpf. Data shown are the pooled results of three independent experiments.

S. Fig. 1. (A) Ordered list of the genes located between markers zK46K9 and zK229B18. Marker zC206L17 is included for reference. A single asterisk indicates the gene where most of the coding sequence was cloned from *gulliver* mutant cDNA. Double asterisks indicate genes where the entire coding sequence was cloned from *gulliver* mutant cDNA. (**B) Nucleotide coding sequence of genes cloned from *gulliver* mutant cDNA.** Primers used for PCR are indicated. Notes are included detailing why any

alterations to the predicted amino acid sequence are not expected to cause the *gul*^{m208} phenotype.

S. Fig. 2. Protein sequence alignment of zebrafish Col8a1 with orthologues from other species. Predicted signal peptides are in bold and the conserved tyrosine at position 628 is in blue. The C1q-like domain is in grey.

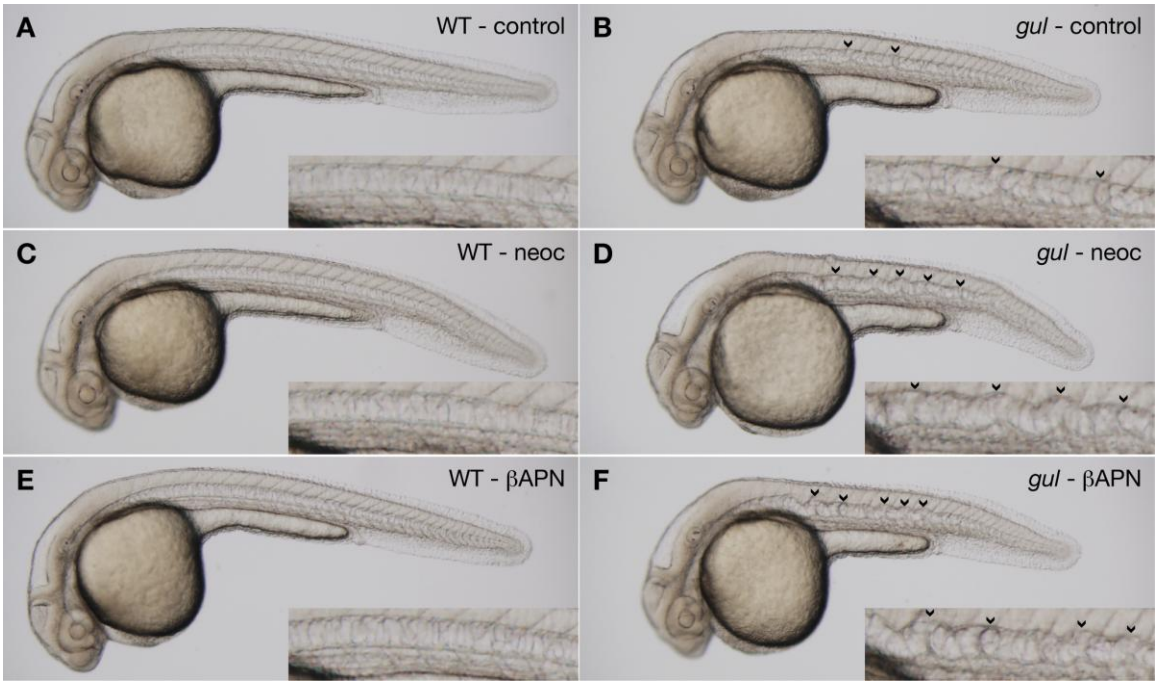
A
WT - control
B
gul - control
C
WT - neoc
D
gul - neoc
E
WT - βAPN
F
gul - βAPN

Figure 1

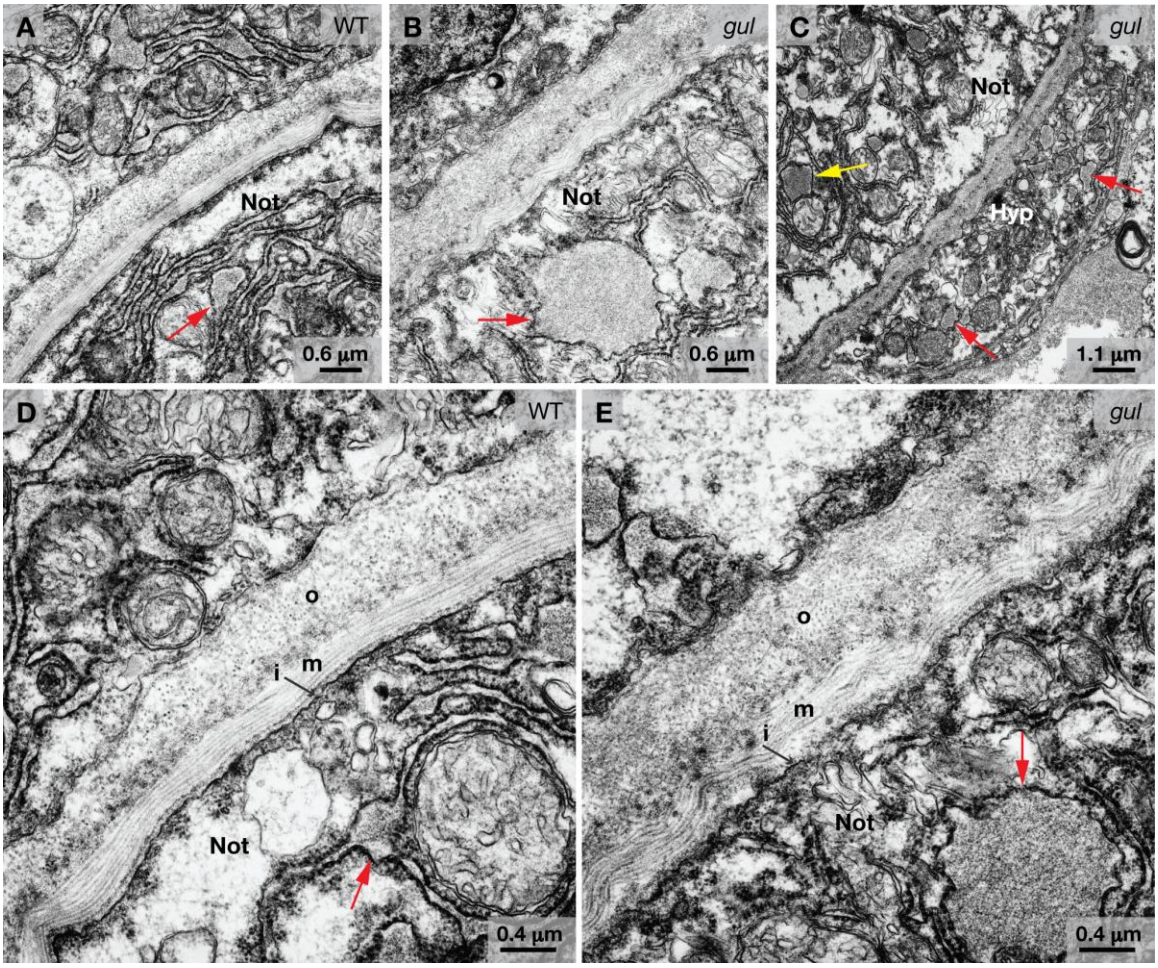
A
WT
Not
0.6 µm
B
gul
Not
0.6 µm
C
gul
Not
Hyp
1.1 µm
D
WT
o
i
m
Not
0.4 µm
E
gul
o
m
i
Not
0.4 µm

Figure 2

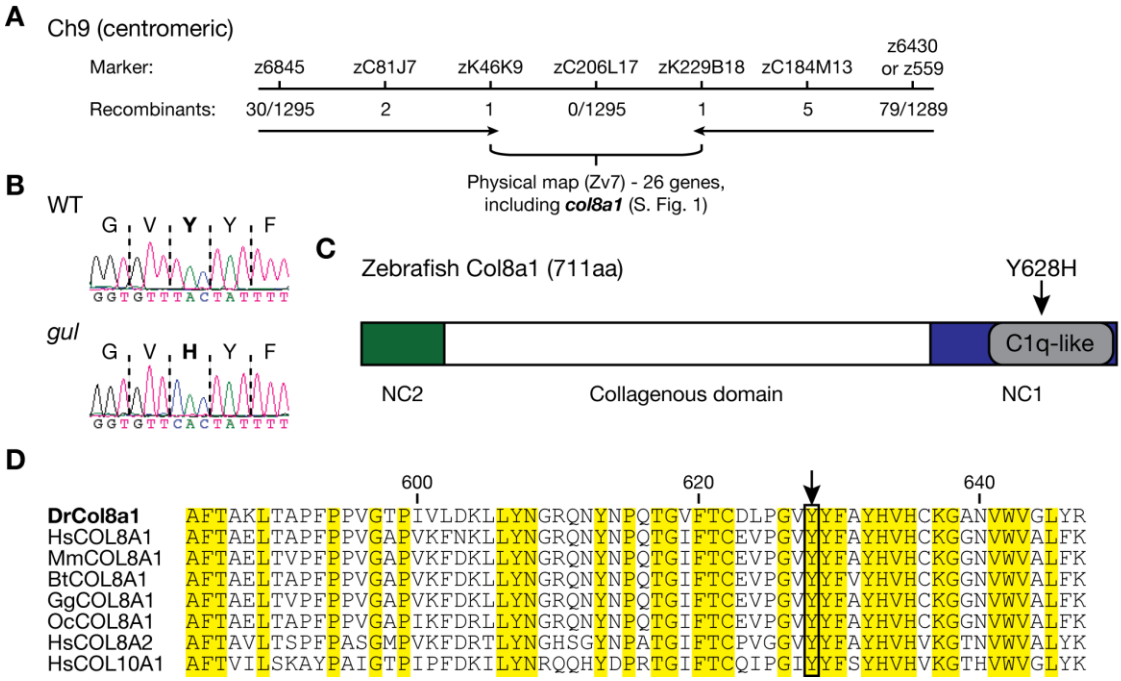
A
Ch9 (centromeric)
Marker:
z6845
zC81J7
zK46K9
zC206L17
zK229B18
zC184M13
z6430 or z559
Recombinants:
30/1295
2
1
0/1295
1
5
79/1289
Physical map (Zv7) - 26 genes, including col8a1 (S. Fig. 1)
B
WT
G V Y Y F
GGTGTTTACTATTTT
gul
G V H Y F
GGTGTTCACTATTTT
C
Zebrafish Col8a1 (711aa)
Y628H
C1q-like
NC2
Collagenous domain
NC1
D
600
620
640
DrCol8a1 AFTAKLTAPFPPVGTPIVLDKLLYNGRQNYNPQTGVFTCDLPGVYYFAYHVHCKGANVWVGLYR
HsCOL8A1 AFTAELTAPFPPVGAPVKFNKLLYNGRQNYNPQTGIFTCEVPGVYYFAYHVHCKGGNVWVALFK
MmCOL8A1 AFTAELTVPFPPVGAPVKFDKLLYNGRQNYNPQTGIFTCEVPGVYYFAYHVHCKGGNVWVALFK
BtCOL8A1 AFTAELTAPFPPVGAPVKFDKLLYNGRQNYNPQTGIFTCEVPGVYYFVYHVHCKGGNVWVALFK
GgCOL8A1 AFTAELTVPFPPVGAPVKFDKLLYNGRQNYNPQTGIFTCEVPGVYYFAYHVHCKGGNVWVALFK
OcCOL8A1 AFTAELTAPFPPVGAPIKFDRLLYNGRQNYNPQTGIFTCEVPGVYYFAYHVHCKGGNVWVALFK
HsCOL8A2 AFTAVLTSPFPASGMPVKFDRTLYNGHSGYNPATGIFTCPVGGVYYFAYHVHVKGTNVWVALYK
HsCOL10A1 AFTVILSKAYPAIGTPIPFDKILYNRQQHYDPRTGIFTCQIPGIYYFSYHVHVKGTHVWVGLYK

Figure 3

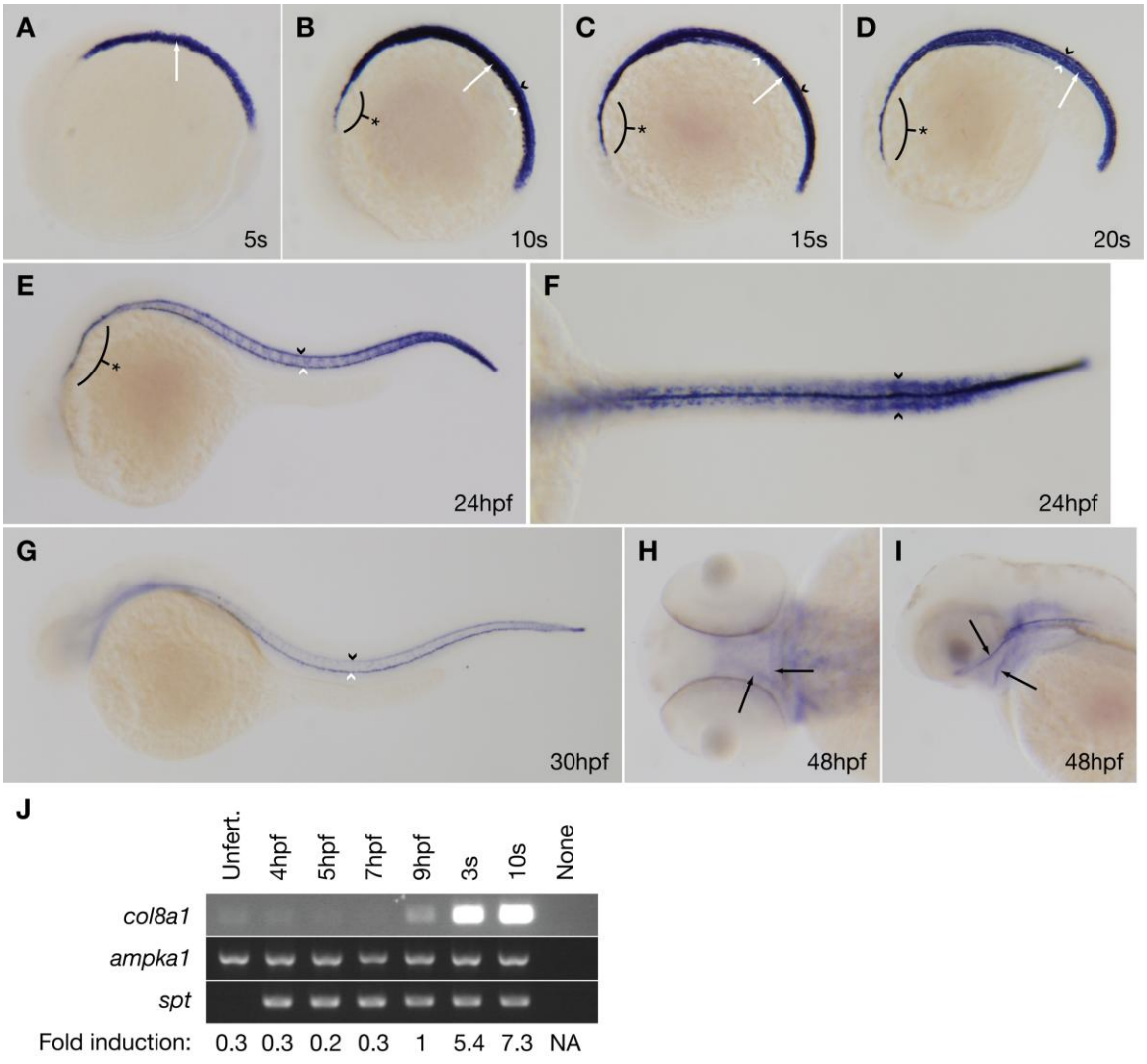
A
5s
B
10s
C
15s
D
20s
E
24hpf
F
24hpf
G
30hpf
H
48hpf
I
48hpf
J
Unfert.
4hpf
5hpf
7hpf
9hpf
3s
10s
None
col8a1
ampka1
spt
Fold induction:
0.3 0.3 0.2 0.3 1 5.4 7.3 NA

Figure 4

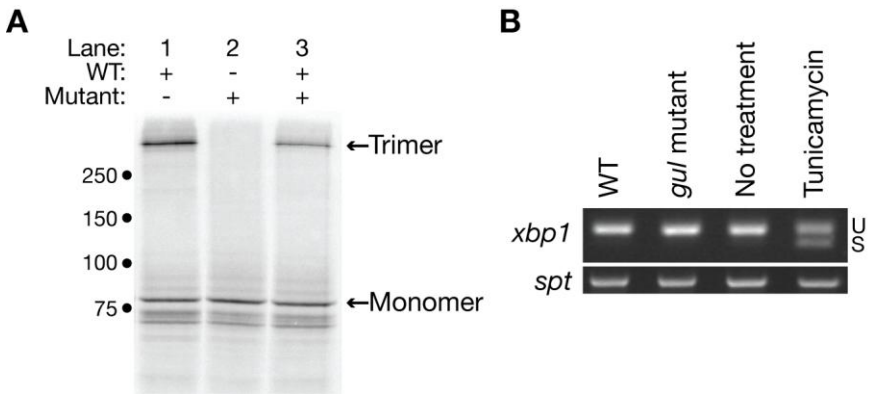
A
Lane: 1 2 3
WT: + - +
Mutant: - + +
250
150
100
75
←Trimer
←Monomer
B
WT
gul mutant
No treatment
Tunicamycin
xbp1
spt
US
UC

Figure 5


A
12 ng control MO
B
2.4 ng col8a1 MO
C
12 ng ctrl
1.2 ng col8a1
2.4 ng col8a1
7.2 ng col8a1
col8a1
spt
% ctrl: 100 19 12 9
D
12 ng col8a1 MO

Figure 6

Specific Morpholino	Dose of morpholino (ng)	Embryos scored (#)	Dead or dysmorphic embryos (#)	Notochord distortion	
				-	+
Control	12	186	10	172 (**98%**)	4 (**2%**)
***col8a1* (splice)**	2.4	170	2	2 (**1%**)	166 (**99%**)

Table 1

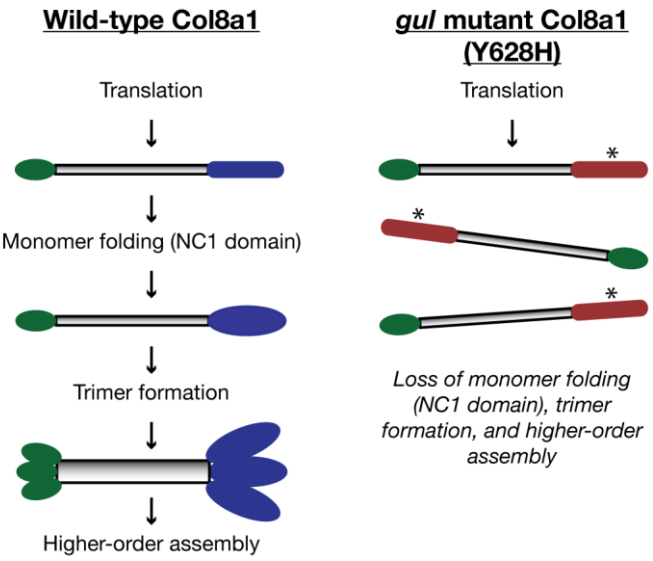
Wild-type Col8a1
Translation
Monomer folding (NC1 domain)
Trimer formation
Higher-order assembly
gul mutant Col8a1 (Y628H)
Translation
*
*
*
Loss of monomer folding (NC1 domain), trimer formation, and higher-order assembly

Figure 7

A)

Marker zK46K9 (1 recombinant)

Q6GML5_DANRE = PHD finger protein 11 (PHF11)
c13orf1 = Chronic lymphocytic leukemia deletion region gene 6 protein
zgc:56602 = Ribonuclease H2 subunit B (RNASEH2B)
zgc:152866 = X-linked interleukin-1 receptor accessory protein-like 1 precursor (IL1RAPL1)

Marker zKC206L17 (0 recombinants)

**zgc:101814 = C3orf26
**zgc:63472 = transmembrane protein 30A (TMEM30A)
*zgc:158743 = Discoidin, CUB and LCCL domain-containing protein 2 precursor (DCBLD2)

col8a1– annotated only on BAC (BX322575)

zgc:101070 = jagunal homolog 1 (JAGN1)
**tfg = TRK-fused gene
LOC100006853 = Target of Nesh-SH3 precursor (ABI3BP)
LOC558093 = interphotoreceptor matrix proteoglycan 2 (IMPG2)
tlr20f = Toll-like receptor 20f
A3KPA1_DANRE = Sentrin-specific protease 7 (SENP7)
g12 = Mid1-interacting protein 1 (MID1IP1)
LOC794667 = Ornithine carbamoyltransferase (OTC)
RPGR = X-linked retinitis pigmentosa GTPase regulator
zgc:110822 = Sushi repeat-containing protein SRPX precursor (SRPX)
SYTL5 = Synaptotagmin-like protein 5
asb11 = Ankyrin repeat and SOCS box protein 11
zgc:56589 = Phosphatidylinositol N-acetylglucosaminyltransferase subunit A (PIGA)
zgc:113314 (novel protein)
LOC795718 = Gap junction alpha-8 protein (GJA8)
cx45.6 = Gap junction alpha-5 protein (GJA5)
LOC558758 = Lysophosphatidic acid phosphatase type 6 precursor (ACP6)
chaf1b = Chromatin assembly factor 1 subunit B

Marker zK229B18 (1 recombinant)

B)

>Sequence for zgc:101814. Forward 5’-GCGATTGCGGTTTGAGACATG-3’ and reverse 5’-GGCATTAAAGTACACAACAATCTCTC-3’.

ATGGCTGATGATTTAGGAGACGAGTGGTGGACCCAGGGCGATAATTCAGATG
TGCCTGAGGTAGAGGAGGAAACAGAGCCTGCAGAAGAAAAACAACCGATTA
AATCTACACCTAAGAAAAGGAAGGTTGAAAAACAGATTCCAGATGCCACAA
AGAAAAAGAAGAAGGCAACAGTTAAGAAAGAATGTTTCATCACGCAAGAGA
GATCAGAGGAAAAGCCTGATAACGAGTCTAACAAAAACAAGAAAAGAAGAA
AGAAGAAGAAAACCATCACAGATGTCCTGACAAGCTCTAAGCCTGTGCCCGG
CTCTCCAGTTGACCTTGTGAGCCTTCTGAAGACTTACCACAGCCAGACCCGCT
CTGTTATTGAGCAGGAGGAACTGACGTTACAAGATTCTTGTTTCCTCAGCTGT

AATGACCTCACACACAGCTTGTCTTCCTACCTCAAAGAAGTTTGTCCAAAGTG
GGCTAAAATGCAGAAACAGCACACCCAGACCAGCTCAGTGGTTTTGCTAATT
GTTTGTGGATCTGCTTTAAGAACCATTGATCTCATTAAGCAGCTGGTGACATT
CAAAGGACAAGCTAAAGTGCTGAAGCTGTTTGCAAAACACATCAAAGTGGA
AGAACAGATAAAGTCATTGAGTAAAGGTGTGACCCATATTGCTGTTGGAACT
CCTGGGAGAATTTGCGCGCTGTTAGAGAAAGAGGGATTGACTGTGCAAGGAC
TACGTTATCTGGTGCTGGACTGGAACTACAGAGACCAGAAGCAAAGGAGGAT
GGTGGATGTACCAGAGGTGAAAGGAGACTTACTAAAAATGATGGACCAAGG
TCTAATCCAGAGCTGCAGAGAAGGAACGGTTAAAATAGGACTCTTCTGA
NOTES: H27P and insertion of K before ATVKKEC vs. zgc:101814 (BC083291), but BAC BX957250 agrees in both cases with the above sequence.

>Sequence for zgc:63472. Forward 5'- GAAAACTTCCTTCGGTGGCAG-3' and reverse 5'- GCTTGTTTTCAGTGATTCTGGG-3'.
ATGGCCAAGAAGGCAGTAGGTTTAGGGCCACTGTCGAGGCGTCCAGATAACT
CGGCGTTTAAACAGCAGAGATTACCAGCCTGGTCTCCATCTCTCACGGCACA
GACCGTCCTGCCAATCTTCTACATCCTAGCTGTCGTGTGCCTGCTGCTGGGCA
TCTGGCTCCTCATCACTGTCCAGAACACACACCAACTGAAGGTGGACTACAC
CGATGCTGGAACATGTGAACAGTGCTTCGAGCTTCATGCCAACAACACCAGA
ACGGTCTGCACATGTTCAGTCAACTTCTACGTTCCAAGACCCTTTCCGGGCGA
CGTGTTCTTCTACTACGGTCTGAGGAACTTTCATCAGAACCTGCGGAGGTACA
TGGACTCCCGCGATGATGCACAGATGGTGGGGAGGAAGAACAACCTGAAGG
CACCGAGTTCATACTGCGCTCCGTTTCATTACGATGCAAACGGGGTACCCATC
GCCCCCTGCGGTGCCGTGGCCAACAGCATGTTCAACGACTCATTTACACTGAT
GTATCATCAAGCTAATGGGGCAGAAGTGCAAGTTCCTCTCTATAGGAAGGGC
ATTGCTTGGTACACAGACAAAAATGTCAAGTTCCGCAACCCTCCGACCAACA
ACACATTTTCCCTTCGACAAGCCTTTGAAGGCACGACTCGGCCCTTATACTGG
CAGCACTCGGTTTATGAGCTGGATGACACAGACTCCAACAACAATGGTTTCA
TAAATGACGACCTGATTGTCTGGATGAGAGAGGCAGCCTTCCCTAATTTCAA
AAAGCTTTATGGGGTTCTCAATCGTGCTCAAGAGCCTTTCACTGAAGGCCTGC
CCGCCGGCAACTACAACATCTCTATAGATTACAATTTTCCTGTTGAGCCCTTC
AGAGGTCGAAAGGAGCTGGTGATCTCAATGGTGACCTGGTTTGGTGGGCAGA
ATTACTTTCTGCCCATTGCGTATCTGGTGACCAGTGGGCTAATCCTGGTGACT
GCTGTCGTTCTCACAACAGTGTTTGTCAAATTTGGCAAAAATGGCAAGAACA
TGGAGGAATAA
Notes: 1) R77Q vs. zgc:63472 (NM_200596) but EST EB861052 agrees with the above sequence. 2) K136N, but EST AL920832 agrees with the above sequence. 3) P268L, but EST CR929675 agrees with the above sequence.

>Sequence for tfg. Forward 5'-GATTGACACGTCCAAAACACCAGC-3' and reverse 5'-GAGGGAAGTTATAGTGAGGTGCTG-3'.
ATGAATGGACAGCTGGACCTGAGTGGGAAGCTGATCATCAAAGCTCAGCTGG
GTGATGATATTCGTCGTATTCCTATCCACAATGAAGACATCACCTACGACGAG
CTCCTGCTGATGATGCAGAGAGTTTTTCGTGGCCAGTTACAGAGCAGCGATG

AAGTCACCATCAAATACAAGGACGAAGATGACGACCTTATCACCATCTTTGA
CAGTTCTGATTTGTCCTTTGCGATCCAGTGCAGTAGAATATTAAAGCTCACTC
TTTTTGTGAATGGGCAGCCTCGGCCACTGGAGTCATCTCAGGTGAAGCACCTG
CGCAGAGAACTGATCCATTTGAGGAATAAAGTCAACAGCCTGCTGGACAGCC
TGGAGCCACCCTTAGAGTCTGTCCCAGAAAGCACCAACCCAGAAACTGAATG
TGTAAATGATGCAGTAGACTCCACAATGAGGCATGCTCCTCCTGTCAGTGCTG
CCAGCATGTCTGCTTTTGACCCACTGAAGAACCAGGAAGAGGTCAACAAGAA
TGTCATTTCTGCATTTGGTTTAACTGAGGAACCTGCCCCAGTTCCAGCTGTAG
CTGCCACCGCTGCTGCAGAGGAGCGCTCTGCTACTCCAGACAGTATTGCCTCT
TCATCCTCTGCAGCGCCCCCTGCTGCTGTGGCTCCACAGGCCCCCCCACCTTA
TTCAGGGGTCCAGCAACCCCCCTCTACTACTATGGATGGTCAGATGTATCAGC
AGTATCAGGCTCCAGGTGGATATCCTCCACCAGCTGGACCGCAGCAGCAGTA
TGGCATGCAGTACCCTGCTGGTTATACTCCTCAATCTGGTGTTCCTCAGGCTC
CGCCTCCTCAACAGCAGTTCCAGAATTACCCCACCCCTACTTCTCAGGCTGCT
GGCGCTCCTGGCTCCGCCCCTGGCTTTTCTGGCCAATCACAGCCTCCTGCTCC
CCAAGCACCTGCTCAGTATCCACCCGGAGCCTTTCCGCCTCAAAACTACACAT
CCCAGGCCTCTCAGCAGCCCGCAAACTACAGCCTGCCTCCAACCTCGCAGGC
CACAGCCGGTTACCAGCCCCGTCCCGGATACACCCCACCACCAGGTGCCACC
CCTCCACCCGGGGGTGCCAATCCCTATGCCCGAAACCGCCCGCCTTACGGCC
AGGGCTACACCCAACCAGGTCCTGGCTATCGGTAA

NOTES: 100% nucleotide agreement with CT726943 and CT700332 (full coverage when both are aligned).

>Sequence for zgc:158743. Forward 5’-CGGCTGATCGGGACACTTTAGC-3’ and reverse 5’-AGGCTCGGGGAGAGATTTCC-3’.

ATGGACGCGTCGGTAATGGTGGGCAGAGGAACCGGAGGGGCTGCGCTCTTCA
TCCTGATCGTCTTCATCGTACTACTAGGTGCCAGAAGCTCACGGGCGCAGAA
GGGGGACGGCTGTGGACACACAGTGCTAGGTGTGGGCAGCGGGAGCCTGGC
GTCTCTGGGTTATCCTCAGTCTTATCCTTCACAGTCTGTGTGTGAGTGGGAGA
TCAGCGTGACCGCTGGGCACAAAGTCCTTGTGCGCATCGCAGATCTTGACATT
GATACAAACAATTGCCAGGTGTCTTACCTGCGACTCTATAATGGGATCGGAC
CGGGACGAACAGAAATTGTGAAGTTTTGTGGCAGTAAAGAATGGAAAGAATT
GGTTATAAAGTCTGAGGGCCATCAGGTCACAGTGCAGTTCATGAGTGGACCA
CACCACAACGGCCGTGGCCTTTTCCTCTCCTACACCAACAGTCAGCACACTGA
CCTCATCACCTGTCTGGAGAAAGGAGAGCACTTCAGTGAAGCAGAGTTCAGT
AAATTCTGTCCTGCTGGATGCCTGATTGATTTCGGAGAGGTTTCGGGAACCAT
ACCGCATGGATACAGAGATTCTTCTCCTCTGTGCCTGGCCGGCATTCATGCGG
GTGTGCTGTCCAACACTCTGGGGGGGCAGATCAGTGTGGTCAGCAGCAAAGG
CATCCCACACTACGAAAGCTCACTGGCTAACAATGTGACATCTGTGCCTGGA
AATCTCTCCCCGAGCCT

NOTES: Fragment. D28A (in signal peptide) vs. zgc:158743 (NM_001080171) but this change is present in CO922572. Larger fragment was also cloned – sequence below.

>Additional sequence for zgc:158743. Forward 5’-GGGACACTTTAGCATTATGC-3’ and reverse 5’-GAGTGCCTCCTGATAGGTGG-3’.

GGGACACTTTAGCATTATGCATTCGGACTGCAGGCTGCTGGGATGGACGCGT
CGGTAATGGTGGGCAGAGGAACCGGAGGGGCTGCGCTCTTCATCCTGATCGT
CTTCATCGTACTACTAGGTGCCAGAAGCTCACGGGCGCAGAAGGGGGACGGC
TGTGGACACACAGTGCTAGGTGTGGGCAGCGGGAGCCTGGCGTCTCTGGGTT
ATCCTCAGTCTTATCCTTCACAGTCTGTGTGTGAGTGGGAGATCAGCGTGACC
GCTGGGCACAAAGTCCTTGTGCGCATCGCAGATCTTGACATTGATACAAACA
ATTGCCAGGTGTCTTACCTGCGACTCTATAATGGGATCGGACCGGGACGAAC
AGAAATTGTGAAGTTTTGTGGCAGTAAAGAATGGAAAGAATTGGTTATAAAG
TCTGAGGGCCATCAGGTCACAGTGCAGTTCATGAGTGGACCACACCACAACG
GCCGTGGCCTTTTCCTCTCCTACACCAACAGTCAGCACACTGACCTCATCACC
TGTCTGGAGAAAGGAGAGCACTTCAGTGAAGCAGAGTTCAGTAAATTCTGTC
CTGCTGGATGCCTGATTGATTTCGGAGAGGTTTCGGGAACCATACCGCATGG
ATACAGAGATTCTTCTCCTCTGTGCCTGGCCGGCATTCATGCGGGTGTGCTGT
CCAACACTCTGGGGGGGCAGATCAGTGTGGTCAGCAGCAAAGGCATCCCACA
CTACGAAAGCTCACTGGCTAACAATGTGACATCTGTGCCTGGAAATCTCTCCC
CGAGCCTTTTTACTTTCAAGACCAGCGGTTGCTATGGTACTTTGGGTTTGGAG
TCGGGGGTGGTGAGCGACTCTCAGATCACGGCCTCGTCCGAGTGGGAATGGG
GCGGTCATGGAAAACAGCCCACCGTCTGGGGCCCTACGGGGGCCCGCCTCAA
AACTCCAGGACGTCCGTGGGCTGCAGCCAACAGCGACACCAAAGAATGGATT
CAAGTGGACCTAAAGAAAGAGAAAAAAATAACAGGCATTACCACCACTGGC
TCCACACTCCCAGAGTATCAGTTTTACGTTTCAGCCTATGAGGTGTTATATAG
CCATGATGGACAGCAGTGGAAAACCTATCAAGAAGTGGGATCAGATAAAAA
CAAGATTTTCCAAGGTAACACCCACTATCTGCAGGAGGTGCGAAACAACTTT
ATTCCTCCAATTGAGGCACGCTTTCTCCGAATATGTCCCTTACAGTGGCACCA
GAGGATCGCCCTTAAAATGGAACTGCTGGGCTGCCAACCACATGCAGCGAGG
CCCAGAATCTTCCACCCAGGCCCTGCACCTCCTCGCAGGAAGAGCACAACAC
CGCCAGCGCAGGACAGGACCACACACACACCCAACATCCGAAACTCCACCAT
GCCTCCACACTCCCATGACGAGGTGGCTCTGGTAGCAGTGTTGGTTCCTGTAT
TGGTGGTGGTTCTGACGACACCAGTTCTGGTGATGGTGTGCTCATGGCTGTGG
AAGAACAGAAAAAGCCCTGAGGTGACGTATGACCTTCCACACTGGGAGCGC
ACGGTGTGGTGGAAGAGTATGAAACAGTTGTTGCCCTCTAAGCTGGATGGAG
AAGACTGTGTTCGCTATAGCTCTACGGCGCGAGTGGACCACCAGAGACCCCG
GGTGGAGCCTGCAGAATACGCCCAACCGCTGGTCACAGGAAACATGGCCTCT
CTTGGACAACGGTCGACATTTAAACCCGAAGAGGCCGATGTTCCCGAATACG
ATGCACCTATTCCTCCAGAACATTACCATGCTTATGCTGAGCCCCTTCCTGCT
TCTGGCACTGAATACGCCATGCCGATCATGATTGACAGGGCTAACCACCTAT
CAGGAGGCACTC

NOTES: Longer than zgc:158743 (NM_001080171). Compare with cds for CAQ14992 – agrees for all amino acids except E121D and L122V, both of which are conservative changes. Missing sequence for the terminal 45 amino acids compared to cds for CAQ14992. Smaller fragment was also cloned – see above.

Supplementary Figure 1

```
BtCOL8A1        MAGPPSPLQLLGVLLTLSVGSIRLIHAGAYYGIKPLPPQIPAQIPPQIPQYQPLGQQVPH 60
GgCOL8A1        MAVQPGPPQLLQVLLTISLGSIRLIQAGAYYGIKPLPPQIPPQMPPQIPQYQPLGQQVPH 60
OcCOL8A1        MAVPPGPPQLLQVLLTISLGSIRLIQAGAYYGIKPLPPQIPPQMPPQIPQYQPLGQQVPH 60
MmCOL8A1        MAVPPRPLQLLGILFIISLNSVRLIQAGAYYGIKPLPPQIPPQIPPQIPQYQPLGQQVPH 60
HsCOL8A1        MAVLPGPLQLLGVLLTISLSSIRLIQAGAYYGIKPLPPQIPPQMPPQIPQYQPLGQQVPH 60
DrCol8a1        MAMAAFLVALVQLTFLP------LAFGGGYYPHKSHP-----------QQHQPL----PQ 39
                **  .    *: : :        *  .*.**  *. *            *:***    *:

BtCOL8A1        MPLGKDGLNVGKELPHMQYGKEYPHLPQYRKEVQPAPRMGKEAAPKKGK-EIPLASLRGE 119
GgCOL8A1        MPLAKDGLTMGKEMPHAQYGKEYPHLPQYMKEVQPVPRMGKEAVPKKGK-EIPLASLRGE 119
OcCOL8A1        MPLAKDGLTMGKEMPHAQYGKEYPHLPQYMKEVQPVPRMGKEAVPKKGK-EIPLASLRGE 119
MmCOL8A1        MPLGKDGLSMGKEMPHMQYGKEYPHLPQYMKEIPPVPRMGKEVVPKKGKGEVPLASLRGE 120
HsCOL8A1        MPLAKDGLAMGKEMPHLQYGKEYPHLPQYMKEIQPAPRMGKEAVPKKGK-EIPLASLRGE 119
DrCol8a1        MHMG-----MGKEMPHMPYPHYRKDLPMHLNKGKDNK---GETIPRGEQ---GVQGQPGA 88
                * :.     :***:**  * :   .** : ::         *. *:  :    : .  *

BtCOL8A1        QGPRGEPGPRGPPGPPGLPGQGIPGVKGKPGPQGYPGIGKPGMPGMPGKPGAMGMPGAKG 179
GgCOL8A1        QGPRGEPGPRGPPGPPGLPGQGIPGIKGKPGPQGYPGVGKPGMPGMPGKPGAMGMPGAKG 179
OcCOL8A1        QGPRGEPGPRGPPGPPGLPGQGIPGIKGKPGPQGYPGVGKPGMPGMPGKPGAMGMPGAKG 179
MmCOL8A1        QGPRGEPGPRGPPGPPGLPGHGMPGIKGKPGPQGYPGIGKPGMPGMPGKPGAMGMPGAKG 180
HsCOL8A1        QGPRGEPGPRGPPGPPGLPGHGIPGIKGKPGPQGYPGVGKPGMPGMPGKPGAMGMPGAKG 179
DrCol8a1        QGPVGPPGPQGPPGPQGNGIQGPPGKPGPPGPPGYPGIGKPGMSGMPGKAGDPGQPGQPG 148
                *** * ***:***** *   :* **  * *** ****:*****.*****.*  * **  *

BtCOL8A1        EIGPKGEIGPMGIPGPQGPPGPHGLPGIGKPGGPGLPGQPGAKGERGPKGPPGPPGLQGP 239
GgCOL8A1        EIGPKGEIGPMGIPGPQGPPGPHGLPGIGKPGGPGLPGQPGAKGDRGPKGPPGPPGLQGP 239
OcCOL8A1        EIGPKGEIGPMGIPGPQGPPGPHGLPGIGKPGGPGLPGQPGAKGDRGPKGPPGPPGLQGP 239
MmCOL8A1        EIGPKGEIGPMGIPGPQGPPGPHGLPGIGKPGGPGLPGQPGAKGERGPKGPPGPPGLQGP 240
HsCOL8A1        EIGQKGEIGPMGIPGPQGPPGPHGLPGIGKPGGPGLPGQPGPKGDRGPKGLPGPQGLRGP 239
DrCol8a1        EQGPRGEDGQPGIAGPPGPPGPSGLPGIGKPGGQGLPGQPGNKGEPGHKGFPGLPGLPGP 208
                * * :** *  **.** ***** ********** ******* **: * ** **  ** **

BtCOL8A1        KGEKGFGMPGLPGLKGPPGMHGPPGPVGLPGVGKPGVTGFPGPQGPLGKPGPPGEPGPQG 299
GgCOL8A1        KGEKGFGMPGLPGLKGPPGMHGPPGPVGLPGVGKPGVTGFPGPQGPLGKPGPPGEPGPQG 299
OcCOL8A1        KGEKGFGMPGLPGLKGPPGMHGPPGPVGLPGVGKPGVTGFPGPQGPLGKPGPPGEPGPQG 299
MmCOL8A1        KGEKGFGMPGLPGLKGPPGMHGPPGPVGLPGVGKPGVTGFPGPQGPLGKPGPPGEPGPQG 300
HsCOL8A1        KGDKGFGMPGAPGVKGPPGMHGPPGPVGLPGVGKPGVTGFPGPQGPLGKPGAPGEPGPQG 299
DrCol8a1        KGDRGIGLPGPQGPKGPVGPPGLRGPAGLPGVGKTGLPGIPGPAGVPGKPGEPGEPGPEG 268
                **::*:*:**  * *** *  *  **.*******.*:.*:*** *  **** ******:*

BtCOL8A1        PIGVPGVQGPPGIPGIGKPGQDGIPGQPGFPGGKGEQGLPGLPGPPGLPGVGKPGFPGPK 359
GgCOL8A1        PIGVPGVQGPPGLPGVGKPGQDGIPGQPGFPGGKGEQGLPGLPGPPGLPGVGKPGFPGPK 359
OcCOL8A1        PIGVPGVQGPPGLPGVGKPGQDGIPGQPGFPGGKGEQGLPGLPGPPGLPGVGKPGFPGPK 359
MmCOL8A1        LIGVPGVQGPPGMPGVGKPGQDGIPGQPGFPGGKGEQGLPGLPGPPGLPGVGKPGFPGPK 360
HsCOL8A1        PIGVPGVQGPPGIPGIGKPGQDGIPGQPGFPGGKGEQGLPGLPGPPGLPGIGKPGFPGPK 359
DrCol8a1        PPGEKGPQGPQGAPGIGSPGEKGLPGQPGTPGHKGLHGPPGLPGKPGLPGFGKPGYPGPK 328
                  *  * *** * **:*.**:.*:***** ** ** :* ***** *****.****:****

BtCOL8A1        GDRGVGGLPGPLGPRGEKGPVGAPGLGGPPGEPGLPGIPGPMGPPGAIGFPGPKGEGGVV 419
GgCOL8A1        GDRGIGGVPGALGPRGEKGPVGAPGMGGPPGEPGLPGIPGPMGPPGAIGFPGPKGEGGIV 419
OcCOL8A1        GDRGIGGVPGALGPRGEKGPVGAPGMGGPPGEPGLPGIPGPMGPPGAIGFPGPKGEGGIV 419
MmCOL8A1        GDRGIGGVPGVLGPRGEKGPIGAPGMGGPPGEPGLPGIPGPMGPPGAIGFPGPKGEGGVV 420
HsCOL8A1        GDRGMGGVPGALGPRGEKGPIGAPGIGGPPGEPGLPGIPGPMGPPGAIGFPGPKGEGGIV 419
DrCol8a1        GDRGMGGLPGPQGPKGEKGHMGQPGMMGPPGQTGLPGPSGPIGAPGEVGSPGLKGEGGAG 388
                ****:**:**  **:**** :* **: ****:.**** .**:*.** :* ** *****

BtCOL8A1        GPQGPPGPKGEPGLQGFPGKPGFLGEVGPPGMRGLPGPIGPKGEAGLKGLPGLPGAPGLL 479
GgCOL8A1        GPQGPPGPKGEPGLQGFPGKPGFLGEVGPPGIRGLPGPIGPKGEAGHKGLPGLPGVPGLL 479
OcCOL8A1        GPQGPPGPKGEPGLQGFPGKPGFLGEVGPPGIRGLPGPIGPKGEAGHKGLPGLPGVPGLL 479
MmCOL8A1        GPQGPPGPKGEPGLQGFPGKPGFLGEVGPPGMRGLPGPIGPKGEGGHKGLPGLPGVPGLL 480
HsCOL8A1        GPQGPPGPKGEPGLQGFPGKPGFLGEVGPPGMRGLPGPIGPKGEAGQKGVPGLPGVPGLL 479
DrCol8a1        GAKGDPGPIGLTGPPGIPGQPGQPGEDGEPGPRGPQGPIGPKGEGGSNGLPGPPGQSGLP 448
                *.:* *** * .*  *:**:**  ** * ** **  ********.* :*:** ** .**
```

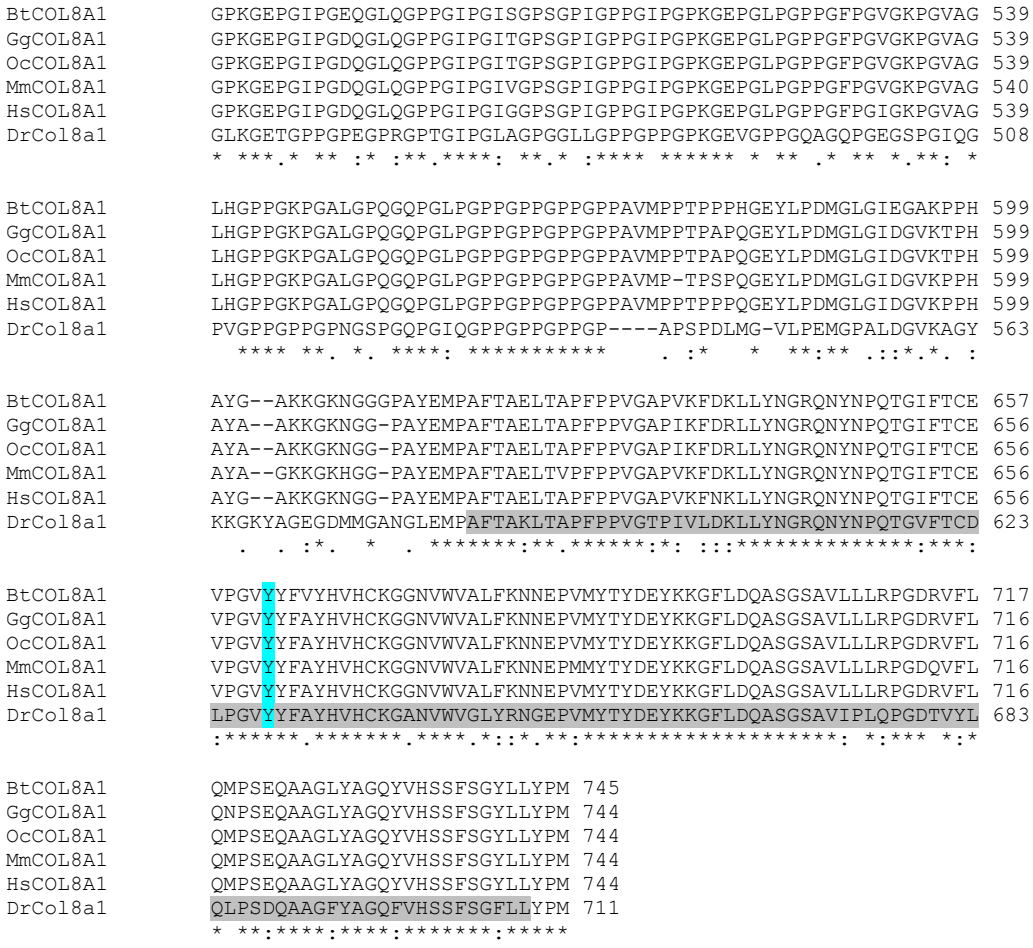

Supplementary Figure 2

CHAPTER 6

Discussion

Discussion: Summary and Future Directions

This thesis originated in the observation that the pleiotropic phenotype of copper deficiency in zebrafish embryos includes a strikingly distorted notochord. The work that followed has elucidated a number of genes essential for notochord morphogenesis in zebrafish and has contributed to an understanding of the gene-nutrient interactions critical for notochord development. Importantly, though our studies focused on a single nutrient involved in the formation of a single organ system, the results are broadly generalizable to other nutrients and organ systems.

Cloning of the lysyl oxidase gene family in zebrafish (Chapter 2) sets the stage for more detailed study of the role of individual family members in early development. Our work concentrated on the notochord-expressed lysyl oxidases, revealing overlapping roles for *loxl1* and *loxl5b* in notochord formation as well as interactions between these genes, the gene encoding collagen II, and copper. However, the embryonic functions of other lysyl oxidase family members, including Lox, Loxl2a, Loxl3a, and Loxl5a are yet to be determined. Studies of these family members will be facilitated by the optical clarity and genetic tractability of the zebrafish.

Our data suggest that studies of notochord formation may be relevant to understanding the etiology of congenital birth defects of the axial skeleton (Chapters 2, 4, and 5). For instance, mutations in human lysyl oxidases may contribute to the development of idiopathic scoliosis, a hypothesis now testable using a candidate gene approach based on our findings in zebrafish. The data may also have implications for certain diseases prevalent in adults. Single nucleotide polymorphisms in the human

LOXL1 gene have recently been associated with pseudoexfoliation syndrome, a late-onset systemic disorder of altered extracellular matrix homeostasis that can lead to glaucoma and blindness (177-186). Interestingly, many carriers of the high-risk polymorphisms do not develop pseudoexfoliation syndrome, and therefore additional environmental or genetic factors must strongly influence the phenotypic expression of the syndrome (180-182). The gene-nutrient interaction demonstrated between copper and zebrafish *loxl1* in notochord formation (Chapter 2) suggests that suboptimal copper nutrition or polymorphisms in genes affecting the delivery of copper to LOXL1 may play a role in the pathogenesis of this disorder.

The identification of a novel lysyl oxidase inhibitor, 2-mercaptopyridine-*N*-oxide, provided an important tool for use in our forward genetic sensitivity screen. 2-mercaptopyridine-*N*-oxide reduces amine oxidase activity in adult zebrafish extracts (Chapter 3), and the kinetics of lysyl oxidase inhibition by 2-mercaptopyridine-*N*-oxide should now be determined using precise radioactive assays and recombinant or purified lysyl oxidases. This potent compound may provide a basis for pharmacologic optimization by medicinal chemists with the goal of creating an inhibitor that is family-member specific. In light of the role of LOX in hypoxia-dependent cancer metastasis (54), such a drug could be important as a chemotherapeutic agent. It would also facilitate studies aimed at delineating the function of individual lysyl oxidases in early development.

Using 2-mercaptopyridine-*N*-oxide, we conducted a forward genetic screen for mutants that exhibit increased notochord distortion after partial lysyl oxidase inhibition.

This screen yielded a mutant in fibrillin-2 with defects in notochord and vascular morphogenesis and provided insight into the pathogenesis of congenital contractural arachnodactyly (Chapter 4). Future screens should focus on mutants that appear wild-type before pharmacologic inhibition and manifest a mutant phenotype only after exposure to 2-mercaptopyridine-*N*-oxide. This approach will identify "nonessential" genes that are actually essential under stress, as elegant work has recently demonstrated in yeast (107). It will also identify hypomorphic alleles of "essential" genes that may not be lethal, permitting studies into the role of these genes in adult fish. Cloning of each mutant locus will provide structure-function information about the affected protein and will further elucidate the molecular mechanisms of notochord formation.

Studies of the notochord mutant *gulliver* demonstrated a gene-nutrient interaction between copper and the gene encoding the alpha 1 chain of type VIII collagen (Chapter 5). This finding reiterates the need to interpret the nutritional status of an organism within the context of its specific genotype. The biological relevance of COL8A1 is poorly defined, and the *gulliver* mutant zebrafish may permit important studies into various aspects of COL8A1 function in the extracellular matrix. The observation that inhibition of lysyl oxidases (Chapter 2), disruption of fibrillin-2 (Chapter 4), or disruption of collagen VIII (Chapter 5) results in notochord distortion underscores the utility of the notochord as a model for understanding extracellular matrix formation.

The gene-gene and gene-nutrient interactions elucidated in this thesis (Chapters 2, 4, and 5) are particularly relevant in the era of personalized medicine that is now upon us. Sequencing individual human genomes has become a reality, with dramatic reductions in

cost and increases in speed (187). Indeed, the sequencing of James Watson's genome was recently completed in less than 2 months at a cost of under $1 million (188, 189). While the goal of the $1000 genome (190) is still out of reach, it will soon become a reality. Even today, single nucleotide polymorphism typing is being commercially exploited to provide interested parties with information regarding their putative health risks, determined mainly on the basis of genome-wide association studies. However, the interpretation of the polymorphisms and other quirks of individual genomes remains a largely unsolved challenge. For the full potential of this information to be realized, the functions and interactions of genetic and environmental networks involved in development and disease must be clarified. This represents one of the greatest challenges now facing science.

References

1. Jirtle, R.L., and Skinner, M.K. 2007. Environmental epigenomics and disease susceptibility. *Nat Rev Genet* 8:253-262.
2. Keen, C.L., Uriu-Hare, J.Y., Hawk, S.N., Jankowski, M.A., Daston, G.P., Kwik-Uribe, C.L., and Rucker, R.B. 1998. Effect of copper deficiency on prenatal development and pregnancy outcome. *Am J Clin Nutr* 67:1003S-1011S.
3. Held, K.R., Cruz, M.E., and Moncayo, F. 1990. Clinical pattern and the genetics of the fetal iodine deficiency disorder (endemic cretinism): results of a field study in Highland Ecuador. *Am J Med Genet* 35:85-90.
4. Wang, H.Y., Zhang, F.C., Gao, J.J., Fan, J.B., Liu, P., Zheng, Z.J., Xi, H., Sun, Y., Gao, X.C., Huang, T.Z., et al. 2000. Apolipoprotein E is a genetic risk factor for fetal iodine deficiency disorder in China. *Mol Psychiatry* 5:363-368.
5. Cao, X.Y., Jiang, X.M., Dou, Z.H., Rakeman, M.A., Zhang, M.L., O'Donnell, K., Ma, T., Amette, K., DeLong, N., and DeLong, G.R. 1994. Timing of vulnerability of the brain to iodine deficiency in endemic cretinism. *N Engl J Med* 331:1739-1744.
6. Guo, T.W., Zhang, F.C., Yang, M.S., Gao, X.C., Bian, L., Duan, S.W., Zheng, Z.J., Gao, J.J., Wang, H., Li, R.L., et al. 2004. Positive association of the DIO2 (deiodinase type 2) gene with mental retardation in the iodine-deficient areas of China. *J Med Genet* 41:585-590.
7. van der Linden, I.J., Afman, L.A., Heil, S.G., and Blom, H.J. 2006. Genetic variation in genes of folate metabolism and neural-tube defect risk. *Proc Nutr Soc* 65:204-215.
8. Finnell, R.H., Shaw, G.M., Lammer, E.J., Brandl, K.L., Carmichael, S.L., and Rosenquist, T.H. 2004. Gene-nutrient interactions: importance of folates and retinoids during early embryogenesis. *Toxicol Appl Pharmacol* 198:75-85.
9. Greve, C., Trachtenberg, E., Opsahl, W., Abbott, U., and Rucker, R. 1987. Diet as an external factor in the expression of scoliosis in a line of susceptible chickens. *J Nutr* 117:189-193.
10. Thiele, D.J., and Gitlin, J.D. 2008. Assembling the pieces. *Nat Chem Biol* 4:145-147.
11. Royce, P.M., and Steinmann, B. 2002. *Connective tissue and its heritable disorders : molecular, genetic, and medical aspects*. New York ; Chichester: Wiley.
12. Kaler, S.G., Holmes, C.S., Goldstein, D.S., Tang, J., Godwin, S.C., Donsante, A., Liew, C.J., Sato, S., and Patronas, N. 2008. Neonatal diagnosis and treatment of Menkes disease. *N Engl J Med* 358:605-614.
13. de Bie, P., Muller, P., Wijmenga, C., and Klomp, L.W. 2007. Molecular pathogenesis of Wilson and Menkes disease: correlation of mutations with molecular defects and disease phenotypes. *J Med Genet* 44:673-688.
14. Mendelsohn, B.A., Yin, C., Johnson, S.L., Wilm, T.P., Solnica-Krezel, L., and Gitlin, J.D. 2006. Atp7a determines a hierarchy of copper metabolism essential for notochord development. *Cell Metab* 4:155-162.

15. Cleaver, O., and Krieg, P.A. 2001. Notochord patterning of the endoderm. *Dev Biol* 234:1-12.
16. Stemple, D.L. 2005. Structure and function of the notochord: an essential organ for chordate development. *Development* 132:2503-2512.
17. Stemple, D.L., Solnica-Krezel, L., Zwartkruis, F., Neuhauss, S.C., Schier, A.F., Malicki, J., Stainier, D.Y., Abdelilah, S., Rangini, Z., Mountcastle-Shah, E., et al. 1996. Mutations affecting development of the notochord in zebrafish. *Development* 123:117-128.
18. Odenthal, J., Haffter, P., Vogelsang, E., Brand, M., van Eeden, F.J., Furutani-Seiki, M., Granato, M., Hammerschmidt, M., Heisenberg, C.P., Jiang, Y.J., et al. 1996. Mutations affecting the formation of the notochord in the zebrafish, Danio rerio. *Development* 123:103-115.
19. Coutinho, P., Parsons, M.J., Thomas, K.A., Hirst, E.M., Saude, L., Campos, I., Williams, P.H., and Stemple, D.L. 2004. Differential requirements for COPI transport during vertebrate early development. *Dev Cell* 7:547-558.
20. Parsons, M.J., Pollard, S.M., Saude, L., Feldman, B., Coutinho, P., Hirst, E.M., and Stemple, D.L. 2002. Zebrafish mutants identify an essential role for laminins in notochord formation. *Development* 129:3137-3146.
21. Shaw, G.C., Cope, J.J., Li, L., Corson, K., Hersey, C., Ackermann, G.E., Gwynn, B., Lambert, A.J., Wingert, R.A., Traver, D., et al. 2006. Mitoferrin is essential for erythroid iron assimilation. *Nature* 440:96-100.
22. Taylor, M.R., Hurley, J.B., Van Epps, H.A., and Brockerhoff, S.E. 2004. A zebrafish model for pyruvate dehydrogenase deficiency: rescue of neurological dysfunction and embryonic lethality using a ketogenic diet. *Proc Natl Acad Sci U S A* 101:4584-4589.
23. Donovan, A., Brownlie, A., Zhou, Y., Shepard, J., Pratt, S.J., Moynihan, J., Paw, B.H., Drejer, A., Barut, B., Zapata, A., et al. 2000. Positional cloning of zebrafish ferroportin1 identifies a conserved vertebrate iron exporter. *Nature* 403:776-781.
24. Patton, E.E., and Zon, L.I. 2001. The art and design of genetic screens: zebrafish. *Nat Rev Genet* 2:956-966.
25. Bahary, N., Davidson, A., Ransom, D., Shepard, J., Stern, H., Trede, N., Zhou, Y., Barut, B., and Zon, L.I. 2004. The Zon laboratory guide to positional cloning in zebrafish. *Methods Cell Biol* 77:305-329.
26. Johnson, S.L., Africa, D., Horne, S., and Postlethwait, J.H. 1995. Half-tetrad analysis in zebrafish: mapping the ros mutation and the centromere of linkage group I. *Genetics* 139:1727-1735.
27. Nasevicius, A., and Ekker, S.C. 2000. Effective targeted gene 'knockdown' in zebrafish. *Nat Genet* 26:216-220.
28. Epstein, C.J. 1995. The new dysmorphology: application of insights from basic developmental biology to the understanding of human birth defects. *Proc Natl Acad Sci U S A* 92:8566-8573.
29. Miles, H.L., Hofman, P.L., and Cutfield, W.S. 2005. Fetal origins of adult disease: a paediatric perspective. *Rev Endocr Metab Disord* 6:261-268.

30. Jensen, P.J., Gitlin, J.D., and Carayannopoulos, M.O. 2006. GLUT1 deficiency links nutrient availability and apoptosis during embryonic development. *J Biol Chem* 281:13382-13387.
31. Scott, A., and Stemple, D.L. 2005. Zebrafish notochordal basement membrane: signaling and structure. *Curr Top Dev Biol* 65:229-253.
32. Geach, T.J., and Dale, L. 2005. Members of the lysyl oxidase family are expressed during the development of the frog Xenopus laevis. *Differentiation* 73:414-424.
33. Westerfield, M. 1993. *The zebrafish book : a guide for the laboratory use of zebrafish (Brachydanio rerio)*. Eugene, OR: M. Westerfield.
34. Kimmel, C.B., Ballard, W.W., Kimmel, S.R., Ullmann, B., and Schilling, T.F. 1995. Stages of embryonic development of the zebrafish. *Dev Dyn* 203:253-310.
35. Kagan, H.M., and Li, W. 2003. Lysyl oxidase: properties, specificity, and biological roles inside and outside of the cell. *J Cell Biochem* 88:660-672.
36. Chenna, R., Sugawara, H., Koike, T., Lopez, R., Gibson, T.J., Higgins, D.G., and Thompson, J.D. 2003. Multiple sequence alignment with the Clustal series of programs. *Nucleic Acids Res* 31:3497-3500.
37. ClustalW WWW Service at the European Bioinformatics Institute.
38. Felsenstein, J. 2005. PHYLIP (Phylogeny Inference Package). [Department of Genome Sciences, University of Washington, Seattle]: Distributed by the author.
39. Bendtsen, J.D., Nielsen, H., von Heijne, G., and Brunak, S. 2004. Improved prediction of signal peptides: SignalP 3.0. *J Mol Biol* 340:783-795.
40. Pagni, M., Ioannidis, V., Cerutti, L., Zahn-Zabal, M., Jongeneel, C.V., and Falquet, L. 2004. MyHits: a new interactive resource for protein annotation and domain identification. *Nucleic Acids Res* 32:W332-335.
41. Borel, A., Eichenberger, D., Farjanel, J., Kessler, E., Gleyzal, C., Hulmes, D.J., Sommer, P., and Font, B. 2001. Lysyl oxidase-like protein from bovine aorta. Isolation and maturation to an active form by bone morphogenetic protein-1. *J Biol Chem* 276:48944-48949.
42. Panchenko, M.V., Stetler-Stevenson, W.G., Trubetskoy, O.V., Gacheru, S.N., and Kagan, H.M. 1996. Metalloproteinase activity secreted by fibrogenic cells in the processing of prolysyl oxidase. Potential role of procollagen C-proteinase. *J Biol Chem* 271:7113-7119.
43. Csiszar, K. 2001. Lysyl oxidases: a novel multifunctional amine oxidase family. *Prog Nucleic Acid Res Mol Biol* 70:1-32.
44. Yan, Y.L., Hatta, K., Riggleman, B., and Postlethwait, J.H. 1995. Expression of a type II collagen gene in the zebrafish embryonic axis. *Dev Dyn* 203:363-376.
45. Thisse, C., Thisse, B., Schilling, T.F., and Postlethwait, J.H. 1993. Structure of the zebrafish snail1 gene and its expression in wild-type, spadetail and no tail mutant embryos. *Development* 119:1203-1215.
46. Kawakami, K., Takeda, H., Kawakami, N., Kobayashi, M., Matsuda, N., and Mishina, M. 2004. A transposon-mediated gene trap approach identifies developmentally regulated genes in zebrafish. *Dev Cell* 7:133-144.

47. Rasband, W.S. 1997-2007. ImageJ, U.S. National Institutes of Health, Bethesda, Maryland, USA.
48. Tang, S.S., Trackman, P.C., and Kagan, H.M. 1983. Reaction of aortic lysyl oxidase with beta-aminopropionitrile. *J Biol Chem* 258:4331-4338.
49. Molnar, J., Fong, K.S., He, Q.P., Hayashi, K., Kim, Y., Fong, S.F., Fogelgren, B., Szauter, K.M., Mink, M., and Csiszar, K. 2003. Structural and functional diversity of lysyl oxidase and the LOX-like proteins. *Biochim Biophys Acta* 1647:220-224.
50. Liu, X., Zhao, Y., Gao, J., Pawlyk, B., Starcher, B., Spencer, J.A., Yanagisawa, H., Zuo, J., and Li, T. 2004. Elastic fiber homeostasis requires lysyl oxidase-like 1 protein. *Nat Genet* 36:178-182.
51. Maki, J.M., Rasanen, J., Tikkanen, H., Sormunen, R., Makikallio, K., Kivirikko, K.I., and Soininen, R. 2002. Inactivation of the lysyl oxidase gene Lox leads to aortic aneurysms, cardiovascular dysfunction, and perinatal death in mice. *Circulation* 106:2503-2509.
52. Maki, J.M., Sormunen, R., Lippo, S., Kaarteenaho-Wiik, R., Soininen, R., and Myllyharju, J. 2005. Lysyl oxidase is essential for normal development and function of the respiratory system and for the integrity of elastic and collagen fibers in various tissues. *Am J Pathol* 167:927-936.
53. Hornstra, I.K., Birge, S., Starcher, B., Bailey, A.J., Mecham, R.P., and Shapiro, S.D. 2003. Lysyl oxidase is required for vascular and diaphragmatic development in mice. *J Biol Chem* 278:14387-14393.
54. Erler, J.T., Bennewith, K.L., Nicolau, M., Dornhofer, N., Kong, C., Le, Q.T., Chi, J.T., Jeffrey, S.S., and Giaccia, A.J. 2006. Lysyl oxidase is essential for hypoxia-induced metastasis. *Nature* 440:1222-1226.
55. Woods, I.G., Kelly, P.D., Chu, F., Ngo-Hazelett, P., Yan, Y.L., Huang, H., Postlethwait, J.H., and Talbot, W.S. 2000. A comparative map of the zebrafish genome. *Genome Res* 10:1903-1914.
56. Lynch, M., and Force, A. 2000. The probability of duplicate gene preservation by subfunctionalization. *Genetics* 154:459-473.
57. Eriksson, J., and Lofberg, J. 2000. Development of the hypochord and dorsal aorta in the zebrafish embryo (Danio rerio). *J Morphol* 244:167-176.
58. Cleaver, O., and Krieg, P.A. 1998. VEGF mediates angioblast migration during development of the dorsal aorta in Xenopus. *Development* 125:3905-3914.
59. Tilton, F., La Du, J.K., Vue, M., Alzarban, N., and Tanguay, R.L. 2006. Dithiocarbamates have a common toxic effect on zebrafish body axis formation. *Toxicol Appl Pharmacol* 216:55-68.
60. Cerda, J., Grund, C., Franke, W.W., and Brand, M. 2002. Molecular characterization of Calymmin, a novel notochord sheath-associated extracellular matrix protein in the zebrafish embryo. *Dev Dyn* 224:200-209.
61. Lau, Y.K., Gobin, A.M., and West, J.L. 2006. Overexpression of lysyl oxidase to increase matrix crosslinking and improve tissue strength in dermal wound healing. *Ann Biomed Eng* 34:1239-1246.

62. Yu, Q., Horak, K., and Larson, D.F. 2006. Role of T lymphocytes in hypertension-induced cardiac extracellular matrix remodeling. *Hypertension* 48:98-104.
63. Grotmol, S., Kryvi, H., Keynes, R., Krossoy, C., Nordvik, K., and Totland, G.K. 2006. Stepwise enforcement of the notochord and its intersection with the myoseptum: an evolutionary path leading to development of the vertebra? *J Anat* 209:339-357.
64. Asuncion, L., Fogelgren, B., Fong, K.S., Fong, S.F., Kim, Y., and Csiszar, K. 2001. A novel human lysyl oxidase-like gene (LOXL4) on chromosome 10q24 has an altered scavenger receptor cysteine rich domain. *Matrix Biol* 20:487-491.
65. Ito, H., Akiyama, H., Iguchi, H., Iyama, K., Miyamoto, M., Ohsawa, K., and Nakamura, T. 2001. Molecular cloning and biological activity of a novel lysyl oxidase-related gene expressed in cartilage. *J Biol Chem* 276:24023-24029.
66. Maki, J.M., Tikkanen, H., and Kivirikko, K.I. 2001. Cloning and characterization of a fifth human lysyl oxidase isoenzyme: the third member of the lysyl oxidase-related subfamily with four scavenger receptor cysteine-rich domains. *Matrix Biol* 20:493-496.
67. Lee, J.E., and Kim, Y. 2006. A tissue-specific variant of the human lysyl oxidase-like protein 3 (LOXL3) functions as an amine oxidase with substrate specificity. *J Biol Chem* 281:37282-37290.
68. Teraoka, H., Urakawa, S., Nanba, S., Nagai, Y., Dong, W., Imagawa, T., Tanguay, R.L., Svoboda, K., Handley-Goldstone, H.M., Stegeman, J.J., et al. 2006. Muscular contractions in the zebrafish embryo are necessary to reveal thiuram-induced notochord distortions. *Toxicol Appl Pharmacol* 212:24-34.
69. Fleming, A., Keynes, R., and Tannahill, D. 2004. A central role for the notochord in vertebral patterning. *Development* 131:873-880.
70. Barrow, M.V., Simpson, C.F., and Miller, E.J. 1974. Lathyrism: a review. *Q Rev Biol* 49:101-128.
71. Tiller, G.E., Polumbo, P.A., Weis, M.A., Bogaert, R., Lachman, R.S., Cohn, D.H., Rimoin, D.L., and Eyre, D.R. 1995. Dominant mutations in the type II collagen gene, COL2A1, produce spondyloepimetaphyseal dysplasia, Strudwick type. *Nat Genet* 11:87-89.
72. Tiller, G.E., Rimoin, D.L., Murray, L.W., and Cohn, D.H. 1990. Tandem duplication within a type II collagen gene (COL2A1) exon in an individual with spondyloepiphyseal dysplasia. *Proc Natl Acad Sci U S A* 87:3889-3893.
73. Yeowell, H.N., and Walker, L.C. 2000. Mutations in the lysyl hydroxylase 1 gene that result in enzyme deficiency and the clinical phenotype of Ehlers-Danlos syndrome type VI. *Mol Genet Metab* 71:212-224.
74. Anderson, C., Bartlett, S.J., Gansner, J.M., Wilson, D., He, L., Gitlin, J.D., Kelsh, R.N., and Dowden, J. 2007. Chemical genetics suggests a critical role for lysyl oxidase in zebrafish notochord morphogenesis. *Mol Biosyst* 3:51-59.
75. Palamakumbura, A.H., and Trackman, P.C. 2002. A fluorometric assay for detection of lysyl oxidase enzyme activity in biological samples. *Anal Biochem* 300:245-251.

76. Shaw, G.M., Carmichael, S.L., Kaidarova, Z., and Harris, J.A. 2003. Differential risks to males and females for congenital malformations among 2.5 million California births, 1989-1997. *Birth Defects Res A Clin Mol Teratol* 67:953-958.
77. Detrait, E.R., George, T.M., Etchevers, H.C., Gilbert, J.R., Vekemans, M., and Speer, M.C. 2005. Human neural tube defects: developmental biology, epidemiology, and genetics. *Neurotoxicol Teratol* 27:515-524.
78. Murray, J.C. 2002. Gene/environment causes of cleft lip and/or palate. *Clin Genet* 61:248-256.
79. Shaw, G.M., Carmichael, S.L., Laurent, C., and Rasmussen, S.A. 2006. Maternal nutrient intakes and risk of orofacial clefts. *Epidemiology* 17:285-291.
80. Gansner, J.M., Mendelsohn, B.A., Hultman, K.A., Johnson, S.L., and Gitlin, J.D. 2007. Essential role of lysyl oxidases in notochord development. *Dev Biol* 307:202-213.
81. Gallagher, B.C., Sakai, L.Y., and Little, C.D. 1993. Fibrillin delineates the primary axis of the early avian embryo. *Dev Dyn* 196:70-78.
82. Wunsch, A.M., Little, C.D., and Markwald, R.R. 1994. Cardiac endothelial heterogeneity defines valvular development as demonstrated by the diverse expression of JB3, an antigen of the endocardial cushion tissue. *Dev Biol* 165:585-601.
83. Quondamatteo, F., Reinhardt, D.P., Charbonneau, N.L., Pophal, G., Sakai, L.Y., and Herken, R. 2002. Fibrillin-1 and fibrillin-2 in human embryonic and early fetal development. *Matrix Biol* 21:637-646.
84. Hubmacher, D., Tiedemann, K., and Reinhardt, D.P. 2006. Fibrillins: from biogenesis of microfibrils to signaling functions. *Curr Top Dev Biol* 75:93-123.
85. Corson, G.M., Charbonneau, N.L., Keene, D.R., and Sakai, L.Y. 2004. Differential expression of fibrillin-3 adds to microfibril variety in human and avian, but not rodent, connective tissues. *Genomics* 83:461-472.
86. Haston, J.L., Engelsen, S.B., Roessle, M., Clarkson, J., Blanch, E.W., Baldock, C., Kielty, C.M., and Wess, T.J. 2003. Raman microscopy and X-ray diffraction, a combined study of fibrillin-rich microfibrillar elasticity. *J Biol Chem* 278:41189-41197.
87. Sakai, L.Y., Keene, D.R., and Engvall, E. 1986. Fibrillin, a new 350-kD glycoprotein, is a component of extracellular microfibrils. *J Cell Biol* 103:2499-2509.
88. Czirok, A., Zamir, E.A., Filla, M.B., Little, C.D., and Rongish, B.J. 2006. Extracellular matrix macroassembly dynamics in early vertebrate embryos. *Curr Top Dev Biol* 73:237-258.
89. Czirok, A., Rongish, B.J., and Little, C.D. 2004. Extracellular matrix dynamics during vertebrate axis formation. *Dev Biol* 268:111-122.
90. Rongish, B.J., Drake, C.J., Argraves, W.S., and Little, C.D. 1998. Identification of the developmental marker, JB3-antigen, as fibrillin-2 and its de novo organization into embryonic microfibrous arrays. *Dev Dyn* 212:461-471.
91. Lawson, N.D., and Weinstein, B.M. 2002. In vivo imaging of embryonic vascular development using transgenic zebrafish. *Dev Biol* 248:307-318.

92. Solnica-Krezel, L., Schier, A.F., and Driever, W. 1994. Efficient recovery of ENU-induced mutations from the zebrafish germline. *Genetics* 136:1401-1420.
93. Johnson, S.L., Gates, M.A., Johnson, M., Talbot, W.S., Horne, S., Baik, K., Rude, S., Wong, J.R., and Postlethwait, J.H. 1996. Centromere-linkage analysis and consolidation of the zebrafish genetic map. *Genetics* 142:1277-1288.
94. Shimoda, N., Knapik, E.W., Ziniti, J., Sim, C., Yamada, E., Kaplan, S., Jackson, D., de Sauvage, F., Jacob, H., and Fishman, M.C. 1999. Zebrafish genetic map with 2000 microsatellite markers. *Genomics* 58:219-232.
95. Geisler, R., Rauch, G.J., Baier, H., van Bebber, F., Bross, L., Dekens, M.P., Finger, K., Fricke, C., Gates, M.A., Geiger, H., et al. 1999. A radiation hybrid map of the zebrafish genome. *Nat Genet* 23:86-89.
96. Larkin, M.A., Blackshields, G., Brown, N.P., Chenna, R., McGettigan, P.A., McWilliam, H., Valentin, F., Wallace, I.M., Wilm, A., Lopez, R., et al. 2007. Clustal W and Clustal X version 2.0. *Bioinformatics* 23:2947-2948.
97. Milne, I., Wright, F., Rowe, G., Marshall, D.F., Husmeier, D., and McGuire, G. 2004. TOPALi: software for automatic identification of recombinant sequences within DNA multiple alignments. *Bioinformatics* 20:1806-1807.
98. Guindon, S., and Gascuel, O. 2003. A simple, fast, and accurate algorithm to estimate large phylogenies by maximum likelihood. *Syst Biol* 52:696-704.
99. Anisimova, M., and Gascuel, O. 2006. Approximate likelihood-ratio test for branches: A fast, accurate, and powerful alternative. *Syst Biol* 55:539-552.
100. Tamura, K., Dudley, J., Nei, M., and Kumar, S. 2007. MEGA4: Molecular Evolutionary Genetics Analysis (MEGA) software version 4.0. *Mol Biol Evol* 24:1596-1599.
101. Skoglund, P., Dzamba, B., Coffman, C.R., Harris, W.A., and Keller, R. 2006. Xenopus fibrillin is expressed in the organizer and is the earliest component of matrix at the developing notochord-somite boundary. *Dev Dyn* 235:1974-1983.
102. Skoglund, P., and Keller, R. 2007. Xenopus fibrillin regulates directed convergence and extension. *Dev Biol* 301:404-416.
103. Behm-Ansmant, I., and Izaurralde, E. 2006. Quality control of gene expression: a stepwise assembly pathway for the surveillance complex that triggers nonsense-mediated mRNA decay. *Genes Dev* 20:391-398.
104. Griffin, K.J., Amacher, S.L., Kimmel, C.B., and Kimelman, D. 1998. Molecular identification of spadetail: regulation of zebrafish trunk and tail mesoderm formation by T-box genes. *Development* 125:3379-3388.
105. Ramirez, F., and Dietz, H.C. 2007. Fibrillin-rich microfibrils: Structural determinants of morphogenetic and homeostatic events. *J Cell Physiol* 213:326-330.
106. Ramirez, F., Sakai, L.Y., Rifkin, D.B., and Dietz, H.C. 2007. Extracellular microfibrils in development and disease. *Cell Mol Life Sci* 64:2437-2446.
107. Hillenmeyer, M.E., Fung, E., Wildenhain, J., Pierce, S.E., Hoon, S., Lee, W., Proctor, M., St Onge, R.P., Tyers, M., Koller, D., et al. 2008. The chemical genomic portrait of yeast: uncovering a phenotype for all genes. *Science* 320:362-365.

108. Chen, E., Larson, J.D., and Ekker, S.C. 2006. Functional analysis of zebrafish microfibril-associated glycoprotein-1 (Magp1) in vivo reveals roles for microfibrils in vascular development and function. *Blood* 107:4364-4374.
109. Bax, D.V., Bernard, S.E., Lomas, A., Morgan, A., Humphries, J., Shuttleworth, C.A., Humphries, M.J., and Kielty, C.M. 2003. Cell adhesion to fibrillin-1 molecules and microfibrils is mediated by alpha 5 beta 1 and alpha v beta 3 integrins. *J Biol Chem* 278:34605-34616.
110. Bax, D.V., Mahalingam, Y., Cain, S., Mellody, K., Freeman, L., Younger, K., Shuttleworth, C.A., Humphries, M.J., Couchman, J.R., and Kielty, C.M. 2007. Cell adhesion to fibrillin-1: identification of an Arg-Gly-Asp-dependent synergy region and a heparin-binding site that regulates focal adhesion formation. *J Cell Sci* 120:1383-1392.
111. Sakamoto, H., Broekelmann, T., Cheresh, D.A., Ramirez, F., Rosenbloom, J., and Mecham, R.P. 1996. Cell-type specific recognition of RGD- and non-RGD-containing cell binding domains in fibrillin-1. *J Biol Chem* 271:4916-4922.
112. Jovanovic, J., Takagi, J., Choulier, L., Abrescia, N.G., Stuart, D.I., van der Merwe, P.A., Mardon, H.J., and Handford, P.A. 2007. alphaVbeta6 is a novel receptor for human fibrillin-1. Comparative studies of molecular determinants underlying integrin-rgd affinity and specificity. *J Biol Chem* 282:6743-6751.
113. Sugi, Y., and Markwald, R.R. 1996. Formation and early morphogenesis of endocardial endothelial precursor cells and the role of endoderm. *Dev Biol* 175:66-83.
114. Visconti, R.P., Barth, J.L., Keeley, F.W., and Little, C.D. 2003. Codistribution analysis of elastin and related fibrillar proteins in early vertebrate development. *Matrix Biol* 22:109-121.
115. Zhang, H., Apfelroth, S.D., Hu, W., Davis, E.C., Sanguineti, C., Bonadio, J., Mecham, R.P., and Ramirez, F. 1994. Structure and expression of fibrillin-2, a novel microfibrillar component preferentially located in elastic matrices. *J Cell Biol* 124:855-863.
116. Zhang, H., Hu, W., and Ramirez, F. 1995. Developmental expression of fibrillin genes suggests heterogeneity of extracellular microfibrils. *J Cell Biol* 129:1165-1176.
117. Werneck, C.C., Trask, B.C., Broekelmann, T.J., Trask, T.M., Ritty, T.M., Segade, F., and Mecham, R.P. 2004. Identification of a major microfibril-associated glycoprotein-1-binding domain in fibrillin-2. *J Biol Chem* 279:23045-23051.
118. Lin, G., Tiedemann, K., Vollbrandt, T., Peters, H., Batge, B., Brinckmann, J., and Reinhardt, D.P. 2002. Homo- and heterotypic fibrillin-1 and -2 interactions constitute the basis for the assembly of microfibrils. *J Biol Chem* 277:50795-50804.
119. Charbonneau, N.L., Dzamba, B.J., Ono, R.N., Keene, D.R., Corson, G.M., Reinhardt, D.P., and Sakai, L.Y. 2003. Fibrillins can co-assemble in fibrils, but fibrillin fibril composition displays cell-specific differences. *J Biol Chem* 278:2740-2749.

120. Freeman, L.J., Lomas, A., Hodson, N., Sherratt, M.J., Mellody, K.T., Weiss, A.S., Shuttleworth, A., and Kielty, C.M. 2005. Fibulin-5 interacts with fibrillin-1 molecules and microfibrils. *Biochem J* 388:1-5.
121. Carta, L., Pereira, L., Arteaga-Solis, E., Lee-Arteaga, S.Y., Lenart, B., Starcher, B., Merkel, C.A., Sukoyan, M., Kerkis, A., Hazeki, N., et al. 2006. Fibrillins 1 and 2 perform partially overlapping functions during aortic development. *J Biol Chem* 281:8016-8023.
122. Arteaga-Solis, E., Gayraud, B., Lee, S.Y., Shum, L., Sakai, L., and Ramirez, F. 2001. Regulation of limb patterning by extracellular microfibrils. *J Cell Biol* 154:275-281.
123. Chaudhry, S.S., Gazzard, J., Baldock, C., Dixon, J., Rock, M.J., Skinner, G.C., Steel, K.P., Kielty, C.M., and Dixon, M.J. 2001. Mutation of the gene encoding fibrillin-2 results in syndactyly in mice. *Hum Mol Genet* 10:835-843.
124. Neptune, E.R., Frischmeyer, P.A., Arking, D.E., Myers, L., Bunton, T.E., Gayraud, B., Ramirez, F., Sakai, L.Y., and Dietz, H.C. 2003. Dysregulation of TGF-beta activation contributes to pathogenesis in Marfan syndrome. *Nat Genet* 33:407-411.
125. Cohn, R.D., van Erp, C., Habashi, J.P., Soleimani, A.A., Klein, E.C., Lisi, M.T., Gamradt, M., ap Rhys, C.M., Holm, T.M., Loeys, B.L., et al. 2007. Angiotensin II type 1 receptor blockade attenuates TGF-beta-induced failure of muscle regeneration in multiple myopathic states. *Nat Med* 13:204-210.
126. Habashi, J.P., Judge, D.P., Holm, T.M., Cohn, R.D., Loeys, B.L., Cooper, T.K., Myers, L., Klein, E.C., Liu, G., Calvi, C., et al. 2006. Losartan, an AT1 antagonist, prevents aortic aneurysm in a mouse model of Marfan syndrome. *Science* 312:117-121.
127. Ng, C.M., Cheng, A., Myers, L.A., Martinez-Murillo, F., Jie, C., Bedja, D., Gabrielson, K.L., Hausladen, J.M., Mecham, R.P., Judge, D.P., et al. 2004. TGF-beta-dependent pathogenesis of mitral valve prolapse in a mouse model of Marfan syndrome. *J Clin Invest* 114:1586-1592.
128. Dean, C., Ito, M., Makarenkova, H.P., Faber, S.C., and Lang, R.A. 2004. Bmp7 regulates branching morphogenesis of the lacrimal gland by promoting mesenchymal proliferation and condensation. *Development* 131:4155-4165.
129. Grishina, I.B., Kim, S.Y., Ferrara, C., Makarenkova, H.P., and Walden, P.D. 2005. BMP7 inhibits branching morphogenesis in the prostate gland and interferes with Notch signaling. *Dev Biol* 288:334-347.
130. Yang, Q., Ota, K., Tian, Y., Kumar, A., Wada, J., Kashihara, N., Wallner, E., and Kanwar, Y.S. 1999. Cloning of rat fibrillin-2 cDNA and its role in branching morphogenesis of embryonic lung. *Dev Biol* 212:229-242.
131. Gupta, P.A., Putnam, E.A., Carmical, S.G., Kaitila, I., Steinmann, B., Child, A., Danesino, C., Metcalfe, K., Berry, S.A., Chen, E., et al. 2002. Ten novel FBN2 mutations in congenital contractural arachnodactyly: delineation of the molecular pathogenesis and clinical phenotype. *Hum Mutat* 19:39-48.
132. Nishimura, A., Sakai, H., Ikegawa, S., Kitoh, H., Haga, N., Ishikiriyama, S., Nagai, T., Takada, F., Ohata, T., Tanaka, F., et al. 2007. FBN2, FBN1, TGFBR1,

and TGFBR2 analyses in congenital contractural arachnodactyly. *Am J Med Genet A* 143:694-698.
133. Park, E.S., Putnam, E.A., Chitayat, D., Child, A., and Milewicz, D.M. 1998. Clustering of FBN2 mutations in patients with congenital contractural arachnodactyly indicates an important role of the domains encoded by exons 24 through 34 during human development. *Am J Med Genet* 78:350-355.
134. Miner, J.H. 2005. *Extracellular matrix in development and disease*. Amsterdam ; Boston: Elsevier.
135. NBDPN. 2002. Congenital Malformations Surveillance Report. A report from the National Birth Defects Prevention Network. *Teratology* 66 Suppl 1:S1-219.
136. Gansner, J.M., Madsen, E.C., Mecham, R.P., and Gitlin, J.D. 2008. Essential role for fibrillin-2 in zebrafish notochord and vascular morphogenesis. *Dev Dyn* 237:2844-2861.
137. Mendelsohn, B.A., Kassebaum, B.L., and Gitlin, J.D. 2008. The zebrafish embryo as a dynamic model of anoxia tolerance. *Dev Dyn* 237:1780-1788.
138. Chan, D., Cole, W.G., Rogers, J.G., and Bateman, J.F. 1995. Type X collagen multimer assembly in vitro is prevented by a Gly618 to Val mutation in the alpha 1(X) NC1 domain resulting in Schmid metaphyseal chondrodysplasia. *J Biol Chem* 270:4558-4562.
139. Chan, D., Weng, Y.M., Hocking, A.M., Golub, S., McQuillan, D.J., and Bateman, J.F. 1996. Site-directed mutagenesis of human type X collagen. Expression of alpha1(X) NC1, NC2, and helical mutations in vitro and in transfected cells. *J Biol Chem* 271:13566-13572.
140. Hu, M.C., Gong, H.Y., Lin, G.H., Hu, S.Y., Chen, M.H., Huang, S.J., Liao, C.F., and Wu, J.L. 2007. XBP-1, a key regulator of unfolded protein response, activates transcription of IGF1 and Akt phosphorylation in zebrafish embryonic cell line. *Biochem Biophys Res Commun* 359:778-783.
141. Mendelsohn, B.A., and Gitlin, J.D. 2008. Coordination of development and metabolism in the pre-midblastula transition zebrafish embryo. *Dev Dyn* 237:1789-1798.
142. Innamorati, G., Bianchi, E., and Whang, M.I. 2006. An intracellular role for the C1q-globular domain. *Cell Signal* 18:761-770.
143. Yamaguchi, N., Mayne, R., and Ninomiya, Y. 1991. The alpha 1 (VIII) collagen gene is homologous to the alpha 1 (X) collagen gene and contains a large exon encoding the entire triple helical and carboxyl-terminal non-triple helical domains of the alpha 1 (VIII) polypeptide. *J Biol Chem* 266:4508-4513.
144. Ron, D., and Walter, P. 2007. Signal integration in the endoplasmic reticulum unfolded protein response. *Nat Rev Mol Cell Biol* 8:519-529.
145. Ozcan, U., Yilmaz, E., Ozcan, L., Furuhashi, M., Vaillancourt, E., Smith, R.O., Gorgun, C.Z., and Hotamisligil, G.S. 2006. Chemical chaperones reduce ER stress and restore glucose homeostasis in a mouse model of type 2 diabetes. *Science* 313:1137-1140.
146. de Almeida, S.F., Picarote, G., Fleming, J.V., Carmo-Fonseca, M., Azevedo, J.E., and de Sousa, M. 2007. Chemical chaperones reduce endoplasmic reticulum

stress and prevent mutant HFE aggregate formation. *J Biol Chem* 282:27905-27912.
147. Greenhill, N.S., Ruger, B.M., Hasan, Q., and Davis, P.F. 2000. The alpha1(VIII) and alpha2(VIII) collagen chains form two distinct homotrimeric proteins in vivo. *Matrix Biol* 19:19-28.
148. Geisler, R., Rauch, G.J., Geiger-Rudolph, S., Albrecht, A., van Bebber, F., Berger, A., Busch-Nentwich, E., Dahm, R., Dekens, M.P., Dooley, C., et al. 2007. Large-scale mapping of mutations affecting zebrafish development. *BMC Genomics* 8:11.
149. Bogin, O., Kvansakul, M., Rom, E., Singer, J., Yayon, A., and Hohenester, E. 2002. Insight into Schmid metaphyseal chondrodysplasia from the crystal structure of the collagen X NC1 domain trimer. *Structure* 10:165-173.
150. Kvansakul, M., Bogin, O., Hohenester, E., and Yayon, A. 2003. Crystal structure of the collagen alpha1(VIII) NC1 trimer. *Matrix Biol* 22:145-152.
151. Tom Tang, Y., Hu, T., Arterburn, M., Boyle, B., Bright, J.M., Palencia, S., Emtage, P.C., and Funk, W.D. 2005. The complete complement of C1q-domain-containing proteins in Homo sapiens. *Genomics* 86:100-111.
152. Mei, J., and Gui, J. 2008. Bioinformatic identification of genes encoding C1q-domain-containing proteins in zebrafish. *J Genet Genomics* 35:17-24.
153. Bonaventure, J., Chaminade, F., and Maroteaux, P. 1995. Mutations in three subdomains of the carboxy-terminal region of collagen type X account for most of the Schmid metaphyseal dysplasias. *Hum Genet* 96:58-64.
154. Brass, A., Kadler, K.E., Thomas, J.T., Grant, M.E., and Boot-Handford, R.P. 1992. The fibrillar collagens, collagen VIII, collagen X and the C1q complement proteins share a similar domain in their C-terminal non-collagenous regions. *FEBS Lett* 303:126-128.
155. Zhang, Y., and Chen, Q. 1999. The noncollagenous domain 1 of type X collagen. A novel motif for trimer and higher order multimer formation without a triple helix. *J Biol Chem* 274:22409-22413.
156. Illidge, C., Kielty, C., and Shuttleworth, A. 2001. Type VIII collagen: heterotrimeric chain association. *Int J Biochem Cell Biol* 33:521-529.
157. Sawada, H., Konomi, H., and Hirosawa, K. 1990. Characterization of the collagen in the hexagonal lattice of Descemet's membrane: its relation to type VIII collagen. *J Cell Biol* 110:219-227.
158. Kapoor, R., Bornstein, P., and Sage, E.H. 1986. Type VIII collagen from bovine Descemet's membrane: structural characterization of a triple-helical domain. *Biochemistry* 25:3930-3937.
159. Labermeier, U., and Kenney, M.C. 1983. The presence of EC collagen and type IV collagen in bovine Descemet's membranes. *Biochem Biophys Res Commun* 116:619-625.
160. Kabosova, A., Azar, D.T., Bannikov, G.A., Campbell, K.P., Durbeej, M., Ghohestani, R.F., Jones, J.C., Kenney, M.C., Koch, M., Ninomiya, Y., et al. 2007. Compositional differences between infant and adult human corneal basement membranes. *Invest Ophthalmol Vis Sci* 48:4989-4999.

161. Kapoor, R., Sakai, L.Y., Funk, S., Roux, E., Bornstein, P., and Sage, E.H. 1988. Type VIII collagen has a restricted distribution in specialized extracellular matrices. *J Cell Biol* 107:721-730.
162. Hopfer, U., Fukai, N., Hopfer, H., Wolf, G., Joyce, N., Li, E., and Olsen, B.R. 2005. Targeted disruption of Col8a1 and Col8a2 genes in mice leads to anterior segment abnormalities in the eye. *Faseb J* 19:1232-1244.
163. Muragaki, Y., Shiota, C., Inoue, M., Ooshima, A., Olsen, B.R., and Ninomiya, Y. 1992. alpha 1(VIII)-collagen gene transcripts encode a short-chain collagen polypeptide and are expressed by various epithelial, endothelial and mesenchymal cells in newborn mouse tissues. *Eur J Biochem* 207:895-902.
164. Bateman, J.F., Freddi, S., Nattrass, G., and Savarirayan, R. 2003. Tissue-specific RNA surveillance? Nonsense-mediated mRNA decay causes collagen X haploinsufficiency in Schmid metaphyseal chondrodysplasia cartilage. *Hum Mol Genet* 12:217-225.
165. Chan, D., Weng, Y.M., Graham, H.K., Sillence, D.O., and Bateman, J.F. 1998. A nonsense mutation in the carboxyl-terminal domain of type X collagen causes haploinsufficiency in schmid metaphyseal chondrodysplasia. *J Clin Invest* 101:1490-1499.
166. Tsang, K.Y., Chan, D., Cheslett, D., Chan, W.C., So, C.L., Melhado, I.G., Chan, T.W., Kwan, K.M., Hunziker, E.B., Yamada, Y., et al. 2007. Surviving endoplasmic reticulum stress is coupled to altered chondrocyte differentiation and function. *PLoS Biol* 5:e44.
167. Ho, M.S., Tsang, K.Y., Lo, R.L., Susic, M., Makitie, O., Chan, T.W., Ng, V.C., Sillence, D.O., Boot-Handford, R.P., Gibson, G., et al. 2007. COL10A1 nonsense and frame-shift mutations have a gain-of-function effect on the growth plate in human and mouse metaphyseal chondrodysplasia type Schmid. *Hum Mol Genet* 16:1201-1215.
168. Maestri, N.E., Brusilow, S.W., Clissold, D.B., and Bassett, S.S. 1996. Long-term treatment of girls with ornithine transcarbamylase deficiency. *N Engl J Med* 335:855-859.
169. Gottsch, J.D., Sundin, O.H., Liu, S.H., Jun, A.S., Broman, K.W., Stark, W.J., Vito, E.C., Narang, A.K., Thompson, J.M., and Magovern, M. 2005. Inheritance of a novel COL8A2 mutation defines a distinct early-onset subtype of fuchs corneal dystrophy. *Invest Ophthalmol Vis Sci* 46:1934-1939.
170. Liskova, P., Prescott, Q., Bhattacharya, S.S., and Tuft, S.J. 2007. British family with early-onset Fuchs' endothelial corneal dystrophy associated with p.L450W mutation in the COL8A2 gene. *Br J Ophthalmol* 91:1717-1718.
171. Mok, J.W., Kim, H.S., and Joo, C.K. 2009. Q455V mutation in COL8A2 is associated with Fuchs' corneal dystrophy in Korean patients. *Eye* 23:895-903.
172. Bateman, J.F., Wilson, R., Freddi, S., Lamande, S.R., and Savarirayan, R. 2005. Mutations of COL10A1 in Schmid metaphyseal chondrodysplasia. *Hum Mutat* 25:525-534.
173. Bateman, J.F., Freddi, S., McNeil, R., Thompson, E., Hermanns, P., Savarirayan, R., and Lamande, S.R. 2004. Identification of four novel COL10A1 missense

mutations in schmid metaphyseal chondrodysplasia: further evidence that collagen X NC1 mutations impair trimer assembly. *Hum Mutat* 23:396.
174. Ridanpaa, M., Ward, L.M., Rockas, S., Sarkioja, M., Makela, H., Susic, M., Glorieux, F.H., Cole, W.G., and Makitie, O. 2003. Genetic changes in the RNA components of RNase MRP and RNase P in Schmid metaphyseal chondrodysplasia. *J Med Genet* 40:741-746.
175. Wallis, G.A., Rash, B., Sykes, B., Bonaventure, J., Maroteaux, P., Zabel, B., Wynne-Davies, R., Grant, M.E., and Boot-Handford, R.P. 1996. Mutations within the gene encoding the alpha 1 (X) chain of type X collagen (COL10A1) cause metaphyseal chondrodysplasia type Schmid but not several other forms of metaphyseal chondrodysplasia. *J Med Genet* 33:450-457.
176. Wagner, D.S., Dosch, R., Mintzer, K.A., Wiemelt, A.P., and Mullins, M.C. 2004. Maternal control of development at the midblastula transition and beyond: mutants from the zebrafish II. *Dev Cell* 6:781-790.
177. Ritch, R., and Schlotzer-Schrehardt, U. 2001. Exfoliation (pseudoexfoliation) syndrome: toward a new understanding. Proceedings of the First International Think Tank. *Acta Ophthalmol Scand* 79:213-217.
178. Thorleifsson, G., Magnusson, K.P., Sulem, P., Walters, G.B., Gudbjartsson, D.F., Stefansson, H., Jonsson, T., Jonasdottir, A., Jonasdottir, A., Stefansdottir, G., et al. 2007. Common sequence variants in the LOXL1 gene confer susceptibility to exfoliation glaucoma. *Science* 317:1397-1400.
179. Aragon-Martin, J.A., Ritch, R., Liebmann, J., O'Brien, C., Blaaow, K., Mercieca, F., Spiteri, A., Cobb, C.J., Damji, K.F., Tarkkanen, A., et al. 2008. Evaluation of LOXL1 gene polymorphisms in exfoliation syndrome and exfoliation glaucoma. *Mol Vis* 14:533-541.
180. Challa, P., Schmidt, S., Liu, Y., Qin, X., Vann, R.R., Gonzalez, P., Allingham, R.R., and Hauser, M.A. 2008. Analysis of LOXL1 polymorphisms in a United States population with pseudoexfoliation glaucoma. *Mol Vis* 14:146-149.
181. Fingert, J.H., Alward, W.L., Kwon, Y.H., Wang, K., Streb, L.M., Sheffield, V.C., and Stone, E.M. 2007. LOXL1 mutations are associated with exfoliation syndrome in patients from the midwestern United States. *Am J Ophthalmol* 144:974-975.
182. Hewitt, A.W., Sharma, S., Burdon, K.P., Wang, J.J., Baird, P.N., Dimasi, D.P., Mackey, D.A., Mitchell, P., and Craig, J.E. 2008. Ancestral LOXL1 variants are associated with pseudoexfoliation in Caucasian Australians but with markedly lower penetrance than in Nordic people. *Hum Mol Genet* 17:710-716.
183. Pasutto, F., Krumbiegel, M., Mardin, C.Y., Paoli, D., Lammer, R., Weber, B.H., Kruse, F.E., Schlotzer-Schrehardt, U., and Reis, A. 2008. Association of LOXL1 Common Sequence Variants in German and Italian Patients with Pseudoexfoliation Syndrome and Pseudoexfoliation Glaucoma. *Invest Ophthalmol Vis Sci* 49:1459-1463.
184. Ramprasad, V.L., George, R., Soumittra, N., Sharmila, F., Vijaya, L., and Kumaramanickavel, G. 2008. Association of non-synonymous single nucleotide

polymorphisms in the LOXL1 gene with pseudoexfoliation syndrome in India. *Mol Vis* 14:318-322.

185. Yang, X., Zabriskie, N.A., Hau, V.S., Chen, H., Tong, Z., Gibbs, D., Farhi, P., Katz, B.J., Luo, L., Pearson, E., et al. 2008. Genetic association of LOXL1 gene variants and exfoliation glaucoma in a Utah cohort. *Cell Cycle* 7:521-524.
186. Fan, B.J., Pasquale, L., Grosskreutz, C.L., Rhee, D., Chen, T., DeAngelis, M.M., Kim, I., del Bono, E., Miller, J.W., Li, T., et al. 2008. DNA sequence variants in the LOXL1 gene are associated with pseudoexfoliation glaucoma in a U.S. clinic-based population with broad ethnic diversity. *BMC Med Genet* 9:5.
187. von Bubnoff, A. 2008. Next-generation sequencing: the race is on. *Cell* 132:721-723.
188. Wheeler, D.A., Srinivasan, M., Egholm, M., Shen, Y., Chen, L., McGuire, A., He, W., Chen, Y.J., Makhijani, V., Roth, G.T., et al. 2008. The complete genome of an individual by massively parallel DNA sequencing. *Nature* 452:872-876.
189. Levy, S., Sutton, G., Ng, P.C., Feuk, L., Halpern, A.L., Walenz, B.P., Axelrod, N., Huang, J., Kirkness, E.F., Denisov, G., et al. 2007. The diploid genome sequence of an individual human. *PLoS Biol* 5:e254.
190. Collins, F.S., Green, E.D., Guttmacher, A.E., and Guyer, M.S. 2003. A vision for the future of genomics research. *Nature* 422:835-847.